OULU 2015
C 541

ACTA UNIVERSITATIS OULUENSIS

Harri Pennanen

COORDINATED BEAMFORMING IN CELLULAR AND COGNITIVE RADIO NETWORKS

*UNIVERSITY OF OULU GRADUATE SCHOOL;
UNIVERSITY OF OULU,
FACULTY OF INFORMATION TECHNOLOGY AND ELECTRICAL ENGINEERING,
DEPARTMENT OF COMMUNICATIONS ENGINEERING;
CENTRE FOR WIRELESS COMMUNICATIONS;
INFOTECH OULU*

ACTA UNIVERSITATIS OULUENSIS
C Technica 541

HARRI PENNANEN

COORDINATED BEAMFORMING IN CELLULAR AND COGNITIVE RADIO NETWORKS

Academic dissertation to be presented with the assent of the Doctoral Training Committee of Technology and Natural Sciences of the University of Oulu for public defence in the OP auditorium (L10), Linnanmaa, on 18 September 2015, at 12 noon

UNIVERSITY OF OULU, OULU 2015

Acta Univ. Oul. C 541, 2015

Supervised by
Professor Matti Latva-aho
Docent Antti Tölli

Reviewed by
Professor Wolfgang Utschick
Professor Wei Yu

ISBN 978-952-62-0896-1 (Paperback)
ISBN 978-952-62-0897-8 (PDF)

ISSN 0355-3213 (Printed)
ISSN 1796-2226 (Online)

Cover Design
Raimo Ahonen

JUVENES PRINT
TAMPERE 2015

Pennanen, Harri, Coordinated beamforming in cellular and cognitive radio networks.
University of Oulu Graduate School; University of Oulu, Faculty of Information Technology and Electrical Engineering, Department of Communications Engineering; Centre for Wireless Communications; Infotech Oulu
Acta Univ. Oul. C 541, 2015
University of Oulu, P.O. Box 8000, FI-90014 University of Oulu, Finland

Abstract

This thesis focuses on the design of coordinated downlink beamforming techniques for wireless multi-cell multi-user multi-antenna systems. In particular, cellular and cognitive radio networks are considered. In general, coordinated beamforming schemes aim to improve system performance, especially at the cell-edge area, by controlling inter-cell interference. In this work, special emphasis is put on practical coordinated beamforming designs that can be implemented in a decentralized manner by relying on local channel state information (CSI) and low-rate backhaul signaling. The network design objective is the sum power minimization (SPMin) of base stations (BSs) while providing the guaranteed minimum rate for each user.

Decentralized coordinated beamforming techniques are developed for cellular multi-user multiple-input single-output (MISO) systems. The proposed iterative algorithms are based on classical primal and dual decomposition methods. The SPMin problem is decomposed into two optimization levels, i.e., BS-specific subproblems for the beamforming design and a network-wide master problem for the inter-cell interference coordination. After the acquisition of local CSI, each BS can independently compute its transmit beamformers by solving the subproblem via standard convex optimization techniques. Interference coordination is managed by solving the master problem via a traditional subgradient method that requires scalar information exchange between the BSs. The algorithms make it possible to satisfy the user-specific rate constraints for any iteration. Hence, delay and signaling overhead can be reduced by limiting the number of performed iterations. In this respect, the proposed algorithms are applicable to practical implementations unlike most of the existing decentralized approaches. The numerical results demonstrate that the algorithms provide significant performance gains over zero-forcing beamforming strategies.

Coordinated beamforming is also studied in cellular multi-user multiple-input multiple-output (MIMO) systems. The corresponding non-convex SPMin problem is divided into transmit and receive beamforming optimization steps that are alternately solved via successive convex approximation method and the linear minimum mean square error criterion, respectively, until the desired level of convergence is attained. In addition to centralized design, two decentralized primal decomposition-based algorithms are proposed wherein the transmit and receive beamforming designs are facilitated by a combination of pilot and backhaul signaling. The results show that the proposed MIMO algorithms notably outperform the MISO ones.

Finally, cellular coordinated beamforming strategies are extended to multi-user MISO cognitive radio systems, where primary and secondary networks share the same spectrum. Here, network optimization is performed for the secondary system with additional interference constraints imposed for the primary users. Decentralized algorithms are proposed based on primal decomposition and an alternating direction method of multipliers.

Keywords: backhaul information exchange, convex optimization, coordinated beamforming, decentralized processing, interference coordination, multi-cell multi-user MIMO system, pilot signaling, sum power minimization, transceiver design

Pennanen, Harri, Yhteistoiminnallinen keilanmuodostus langattomissa solukko- ja kognitiiviradioverkoissa.
Oulun yliopiston tutkijakoulu; Oulun yliopisto, Tieto- ja sähkötekniikan tiedekunta, Tietoliikennetekniikan osasto; Centre for Wireless Communications; Infotech Oulu
Acta Univ. Oul. C 541, 2015
Oulun yliopisto, PL 8000, 90014 Oulun yliopisto

Tiivistelmä

Tämä väitöskirja keskittyy yhteistoiminnallisten keilanmuodostustekniikoiden suunnitteluun langattomissa monisolu- ja moniantennijärjestelmissä, erityisesti solukko- ja kognitiiviradioverkoissa. Yhteistoiminnalliset keilanmuodostustekniikat pyrkivät parantamaan verkkojen suorituskykyä kontrolloimalla monisoluhäiriötä, erityisesti tukiasemasolujen reuna-alueilla. Tässä työssä painotetaan erityisesti käytännöllisten yhteistoiminnallisten keilanmuodostustekniikoiden suunnittelua, joka voidaan toteuttaa hajautetusti perustuen paikalliseen kanavatietoon ja tukiasemien väliseen informaationvaihtoon. Verkon suunnittelutavoite on minimoida tukiasemien kokonaislähetysteho samalla, kun jokaiselle käyttäjälle taataan tietty vähimmäistiedonsiirtonopeus.

Hajautettuja yhteistoiminnallisia keilanmuodostustekniikoita kehitetään moni-tulo yksi-lähtö -solukkoverkoille. Oletuksena on, että tukiasemat ovat varustettuja monilla lähetysantenneilla, kun taas päätelaitteissa on vain yksi vastaanotinantenni. Ehdotetut iteratiiviset algoritmit perustuvat klassisiin primaali- ja duaalihajotelmiin. Lähetystehon minimointiongelma hajotetaan kahteen optimointitasoon: tukiasemakohtaisiin aliongelmiin keilanmuodostusta varten ja verkkotason pääongelmaan monisoluhäiriön hallintaa varten. Paikallisen kanavatiedon hankkimisen jälkeen jokainen tukiasema laskee itsenäisesti lähetyskeilansa ratkaisemalla aliongelmansa käyttäen apunaan standardeja konveksioptimointitekniikoita. Monisoluhäiriötä kontrolloidaan ratkaisemalla pääongelma käyttäen perinteistä aligradienttimenetelmää. Tämä vaatii tukiasemien välistä informaationvaihtoa. Ehdotetut algoritmit takaavat käyttäjäkohtaiset tiedonsiirtonopeustavoitteet jokaisella iterointikierroksella. Tämä mahdollistaa viiveen pienentämisen ja tukiasemien välisen informaatiovaihdon kontrolloimisen. Tästä syystä ehdotetut algoritmit soveltuvat käytännön toteutuksiin toisin kuin useimmat aiemmin ehdotetut hajautetut algoritmit. Numeeriset tulokset osoittavat, että väitöskirjassa ehdotetut algoritmit tuovat merkittävää verkon suorituskyvyn parannusta verrattaessa aiempiin nollaanpakotus -menetelmiin.

Yhteistoiminnallista keilanmuodostusta tutkitaan myös moni-tulo moni-lähtö -solukkoverkoissa, joissa tukiasemat sekä päätelaitteet ovat varustettuja monilla antenneilla. Tällaisessa verkossa lähetystehon minimointiongelma on ei-konveksi. Optimointiongelma jaetaan lähetys- ja vastaanottokeilanmuodostukseen, jotka toistetaan vuorotellen, kunnes algoritmi konvergoituu. Lähetyskeilanmuodostusongelma ratkaistaan peräkkäisillä konvekseilla approksimaatioilla. Vastaanottimen keilanmuodostus toteutetaan summaneliövirheen minimoinnin kautta. Keskitetyn algoritmin lisäksi tässä työssä kehitetään myös kaksi hajautettua algoritmia, jotka perustuvat primaalihajotelmaan. Hajautettua toteutusta helpotetaan pilottisignaloinnilla ja tukiasemien välisellä informaationvaihdolla. Numeeriset tulokset osoittavat, että moni-tulo moni-lähtö -tekniikoilla on merkittävästi parempi suorituskyky kuin moni-tulo yksi-lähtö -tekniikoilla.

Lopuksi yhteistoiminnallista keilanmuodostusta tarkastellaan kognitiiviradioverkoissa, joissa primaari- ja sekundaarijärjestelmät jakavat saman taajuuskaistan. Lähetystehon optimointi suoritetaan sekundaariverkolle samalla minimoiden primaarikäyttäjille aiheuttamaa häiriötä. Väitöskirjassa kehitetään kaksi hajautettua algoritmia, joista toinen perustuu primaalihajotelmaan ja toinen kerrointen vaihtelevan suunnan menetelmään.

Asiasanat: hajautettu prosessointi, häiriönhallinta, kokonaislähetystehon minimointi, konveksi optimointi, lähetin- ja vastaanotinkeilojen suunnittelu, monisoluinen monikäyttäjä- ja moniantennijärjestelmä, pilottisignalointi, tukiasemien välinen informaationvaihto, yhteistoiminnallinen keilanmuodostus

To my parents and my siblings

Preface

This doctoral thesis is the outcome of the research work conducted at the Centre for Wireless Communications (CWC), University of Oulu, Finland, during the years 2010 – 2015. These years have been extremely educational, both scientifically and personally. Choosing an academic career path and pursuing a doctoral degree has definitely been one of the best decisions in my life.

First, I would like to thank my supervisor, Professor Matti Latva-aho, for hiring me in the first place at CWC and giving me the opportunity to work in a top-notch research unit. I am deeply grateful to him for his firm guidance, invaluable encouragement and unreserved support during my doctoral research. I also wish to express my deep gratitude to my co-supervisor, Docent Antti Tölli, for his inspiring guidance and excellent scientific support. Without his profound and vast technical knowledge, ingenuity, and enthusiasm, completing a thesis of this quality would not have been possible. I further wish to thank the pre-examiners, Professor Wolfgang Utschick from the Technical University of Munich, Germany, and Professor Wei Yu from the University of Toronto, Canada. Their insightful comments and constructive feedback helped me further improve the quality of the thesis.

I thank all personnel at the CWC including my superiors, colleagues and fellow researchers for creating such an open and inspiring working environment. A special thanks goes to my former office mate, Dr. Petri Komulainen, who, besides being a great colleague, also served as a good example for how to be an excellent researcher. I am also grateful to Jarkko Kaleva and Dr. Valtteri Tervo for the cooperation and fruitful technical discussions that we had. I wish to thank my close colleagues for making an average work day always a positive experience and creating a joyful, supportive, and inspiring atmosphere. These colleagues are Dr. Valtteri Tervo, Tuomo Hänninen, Oskari Tervo, Jarkko Kaleva, Dr. Mehdi Bennis, Marko Mäkeläinen, Brett Kaufmann, Dr. Marian Codreanu, Nuutti Tervo, Petri Luoto, Markus Leinonen, Markku Jokinen and Pasi Maliniemi. I have also had the privilege to guide the Master's thesis of Amin Ghazanfari, and this experience turned out to be very educational. The administrative support of Hanna Saarela, Kirsi Ojutkangas, Eija Pajunen, Mari Lehmikangas, and Jari

Sillanpää is gratefully acknowledged as well.

During the years at the CWC, I have had the privilege to work in many projects, namely, Energy-Efficient Wireless Networks and Connectivity of Devices-Densification (EWINE-D), Interference Management for Wireless Networks beyond Present Horizon (IMANET and IMANET+), Wireless World Initiative New Radio+ (WINNER+), 5G radio access solutions to 10 GHz and beyond frequency bands (5Gto10G) and Broadband Evolved Femto Networks (BEFEMTO). The main funding for these projects was received from the Finnish Funding Agency for Technology and Innovation (Tekes). The main industrial funders were Nokia, Nokia Siemens Networks and Renesas Mobile Europe. I thank the project managers of these projects as well as all my fellow researchers and industrial representatives who either directly or indirectly influenced my research work. My doctoral research was partly supported by the Graduate Schools in Electronics, Telecommunications, and Automation (GETA). I was also fortunate to receive personal grants from several Finnish funding organizations: Nokia säätiö, Tauno Tönningin säätiö, Walter Ahlströmin säätiö, Riitta and Jorma J. Takasen säätiö and Tekniikan edistämisäätio. All these funders are highly appreciated.

Finally, I wish to express my deepest gratitude to my wonderful parents, Pekka and Arja, for their unconditional support and encouragement throughout my life. Their positive attitude towards education has certainly influenced on my motivation and choice of studies. I am grateful for my elder brother, Teemu, who has been a great role model for me, both in research and in life. I also wish to thank my little sister for her constant encouragement and endless faith in me.

Oulu, August 13, 2015 Harri Pennanen

Abbreviations

a	path gain from a BS to its own cell's users
$\bar{a}$	path gain from a BS to other cells' users
A_{R}	number of receive antennas
A_{T}	number of transmit antennas
b_k	serving BS for user k
B	number of base stations
$\mathcal{B}$	set of all BSs
$c_{k,l}$	SCA coefficient for stream (k, l)
$d_{k,l}$	SCA coefficient for stream (k, l)
e	radius of CSI error region
$\mathbf{e}_{b,k,l}$	effective channel vector for stream l of user k as seen by BS b
$\mathcal{E}_{b,k}$	ellipsoid bounding CSI error vector $\mathbf{u}_{b,k}$
$\mathcal{E}_{t,s}$	ellipsoid bounding CSI error vector $\mathbf{u}_{t,s}$
$\mathbf{E}_{b,k}$	matrix defining the shape and size of the ellipsoid that bounds CSI error vector $\mathbf{u}_{b,k}$
$\mathbf{E}_{t,s}$	matrix defining the shape and size of the ellipsoid that bounds CSI error vector $\mathbf{u}_{t,s}$
f_{D}	maximum doppler shift
f'	first-order partial derivative of f
$\mathcal{F}_{t,p}$	ellipsoid bounding CSI error vector $\mathbf{v}_{t,p}$
$\mathbf{F}_{t,p}$	matrix defining the shape and size of the ellipsoid that bounds CSI error vector $\mathbf{v}_{t,p}$
$g_b^\star$	optimal objective value of subproblem b in primal decomposition method
$g_t^\star$	optimal objective value of subproblem t in primal decomposition method
$\bar{g}_b^\star$	optimal objective value of inner maximization of $\boldsymbol{\lambda}_b$
$\bar{g}_t^\star$	optimal objective value of inner maximization of $\boldsymbol{\lambda}_t$
$\mathbf{g}_{t,p}$	MISO channel vector from secondary transmitter t to PU p
$\hat{\mathbf{g}}_{t,p}$	estimated MISO channel vector from secondary transmitter t to PU p

$\mathbf{h}_{b,k}$	MISO channel vector from BS b to user k
$\hat{\mathbf{h}}_{b,k}$	estimated MISO channel vector from BS b to user k
$\mathbf{h}_{t,s}$	MISO channel vector from secondary transmitter t to SU s
$\hat{\mathbf{h}}_{t,s}$	estimated MISO channel vector from secondary transmitter t to SU s
$\mathbf{H}_{b,k}$	MIMO channel matrix from BS b to user k
K	number of users
K_b	number of users served by BS b
$\mathcal{K}$	set of all users
$\mathcal{K}_b$	set of users served by BS b
$\bar{\mathcal{K}}_b$	set of users served by other BS than b
L_k	number of allocated streams for user k
$\mathcal{L}_k$	set of allocated streams for user k
m	iteration index for fixed-point iteration method
$\mathbf{m}_k$	transmit beamforming vector for user k
$\mathbf{m}_{k,l}$	transmit beamforming vector for stream l of user k
$\mathbf{m}_s$	transmit beamforming vector for SU s
$\bar{\mathbf{m}}$	all transmit beamforming vectors stacked into a column vector
$\bar{\mathbf{m}}_b$	transmit beamforming vectors of BS b stacked into a column vector
$\mathbf{M}$	all transmit beamforming vectors in the system stacked into a matrix
$\mathbf{M}_b$	transmit beamforming vectors of BS b stacked into a matrix
$\mathbf{M}_t$	transmit beamforming vectors of secondary transmitter t stacked into a matrix
$\bar{\mathbf{M}}_b$	stacked matrix of transmit beamforming vectors of BS b excluding the beamformer for stream (k,l)
n	iteration index for the subgradient update of dual variable $\mu_{b,k}$
n_k	noise sample for user k
$\mathbf{n}_k$	noise vector for user k
N_0	Gaussian noise variance
p^{tx}	square root of P^{tx}
p_b^{tx}	square root of P_b^{tx}
p_t^{tx}	square root of P_t^{tx}
P	number of PUs
P^{tx}	total transmission power of system

P_b^{tx}	Transmission power of BS b
P_t^{tx}	Transmission power of secondary transmitter t
$P_{\text{opt}}^{\text{tx}}$	optimal total transmission power of the system
$\mathcal{P}$	set of all PUs
$\mathcal{P}_{+}$	projection onto the set of nonnegative real numbers
$\mathcal{P}_{++}$	projection onto the set of positive real numbers
q	iteration index for the SCA method
$\mathbf{Q}_k$	transmit covariance matrix of user k
$\mathbf{Q}_{k,l}$	transmit covariance matrix for stream l of user k
$\mathbf{Q}_s$	transmit covariance matrix of SU s
$\hat{\mathbf{Q}}_t$	transmit beamforming vectors of secondary transmitter t stacked into a matrix
r	iteration index for subgradient method
r_k	rate of user k
r_s	rate of SU s
R_k	minimum rate target of user k
R_s	minimum rate target of SU s
S	number of SUs
S_t	number of SUs served by secondary transmitter t
$\mathcal{S}$	set of all SUs
$\mathcal{S}_t$	set of SUs served by secondary transmitter t
$\bar{\mathcal{S}}_t$	set of SUs served by secondary transmitters other than t
$t_{k,l}$	auxiliary variable associated with the SCA method
t_s	serving secondary transmitter for SU s
T	number of secondary transmitters
T_{F}	duration of uplink and downlink frames
$\mathcal{T}$	set of all secondary transmitters
u	iteration index for transmitter-receiver optimization step
$u_{b,k}$	subgradient evaluated at point $\chi_{b,k}$
$u_{b,k,l}$	subgradient evaluated at point $\chi_{b,k,l}$
$u_{t,s}$	subgradient evaluated at point $\mu_{t,s}$
$\tilde{u}_{t,s}$	subgradient evaluated at point $\nu_{t,p}$
$\mathbf{u}_{b,k}$	CSI error vector associated with channel $\hat{\mathbf{h}}_{b,k}$
$\mathbf{u}_{t,s}$	CSI error vector associated with channel $\hat{\mathbf{h}}_{t,s}$
$\mathbf{v}_{t,p}$	CSI error vector associated with channel $\hat{\mathbf{g}}_{t,p}$

$\mathbf{w}_{k,l}$	receive beamforming vector of stream l of user k
$\acute{\mathbf{w}}_k$	virtual uplink normalized receive beamforming vector of user k
$\grave{\mathbf{w}}_k$	virtual uplink unnormalized receive beamforming vector of user k
$\tilde{\mathbf{w}}_{k,l}$	normalized MMSE receive beamforming vector for stream l of user k
$\hat{\mathbf{w}}_{k,l}$	worst case MMSE receive beamforming vector for stream l of user k
$\bar{\mathbf{w}}_k$	unnormalized MMSE receive beamforming vector for user k
$\tilde{\mathbf{w}}_{k,l}$	unnormalized MMSE receive beamforming vector for stream l of user k
$\hat{\mathbf{W}}_k$	worst case MMSE receive covariance matrix of user k
x_k	information symbol for user k
$x_{k,l}$	information symbol for stream l of user k
x_s	information symbol for SU s
y_k	received signal of user k
y_s	received signal of SU s
$\mathbf{y}_k$	received signal vector of user k
z_s	noise sample for SU s
Z_0	noise plus interference variance

$\beta_{b,k}$	slack variable for user k in robust subproblem b
$\beta_{t,s}$	slack variable for SU s in robust subproblem t
γ_k	minimum SINR target of user k
γ_s	minimum SINR target of SU s
Γ_k	SINR of user k
$\Gamma_{k,l}$	SINR for stream l of user k
Γ_s	SINR of SU s
$\tilde{\Gamma}_{k,l}$	SINR for stream l of user k, assuming that MMSE receiver is used
$\delta_{b,k}$	dual variable associated with consistency constraint of local inter-cell interference variables
$\boldsymbol{\delta}_b$	stacked vector of dual variables associated with consistency constraint of local inter-cell interference variables in subproblem b
$\epsilon_{k,l}$	MSE of stream l of user k
$\tilde{\epsilon}_{k,l}$	MSE of stream l of user k assuming that MMSE receiver is used
η	cell separation parameter

$\bar{\eta}$	network separation parameter
$\lambda_{\max}(\mathbf{X})$	maximum eigenvalue of a symmetric matrix $\mathbf{X}$
$\lambda_{b,k}$	dual variable associated with $\chi_{b,k}$ in SINR constraint of subproblem b
$\lambda_{b,k,l}$	dual variable associated with $\chi_{b,k,l}$ in MSE constraint of subproblem b
$\lambda_{t,s}$	dual variable associated with $\chi_{t,s}$ in SINR constraint of subproblem t
$\boldsymbol{\lambda}_b$	dual variables associated with SINR constraints of subproblem b stacked into a column vector
$\boldsymbol{\lambda}_t$	dual variables associated with SINR constraints of subproblem t stacked into a column vector
$\mu_{b,k}$	dual variable associated with $\chi_{b,k}$ in inter-cell interference constraint of subproblem b
$\mu_{b,k,l}$	dual variable associated with $\chi_{b,k,l}$ in inter-cell interference constraint of subproblem b
$\mu_{t,s}$	dual variable associated with $\chi_{t,s}$ in inter-cell interference constraint of subproblem t
$\boldsymbol{\mu}_b$	dual variables associated with inter-cell interference constraints of subproblem b stacked into a column vector
$\boldsymbol{\mu}_t$	dual variables associated with inter-cell interference constraints of subproblem t stacked into a column vector
$\nu_{t,p}$	dual variable associated with $\phi_{t,p}$ of subproblem t
$\boldsymbol{\nu}_t$	dual variables associated with PU-specific inter-cell interference constraints of subproblem t stacked into a column vector
ρ	penalty parameter for the ADMM method
$\sigma^{(r)}$	step-size at iteration r in subgradient method
$\upsilon_{t,p}$	dual variable associated with $\phi_{t,p}$ of subproblem t
$\phi_{t,p}$	inter-cell interference power from secondary transmitter t to PU p
$\tilde{\phi}_{t,p}$	secondary transmitter t specific auxiliary variable associated with inter-cell interference from secondary transmitter t to PU p
$\boldsymbol{\phi}$	stacked vector of all PU-specific inter-cell interference variables
$\boldsymbol{\phi}_t$	stacked vector of PU-specific inter-cell interference variables associated with secondary transmitter t

$\bar{\boldsymbol{\phi}}_p$	stacked vector of inter-cell interference experienced by PU p from all secondary transmitters
$\bar{\boldsymbol{\phi}}_t$	stacked vector of all secondary transmitter t specific local PU-specific inter-cell interference variables
Φ_p	maximum aggregate interference power constraint from secondary transmitters to PU p
$\varphi_{t,p}$	slack variable associated with S-procedure method
$\chi_{b,k}$	inter-cell interference from BS b to user k
$\chi_{b,k,l}$	inter-cell interference from BS b to stream l of user k
$\chi_{t,s}$	inter-cell interference from secondary transmitter t to SU s
$\bar{\chi}_{b,k}$	square root of $\chi_{b,k}$
$\bar{\chi}_{b,k,l}$	square root of $\chi_{b,k,l}$
$\bar{\chi}_{t,s}$	square root of $\chi_{t,s}$
$\bar{\chi}_{b,k}^{b}$	BS b specific auxiliary variable associated with inter-cell interference from BS b to user k
$\bar{\chi}_{t,s}^{t}$	secondary transmitter t specific auxiliary variable associated with inter-cell interference from secondary transmitter t to SU s
$\boldsymbol{\chi}$	stacked vector of all inter-cell interference variables
$\boldsymbol{\chi}_t$	stacked vector of inter-cell interference variables associated with secondary transmitter t
$\boldsymbol{\chi}_b$	stacked vector of inter-cell interference variables associated with BS b
$\bar{\boldsymbol{\chi}}_b$	stacked vector of all BS b specific local inter-cell interference variables
$\bar{\boldsymbol{\chi}}_k$	stacked vector of inter-cell interference experienced by user k from other BSs
$\bar{\boldsymbol{\chi}}_s$	stacked vector of inter-cell interference experienced by SU s from other secondary transmitters
$\bar{\boldsymbol{\chi}}_t$	stacked vector of all secondary transmitter t specific local inter-cell interference variables
ω_k	slack variable for user k associated with S-procedure method
ω_s	slack variable for SU s associated with S-procedure method
$(\cdot)^{\mathrm{T}}$	transpose
$(\cdot)^{\mathrm{H}}$	complex conjugate transpose (Hermitian)

$(\cdot)^{\star}$	solution of an optimization problem
$\vert\mathcal{X}\vert$	cardinality of set $\mathcal{X}$
$\mathbf{X}^{-1}$	inverse of matrix $\mathbf{X}$
$\mathcal{CN}(0, N_0)$	complex Gaussian distribution with zero mean and variance N_0
$\mathcal{CN}(\mathbf{m}, \mathbf{C})$	complex circularly symmetric Gaussian vector distribution with mean $\mathbf{m}$ and covariance matrix $\mathbf{C}$
$\mathbf{I}_x$	identity matrix with dimension x
$\mathrm{diag}(\mathbf{x})$	diagonal matrix with elements of vector $\mathbf{x}$ on the main diagonal
$\mathrm{E}(\cdot)$	statistical expectation
$\log_2(\cdot)$	logarithm in base 2
$\log_e(\cdot)$	logarithm in base e
$\vert x\vert$	absolute value of scalar x
$\Vert\mathbf{x}\Vert_2$	Euclidean norm of vector $\mathbf{x}$
$\mathrm{tr}(\mathbf{X})$	trace of matrix $\mathbf{X}$
$\succeq$	generalized inequality in a proper cone
$\mathbb{R}$	set of real numbers
$\mathbb{R}_+$	set of nonnegative real numbers
$\mathbb{R}_{++}$	set of positive real numbers
$\mathbb{C}$	set of complex numbers
$\mathbb{R}_+^n$	set of nonnegative n-dimensional real vectors
$\mathbb{C}^{m\times n}$	set of $m \times n$ complex matrices

3G	third generation cellular systems
4G	fourth generation cellular systems
5G	fifth generation cellular systems
ADMM	alternating direction method of multipliers
BS	base station
CoMP	coordinated multi-point
CSI	channel state information
D2D	device-to-device
DL	downlink
DCP	difference of convex functions program
DPC	dirty-paper coding
FDD	frequency division duplex
GP	geometric program

HSPA	High-Speed Packet Access
IBC	interfering broadcast channel
IC	interference channel
IID	independent and identically distributed
KKT	Karush-Kuhn-Tucker
LMI	linear matrix inequality
LTE	Long-Term Evolution
LTE-A	Long-Term Evolution Advanced
MIMO	multiple-input multiple-output
MISO	multiple-input single-output
M-MIMO	multi-stream MIMO
MMSE	minimum mean square error
MSE	mean square error
PU	primary user
QoS	quality of service
SCA	successive convex approximation
SDP	semidefinite program
SDR	semidefinite relaxation
SNR	signal-to-interference-plus-noise ratio
SINR	signal-to-interference-plus-noise ratio
SISO	single-input single-output
S-MIMO	single-stream MIMO
SOC	second-order cone
SOCP	second-order cone program
SPMin	sum power minimization
SU	secondary user
SVD	singular value decomposition
TDD	time division duplex
UL	uplink
WCRX	worst case receiver
ZF	zero-forcing

Contents

1 Introduction

Since mobile data traffic is constantly growing, it is of the uttermost importance to enhance the capacity of mobile networks. Coordinated beamforming is a promising candidate to improve the performance of wireless communications systems, e.g., in terms of power or spectral efficiency, especially at the cell-edge area. This thesis studies practical coordinated beamforming strategies for cellular and cognitive radio networks.

This introductory chapter offers an overview of the topic by introducing the related background and reviewing the existing literature. In Section 1.1, the motivation for the use of coordinated beamforming is presented. Section 1.2 introduces the main steps in the evolution path from single-user multiple-input multiple-output (MIMO) communications to cooperative/coordinated multi-cell multi-user MIMO techniques. The concepts of joint processing and coordinated beamforming are described in Section 1.3. Section 1.4 discusses main network design objectives for coordinated beamforming. Section 1.5 reviews the previous and parallel work of coordinated beamforming in cellular and cognitive radio networks. Section 1.6 describes the goal for the thesis and its outline. Finally, the author's contributions to the publications are specified in Section 1.7.

1.1 Motivation

The use of the mobile internet started to boom after the introduction of easy-to-use touch screen devices, such as smartphones and tablets. It has been predicted that within the next ten years, mobile data traffic will increase 1000-fold compared to what is being experienced today [1, 2]. To meet this huge growth in traffic, next generation mobile networks, i.e., fifth generation (5G) [1–9], will need 1000 times more capacity than what the current third generation (3G), High-Speed Packet Access, and fourth generation (4G), Long-Term Evolution (LTE) [10] and LTE-Advanced [11], networks can provide [1, 2]. From a global perspective, increased research effort is being put on the development of future 5G networks [4, 5]. The main expectations for 5G networks are discussed and summarized in [5]. In short, there is an expectation of 1000 and 100 times higher area capacity and edge rates, respectively, compared with the current 4G technology. The aim for future peak data rates will be in the range of multiple tens of Gigabits per second (Gbps). In addition, roundtrip latency will need to be reduced by an order of magnitude from 4G. Therefore, it is clearly important to study and develop new technologies to meet the high requirements of future mobile networks. The most promising key elements/technologies in the evolution path toward and beyond 5G are increased bandwidth using higher frequencies (possibly millimeter waves), cell densification through smaller cells and increased spectral efficiency via advanced MIMO and interference coordination techniques [5]. The main focus of this thesis is on designing advanced MIMO and interference coordination techniques for future wireless communication networks. Advanced MIMO techniques can increase spectral efficiency significantly, if properly designed. However, without proper interference coordination between neighboring cells, inter-cell interference may limit the increase of spectral efficiency or even decrease system-level performance. In this respect, coordinated multi-point (CoMP) transmission, which combines advanced MIMO and interference coordination techniques, has been recognized as a powerful approach to improve the performance of cellular systems, especially at the cell-edge area, by controlling inter-cell interference [11–13]. CoMP transmission refers to a system wherein data transmissions are dynamically coordinated between multiple BSs in order to improve received signal quality and control generated interference for other users. CoMP can be seen as the latest evolution of MIMO communication, which started from single-user MIMO and evolved through multi-user MIMO to coordinated/cooperative multi-cell MIMO concepts [12, 14, 15], as depicted in Fig. 1. In the following section, the main steps in the evolution path from MIMO to CoMP are summarized.

1.2 From MIMO to CoMP

Traditionally, the performance of a single-antenna communication link, i.e., a single-input single-output (SISO) system, is improved by increasing either the transmission power or the bandwidth. However, it has been shown that the capacity of a communication link can be substantially increased without extra power or extra bandwidth by using multiple antennas at the transmitter and the receiver [16–18]. The achievable rate scales linearly with the minimum number of transmit and receive antennas in ideal rich scattering channel conditions [17, 18].

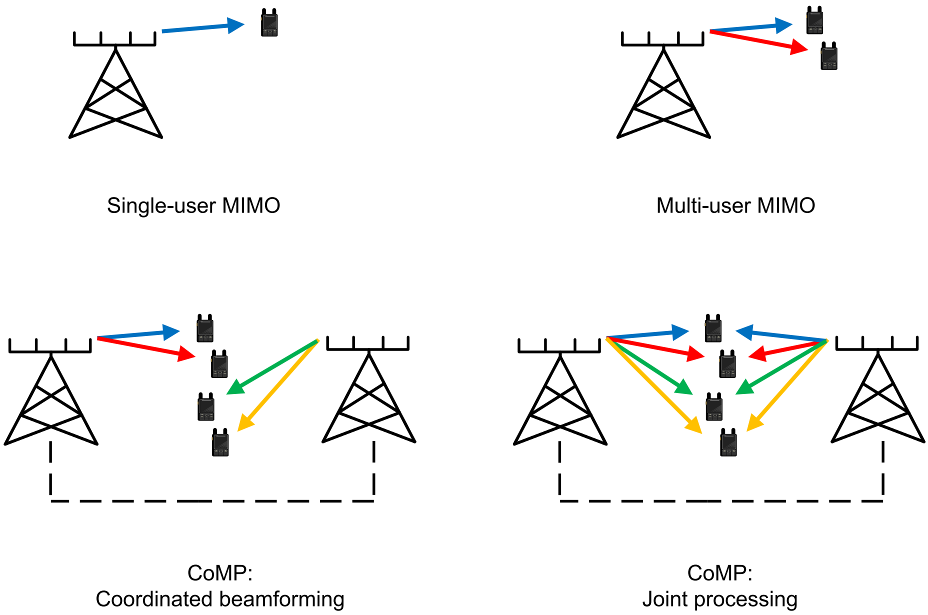

Fig 1. Main evolution steps from MIMO to CoMP.

In general, there are three kinds of gains available in a (single-user) MIMO system, i.e., diversity gain, array gain and multiplexing gain. The diversity and array gains are mostly intended to improve the reliability of a communication link, whereas the multiplexing gain aims to increase spectral efficiency. Diversity gain prevents drastic fluctuations of the received signal-to-noise-ratio (SNR) and is obtained by receiving or transmitting independently faded copies of the same signal. Array gain, which improves the average received SNR, is achieved by coherently combining the desired signal over multiple receiving or transmitting antennas. The most efficient way to increase data rate is to provide multiplexing gain by transmitting multiple spatially separable data streams at the same time and frequency slot. The available gains in a single-user MIMO system are summarized in Fig. 2.

The design and performance of a MIMO system is greatly influenced by the availability of channel state information (CSI) at the transmitter. The knowledge of CSI at the receiver is presumed by default. Diversity and multiplexing gains can be achieved without CSI knowledge at the transmitter, as proposed in [17, 19–21]. A study of optimal trade-off between diversity and multiplexing gains has

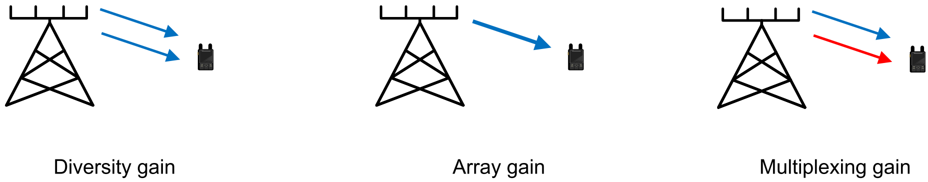

Fig 2. Gains in single-user MIMO system.

been provided in [22]. A remarkably simple diversity technique called Alamouti code was proposed in [19]. It achieves optimal diversity and multiplexing order in a simple case of two transmit and one receive antennas. Due to its simplicity, it has been adopted for many wireless systems standards. In the case of having CSI both at the transmitter and receiver, the MIMO channel can be turned into parallel independent SISO channels through singular value decomposition (SVD) of the channel matrix. The capacity achieving communication strategy is to use the right and left singular vectors of the channel matrix as transmit precoders and receive filters, respectively, and allocate the total transmission power to the independent SISO channels using a water-filling principle based on the eigenvalues of the channel matrix [18].

The linear scaling of capacity in a single-user MIMO system is largely based on the assumption of a rich scattering environment. Thus, the capacity is limited by the communication channel. In terms of a cellular system, base stations (BSs) can be equipped with large antennas arrays, however, the size of a user terminal is physically more limiting. Hence, the capacity in a single-user MIMO system is limited by the number of antennas at the user terminal. To overcome the propagation channel limitation and take advantage of multiple BS antennas, multi-user MIMO communications can be applied. There are several benefits of multi-user MIMO over single-user MIMO communications. For example, challenging per-user channel conditions, such as poor scattering channels, is no longer a fundamental problem. Moreover, (multi-user) spatial multiplexing gain can be obtained without the use of multiple antennas at the user terminal. Since users cannot cooperate in a multi-user MIMO environment, a new type of interference is introduced, i.e., inter-user interference. This interference is referred to intra-cell interference in the context of cellular networks. Due to non-cooperating users, transmitter side processing is emphasized to improve the performance of a multi-user MIMO system. Thus, the availability of CSI at the transmitter plays a more critical role for the multi-user MIMO communication than for the single-user MIMO case.

In a multi-user MIMO system (i.e., MIMO broadcast channel), the capacity is characterized by a capacity region. It is given by a set of achievable rates that can be simultaneously achieved with an arbitrary small joint probability of error. The capacity-achieving transmission strategy for a MIMO broadcast channel is known as dirty paper coding (DPC) [23–25]. This scheme is based on a successive encoding strategy that completely cancels out interference at the transmitter side without requiring extra transmit power. The idea behind DPC was first introduced in [23], and further extended to the multi-user MIMO setting in [24]. Finally, it was shown in [25] that DPC is an optimal transmission scheme for the MIMO broadcast channel. Due to its high computational complexity, DPC is very challenging to be implemented in practice, especially when the number of users is high.

In general, sub-optimal linear transmission and reception strategies allow a reasonable balance between complexity and performance. A conceptually simple linear strategy is zero-forcing (ZF) beamforming, which is designed to completely avoid inter-user interference [26]. This scheme has a practical advantage since the beamforming design and power allocation are decoupled. A regularized ZF strategy was also introduced in [26] where limited amount of inter-user interference is allowed. An extension of ZF scheme to the case of multiple antenna users was provided in [27–29]. It was shown in [30] that ZF strategy can asymptotically approach the performance of DPC if the number of users is large. However, in practical scenarios with a moderate number of users, ZF strategy suffers from power penalty making it highly sub-optimal. Moreover, ZF beamforming scheme is applicable only when the number of transmit antennas is greater or equal than the aggregate number of receiver antennas in the system.

By allowing a small amount of inter-user interference and jointly optimizing the linear beamformers and powers, the performance of a multi-cell MIMO system can be improved. In this respect, linear beamformers can be optimized according to certain performance criteria while satisfying some practical constraints [31–42], e.g., sum rate or minimum rate maximization with transmission power constraints or transmission power minimization with user-specific rate constraints. In general, convex optimization methods have been found as powerful tools for solving many problems in wireless communications [43, 44], especially linear beamforming design problems [31–42]. To optimize linear beamformers properly, the CSI of all active users need to be acquired.

In a multi-cell MIMO network where each cell operates independently, the performance of multi-user MIMO techniques may be degraded due to inter-cell interference that occurs when the same radio resources are reused in nearby cells. Inter-cell interference that is experienced by each user constantly varies since it depends on the transmissions from neighboring cells. Thus, the signal-to-interference-plus-noise ratio (SINR) of a user can change significantly, depending on the time and the user's location in the network. Inter-cell interference limits the performance, especially for cell-edge users, thus leading to performance discrepancies between different users in the network. In order to mitigate the effect of inter-cell interference, designing advanced interference coordination techniques is of uttermost importance. In this regard, the key idea is to allow BSs to collaborate and share information between each other.

It has been shown that CoMP is a promising candidate for efficient interference coordination [12, 13]. The idea is to control inter-cell interference and improve network performance by allowing nearby BSs to cooperate/coordinate when designing their transmission/reception parameters. The use of CoMP is especially beneficial for cell-edge users, which usually suffer from low data rates. CoMP can be divided into transmission and reception parts, i.e., downlink and uplink communications, respectively. Here, the focus is on CoMP transmission for downlink. CoMP transmission usually employs beamforming (i.e., precoding) to manage interference. The concept of CoMP has been already included in LTE-A specifications [13]. At a high level, CoMP transmission techniques can be classified into two main categories, namely joint processing and coordinated beamforming [12, 13]. Joint processing refers to full cooperation, where user payload data and CSI are both shared between BSs. In coordinated beamforming, coordination can be interpreted as a reduced level of cooperation, where only CSI is shared among BSs and user data is communicated only to its serving BS. Both techniques can be implemented either centralized or decentralized way. Centralized algorithms require knowledge of the channels between all BSs and all users in the system, i.e., global CSI. Decentralized approaches rely on the availability of local CSI, i.e., knowledge of the channels between a BS and all users in the system. In addition to local CSI, BSs may exchange limited amount of information between each other. The categorization of CoMP techniques is

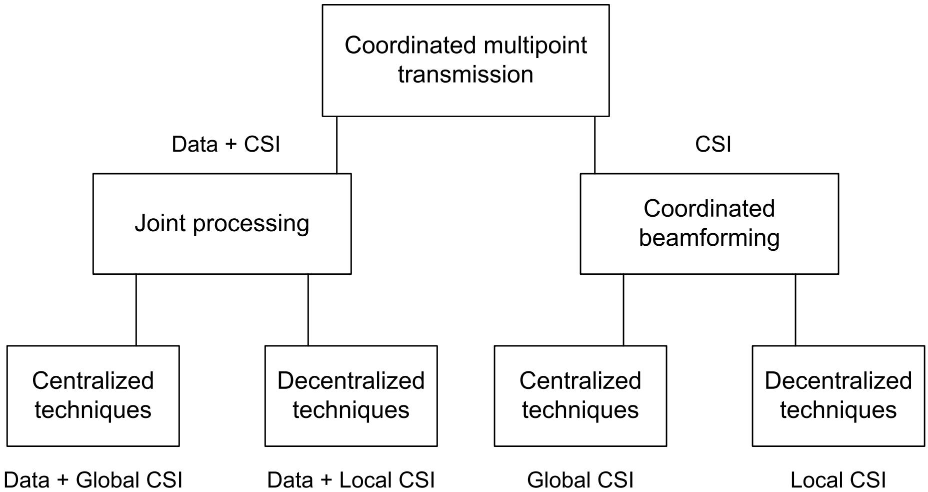

Fig 3. Categorization of CoMP.

shown in Fig. 3. In the following section, the concepts of joint processing and coordinated beamforming are discussed in detail.

1.3 Joint processing and coordinated beamforming

In joint processing, each data stream can be coherently transmitted over multiple cooperative BSs, as depicted in Fig. 1. This concept is also known as network MIMO and has been intensively studied over a decade [12, 45–55]. The operation of joint processing is based on multiple premises, i.e., the sharing of user data among all BSs, the availability of global or local CSI, as well as full synchronization of signals transmitted from different BSs. Joint processing can be interpreted as a single transmitter with distributed clusters of antennas serving all the users in the network. Consequently, a multi-cell environment is turned into a benefit by transmitting useful data from all BSs through the channels that are considered to be interfering in a non-cooperative system. It is worth mentioning that there still exists inter-stream and inter-user interferences in the networks with fully cooperative BSs. However, these interferences can be managed by proper joint processing beamforming techniques, which may aim to optimize a practical system design target while guaranteeing certain constraints set on the BSs and users. Joint processing can be divided into centralized and decentralized techniques [12, 53–55]. Centralized algorithms rely on user data and local CSI sharing among the BSs via backhaul. As a result, each BS has access to the data of all users and global CSI. Alternatively, the availability of global CSI can be achieved by each BS sending its local CSI to a central controlling unit via backhaul. Decentralized algorithms aim to reduce backhaul signalling by exploiting only local CSI without the need to share it with other BSs. However, a small amount of information exchange can be allowed via backhaul and/or over-the-air signaling. By using decentralized algorithms, the cost is a degradation of performance. Note that the amount of user payload data sharing via backhaul is still the same as in the centralized case. In the literature, most of the proposed joint processing techniques are centralized. The implementation of joint processing techniques is challenging due to the requirement of carrier phase synchronism for the cooperative BSs and the large amount of required backhaul signaling. From an implementation point of view, coordinated beamforming approaches are more appealing than joint processing ones. This work concentrates solely on coordinated beamforming strategies.

In coordinated beamforming, each data stream is linearly precoded in the spatial domain and transmitted from a single BS, as illustrated in Fig. 1. The transmissions of other data streams in one's own cell and other cells are treated as interference. Thus, inter-stream, intra-cell, and inter-cell interferences exist. To control these interferences, precoded data transmissions may be jointly designed among the coordinated BSs such that a network design target is achieved while providing guaranteed Quality of Service (QoS) to users and satisfying practical power constraints imposed on BSs. In coordinated beamforming, the carrier phase synchronism between the BSs is not required, and a lower amount of data needs to be communicated via backhaul compared to the joint processing strategies. For example, user payload data is communicated only for the serving BS. The performance of coordinated beamforming schemes rests on the availability of channel knowledge at the BSs. For centralized algorithms, knowledge of global CSI is usually required. Global CSI can be achieved via the same means as that described for the joint processing case, i.e., each BS communicating its local CSI to the central controlling unit or sharing it directly with all BSs.

A common assumption for decentralized algorithms is that, at least, local CSI is available at each BS, and coordination is performed directly between the BSs via low-rate backhaul links, possibly along with over-the-air (pilot) signaling. The methods for acquiring local CSI depend on the employed duplexing mode. In those systems operating in a time-division duplexing (TDD) mode, the reciprocity of the uplink and downlink channels can be exploited since the used frequency bands are the same for both directions. In this case, it is possible to use antenna-specific uplink pilot signaling, also known as channel sounding [56]. Each user transmits known training signals that are used at the BS side to estimate the channels. In those systems based on frequency-division duplexing (FDD), each user estimates its channel and sends the information, usually in a quantized form, to the BS via a feedback channel. In general, TDD-based CSI acquisition is more resource efficient compared to the FDD-based one [57]. Antenna-specific uplink pilots have already been adopted in the LTE-Advanced standards [11]. In the case of single-antenna users, having local CSI at each BS usually enables the use of decentralized techniques. However, decentralized processing becomes more problematic if the users are equipped with multiple receive antennas. This is due to the fact that even if the channels from the BS to neighboring cells' users are known via antenna-specific uplink pilots, the receivers there users are employing may not be. In other words, using antenna-specific pilots, there is no information available on the users' receivers at the BSs.

A simple strategy to convey implicit knowledge of the user's receiver to the BS is to use precoded uplink pilots. More precisely, each user employs its receiver as a precoder for uplink pilot signaling observed by each BS. Instead of knowing a given user's receiver explicitly, implicit information about the receiver, also known as the effective channel, is available at each BS, i.e., the user channel multiplied by the user's receiver. Precoded uplink pilots can carry more information to the BSs than antenna-specific pilots. The use of precoded pilots can potentially lead to improved system performance since the generated interference can be coordinated more efficiently by the BSs. In addition to uplink pilots, downlink pilot signaling can also be used to aid decentralized design. In this respect, downlink demodulation pilots, which are precoded similarly as user data, can be used to provide an effective CSI for users to facilitate data reception. Downlink demodulation pilot strategy has already been specified for LTE-Advanced [11]. In addition to pilot signaling, decentralized design may require that a limited amount of information is exchanged between the neighboring BSs via backhaul links. Decentralized schemes are often more practically realizable than centralized ones are due to possibly reduced signaling overhead, simpler network structure (i.e., no central controlling unit needed) and lower computational requirements per processing unit.

If not designed properly, however, decentralized coordinated beamforming schemes may cause extra delays and increase signaling overhead in the system. This thesis designs practical decentralized coordinated beamforming algorithms where delay and signaling aspects are also taken into account. Unlike most of the existing decentralized approaches, the proposed algorithms can prevent long delays and notably reduce signaling overhead while still obtaining performance close to that of centralized algorithms.

1.4 Network design objectives for coordinated beamforming

Coordinated beamforming has been intensively studied for a variety of practical network design objectives such as sum power minimization (SPMin) [33, 58–63], minimum rate maximization [64–66], sum rate maximization [56, 67–71] and energy efficiency maximization [72–75]. Other widely studied network optimization problems are mean square error (MSE)-based design problems [76–80]. In the following discussion, the main three design objectives are introduced and discussed in detail.

In the classical SPMin problem [58], the goal is to minimize the sum transmission power of the BSs while guaranteeing the minimum data rate targets to all active users in the system. This system design objective is of practical interest for wireless applications, where there are stringent data rate and delay constraints for active users. Different users may get different rate targets depending on the application or operator settings. Note that when minimizing total transmitted power in the network, the overall interference is implicitly reduced as well. Among the aforementioned network optimization problems, the SPMin problem is the simplest one to solve in terms of computational complexity, due to the fact that it can be usually cast as a convex problem in the case of single-antenna users. The problem can be cast as a convex optimization problem in a multi-cell multi-user MISO setting [59, 60]. In the case of a convex problem, an optimal solution can be found via efficient numerical methods [81]. In this respect, the SPMin problem can also be seen as a good starting point for finding solutions to other (more complex) network optimization problems. For example, it can be used as a part of the algorithms that solve the minimum rate maximization and sum rate maximization problems as shown in [82] and [52], respectively. The SPMin problem is also a special case of the weighted energy efficiency maximization problem.

In general, the SPMin problem can be infeasible when the total number of (single antenna) users in the entire coordinated system is greater than the number of transmit antennas at each BS. In this setting, the network can be interference limited, meaning that when increasing the transmit power the increase of the generated interference blocks the increase of system performance. However, if the number of users is equal or less than the number of antennas in each BS, the system is always feasible, provided that the elements of the user channels are independent and there is no maximum transmit power constraints for BSs. In interference limited scenarios, the higher the rate targets or the number of users, the higher will be the probability that the problem becomes infeasible. If infeasibility is detected, the problem can be made feasible by letting admission control relax the rate targets or inactivate the critical users that compromise the feasibility [83]. In Section 2.1, further discussion is provided on the feasibility of the SPMin problem in a multi-cell multi-user MISO system. The original SPMin problem formulation does not involve practical transmit power constraints [58]. However, it is straightforward to add power constraints to the SPMin problems. For example, per-antenna power constraints were involved in a single-cell multi-user MISO system in [35]. Transmit power constraints are fairly easy to handle since they can be cast as convex constraints (e.g., SOC constraints). Thus, the original problem structure does not radically change from a mathematical perspective. In addition, per-BS and per-antenna power constraints are separable between BSs and hence, they naturally lend themselves to decentralized implementation if necessary. Nevertheless, the power constraints do affect the feasibility of the SPMin problem. The lower the maximum power constraints are, the higher is the probability that the problem is infeasible.

The objective of maximizing the minimum rate of active users with transmit power constraints at the BSs is fair for users since each user is getting the same rate at the optimal solution. This problem is also known as rate balancing or common rate maximization. The rate balancing design seems suitable for traffic scenarios where many users have similar constraints for data rates and latency. In a general setting, this problem is feasible. However, it is usually more difficult to solve than the SPMin problem. For example, the problem is quasi-convex for a multi-cell multi-user MISO system. In that setting, a classical way of optimally solving the problem is to use an iterative bisection method, where the feasibility of a convex problem (i.e., SPMin problem) is checked at each iteration [82]. In general, the cost of fairness is highly sub-optimal sum rate performance since equalizing the data rates among users leads to a beamforming design where less resources (i.e., transmit power) are given to the users with good channel and interference conditions, and more resources are given to the users with bad conditions. However, priority weights can be added to the rates of different users to improve the sum rate performance at the expense of fairness.

In the standard sum rate maximization problem, the aim is to maximize the sum of the users' rates while satisfying the maximum transmission power constraint at each BS. In principle, this problem is not fair to users since most of the resources are given to the users with good channel and interference conditions. In contrast, users with bad conditions may get very low data rates. However, fairness can be included by adding priority weights to different users. Moreover, fairness can be included in scheduling, e.g., using different types of proportional fair scheduling algorithms [84]. In general, the weighted sum rate maximization problem is always feasible if there are no given minimum QoS targets for users. This network design objective is most suitable for wireless applications where there are no strict delay or rate constraints for users. In order to support stringent rate or delay requirements, per-user QoS constraints can be added. This comes at the cost of a more difficult problem structure and possible infeasibility. Weighted sum rate maximization is, in general, a non-convex problem, even in the case of single-antenna users. Thus, it cannot be solved in its original form. There are many algorithms proposed, where the problem is first reformulated/approximated and then solved efficiently. In general, the proposed solutions cannot guarantee global optimality since the original problem is non-convex. It is worth mentioning that in some iterative sum rate maximization algorithms, the SPMin problem is solved as an inner optimization step [52, 85].

Due to its importance, the sole focus of this thesis is on coordinated beamforming for SPMin with user-specific rate constraints. In this regard, the main literature is reviewed in the next section.

1.5 Literature review

This section provides a detailed review of the existing literature associated with the scope of this thesis. Coordinated beamforming techniques for SPMin in cellular and cognitive radio networks are surveyed in Sections 1.5.1 and 1.5.2, respectively.

1.5.1 Coordinated beamforming for SPMin in cellular networks

One of the earliest coordinated beamforming approaches was introduced in [58], where a downlink beamformer design problem for minimizing the multi-cell sum power subject to the received SINR constraint per each single antenna user was solved by using uplink-downlink SINR duality. The optimality of this approach was proved for a single-cell case in [86, 87]. Alternative optimal approaches were proposed in [31] and [33]. The solutions were based on convex optimization methods called semidefinite programming (SDP) and second order cone programming (SOCP), respectively. If an optimization problem could be formulated as a convex problem, it could be solved via efficient numerical methods with a guarantee of global optimality [81]. Standard convex optimization solvers have been developed to solve various forms of convex problems. One such solver is CVX [88], which is also used to produce the numerical results in this thesis. Some of the most common convex formulations include SDP, SOCP and geometric programming (GP) [81].

The single-cell method in [33] can be readily extended to the centralized multi-cell setting as shown in [59, 60]. This observation was utilized to show that uplink-downlink duality can be exploited to produce an optimal solution for the multi-cell case [59]. The iterative approach proposed in [59] naturally leads to a decentralized implementation for TDD-based systems. In general, decentralized uplink-downlink duality- based approaches usually need to converge before they can satisfy the user-specific SINR constraints. By employing these iterative schemes may cause extra delay and increased signaling overhead on the system. Practical decentralized approaches, which can reduce delay and signaling overhead, have been proposed in the author's contributions [60, 61, 63], where feasible beamformers can be obtained at each iteration by relying on scalar backhaul information exchange between the BSs. In these algorithms, a network-wide multiple-input single-output (MISO) transmit beamforming design was turned into independent BS-level designs via dual and primal decomposition methods. In all the algorithms, each local beamforming design was iteratively managed via a scalar backhaul information exchange between the BSs, leading to a network-wide solution. Inspired by [60, 61] other decentralized algorithms were proposed in [89, 90], wherein the beamforming designs were based on an alternating direction method of multipliers (ADMM) method.

The problem of multi-cell coordination evolves further when the users employ more than one receive antenna. In this case, each user may be allocated with one (i.e., single-stream MIMO) or multiple data streams (i.e., multi-stream MIMO). Each of the streams can be distinguished by a dedicated linear receive beamformer. Having multiple receive antennas per user, the SPMin problem is not jointly convex in transmit and receive beamformers [91]. Linear transceiver design algorithms are proposed in [62, 92–95] and [91, 96] for both single-cell and multi-cell MIMO systems, respectively. All these algorithms are inherently centralized, requiring a central processing unit for their transmit and receive beamforming designs. Since the non-convexity of the original problem, global optimality cannot be guaranteed for the proposed solutions.

In [96], a linear uplink transmit and receive beamforming design was proposed for the SPMin with per-user SINR constraints in a multi-cell single-stream MIMO system. Receive and transmit beamformer weights with minimized powers were resolved with the aid of an uplink-downlink duality concept by repeatedly solving a four-step optimization process. The same idea is also applicable to downlink communication [96]. In [91, 92, 94], linear transceiver design algorithms were proposed for SPMin with per-stream SINR constraints in a multi-stream MIMO system. In [91], the sum power is guaranteed to converge by consecutively optimizing the transmit and receive beamformers. The uplink-downlink duality-based MISO algorithm in [87] was generalized to the multi-stream MIMO case in [92]. In [94], the same problem as considered in [92] was solved, but with a weighted objective function. Sum power minimization with per-user and per-stream MSE constraints was studied for multi-user MIMO systems in [76, 97, 98] and [76], respectively. However, there is no direct mapping between these MSE constraints and per-user rate constraints in multi-stream MIMO systems. In [93], the per-user rate constraints of the SPMin problem were approximated with the aid of a MSE-based reformulation. Since this approximation is not necessarily tight, the constraints are not exactly equivalent to per-user rate constraints, thus yielding higher achieved rates than necessary and consequently sub-optimal sum power.

Sum power minimization with per-user rate constraints was considered for a single-cell MIMO system in [62, 95]. In [95], each iteration of the proposed algorithm consists of the optimization of uplink powers via GPs, while the optimization of uplink and downlink receive beamformers via the minimum MSE (MMSE) criterion. In [62], a gradient-based algorithm with linear transmit and receive beamformers was proposed. In this scheme, the main idea is to divide per-user rate targets into per-stream rate targets and find the optimal per-stream rates. This optimization procedure is combined with the alternating updates of transmit and receive beamformers. It is straightforward to extend the aforementioned single-cell MIMO algorithms to a centralized multi-cell scenario. However, there remains a lack of decentralized coordinated beamforming algorithms for the SPMin problem in a multi-cell MIMO system.

The SPMin problem becomes more complicated for a decentralized implementation since global CSI is not available at each BS. In a decentralized processing mode, each BS should attempt to control the inter-cell interference seen via the receive beamformers of the users that are served by the neighboring BSs. Here, a problem arises that even if the channels from the BS to the neighboring cells' users are known, the receivers they are employing may not be known. Most of the linear transmitter and receiver design algorithms proposed in the literature do not generally consider practical signaling strategies for distributed implementation. Instead, the focus is mainly on optimization designs rather than studying practical implementation strategies with the goal to limit signaling overhead. To facilitate decentralized processing, different pilot and backhaul signaling strategies were recently proposed in [56] for the weighted sum rate maximization problem. These strategies are designed for TDD-based systems where the reciprocity of downlink and uplink channels can be exploited. The author's contributions in [99] considered decentralized beamforming algorithms in multi-cell multi-stream MIMO systems by exploiting a combination of pilot and backhaul signaling.

Perfect CSI was presumed for the design of the aforementioned algorithms. In practice, however, only imperfect CSI can be made available at each BS. If imperfect CSI is not taken into account in the system optimization, per-user

QoS constraints cannot usually be satisfied. In order to guarantee the QoS constraints, the worst case robust optimization methods can be applied where the CSI errors are assumed to lie in a bounded region. In this setting, the minimum power beamforming problem is non-convex, even for the multi-cell MISO case. Many robust designs that approximate the non-convex problem with a convex one have been proposed, such as [89, 100–104]. In [100–102], convex approximations are achieved by approximating the non-convex constraints by tighter convex constraints. Globally optimal solutions cannot be guaranteed due to the restrictive nature of the approximations. In [89, 103, 104], a semidefinite relaxation (SDR) method was used to achieve a convex approximation of the problem. In this case, a non-convex feasible solution set is approximated by a larger convex set. If the resulting transmit covariance matrices are rank-one, then the achieved solution is also globally optimal for the original non-convex problem [103]. Most of the proposed approaches assume a single-cell system, thus the algorithms are inherently centralized. Recently, decentralized robust algorithms were proposed for multi-cell MISO systems in [102] and [89]. The dual decomposition-based approach in [102] is inherently sub-optimal. In [89], the proposed algorithm is based on ADMM, and it is globally optimal if the obtained transmit covariance matrices are all rank-one. An alternative decentralized algorithm based on primal decomposition was proposed in the author's contribution [105].

1.5.2 Coordinated beamforming for SPMin in cognitive radio networks

Cognitive radio is a promising approach for effectively utilizing the radio spectrum by allowing cognitive secondary users (SUs) to access the bandwidth of the licensed primary users (PUs) [106, 107]. Many of the traditional cognitive radio approaches are designed to exploit the spectrum holes of the licensed band [108]. However, higher spectrum efficiency is provided in underlay spectrum sharing cognitive radio networks where the primary network allows the secondary network to access the occupied primary bandwidth, provided that the generated interference toward PUs is under a tolerable threshold [109, 110]. Within this interference limitation, a secondary network can optimize its own system performance. In this respect, multiantenna beamforming is seen as a promising approach to provide efficient spectrum usage while satisfying the PU specific interference power constraints since the generated interference can be spatially controlled [111]. Recent achievements in cellular beamforming, especially in coordinated beamforming (see Section 1.5.1), have evoked an interest in extending these solutions to spectrum sharing cognitive radio networks.

Extending cellular beamforming approaches to cognitive radio networks requires introducing additional constraints to the maximum allowed interference levels experienced by the PUs [111]. Recently, cognitive beamforming approaches have been widely studied with various secondary network optimization objectives, e.g., sum power minimization [65, 112–120], sum rate maximization [121–124] and minimum rate maximization [125–127]. Cognitive multicast MISO beamforming strategy was studied in [65, 114]. Convex optimization and uplink-downlink duality based beamforming solutions were proposed for a cognitive radio network with a single secondary and primary transmitter in [113, 115] and [112, 113, 115], respectively. In [116], [115] was extended to the cognitive MISO interference channel (IC), i.e., a cognitive radio network with multiple secondary/primary transmitter-receiver pairs. Most of the aforementioned cognitive beamforming approaches are inherently centralized. Hence, they require a central controlling unit with global CSI for the secondary network coordination in a general multi-cell multiuser cognitive radio network setting.

In [126], minimum power beamformers were solved as an intermediate result of the original rate balancing problem in the cognitive MISO IC. It was shown that the centralized problem could be cast as an SOCP and solved efficiently. In addition, the problem was solved in a decentralized manner via a two-level algorithm, where the outer and inner optimizations were solved using a subgradient method and an uplink-downlink duality based approach, similar to that in [59], respectively. The outer optimization requires limited backhaul signaling between secondary transmitters, whereas the inner optimization requires real physical transmissions and receptions along with some over-the-air signaling. As discussed in Section 1.5.1, employing decentralized uplink-downlink duality based algorithms may cause extra delay and increased signaling overhead. In [63, 119], decentralized beamforming algorithms were proposed for the cognitive interference broadcast channel (IBC), where each transmitter serves multiple simultaneous users. In the author's contribution [63], the proposed algorithm was based on primal decomposition. An ADMM-based approach was developed in [119]. In these algorithms, it is possible to provide feasible beamformers at intermediate iterations. Consequently, long delays and increased signaling overhead can be avoided at the cost of sub-optimal performance by stopping the algorithms after a fixed number of iterations. In the case of multiple antenna users, a centralized single-cell MIMO beamforming strategy was proposed in [120]. This scheme can be seen as an extension of the cellular algorithm proposed in [91] for the cognitive radio networks.

The aforementioned algorithms require perfect CSI in order to operate properly. As discussed in the cellular case in Section 1.5.1, CSI is imperfect in practice, mainly due to errors in channel estimation and quantization. If the imperfections in the CSI are not taken into account in the cognitive beamforming design, there may be significant performance degradation and violation of the QoS constraints for the secondary network. In the cognitive radio literature, CSI uncertainty is usually modeled by bounding all the error realizations with a known region (e.g., spherical or ellipsoidal) [125] or assuming that the error realizations are drawn from a known distribution [128, 129]. Various cognitive MISO beamforming optimization problems with the former error modeling approach were handled by worst-case optimization in [117, 118, 123, 125, 129–133]. Single-cell and multi-cell cognitive radio networks were considered in [117, 118, 123, 125, 128, 129, 131] and [129, 130, 132, 133], respectively. All these algorithms are centralized except for the one in [132]. In [132], the sum MSE was minimized in an underlay cognitive radio network with imperfect CSI between secondary transmitters and PUs. However, perfect CSI was assumed between secondary transmitters and the SUs. The focus in this thesis is on the SPMin via the worst-case optimization, as the QoS constraints need to be satisfied for all error realizations. Beamforming designs wherein this non-convex problem is reformulated as a convex one were proposed in [117, 118, 125, 133]. In [117], the problem is approximated conservatively leading to sub-optimal algorithms. In [118, 125, 133], the proposed algorithms use the standard SDR method for the convex approximation. Global optimality is guaranteed for those cases when the solution of the approximated problem is rank-one. It was shown in [133] that rank-one solutions can always be guaranteed for the cognitive interference channel, i.e., where multiple secondary and primary transmitter-receiver pairs co-exist. All the proposed power minimization algorithms in [117, 118, 125, 133] are centralized. In the author's contribution [134] an ADMM-based robust decentralized algorithm was proposed for the cognitive multi-cell MISO system. In the case of multi-antenna users, a robust MIMO beamforming algorithm was proposed in [120] for a cognitive single-cell case.

1.6 Aims and outline of the thesis

The aim of this thesis is to develop coordinated beamforming techniques for multi-antenna cellular and cognitive radio networks. In particular, decentralized algorithms are proposed since they are often more applicable to practical implementation than centralized ones. The main focus of this work is on a practical network design where the objective is to minimize the sum transmission power of the system while providing a guaranteed data rate for each active user. The starting point of the work is a multi-cell multi-user MISO system with an assumption of perfect local CSI at the BSs. This scenario is extended by taking into account some special features of the wireless systems, such as multi-antenna users, imperfect CSI at the transmitters, and a two-tier cognitive radio network architecture. The performance of the proposed coordinated beamforming techniques is evaluated in simplified multi-cell environments via Matlab-based computer simulations. In order to demonstrate possible performance gains, the proposed algorithms are compared with state-of-the-art techniques.

This thesis is written as a monograph for the sake of clarity and coherence. Most of the contributions and results have been published in ten original publications, including four published journal papers [60, 61, 63, 105], one submitted journal paper [99] and five published conference papers [134–138]. To form a coherent piece of work, the presentation of the original contributions was modified accordingly, and some new numerical results were added.

Chapter 2 is mainly founded on [60, 61, 63, 105, 135, 136]. Novel decentralized coordinated beamforming algorithms are proposed for the SPMin problem in a cellular MISO network. First, primal and dual decomposition-based algorithms are proposed with the assumption that local CSI at each BS is perfect. Then, the case of imperfect local CSI is considered, and a primal decomposition-based algorithm is introduced. The sum power performance of the proposed algorithms is examined via numerical examples in a simplified cellular environment.

The results of Chapter 3 rest on [99, 137, 138]. In addition to a centralized solution, two decentralized coordinated beamforming algorithms are proposed for the SPMin problem with per-user rate constraints in a cellular MIMO system. CSI acquisition is assumed to be error-free. To facilitate decentralized implementation, the proposed algorithms exploit a combination of pilot signaling and scalar backhaul information exchange between the BSs. The algorithms are numerically evaluated in terms of sum power under different system settings.

Chapter 4, part of which has been presented in [63, 134] considers a MISO cognitive radio network, where primary and secondary users share the same spectrum. Spatial domain processing, i.e., coordinated beamforming, is employed to keep the generated interference from the secondary network toward PUs below a predefined threshold while guaranteeing a minimum rate target for each SU. Specifically, decentralized coordinated beamforming algorithms are proposed for the sum power minimization of secondary network with additional constraints imposed on the PUs. Both perfect and imperfect local CSI at the transmitter cases are considered. Numerical evaluation is conducted to show the effectiveness of the proposed algorithms.

In Chapter 5, conclusions are drawn and future research directions are discussed.

The main contributions of this thesis are summarized as follows.

– Chapter 2 [60, 61, 63, 105, 135, 136]: Decentralized coordinated beamforming algorithms for the SPMin problem in multi-user MISO cellular networks.
– Chapter 3 [99, 137, 138]: Centralized and decentralized coordinated beamforming algorithms for the SPMin problem in multi-user MIMO cellular networks.
– Chapter 4 [63, 134]: Decentralized coordinated beamforming algorithms for the SPMin problem in multi-user MISO cognitive radio networks.

1.7 Author's contributions to the publications

The author of this thesis has contributed to twenty-seven papers altogether [60, 61, 63, 84, 99, 105, 134–154]. For consistency, the thesis is mainly based on ten original papers, including four published journal papers [60, 61, 63, 105], one submitted journal paper [99] and five published conference papers [134–138]. The author had the main responsibility for creating the ideas, performing the analysis, deriving the mathematical algorithms, developing the Matlab-based simulation software, conducting the numerical evaluation via computer simulations, and writing the papers [61, 63, 99, 105, 134–138]. The role of the co-authors was mainly to provide guidance, comments, and support during the research process.

As the second author in [60], the author of this thesis was actively involved in the research and writing process, by taking part of the analysis as well as providing ideas, comments, and criticism. In addition to the papers [60, 61, 63, 99, 105, 134–138], on which the thesis is based, the author has written other related papers, including a journal paper [152] and five conference papers [140–142, 150, 151], and also co-authored another nine conference papers [84, 139, 143–149]. Still further, the author has acted as technical advisor and co-author for another journal paper [154], currently under revision, and a conference paper [153].

2 Coordinated beamforming in MISO cellular networks

This chapter consider coordinated beamforming in cellular multi-user MISO systems. The network optimization objective is to minimize the sum transmission power of the coordinating BSs while also providing a guaranteed minimum rate for each active user. In particular, decentralized coordinated beamforming techniques are derived and analyzed.

In Section 2.1, the multi-cell multi-user MISO system model is introduced, and the SPMin problem is mathematically formulated applying perfect and imperfect CSI assumptions. Novel decentralized beamforming designs are proposed for perfect and imperfect CSI cases in Sections 2.2 and 2.3, respectively. In the proposed algorithms, primal or dual decomposition methods are used to facilitate decentralized implementation. The optimal transmit beamformers are designed using standard convex optimization techniques or alternatively by exploiting the uplink-downlink duality-based method. The performance of the proposed algorithms is evaluated in a simplified multi-cell environment. Finally, the chapter is summarized and discussed in Section 2.4.

2.1 System model and SPMin problem formulation

The considered system is a multi-cell multi-user MISO network with B BSs and K users, as depicted in Fig. 4. Each BS is equipped with A_{T} transmit antennas and each user with a single receive antenna. The sets of B BSs and K users are denoted by $\mathcal{B}$ and $\mathcal{K}$, respectively. BS b serves its own set of K_b users. This set is denoted by $\mathcal{K}_b$. The set of other cells' users is given by $\bar{\mathcal{K}}_b = \mathcal{K} \setminus \mathcal{K}_b$. A coordinated beamforming system is considered where each user is served by a single BS. User allocation is assumed to be predefined and fixed. The serving BS for user k is denoted by b_k. The signal received by the kth user is given by

$$y_k = \mathbf{h}_{b_k,k}\mathbf{m}_k x_k + \sum_{i\in\mathcal{K}\setminus\{k\}} \mathbf{h}_{b_i,k}\mathbf{m}_i x_i + n_k \qquad (1)$$

where $\mathbf{h}_{b_k,k} \in \mathbb{C}^{1\times A_{\mathrm{T}}}$ is the channel vector from BS b_k to user k, $\mathbf{m}_k \in \mathbb{C}^{A_{\mathrm{T}}\times 1}$ is the unnormalized transmit beamforming vector for user k, x_k is the correspond-

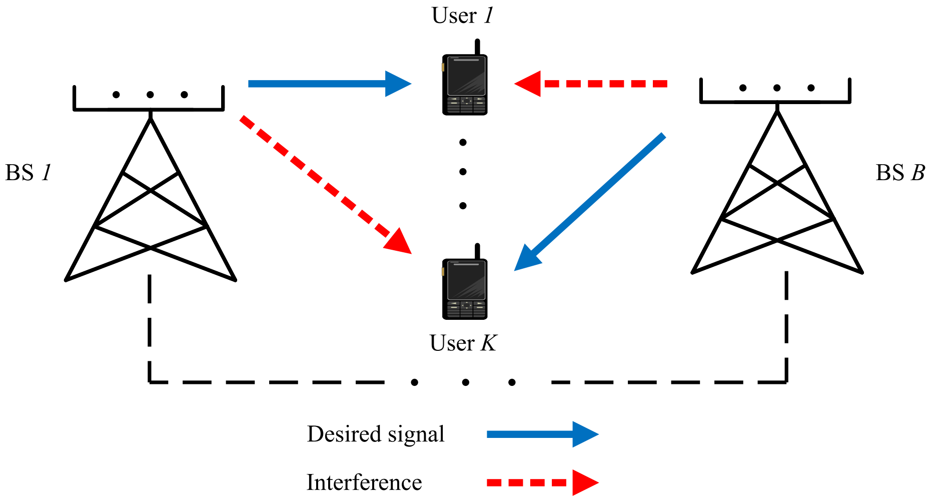

Fig 4. Multi-cell multi-user MISO system.

ing normalized complex data symbol, and $n_k \sim \mathcal{CN}(0, N_0)$ is the complex white Gaussian noise sample with zero mean and variance N_0. The sum transmission power of BSs is expressed as

$$P^{\text{tx}} = \sum_{k \in \mathcal{K}} \text{Tr}\left(\mathbf{m}_k \mathbf{m}_k^{\text{H}}\right) = \sum_{k \in \mathcal{K}} \left\|\mathbf{m}_k\right\|_2^2 \tag{2}$$

By assuming that a Gaussian codebook is used for each data stream, the rate for user k can be written as

$$r_k = \log_2\left(1 + \Gamma_k\right) \tag{3}$$

where the SINR of user k is given by

$$\Gamma_k = \frac{\left|\mathbf{h}_{b_k,k}\mathbf{m}_k\right|^2}{N_0 + \sum\limits_{i \in \mathcal{K}\setminus\{k\}} \left|\mathbf{h}_{b_i,k}\mathbf{m}_i\right|^2} \tag{4}$$

The network design problem is to minimize the sum power of the BSs while guaranteeing a minimum predefined rate for each active user. The resulting optimization problem is expressed as

$$\begin{aligned} \underset{\{\mathbf{m}_k\}_{k \in \mathcal{K}}}{\min.} \quad & \sum_{k \in \mathcal{K}} \left\|\mathbf{m}_k\right\|_2^2 \\ \text{s. t.} \quad & \log_2\left(1 + \Gamma_k\right) \geq R_k, \forall k \in \mathcal{K} \end{aligned} \tag{5}$$

where R_k is the fixed rate target for user k. In this MISO problem setting, the user-specific rate targets $\{R_k\}_{k\in\mathcal{K}}$ can be changed into user-specific SINR targets $\{\gamma_k\}_{k\in\mathcal{K}}$ since there exists direct mapping between the rate and SINR. Now the problem can be written as

$$\begin{array}{ll} \underset{\{\mathbf{m}_k\}_{k\in\mathcal{K}}}{\min.} & \sum_{k\in\mathcal{K}} \left\|\mathbf{m}_k\right\|_2^2 \\ \text{s. t.} & \Gamma_k \geq \gamma_k, \forall k \in \mathcal{K} \end{array} \tag{6}$$

where $\gamma_k = 2^{R_k} - 1$ is the fixed SINR target. In (6), the SINR constraints are tight at the optimal solution. Problem (6) can be infeasible in some channel conditions and network scenarios, e.g., the number of users and/or the SINR targets are too high. In those cases, it is the duty of admission control to loosen the system requirements by decreasing the SINR targets and/or limiting the number of active users [83]. The feasibility of the single-cell version of (6) was discussed in [33]. As an example, a sufficient condition for (6) to be feasible is when $A_{\mathrm{T}} \geq K$, provided that the channel elements are independent of each other. In the following sections, it is assumed that (6) is strictly feasible, and an optimal solution exists. Problem (6) can be solved in a centralized manner by using state-of-the-art algorithms based on uplink-downlink duality [58, 59], SDP [31] and SOCP [33]. In addition, uplink-downlink duality-based decentralized algorithms were proposed in [58, 59]. Novel decentralized algorithms are developed in Sections 2.2.1 and 2.2.2.

In (6), it is assumed that all the channels are known perfectly at the corresponding BSs. In practice, however, there is uncertainty in the CSI acquisition. That issue is addressed in the following by assuming a worst case network design perspective wherein the CSI errors lie in ellipsoidal regions. Assuming imperfect CSI, the channel vector from the bth BS to the kth user is expressed as

$$\mathbf{h}_{b,k} = \hat{\mathbf{h}}_{b,k} + \mathbf{u}_{b,k}, \forall b \in \mathcal{B}, \forall k \in \mathcal{K} \tag{7}$$

where $\hat{\mathbf{h}}_{b,k}$ and $\mathbf{u}_{b,k}$ are the estimated channel at the BS and the CSI error, respectively. Ellipsoid that bounds the CSI errors is given by

$$\mathcal{E}_{b,k} = \left\{\mathbf{u}_{b,k} : \mathbf{u}_{b,k}\mathbf{E}_{b,k}\mathbf{u}_{b,k}^{\mathrm{H}} \leq 1\right\}, \forall b \in \mathcal{B}, \forall k \in \mathcal{K} \tag{8}$$

where the positive definite matrix $\mathbf{E}_{b,k}$ is known at the BS, and it determines the accuracy of the CSI by defining the shape and size of the ellipsoid. Here, the network design problem is to minimize the sum power of the BSs while satisfying the worst case per-user SINR targets. The resulting robust optimization problem is given by

$$\begin{aligned}
\min_{\{\mathbf{m}_k\}_{k\in\mathcal{K}}} \quad & \sum_{k\in\mathcal{K}} \mathrm{tr}\left(\mathbf{m}_k\mathbf{m}_k^{\mathrm{H}}\right) \\
\text{s. t.} \quad & \frac{\left(\hat{\mathbf{h}}_{b_k,k}+\mathbf{u}_{b_k,k}\right)\left(\mathbf{m}_k\mathbf{m}_k^{\mathrm{H}}\right)\left(\hat{\mathbf{h}}_{b_k,k}+\mathbf{u}_{b_k,k}\right)^{\mathrm{H}}}{N_0+\sum\limits_{i\in\mathcal{K}\setminus\{k\}}\left(\hat{\mathbf{h}}_{b_i,k}+\mathbf{u}_{b_i,k}\right)\left(\mathbf{m}_i\mathbf{m}_i^{\mathrm{H}}\right)\left(\hat{\mathbf{h}}_{b_i,k}+\mathbf{u}_{b_i,k}\right)^{\mathrm{H}}} \geq \gamma_k, \\
& \forall \mathbf{u}_{b_k,k} \in \mathcal{E}_{b_k,k}, \forall\ k \in \mathcal{K}
\end{aligned} \tag{9}$$

The problem (9) is non-convex, and thus, it cannot be solved in this form. In [89], (9) was first approximated and then solved in a decentralized manner by exploiting the ADMM method. In Section 2.3, (9) is also approximated and reformulated as a tractable convex form, and an alternative decentralized beamforming algorithm is derived.

2.2 Decentralized transmit beamforming design

In this section, decentralized coordinated beamforming algorithms are developed to solve the SPMin problem in a cellular multi-user MISO system. The proposed algorithms are based on standard primal and dual decomposition methods. In general, decomposition methods turn the original one-level optimization problem into two optimization levels: a higher level master problem that controls the lower level sub-problems [155]. The resulting problem structure can be exploited to solve the original problem in a decentralized way. In the following subsections, a primal decomposition-based algorithm is derived first, after which a dual decomposition-based algorithm is developed.

2.2.1 Primal decomposition-based algorithm

A primal decomposition-based decentralized algorithm is derived to solve the SPMin problem (6). The problem is first reformulated such that the primal decomposition method can be applied to turn the one-level problem into two optimization levels, i.e., a network-wide master problem for inter-cell interference coordination and BS-specific subproblems for independent transmit beamforming design. A projected subgradient method is applied to solve the higher level master problem by iteratively updating inter-cell interference power levels. The lower level subproblems are solved for the transmit beamformers with fixed interference levels either by using convex optimization techniques or the uplink-downlink duality-based method.

Reformulation of SPMin problem

The primal decomposition method is applicable to problems that include coupling variables such that by fixing them the problem decouples [155]. The primal decomposition method cannot be directly applied to the original SPMin problem (6) since it is coupled between the BSs by the transmit beamformers. However, (6) can be reformulated by separating inter-cell interference powers as auxiliary optimization variables. Consequently, the coupling is transferred from the beamformers to the inter-cell interference power variables. After the reformulation, the primal decomposition method can be applied since the resulting problem decouples by fixing the interference power variables. The primal decomposition-based problem structure allows two-level optimization, where the inter-cell interference is coordinated in a network-level by iteratively solving the master problem, and the transmit beamformers are designed in a BS-level by solving the corresponding subproblem with the given interference levels.

Inter-cell interference power from BS b to user k is denoted by

$$\chi_{b,k} = \sum_{i \in \mathcal{K}_b} \left| \mathbf{h}_{b,k} \mathbf{m}_i \right|^2. \tag{10}$$

By using (10), the SINR of user k is rewritten as

$$\Gamma_k = \frac{\left| \mathbf{h}_{b_k,k} \mathbf{m}_k \right|^2}{N_0 + \sum_{b' \in \mathcal{B} \setminus \{b_k\}} \chi_{b',k} + \sum_{i \in \mathcal{K}_b \setminus \{k\}} \left| \mathbf{h}_{b_i,k} \mathbf{m}_i \right|^2}. \tag{11}$$

The SPMin problem (6) can then be reformulated accordingly. The resulting problem is expressed as

$$
\begin{aligned}
\min_{P^{\mathrm{tx}},\{\mathbf{m}_k\}_{k\in\mathcal{K}},\boldsymbol{\chi}}. \quad & P^{\mathrm{tx}} \\
\text{s. t.} \quad & \sum_{k\in\mathcal{K}} \left\|\mathbf{m}_k\right\|_2^2 \leq P^{\mathrm{tx}} \\
& \frac{\left|\mathbf{h}_{b_k,k}\mathbf{m}_k\right|^2}{N_0 + \sum_{b'\in\mathcal{B}\setminus\{b_k\}} \chi_{b',k} + \sum_{i\in\mathcal{K}_b\setminus\{k\}} \left|\mathbf{h}_{b_i,k}\mathbf{m}_i\right|^2} \geq \gamma_k, \forall k\in\mathcal{K} \\
& \sum_{i\in\mathcal{K}_b} \left|\mathbf{h}_{b,k}\mathbf{m}_i\right|^2 \leq \chi_{b,k}, \forall b\in\mathcal{B}, \forall k\in\bar{\mathcal{K}}_b
\end{aligned}
\tag{12}
$$

For notational convenience, all the inter-cell interference power variables are gathered into a single vector $\boldsymbol{\chi}$, i.e., the elements of $\boldsymbol{\chi}$ are taken from the set $\{\chi_{b,k}\}_{b\in\mathcal{B},k\in\bar{\mathcal{K}}_b}$. Problem (12) is written in epigraph form [81]. The optimal solution for (6) is equivalent to that for (12) since all the inequality constraints in (12) hold with equality at the optimal point. For a strict feasibility assumption, it needs to be that $\chi_{b,k} > 0$, $\forall b\in\mathcal{B}, \forall k\in\bar{\mathcal{K}}_b$, since interference power cannot be negative.

Following the derivation in [33], (12) can be reformulated as a convex SOCP

$$
\begin{aligned}
\min_{p^{\mathrm{tx}},\{\mathbf{m}_k\}_{k\in\mathcal{K}},\boldsymbol{\chi}}. \quad & p^{\mathrm{tx}} \\
\text{s. t.} \quad & \left\| \bar{\mathbf{m}} \right\|_2 \leq p^{\mathrm{tx}} \\
& \left\| \begin{matrix} \mathbf{M}_{b_k}^{\mathrm{H}}\mathbf{h}_{b_k,k}^{\mathrm{H}} \\ \bar{\boldsymbol{\chi}}_k \\ \sqrt{N_0} \end{matrix} \right\|_2 \leq \sqrt{1+\frac{1}{\gamma_k}}\mathbf{h}_{b_k,k}\mathbf{m}_k, \forall k\in\mathcal{K} \\
& \left\| \mathbf{M}_b^{\mathrm{H}}\mathbf{h}_{b,k}^{\mathrm{H}} \right\|_2 \leq \bar{\chi}_{b,k}, \forall b\in\mathcal{B}, \forall k\in\bar{\mathcal{K}}_b
\end{aligned}
\tag{13}
$$

where $\bar{\mathbf{m}} = [\mathbf{m}_1^{\mathrm{T}},\ldots,\mathbf{m}_K^{\mathrm{T}}]^{\mathrm{T}}$, $\mathbf{M}_b = [\mathbf{m}_{\mathcal{K}_b(1)},\ldots,\mathbf{m}_{\mathcal{K}_b(K_b)}]$ and $\bar{\chi}_{b,k} = \sqrt{\chi_{b,k}}$. The elements of $\bar{\boldsymbol{\chi}}_k$ are taken from the set $\{\bar{\chi}_{b',k}\}_{b'\in\mathcal{B}\setminus\{b_k\}}$, i.e., the interference experienced by user k from the other BSs. The optimal sum power is given by $(p^{\mathrm{tx}})^2 = P^{\mathrm{tx}}$. The problem (12) is a standard form SOCP [81] since the objective function is linear and the constraints are SOC constraints.

In the following proposition, it is shown via strong duality that (12) can be solved via its Lagrange dual problem. This valuable property is used later in the algorithm derivation. Strong duality implies that the duality gap between a primal problem and its Lagrangian dual problem is zero, i.e., both problems have the same solution [81]. Therefore, the primal problem can be solved via its dual problem.

Proposition 1. *Strong duality holds for problem* (12).

Proof. See Appendix 1. □

Two-level problem structure via primal decomposition

Problem (12) is coupled between the BSs by the inter-cell interference variables, i.e., the elements of $\boldsymbol{\chi}$. Precisely, each element of $\boldsymbol{\chi}$ couples exactly two BSs. The sum power P^{tx} is inherently separable between the BS, i.e., $P^{\text{tx}} = \sum_{b\in\mathcal{B}} P_b^{\text{tx}} = \sum_{b\in\mathcal{B}}\sum_{k\in\mathcal{K}_b}\|\mathbf{m}_k\|_2^2$, where P_b^{tx} is the transmission power of BS b. Consequently, (12) decouples if $\boldsymbol{\chi}$ is fixed. Now, primal decomposition is an adequate method to decompose (12) into a higher level master problem and $\mathcal{B}$ lower level subproblems, one for each BS. The resulting master problem and subproblems are convex since the original problem is convex [155]. For notational purposes, BS-specific inter-cell interference vectors are introduced, i.e., $\boldsymbol{\chi}_b$, $\forall b \in \mathcal{B}$, which consist of all $\chi_{b,k}$ that are coupled with BS b. Precisely, the elements of $\boldsymbol{\chi}_b$ are taken from the sets $\{\chi_{b,k}\}_{k\in\bar{\mathcal{K}}_b}$ and $\{\chi_{b',k}\}_{b'\in\mathcal{B}\setminus\{b_k\},k\in\mathcal{K}_b}$.

The lower level subproblem at BS b for a fixed $\boldsymbol{\chi}_b$ is written as

$$\begin{aligned}
\underset{P_b^{\text{tx}},\{\mathbf{m}_k\}_{k\in\mathcal{K}_b}}{\text{min.}} \quad & P_b^{\text{tx}} \\
\text{s. t.} \quad & \sum_{k\in\mathcal{K}_b}\|\mathbf{m}_k\|_2^2 \le P_b^{\text{tx}} \\
& \frac{|\mathbf{h}_{b_k,k}\mathbf{m}_k|^2}{N_0 + \sum\limits_{b'\in\mathcal{B}\setminus\{b_k\}}\chi_{b',k} + \sum\limits_{i\in\mathcal{K}_b\setminus\{k\}}|\mathbf{h}_{b_i,k}\mathbf{m}_i|^2} \ge \gamma_k, \forall k \in \mathcal{K}_b \\
& \sum_{i\in\mathcal{K}_b}|\mathbf{h}_{b,k}\mathbf{m}_i|^2 \le \chi_{b,k}, \forall k \in \bar{\mathcal{K}}_b
\end{aligned} \tag{14}$$

Proposition 1 holds true for (14) since it is a simplified version of (12), i.e., strong duality holds true.

The network-level master problem manages the subproblems by updating $\{\boldsymbol{\chi}_b\}_{b\in\mathcal{B}}$. The master problem is expressed as

$$\begin{aligned}
\underset{\{\boldsymbol{\chi}_b\}_{b\in\mathcal{B}}}{\text{min.}} \quad & \sum_{b\in\mathcal{B}} g_b^\star(\boldsymbol{\chi}_b) \\
\text{s. t.} \quad & \boldsymbol{\chi}_b \in \mathbb{R}_{++}^{N_b}, \forall b \in \mathcal{B}
\end{aligned} \tag{15}$$

where $g_b^\star(\boldsymbol{\chi}_b)$ denotes the optimal objective value of the subproblem (14) for a given $\boldsymbol{\chi}_b$, and $\mathbb{R}_{++}^{N_b}$ is the set of N_b dimensional positive real vectors. The following subsections show how to solve (14) and (15).

Master problem: network-wide optimization step

The projected subgradient method is applied to solve the network-wide master problem (15) by iteratively updating the inter-cell interference power variables, i.e.,

$$\chi_{b,k}^{(r+1)} = \mathcal{P}_{++}\left\{\chi_{b,k}^{(r)} - \sigma^{(r)}u_{b,k}^{(r)}\right\}, \forall b \in \mathcal{B}, \forall k \in \bar{\mathcal{K}}_b \tag{16}$$

where $\mathcal{P}_{++}$ is the projection onto the set of positive real numbers. Step-size at iteration r is denoted by $\sigma^{(r)}$. The scalar $u_{b,k}^{(r)}$ is any (network-level) subgradient of (15) evaluated at point $\chi_{b,k}^{(r)}$. Finding subgradients for the interference update process (16) is described in the following proposition.

Proposition 2. *A valid subgradient of* (15) *at point* $\chi_{b,k}$ *is given by*

$$u_{b,k}^{(r)} = \lambda_{b_k,k}^{(r)} - \mu_{b,k}^{(r)}, \forall b \in \mathcal{B}, \forall k \in \bar{\mathcal{K}}_b \tag{17}$$

where $\lambda_{b_k,k}^{(r)}$ *is the optimal dual variable associated with* $\chi_{b,k}^{(r)}$ *in the SINR constraint of user* k *at its serving BS* b_k *(i.e., in subproblem* b_k*) and* $\nu_{b,k}^{(r)}$ *is the optimal dual variable associated with* $\chi_{b,k}^{(r)}$ *in the inter-cell interference constraint of user* k *at the interfering BS* b *(i.e., in subproblem* b*). This is due to the inter-cell interference term* $\chi_{b,k}$ *being coupled with exactly two BSs, i.e., user* k*'s serving BS* b_k *and user* k*'s interfering BS* b*.*

Proof. See Appendix 2. □

In the literature, there are multiple results on the convergence of the (projected) subgradient method with different step-size rules, see [156, 157]. For example, the subgradient method converges to the optimal value for a convex problem when the non-negative step-size $\sigma^{(r)}$ is nonsummable and diminishing with r, i.e., $\lim_{r\to\infty}\sigma^{(r)} = 0$ and $\sum_{r=1}^{\infty}\sigma^{(r)} = \infty$. In this respect, a valid step-size is, for example, $\sigma^{(r)} = \frac{\varphi}{\sqrt{r}}$, where φ gets a fixed and positive value. For a fixed step-size, the subgradient method converges within some range of the optimal value, and the range decreases with the decreasing step-size. As an inherent property of the subgradient method, monotonic convergence can not be guaranteed [155]. Thus, it is important to keep track of the best solution for the previous iterations.

Subproblems: BS-specific optimization step

Alternative methods are introduced to solve the BS-specific subproblems for the transmit beamformers and dual variables. The first method is based on standard convex optimization techniques by solving (14) and its dual problem as SOCP and SDP, respectively. The second approach relies on an uplink-downlink duality method that includes optimization steps for uplink powers, uplink receive beamformers, and downlink transmit beamformers. In general, the latter approach has lower computational complexity compared with the former one since it does not use convex optimization methods. For notational convenience, the iteration index r is dropped in the following subsections.

Convex optimization-based solution

Here, the subproblem (14) and its dual problem are reformulated as convex problems. In this respect, (14) can be cast as an SOCP

$$\begin{aligned} \min_{p_b^{\mathrm{tx}}, \{\mathbf{m}_k\}_{k\in\mathcal{K}_b}} \quad & p_b^{\mathrm{tx}} \\ \text{s. t.} \quad & \left\| \bar{\mathbf{m}}_b \right\|_2 \leq p_b^{\mathrm{tx}} \\ & \left\| \begin{matrix} \mathbf{M}_{b_k}^{\mathrm{H}} \mathbf{h}_{b_k,k}^{\mathrm{H}} \\ \bar{\boldsymbol{\chi}}_k \\ \sqrt{N_0} \end{matrix} \right\|_2 \leq \sqrt{1+\frac{1}{\gamma_k}} \mathbf{h}_{b_k,k}\mathbf{m}_k, \forall k \in \mathcal{K}_b \\ & \left\| \mathbf{M}_b^{\mathrm{H}} \mathbf{h}_{b,k}^{\mathrm{H}} \right\|_2 \leq \bar{\chi}_{b,k}, \forall k \in \bar{\mathcal{K}}_b \end{aligned} \tag{18}$$

where $\bar{\mathbf{m}}_b = [\mathbf{m}_{\mathcal{K}_b(1)}^{\mathrm{T}}, \ldots, \mathbf{m}_{\mathcal{K}_b(K_b)}^{\mathrm{T}}]^{\mathrm{T}}$ and the optimal per-BS power is given by $(p_b^{\mathrm{tx}})^2 = P_b^{\mathrm{tx}}$. In general, the optimal dual variables are provided as a certificate for optimality by solving a convex optimization problem via standard convex optimization software packages, e.g., CVX [88]. However, CVX cannot provide the dual variables for the primal problems which are formulated as SOCPs. Since strong duality holds for (14), the optimal dual variables can be found by solving the Lagrange dual problem of (14). The dual problem is expressed as

$$\begin{aligned}
\max_{\boldsymbol{\lambda}_b, \boldsymbol{\mu}_b}. \quad & \sum_{k \in \mathcal{K}_b} \lambda_{b,k} \left(N_0 + \sum_{b' \in \mathcal{B} \setminus \{b_k\}} \chi_{b',k} \right) - \sum_{k \in \bar{\mathcal{K}}_b} \mu_{b,k} \chi_{b,k} \\
\text{s. t.} \quad & \mathbf{I} + \sum_{i \in \mathcal{K}_b} \lambda_{b,i} \mathbf{h}_{b_k,i}^{\mathrm{H}} \mathbf{h}_{b_k,i} + \sum_{j \in \bar{\mathcal{K}}_b} \mu_{b,j} \mathbf{h}_{b_k,j}^{\mathrm{H}} \mathbf{h}_{b_k,j} - \left(1 + \tfrac{1}{\gamma_k}\right) \lambda_{b,k} \mathbf{h}_{b_k,k}^{\mathrm{H}} \mathbf{h}_{b_k,k} \\
& \succeq 0, \forall k \in \mathcal{K}_b \\
& \boldsymbol{\lambda}_b \succeq 0, \boldsymbol{\mu}_b \succeq 0
\end{aligned} \tag{19}$$

where $\boldsymbol{\lambda}_b = [\lambda_{b,1}, \ldots, \lambda_{b,K_b}]^{\mathrm{T}}$ and $\boldsymbol{\mu}_b = [\mu_{b,1}, \ldots, \mu_{b,|\bar{\mathcal{K}}_b|}]^{\mathrm{T}}$. Since the objective function is linear and the inequality constraints are linear matrix inequalities, (19) can be cast as a standard form SDP by turning the maximization into minimization and changing the sign of the objective function. Thus, the resulting problem can be efficiently solved via standard SDP solvers.

Uplink-downlink duality-based solution

The concept of uplink-downlink SINR duality implies that the optimal sum power is the same for the downlink and uplink transmissions assuming the same SINR targets for the active users [35]. In general, this concept can be used to solve downlink beamforming problems via uplink problems, which are usually easier to solve. In the following, an uplink-downlink duality-based algorithm is derived to solve the BS-level subproblem (14).

First, the dual problem (19) is split into an outer maximization of $\boldsymbol{\mu}_b$ and an inner maximization of $\boldsymbol{\lambda}_b$. The vectors $\boldsymbol{\mu}_b$ and $\boldsymbol{\lambda}_b$ consist of the dual variables associated with the inter-cell interference and SINR constraints in (14), respectively. Since (19) is concave, both the outer and inner problems are also concave.

The outer maximization can be expressed as

$$\begin{aligned}
\max_{\boldsymbol{\mu}_b}. \quad & \bar{g}_b^{\star}(\boldsymbol{\mu}_b) \\
\text{s. t.} \quad & \boldsymbol{\mu}_b \in \mathbb{R}_+^{K_b}
\end{aligned} \tag{20}$$

where $\bar{g}_b^{\star}(\boldsymbol{\mu}_b)$ is the optimal objective value of the inner maximization of $\boldsymbol{\lambda}_b$ for the given $\boldsymbol{\mu}_b$, and $\mathbb{R}_+^{K_b}$ is the set of positive real vectors of length K_b. The projected subgradient method is used to optimally solve the outer maximization problem (20) for $\boldsymbol{\mu}_b$. Projected subgradient updates are given by

$$\mu_{b,k}^{(n+1)} = \mathcal{P}_+ \left\{ \mu_{b,k}^{(n)} + \sigma^{(n)} u_{b,k}^{(n)} \right\}, \forall k \in \bar{\mathcal{K}}_b \tag{21}$$

where $\mathcal{P}_+$ is the projection onto the set of non-negative real numbers. At iteration n, the step-size is denoted by $\sigma^{(n)}$. Based on Proposition 2, the subgradient $u_{b,k}^{(n)}$ at point $\mu_{b,k}^{(n)}$ can be expressed as

$$u_{b,k}^{(n)} = \textstyle\sum_{i \in \mathcal{K}_b} |\mathbf{h}_{b,k} \mathbf{m}_i|^2 - \chi_{b,k}, \forall k \in \bar{\mathcal{K}}_b \tag{22}$$

In order to solve (22), the optimal beamformers $\{\mathbf{m}_k\}_{k \in \mathcal{K}_b}$ need to be found at each iteration n. For ease of presentation, the iteration index n with respect to $\boldsymbol{\mu}_b$ is omitted in the rest of this subsection.

The inner optimization problem for $\boldsymbol{\lambda}_b$ is expressed as

$$\begin{aligned} \max_{\boldsymbol{\lambda}_b}. \quad & \sum_{k \in \mathcal{K}_b} \lambda_{b,k} \left(N_0 + \sum_{b' \in \mathcal{B} \setminus \{b_k\}} \chi_{b',k} \right) \\ \text{s. t.} \quad & \mathbf{I} + \sum_{i \in \mathcal{K}_b} \lambda_{b,i} \mathbf{h}_{b_k,i}^{\mathrm{H}} \mathbf{h}_{b_k,i} + \sum_{j \in \bar{\mathcal{K}}_b} \mu_{b,j} \mathbf{h}_{b_k,j}^{\mathrm{H}} \mathbf{h}_{b_k,j} \\ & - \left(1 + \frac{1}{\gamma_k}\right) \lambda_{b,k} \mathbf{h}_{b_k,k}^{\mathrm{H}} \mathbf{h}_{b_k,k} \succeq 0, \forall\, k \in \mathcal{K}_b \\ & \boldsymbol{\lambda}_b \succeq 0. \end{aligned} \tag{23}$$

The fixed term $\sum_{k \in \bar{\mathcal{K}}_b} \mu_{b,k} \chi_{b,k}$ is omitted from the objective since it does not have any impact on finding the optimal $\boldsymbol{\lambda}_b$. Inspired by [33, 35, 59], next it is shown how to find the optimal $\boldsymbol{\lambda}_b$ and $\{\mathbf{m}_k\}_{k \in \mathcal{K}_b}$ with the aid of uplink-downlink duality.

Theorem 1. *Problem* (23) *is equivalent to the following problem:*

$$\begin{aligned} \min_{\boldsymbol{\lambda}_b, \{\acute{\mathbf{w}}_k\}_{k \in \mathcal{K}_b}}. \quad & \sum_{k \in \mathcal{K}_b} \lambda_{b,k} \left(N_0 + \sum_{b' \in \mathcal{B} \setminus \{b_k\}} \chi_{b',k} \right) \\ \text{s. t.} \quad & \frac{1}{\gamma_k} \lambda_{b,k} \left| \acute{\mathbf{w}}_k^H \mathbf{h}_{b_k,k} \right|^2 - \sum_{i \in \mathcal{K}_{b_k} \setminus \{k\}} \lambda_{b,i} \left| \acute{\mathbf{w}}_k^H \mathbf{h}_{b_i,i} \right|^2 \\ & \geq \sum_{j \in \bar{\mathcal{K}}_b} \mu_{b,j} \left| \acute{\mathbf{w}}_k^H \mathbf{h}_{b_k,j} \right|^2 + \acute{\mathbf{w}}_k^H \mathbf{I} \acute{\mathbf{w}}_k, \forall\, k \in \mathcal{K}_b \\ & \boldsymbol{\lambda}_b \succeq 0. \end{aligned} \tag{24}$$

where $\acute{\mathbf{w}}_k \in \mathbb{C}^{A_{\mathrm{T}} \times 1}$ *is interpreted as a virtual uplink beamformer for user* k. *Problem* (24) *can be interpreted as a virtual dual uplink (weighted) SPMin problem for a cellular multi-user MISO system where the user-specific SINR constraints remain the same as in the downlink.*

Proof. See Appendix 3. □

A fixed-point iteration method is introduced in the following proposition to solve (24).

Proposition 3. *The problem* (24) *is solved optimally for* $\boldsymbol{\lambda}_b$ *via the following fixed point iteration:*

$$\lambda_{b,k}^{(m+1)} = \frac{1}{\left(1 + \frac{1}{\gamma_k}\right) \mathbf{h}_{b_k,k} \left(\boldsymbol{\Omega}_b^{(m)}\right)^{-1} \mathbf{h}_{b_k,k}^H}, \forall k \in \mathcal{K}_b \tag{25}$$

where

$$\boldsymbol{\Omega}_b^{(m)} = \mathbf{I} + \sum_{i \in \mathcal{K}_b} \lambda_{b,i}^{(m)} \mathbf{h}_{b_k,i}^H \mathbf{h}_{b_k,i} + \sum_{j \in \bar{\mathcal{K}}_b} \mu_{b,j} \mathbf{h}_{b_k,j}^H \mathbf{h}_{b_k,j}. \tag{26}$$

Proof. See Appendix 4. □

For the fixed (optimal) $\boldsymbol{\lambda}_b$, the optimal virtual uplink beamformers $\{\acute{\mathbf{w}}_k\}_{k \in \mathcal{K}_b}$ can be computed using the linear MMSE receiver, presented in (154) in Appendix 3. The following proposition shows how the optimal downlink beamformers can be acquired with the aid of the optimal uplink beamformers.

Proposition 4. *The optimal downlink beamformers* $\{\mathbf{m}_k\}_{k \in \mathcal{K}_b}$ *are solved via the optimal virtual uplink beamformers* $\{\acute{\mathbf{w}}_k\}_{k \in \mathcal{K}_b}$ *by scaling, i.e.,*

$$\mathbf{m}_k = \sqrt{\varepsilon_k} \acute{\mathbf{w}}_k, \forall k \in \mathcal{K}_b. \tag{27}$$

The scaling factors $\{\varepsilon_k\}_{k \in \mathcal{K}_b}$ *are solved via the matrix equation:*

$$[\varepsilon_1, \ldots, \varepsilon_{K_b}]^T = \mathbf{A}^{-1} \mathbf{b} \tag{28}$$

where the (i,j)*-th and* k*th elements of the matrix* $\mathbf{A}$ *and the vector* $\mathbf{b}$ *are given by*

$$[\mathbf{A}]_{ij} = \begin{cases} (1/\gamma_i) |\mathbf{h}_{b_i,i} \acute{\mathbf{w}}_i|^2, & \text{if} \quad i = j \\ -|\mathbf{h}_{b_i,i} \acute{\mathbf{w}}_j|^2, & \text{if} \quad i \neq j \end{cases}, \forall i,j \in \mathcal{K}_b \tag{29}$$

and $[\mathbf{b}]_k = \sum_{b' \in \mathcal{B} \setminus \{b_k\}} \chi_{b',k} + N_0$, $\forall k \in \mathcal{K}_b$, *respectively.*

Proof. See Appendix 5. □

Following from the previous findings and Proposition 1, the optimal objective value of the downlink problem (14) is the same as the optimal objective value obtained by solving the outer maximization (20) via the projected subgradient method (21) and the inner minimization via the virtual uplink problem (24). Consequently, the obtained downlink beamformers and the dual variables are optimal. These optimization steps can be solved independently at BS b, for all $b \in \mathcal{B}$ in parallel. The proposed BS-level optimization is summarized in *Algorithm 1*.

Algorithm 1 BS-specific subproblem optimization via uplink-downlink duality

1: Set $m = 0$ and $n = 0$. Initialize $\boldsymbol{\lambda}_b^{(0)}$, $\boldsymbol{\mu}_b^{(0)}$.
2: **repeat**
3:     **repeat**
4:         Update virtual uplink powers $\boldsymbol{\lambda}_b^{(m+1)}$ via fixed-point iteration (25).
5:         Set $m = m + 1$.
6:     **until** desired level of convergence
7:     Compute virtual uplink receive beamformers $\{\acute{\mathbf{w}}_k\}_{k\in\mathcal{K}_b}$ via MMSE criterion (154).
8:     Compute downlink transmit beamformers $\{\mathbf{m}_k\}_{k\in\mathcal{K}_b}$ via scaling (27).
9:     Update dual variables $\boldsymbol{\mu}_b^{(n+1)}$ via projected subgradient method (21).
10:     Set $n = n + 1$.
11: **until** desired level of convergence

Decentralized implementation

Decentralized implementation is enabled by having local CSI at each BS (see Fig. 5), and allowing an exchange of the BS-specific subgradients between the coupled BSs via low-rate backhaul links. Specifically, the subproblem b in (14) and the corresponding part of the master problem in (15), i.e., the update of $\boldsymbol{\chi}_b$, can be solved independently at BS b for all $b \in \mathcal{B}$ in parallel. At the subgradient iteration r, the backhaul information exchange is performed by BS b as follows. BS b signals the dual variables associated with the SINR constraints, i.e., $\{\lambda_{b,k}\}_{k\in\mathcal{K}_b}$, to all the interfering BSs. Whereas the dual variables associated with the inter-cell interference constraints, i.e., $\{\mu_{b,k}\}_{k\in\bar{\mathcal{K}}_b}$, are signaled to the

Algorithm 2 Decentralized transmit beamforming design based on primal decomposition for cellular MISO system

1: Set $r = 0$. Initialize inter-cell interference variables $\boldsymbol{\chi}_b^{(0)}$.
2: **repeat**
3: Compute transmit beamformers $\{\mathbf{m}_k\}_{k\in\mathcal{K}_b}$ and dual variables $\{\lambda_{b,k}\}_{k\in\mathcal{K}_b}$ and $\{\mu_{b,k}\}_{k\in\bar{\mathcal{K}}_b}$ by solving SOCP (18) and SDP (19), respectively, or alternatively by using uplink-downlink duality-based *Algorithm 1*.
4: Communicate $\{\lambda_{b,k}\}_{k\in\mathcal{K}_b}$ and $\{\mu_{b,k}\}_{k\in\bar{\mathcal{K}}_b}$ to the coupled BSs via backhaul.
5: Update inter-cell interference variables $\boldsymbol{\chi}_b^{(r+1)}$ via projected subgradient method (16).
6: Set $r = r + 1$.
7: **until** desired level of convergence

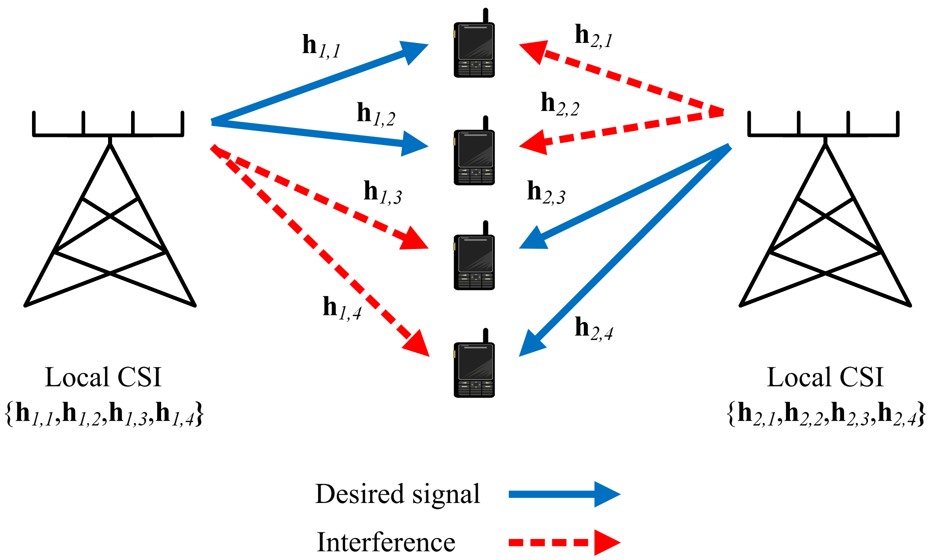

Fig 5. Definition of local CSI in a simple two-cell system.

BS, the user of which is being interfered by BS b. Assuming a fully connected network and an equal number of users at each BS (i.e., $K_b = K/B$, $\forall b \in \mathcal{B}$), the total amount of the required backhaul signaling at each network-wide subgradient iteration r is the sum of the real-valued terms exchanged between the coupled BS pairs, i.e., $2B(B-1)K_b$. The same assumptions are also applied to other backhaul signaling overhead studies in the remainder of this thesis. The primal decomposition-based decentralized coordinated beamforming design is summarized in *Algorithm 2*. All the calculations in *Algorithm 2* take place at BS b, for all $b \in \mathcal{B}$ in parallel. *Algorithm 2* converges to the optimal solution if the step-size is properly chosen and the iterates are feasible.

Practical considerations

To obtain optimal performance, *Algorithm 2* must be run until convergence. However, aiming for the optimal solution is somewhat impractical since the more iterations are run, the higher the signaling/computational load and the longer the caused delay. Unlike the existing decentralized algorithms, *Algorithm 2* naturally lends itself to a more practical design where a limited number of iterations can be used as a stopping criterion. *Algorithm 2* is able to directly compute feasible beamformers, which satisfy the rate constraints, at intermediate subgradient iterations since each $\chi_{b,k}$ is fixed and known at the coupled BSs b and b_k. At the cost of sub-optimal performance, *Algorithm 2* can be stopped at any feasible iteration to reduce delay and signaling/computational load.

In Table 1, the backhaul signaling overhead of the centralized scheme and decentralized *Algorithm 2* are compared under different system settings. In the centralized algorithm, it is assumed that each BS exchanges its local CSI with all other BSs via backhaul links. Thus, global CSI is made available for each BS. Assuming equal number of users at each cell, the total backhaul signaling load in terms of scalar-valued channel coefficients in the centralized system is given by $2A_{\mathrm{T}}K(B-1)B$. Here, one complex channel coefficient is considered as two real valued coefficients. For *Algorithm 2*, the total backhaul signaling load is presented per subgradient iteration. In Table 1, the values inside the brackets denote the percentage of the signaling load required per decentralized iteration, compared with the overall signaling load required by the centralized algorithm. One can see that *Algorithm 2* requires a notably less amount of backhaul signaling per iteration compared to the centralized algorithm. The difference is emphasized, as the network size is increased. For example, with four BSs and eight users, the per-iteration signaling load of *Algorithm 2* is about 3 % of the total signaling load of the centralized algorithm. In conclusion, backhaul signaling overhead can be significantly reduced by limiting the number of iterations.

Table 1. Total backhaul signaling load per iteration.

	Centralized	Decentralized *Algorithm 2*
$\{B, K, A_{\mathrm{T}}\} = \{2, 4, 4\}$	64	8 (12.5%)
$\{B, K, A_{\mathrm{T}}\} = \{3, 6, 6\}$	432	24 (5.6%)
$\{B, K, A_{\mathrm{T}}\} = \{4, 8, 8\}$	1536	48 (3.1%)

Algorithm 2 allows some special case designs where the number of optimization variables is reduced, leading to a lower computational load and even a further decreased signaling overhead. These special case designs come at the cost of somewhat decreased performance. Some of the possible special cases are presented below:

– Common interference constraint: $\chi_{b,k} = \chi, \forall b \in \mathcal{B}, \forall k \in \bar{\mathcal{K}}_b$.
– Fixed interference constraints: $\chi_{b,k} = c_{b,k}$, $\forall b \in \mathcal{B}, \forall k \in \bar{\mathcal{K}}_b$, where $c_{b,k}$ is a predefined constant. Does not require any backhaul signaling.
– Zero-forcing (ZF) beamforming for inter-cell interference, i.e., $\chi_{b,k} = 0$, $\forall b \in \mathcal{B}, \forall k \in \bar{\mathcal{K}}_b$, with requirement of $K \leq A_{\mathrm{T}}$. Does not require any backhaul signaling.

The last two special designs are applicable for rapidly varying channel conditions where the backhaul signaling information is highly outdated. In this kind of channel conditions, performance gains provided by iterative interference coordination via backhaul signaling may be marginal.

If the BSs do not have any prior information on the inter-cell interference power levels, it is fair to use equal elements in the initialization of $\{\boldsymbol{\chi}_b\}_{b\in\mathcal{B}}$ in *Algorithm 2*, i.e., $\chi_{b,k}^{(0)} = \chi^{(0)}$, $\forall b \in \mathcal{B}$, $\forall k \in \bar{\mathcal{K}}_b$. In practice, there can be a mechanism that stops after a fixed number of initialization tries if feasible initialization is not found, and declares the problem infeasible. Then, it is up to admission control to relax the system requirements, e.g., lower the rate targets or decrease the number of active users.

2.2.2 Dual decomposition-based algorithm

In this section, a dual decomposition-based decentralized algorithm is developed to solve the SPMin problem (6). The original problem is first reformulated by introducing auxiliary variables, i.e., the BS-specific inter-cell interference terms, which can be relaxed using the dual decomposition method. In the resulting two-level problem structure, the higher level master problem sets the prices for the interference levels, while the lower level subproblems optimize the interference levels with the given prices. The master problem is iteratively solved by using a subgradient method. The subproblems are solved as SOCPs via standard convex optimization solvers.

Reformulation of SPMin problem

The dual decomposition method can be applied to optimization problems that have a coupling constraint such that the problem decouples into multiple subproblems by relaxing the constraint [155]. In this respect, the SPMin problem (6) can be reformulated by introducing BS-specific auxiliary variables (i.e., inter-cell interference levels) and additional equality constraints that enforce network-wide consistency between the BS-specific variables. For example, $(\bar{\chi}_{b,k}^{b_k})^2$ is a local copy of the interference variable $\chi_{b,k}$ at BS b_k. The coupling in the SINR constraints is transferred to the coupling in the equality constraints, which can then be decoupled using the dual decomposition method. As a result, a two-level optimization problem is allowed, where there are multiple subproblems with fixed dual variables (i.e., prices) at the lower level and a master dual problem coordinating the update process of the dual variables at the higher level. In other words, the network-wide master problem sets the prices for the resources (i.e., inter-cell interference levels), while the resources are optimized by solving the BS-specific subproblems with the given prices.

The reformulated optimization problem is given by

$$\begin{aligned}
\min_{\{\mathbf{m}_k\}_{k\in\mathcal{K}},\{\bar{\boldsymbol{\chi}}_b\}_{b\in\mathcal{B}}} \quad & \sum_{k\in\mathcal{K}} \|\mathbf{m}_k\|_2^2 \\
\text{s. t.} \quad & \frac{|\mathbf{h}_{b_k,k}\mathbf{m}_k|^2}{N_0 + \sum_{b'\in\mathcal{B}\setminus\{b_k\}} (\bar{\chi}_{b',k}^{b_k})^2 + \sum_{i\in\mathcal{K}_{b_k}\setminus\{k\}} |\mathbf{h}_{b_k,k}\mathbf{m}_i|^2} \geq \gamma_k, \forall k\in\mathcal{K} \\
& \sum_{i\in\mathcal{K}_b} |\mathbf{h}_{b,k}\mathbf{m}_i|^2 \leq (\bar{\chi}_{b,k}^{b})^2, \forall b\in\mathcal{B}, \forall k\in\bar{\mathcal{K}}_b \\
& \bar{\chi}_{b,k}^{b} = \bar{\chi}_{b,k}^{b_k}, \forall b\in\mathcal{B}, \forall k\in\bar{\mathcal{K}}_b
\end{aligned} \tag{30}$$

where the vector $\bar{\boldsymbol{\chi}}_b$ consists of the BS b specific inter-cell interference power variables, i.e., the elements of $\bar{\boldsymbol{\chi}}_b$ are taken in a specific order from the sets $\{\bar{\chi}^b_{b,k}\}_{k\in\bar{\mathcal{K}}_b}$ and $\{\bar{\chi}^b_{b',k}\}_{b'\in\mathcal{B}\setminus\{b_k\},k\in\mathcal{K}_b}$. In (30), the objective function and the inequality constraints can be cast as SOC constraints, and they are decoupled between the BSs. However, the equality constraints are coupled and need to be handled by the dual decomposition method, as described in the following section.

Two-level problem structure via dual decomposition

In order to obtain a decentralized algorithm, a standard dual decomposition approach [155] is applied where the equality constraints $\bar{\chi}^b_{b,k} - \bar{\chi}^{b_k}_{b,k} = 0, \forall b \in \mathcal{B}, \forall k \in \bar{\mathcal{K}}_b$ in (30) are relaxed by forming the partial Lagrangian as

$$\begin{aligned} & L\left(\mathbf{M}_1,\ldots,\mathbf{M}_B,\bar{\boldsymbol{\chi}}_1,\ldots,\bar{\boldsymbol{\chi}}_B,\boldsymbol{\delta}_1,\ldots,\boldsymbol{\delta}_B\right) \\ = & \sum_{b\in\mathcal{B}}\sum_{k\in\mathcal{K}_b}\left\|\mathbf{m}_k\right\|_2^2 + \sum_{b\in\mathcal{B}}\sum_{k\in\bar{\mathcal{K}}_b}\delta_{b,k}(\bar{\chi}^b_{b,k} - \bar{\chi}^{b_k}_{b,k}) \\ = & \sum_{b\in\mathcal{B}}\sum_{k\in\mathcal{K}_b}\left\|\mathbf{m}_k\right\|_2^2 + \sum_{b\in\mathcal{B}}\boldsymbol{\delta}_b^{\mathrm{T}}\bar{\boldsymbol{\chi}}_b \end{aligned} \qquad (31)$$

where $\delta_{b,k}$ is the dual variable associated with the equality constraint $\bar{\chi}^b_{b,k} - \bar{\chi}^{b_k}_{b,k}$ and $\boldsymbol{\delta}_b$ consists of the dual variables associated with the BS b specific inter-cell interference terms. Specifically, the elements of $\boldsymbol{\delta}_b$ are taken in a specific order from the sets $\{\delta_{b,k}\}_{k\in\bar{\mathcal{K}}_b}$ and $\{-\delta_{b',k}\}_{b'\in\mathcal{B}\setminus\{b_k\},k\in\mathcal{K}_b}$. The dual function can be written as

$$g(\boldsymbol{\delta}_1,\ldots,\boldsymbol{\delta}_B) = \sum_{b\in\mathcal{B}} g_b(\boldsymbol{\delta}_b) \qquad (32)$$

where the BS b specific function $g_b(\boldsymbol{\delta}_b)$ is the minimum value of the partial Lagrangian solved for a given $\boldsymbol{\delta}_b$

$$g_b(\boldsymbol{\delta}_b) = \inf_{\{\mathbf{m}_k\}_{k\in\mathcal{K}_b},\bar{\boldsymbol{\chi}}_b} \sum_{k\in\mathcal{K}_b}\left\|\mathbf{m}_k\right\|_2^2 + \boldsymbol{\delta}_b^{\mathrm{T}}\bar{\boldsymbol{\chi}}_b. \qquad (33)$$

The dual function $\sum_{b\in\mathcal{B}} g_b(\boldsymbol{\delta}_b)$ is separable between the BSs, and thus, each $g_b(\boldsymbol{\delta}_b)$ can be considered as a BS-specific subproblem. The subproblem $g_b(\boldsymbol{\delta}_b)$

can be solved independently at BS b as the following minimization problem

$$\begin{array}{ll}\underset{\{\mathbf{m}_k\}_{k\in\mathcal{K}_b},\bar{\boldsymbol{\chi}}_b}{\min.} & \sum_{k\in\mathcal{K}_b}\left\|\mathbf{m}_k\right\|_2^2+\boldsymbol{\delta}_b^{\mathrm{T}}\bar{\boldsymbol{\chi}}_b \\ \text{s. t.} & \frac{\left|\mathbf{h}_{b_k,k}\mathbf{m}_k\right|^2}{N_0+\sum_{b'\in\mathcal{B}\setminus\{b_k\}}(\bar{\chi}_{b',k}^{b_k})^2+\sum_{i\in\mathcal{K}_{b_k}\setminus\{k\}}\left|\mathbf{h}_{b_k,k}\mathbf{m}_i\right|^2}\geq\gamma_k,\forall k\in\mathcal{K}_b \\ & \sum_{i\in\mathcal{K}_b}\left|\mathbf{h}_{b,k}\mathbf{m}_i\right|^2\leq(\bar{\chi}_{b,k}^b)^2,\forall k\in\bar{\mathcal{K}}_b\end{array} \tag{34}$$

The master problem, in charge of optimizing the dual variables $\{\boldsymbol{\delta}_b\}_{b\in\mathcal{B}}$, can be written as

$$\begin{array}{ll}\underset{\{\boldsymbol{\delta}_b\}_{b\in\mathcal{B}}}{\max.} & \sum_{b\in\mathcal{B}} g_b(\boldsymbol{\delta}_b) \\ \text{s. t.} & \boldsymbol{\delta}_b\in\mathbb{R}^{M_b},\forall b\in\mathcal{B}\end{array} \tag{35}$$

where $\mathbb{R}$ is the set of real numbers and M_b is the length of the vector $\boldsymbol{\delta}_b$. In the following subsections, it is shown how to efficiently solve (34) and (35).

Master problem: network-wide optimization step

The master problem (35) can be solved by using a standard subgradient method [155], which iteratively updates the dual variables $\{\boldsymbol{\delta}_b\}_{b\in\mathcal{B}}$. The subgradient updates are given by

$$\delta_{b,k}^{(r+1)}=\delta_{b,k}^{(r)}+\sigma^{(r)}u_{b,k}^{(r)},\forall b\in\mathcal{B},\forall k\in\bar{\mathcal{K}}_b \tag{36}$$

where r is the iteration index, $\sigma^{(r)}$ is a positive step-size and $u_{b,k}^{(r)}$ is a subgradient of (35) at the point $\delta_{b,k}^{(r)}$. Based on Proposition 2, it can be shown that $u_{b,k}^{(r)}=\bar{\chi}_{b,k}^{b,(r)}-\bar{\chi}_{b,k}^{b_k,(r)}$, where $\bar{\chi}_{b,k}^{b,(r)}$ and $\bar{\chi}_{b,k}^{b_k,(r)}$ are the optimized inter-cell interference power variables in subproblems b and b_k, respectively. Note that the intermediate iterates $\bar{\boldsymbol{\chi}}_b^{(r)}$ in the dual decomposition do not necessarily result in feasible solutions, i.e., $\Gamma_k\geq\gamma_k$, since $\bar{\chi}_{b,k}^{b_k,(r)}\neq\bar{\chi}_{b,k}^{b,(r)}$. In other words, it is possible to get $\Gamma_k<\gamma_k$ for some k when using the optimized beamformers from (39). However, it is possible to obtain a feasible set of beamformers by solving an additional subproblem per BS, i.e., (14) is solved for fixed average inter-cell interference power values $\boldsymbol{\chi}_b$. Since each inter-cell interference power variable $\chi_{b,k}$ couples exactly two BSs, i.e., the serving BS b_k and the interfering BS b, the average interference power can be easily calculated as

$$\chi_{b,k} = 1/2\left(\left(\bar{\chi}_{b,k}^{b_k,(r)}\right)^2 + \left(\bar{\chi}_{b,k}^{b,(r)}\right)^2\right) \tag{37}$$

Subproblems: BS-specific optimization step

The subproblem (34) can be cast as an SOCP by using an epigraph form representation [81] and reformulating all the inequality constraints as SOC constraints. The epigraph form of (34) is given by

$$\begin{array}{ll} \underset{a_b,\{\mathbf{m}_k\}_{k\in\mathcal{K}_b},\bar{\boldsymbol{\chi}}_b}{\min.} & a_b \\ \text{s. t.} & \sum_{k\in\mathcal{K}_b} \left\|\mathbf{m}_k\right\|_2^2 + \boldsymbol{\delta}_b^{\mathrm{T}}\bar{\boldsymbol{\chi}}_b \le a_b \\ & \dfrac{\left|\mathbf{h}_{b_k,k}\mathbf{m}_k\right|^2}{N_0 + \sum_{b'\in\mathcal{B}\setminus\{b_k\}} (\bar{\chi}_{b',k}^{b_k})^2 + \sum_{i\in\mathcal{K}_{b_k}\setminus\{k\}} \left|\mathbf{h}_{b_k,k}\mathbf{m}_i\right|^2} \ge \gamma_k, \forall k \in \mathcal{K}_b \\ & \sum_{i\in\mathcal{K}_b} \left|\mathbf{h}_{b,k}\mathbf{m}_i\right|^2 \le \left(\bar{\chi}_{b,k}^{b}\right)^2, \forall k \in \bar{\mathcal{K}}_b \end{array} \tag{38}$$

where a_b is introduced as an auxiliary variable to upper bound the relaxed objective function. The resulting quadratic constraint can be reformulated as an SOC constraint

$$\sum_{k\in\mathcal{K}_b} \left\|\mathbf{m}_k\right\|_2^2 + (1 + \boldsymbol{\delta}_b^{\mathrm{T}}\bar{\boldsymbol{\chi}}_b - a_b)^2/4 \le (1 - \boldsymbol{\delta}_b^{\mathrm{T}}\bar{\boldsymbol{\chi}}_b + a_b)^2/4$$

After writing other constraints also as SOC constraints, the resulting SOCP can be expressed as

$$\begin{array}{ll} \underset{a_b,\{\mathbf{m}_k\}_{k\in\mathcal{K}_b},\bar{\boldsymbol{\chi}}_b}{\min.} & a_b \\ \text{s. t.} & \left\| \begin{array}{c} (1 + \boldsymbol{\delta}_b^{\mathrm{T}}\bar{\boldsymbol{\chi}}_b - a_b)/2 \\ \mathrm{vec}(\mathbf{M}_b) \end{array} \right\|_2 \le (1 - \boldsymbol{\delta}_b^{\mathrm{T}}\bar{\boldsymbol{\chi}}_b + a_b)/2 \\ & \left\| \begin{array}{c} \mathbf{M}_{b_k}^{\mathrm{H}}\mathbf{h}_{b_k,k}^{\mathrm{H}} \\ \bar{\boldsymbol{\chi}}_{b,k} \\ \sqrt{N_0} \end{array} \right\|_2 \le \sqrt{1 + \frac{1}{\gamma_k}}\mathbf{h}_{b_k,k}\mathbf{m}_k, \forall k \in \mathcal{K}_b \\ & \left\| \mathbf{M}_b^{\mathrm{H}}\mathbf{h}_{b,k}^{\mathrm{H}} \right\|_2 \le \bar{\chi}_{b,k}^{b}, \forall k \in \bar{\mathcal{K}}_b \end{array} \tag{39}$$

where the elements of $\bar{\boldsymbol{\chi}}_{b,k}$ are taken from the set $\{\bar{\chi}_{b',k}^{b_k}\}_{b'\in\mathcal{B}\setminus\{b_k\}}$, i.e., the interference power from other BSs to user k.

Decentralized implementation

Decentralized implementation is possible if each BS can acquire local CSI, and exchanging the BS-specific inter-cell interference power values between the coupled BSs via low-rate backhaul links is allowed. Consequently, the subproblem b and the corresponding part of the master problem can be solved independently at BS b. The total amount of the required backhaul signaling at each subgradient iteration is given by $2B(B-1)K_b$, which is exactly the same amount as used in the primal decomposition-based algorithm. Finally, the decentralized dual decomposition-based approach is summarized in *Algorithm 3*, which is performed at BS b, for all $b \in \mathcal{B}$ in parallel. Convergence to the optimal solution is guaranteed for *Algorithm 3* as long as the step-size is properly chosen.

Algorithm 3 Decentralized transmit beamforming design based on dual decomposition for cellular MISO system

1: Set $r = 0$. Initialize dual variables $\boldsymbol{\delta}_b^{(0)}$.
2: **repeat**
3: Compute transmit beamformers $\{\mathbf{m}_k\}_{k\in\mathcal{K}_b}$ and inter-cell interference variables $\bar{\boldsymbol{\chi}}_b$ by solving SOCP (39).
4: Communicate the elements of $\bar{\boldsymbol{\chi}}_b$ to the coupled BSs via backhaul.
5: Update dual variables $\boldsymbol{\delta}_b^{(r+1)}$ via subgradient method (36).
6: Optional: Compute feasible transmit beamformers $\{\mathbf{m}_k\}_{k\in\mathcal{K}_b}$ by solving (14) with fixed average inter-cell interference variables $\boldsymbol{\chi}_b$ taken from (37).
7: Set $r = r + 1$.
8: **until** desired level of convergence

Practical considerations and comparison to primal decomposition

Due to the similarities between the primal and dual decomposition methods, most of the practicalities discussed in Section 2.2.1 apply here. However, there are also some differences. The main difference is in the problem reformulation where either the primal problem or the dual problem is decomposed into a two-level structure. Higher level interference coordination via a master problem is either performed directly in the primal decomposition or indirectly via prices (i.e., dual variables) in the dual decomposition. Thus, the content of exchanged backhaul information is different. However, the amount of exchanged information remains the same.

The formulation of subproblems are also different. In primal decomposition, an SOCP needs to be solved for the beamformers and an SDP for the dual variables. In dual decomposition, two SOCPs are solved, one for the feasible beamformers and the other for the inter-cell interference power levels. Note that the SOCPs for computing feasible beamformers are the same for both algorithms. Standard complexity analysis as described in [158] and [159] for the SOCPs and SDPs, respectively, is valid here. In general, the worst-case computational complexity of a convex optimization problem is known to be dominated by the number of optimization variables and the number and size of constraints [101, 125]. Moreover, it is well-known that, in general, SOCPs are less complex than SDPs [158]. It is worth mentioning as well that the primal decomposition method also allows for decentralized implementation by using the uplink-downlink duality method described in Section 2.2.1. This approach combines the benefits of the algorithms proposed in [61] and [35], i.e., feasible beamformers are provided at each iteration and there is no need for using convex optimization tools. This algorithm is mainly based on fixed-point iterations and MMSE calculations, which are, in general, computationally less complex compared to SOCPs and SDPs. Thus, the proposed uplink-downlink duality-based primal decomposition approach has a lower computational complexity than that of the convex optimization-based primal and dual decomposition methods.

Both primal and dual decomposition algorithms converge to an optimal solution if the step-sizes are properly selected. Unlike the primal decomposition method, dual decomposition can find an optimal solution even if some iterates are not feasible in the primal problem sense. This feature makes the initialization of the algorithm less restricted. However, it is still possible to obtain feasible beamformers at intermediate iterations by utilizing fixed average inter-cell interference values as calculated in (37). Thus, the dual decomposition-based algorithm also holds the practical feature that it can be stopped after a limited number of iterations. Therefore, backhaul signaling overhead can be notably reduced compared to the centralized scheme, as shown in Section 2.2.1. The special case designs described in Section 2.2.1 are also applicable.

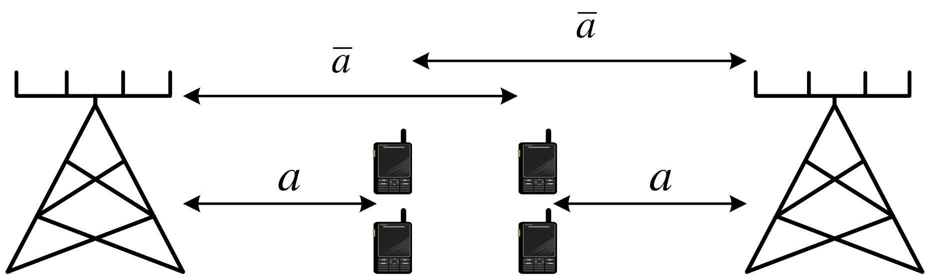

Fig 6. Simplified simulation model using cell separation. Cell separation parameter is defined as a ratio of the path gains, i.e., $\eta = a/\bar{a}$**.**

2.2.3 Numerical evaluation

In this section, the performance of the proposed algorithms is evaluated via numerical examples. First, the optimal coordinated beamforming and ZF strategies are compared under different system settings. Then, the convergence behavior of the proposed decentralized algorithms is examined. Finally, the sum powers and achieved user rates are plotted in time-correlated channel conditions. The used simulation model consists of $B = 2$ BSs, each of which serves a predefined set of two users, i.e., $K_1 = K_2 = 2$. Each BS is equipped with $A_{\mathrm{T}} = 4$ transmit antennas and each user has a single receive antenna.

The pathloss between a BS and its own served users is set to 0 dB. As illustrated in Fig. 6, a cell separation parameter η is defined as the path loss between BS 1 and the users of BS 2, and vice versa [56, 60]. In other words, interference towards the other cell's users is attenuated by the value of η. For $\eta = 0$ dB, the path loss between BS 1 and its own users is the same as the pathloss between BS 1 and the users of BS 2, and vice versa. This case can be seen as a scenario where all four users are located at the cell-edge. This is a worst case scenario at the performance point of view since the inter-cell interference is the most severe (on average). By increasing the value of η, the cells become more isolated. Thus, the other extreme is a best case scenario where the cells do not interfere with each other at all, i.e., $\eta = \infty$. Unless otherwise stated, we assume frequency-flat Rayleigh fading channel conditions with uncorrelated channel coefficients between antennas, i.e., each element of the channel vector is an i.i.d. complex Gaussian random variable with zero mean and unit variance.

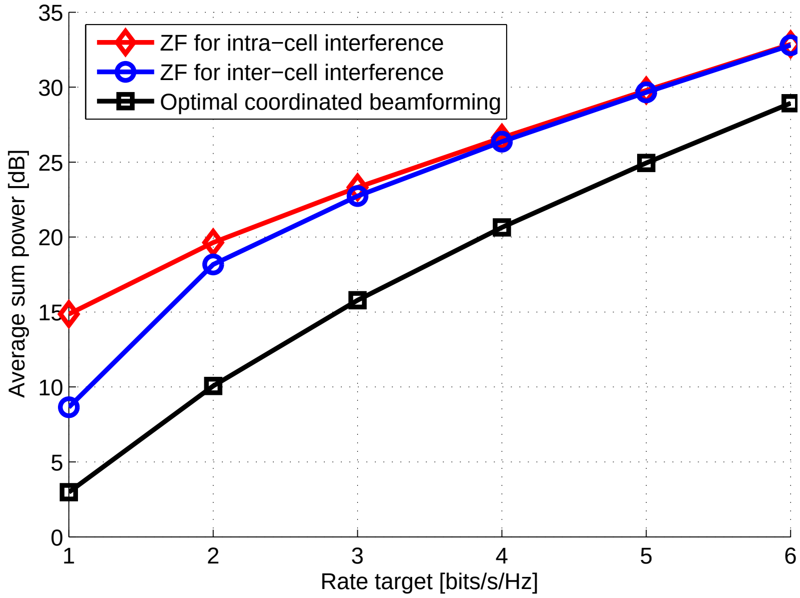

(a) $\eta = 3\text{dB}$

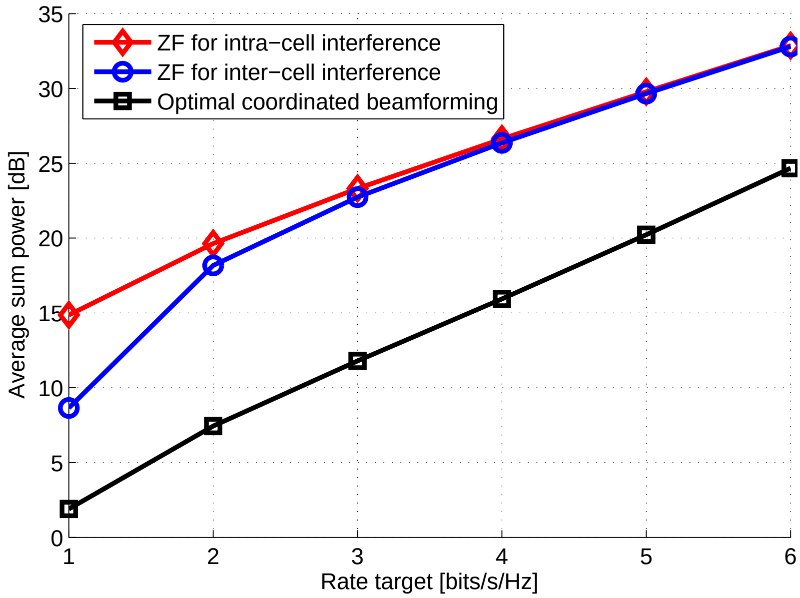

(b) $\eta = 15\text{dB}$

Fig 7. Average sum power versus rate target.

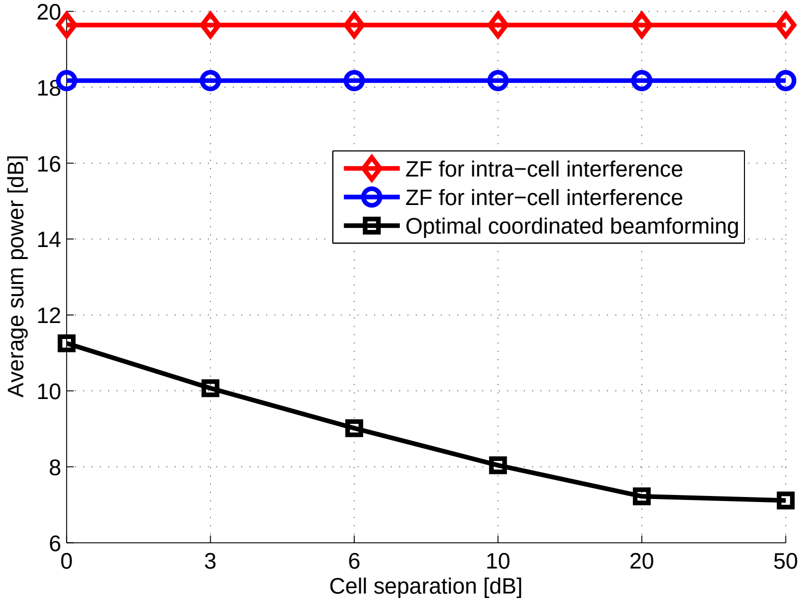

(a) $R = 2$ bits/s/Hz

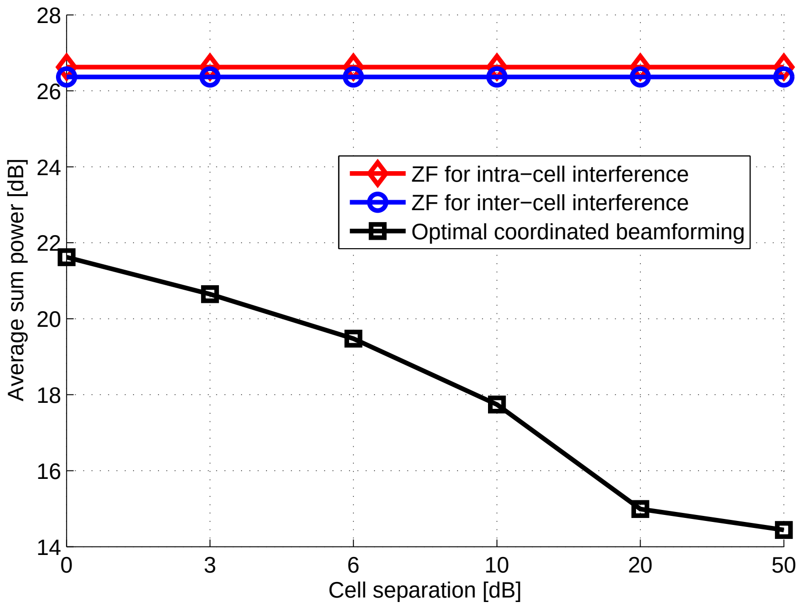

(b) $R = 4$ bits/s/Hz

Fig 8. Average sum power versus cell separation.

Per-user rate constraints are set equal for the users, i.e., $R_k = R$, $\forall k \in \mathcal{K}$. Dual variables and inter-cell interference variables are initialized as follows: $\delta_{b,k}^{(0)} = \delta^{(0)}$, $\chi_{b,k}^{(0)} = \chi^{(0)}$, $\forall b \in \mathcal{B}$, $\forall k \in \bar{\mathcal{K}}_b$.

In Figs. 7-8, the average sum power of various algorithms is evaluated in different system settings. The results are achieved by averaging over 1000 channel realizations. The following algorithms are compared to each other

– ZF beamforming for intra-cell interference
– ZF beamforming for inter-cell interference
– Optimal coordinated beamforming

In the simulations, the optimal results were achieved via centralized processing. However, optimal performance can also be obtained by allowing the decentralized dual and primal decomposition-based algorithms to converge. Fig. 7 illustrates the sum power as a function of the rate target. It can be observed that the coordinated beamforming scheme significantly outperforms the ZF-based algorithms. The performance gap increases with the increasing cell separation and decreases as the rate target increases. In Fig. 8, the sum power is plotted against cell separation. Again, the coordinated beamforming strategy has a superior performance when compared with the ZF strategies. The gain increases, as the cells become more isolated. For the higher rate target, the performance difference is smaller near the cell-edge.

Next, the convergence behavior of the proposed decentralized algorithms is examined by plotting the normalized sub-optimality as a function of the number of subgradient iterations in a single channel realization. The cell separation parameter is set to $\eta = 3$ dB for the rest of the simulations. The normalized sub-optimality is measured on a linear scale, and it is given by

$$\frac{P^{\mathrm{tx}(r)} - P^{\mathrm{tx}}_{\mathrm{opt}}}{P^{\mathrm{tx}}_{\mathrm{opt}}} \tag{40}$$

where $P^{\mathrm{tx}(r)}$ is the feasible sum power of the decentralized algorithm at iteration r and $P^{\mathrm{tx}}_{\mathrm{opt}}$ is the optimal centralized sum power. It is shown in Fig. 9 that the choice of step-size impacts the speed of convergence. Thus, properly chosen values can improve the convergence properties. In general, if the step-size is too small, the convergence speed can be slow but the convergence is more accurate. On the other hand, if the step-size is too large, the convergence can be fast at

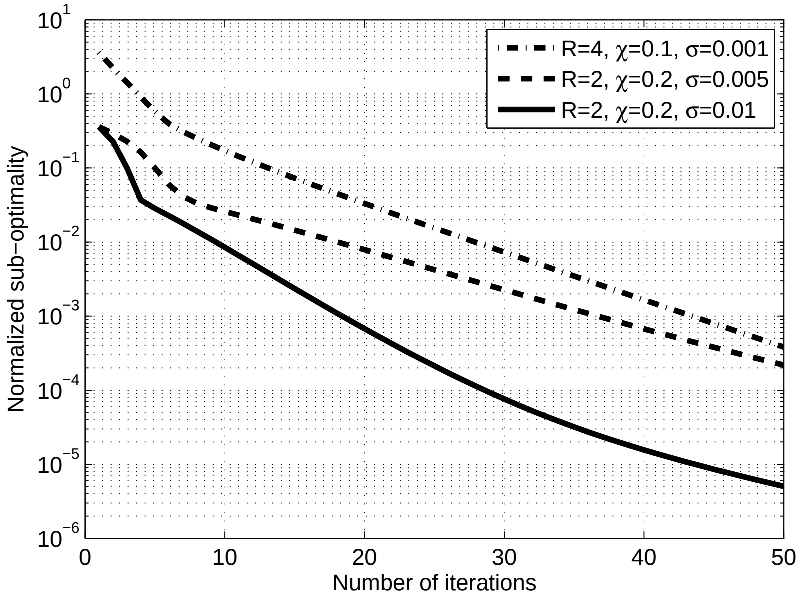

(a) Primal decomposition

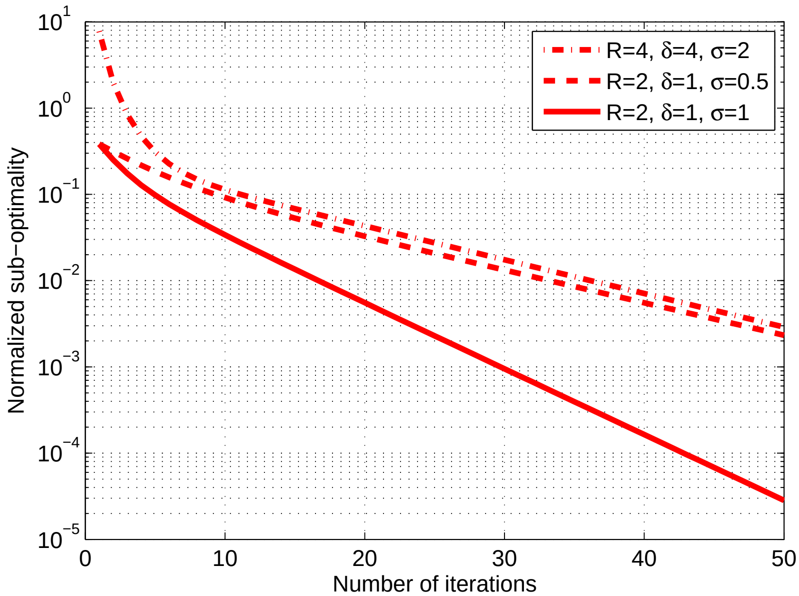

(b) Dual decomposition

Fig 9. Convergence behavior of primal and dual decomposition-based decentralized algorithms.

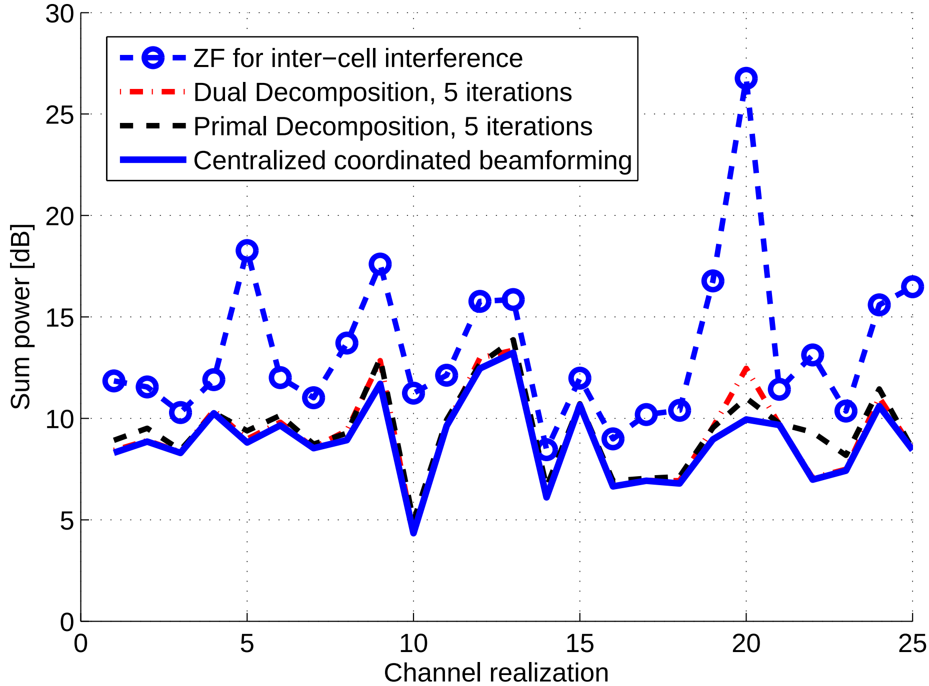

Fig 10. Sum power performance in quasi-static channel conditions.

the beginning, however, leading to the oscillation of the sum power near the optimal value. In other words, the accuracy of the convergence may not be as high as for the smaller step-size case. The speed of convergence is also affected by the initial values χ and δ, as shown in [61] and [60], respectively. The results also imply that the rate of convergence gets slower as the value of the rate target increases. Given the chosen parameters, the primal and dual decomposition-based algorithms seem to have somewhat similar convergence behavior. It can be seen that with properly chosen parameters, the convergence can be relatively fast for both algorithms. In terms of convergence comparison, it is difficult to provide ambiguous results since the convergence depends on the choice of the initial values and step-sizes. Thus, the results here act as suggestive examples.

It is worth noting that in general if the used step-size value of the projected subgradient method in primal decomposition method is too large, that may lead to a momentary increase of the sum power, especially when the resulting updated interference values go outside the feasible region (i.e., positive values) and need

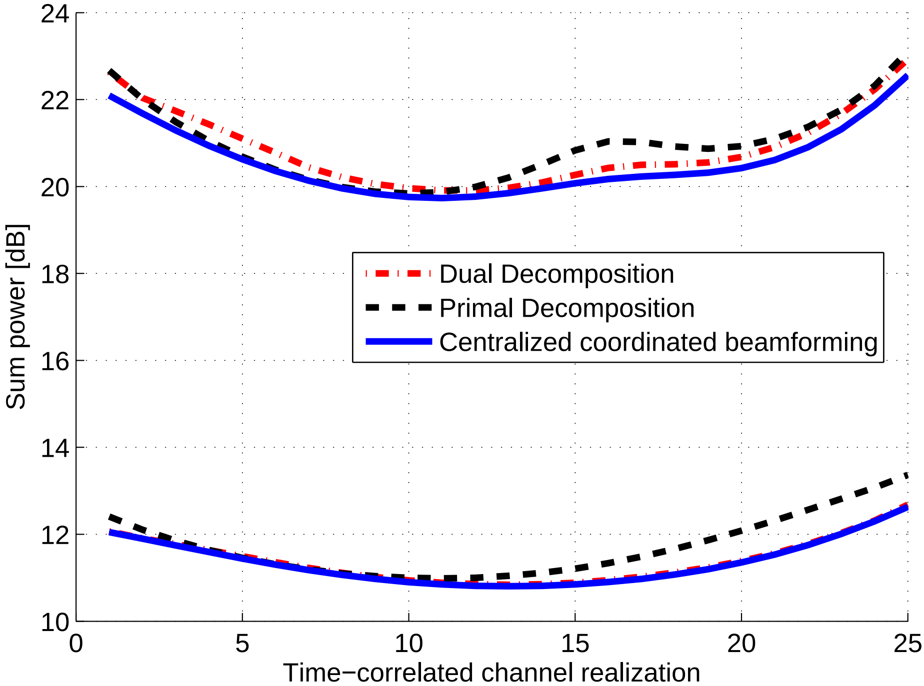

Fig 11. Sum power performance in time-correlated channel conditions.

to be projected back. To smooth and possibly speed up the convergence of the projected subgradient method, an adaptive step-size can be applied. The value of the step-size can be reduced such that the updated interference values remain always positive at any iteration, e.g., by dividing the current step-size (possible for many times) by two. This procedure can be performed locally without any extra backhaul signaling since each BS has the required knowledge of the corresponding interference values. In general, to guarantee the overall convergence of the projected subgradient method, we can switch back to a step-size with guaranteed convergence properties (e.g., non-summable and diminishing [156]) at any iteration. In the remainder of this section, adaptive step-sizes are used in the simulations for the projected subgradient method.

In Fig. 10, the sum powers of different transmission schemes are examined for quasi-static channel conditions. 25 independent Rayleigh faded channel realizations were generated. The dual and primal decomposition-based algorithms with different number of iterations are compared to the ZF and centralized beam-

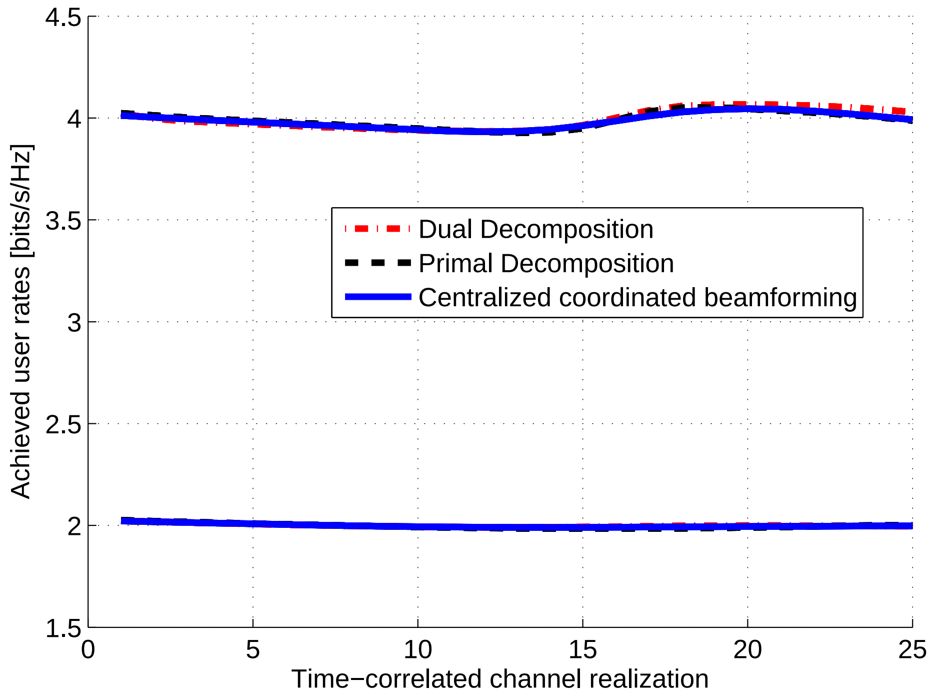

Fig 12. Achieved rate of user 4 in time-correlated channel conditions.

forming schemes. The rate target is set to $R = 2$ bits/s/Hz. As observed, both algorithms obtain near to optimal performance even after a few iterations. Moreover, the performance is superior to the ZF strategy.

Finally, the sum power performance of the decentralized algorithms is evaluated in time-correlated flat fading channel conditions. The corresponding channel realizations are generated using the Jakes' Doppler spectrum model. The channel variation rate is determined via a normalized user velocity parameter $T_{\mathrm{F}} f_{\mathrm{D}}$, where T_{F} is the duration of each uplink and downlink frame and f_{D} is the maximum Doppler shift. In the simulations, the sum power is measured after each transmit beamforming update phase, while the achieved user rates are computed after each reception phase. Channel conditions are let to change during each uplink and downlink frame. Thus, the exchanged backhaul information is always outdated for the decentralized algorithms.

Fig. 11 presents the sum power performance in 25 time-correlated channel realizations for $R = 2$ and $R = 4$ bits/s/Hz rate targets. In addition, the achieved instantaneous rate of user 4 is shown in Fig. 12 and the achieved average rates (over iterations and users) and their ratios to the target rate (in percentages) are presented in *Table 2*. The normalized user velocity is set to $T_{\mathrm{F}} f_{\mathrm{D}} = 0.005$. This can be interpreted as 2.7 km/h user velocity, assuming 2 GHz carrier frequency and 1 ms frame duration. The numerical results show that the dual and primal decomposition-based algorithms have comparable performance close to the centralized one. As expected, the instantaneous user rates may not always satisfy the minimum target rates, even when applying the centralized strategy, due to outdated channel and signaling information. However, it can also be seen that the average rates are very close to (or even equal to) the target rates.

Table 2. Average rates in time-correlated channel conditions.

	Centralized	Primal	Dual
$T_{\mathrm{F}} f_{\mathrm{D}} = 0.005,\ R = 2$	1.994 (99.7%)	2.000 (100%)	1.995 (99.7%)
$T_{\mathrm{F}} f_{\mathrm{D}} = 0.005,\ R = 4$	3.973 (99.3%)	3.968 (99.2%)	3.981 (99.5%)

2.3 Decentralized transmit beamforming design with imperfect CSI

In this section, the primal decomposition-based decentralized beamforming design is developed to solve the SPMin problem in a multi-cell multi-user MISO system, where CSI is assumed to be imperfect. Since the corresponding worst-case SPMin problem is not convex, it cannot be solved in its original form. In this respect, the non-convex problem needs to be approximated and reformulated as a tractable convex problem. The primal decomposition method can then be applied to solve the resulting problem in a decentralized manner relying on local imperfect CSI and low-rate backhaul signaling between the BSs. The primal decomposition part of the design is similar to that of the SPMin problem with perfect CSI, as described in Section 2.2. The proposed algorithm provides an optimal solution for the original non-convex problem if the convex approximation is tight.

2.3.1 Primal decomposition-based algorithm

The derivation of the algorithm begins by first reformulating the non-convex robust SPMin problem in (9) by adding auxiliary inter-cell interference variables so as to apply primal decomposition method in a later phase. The resulting problem is still non-convex, and thus, it is approximated and reformulated as a tractable convex SDP via the conventional SDR approximation [103] and the S-Procedure [81] methods. The primal decomposition method is then proposed to solve the resulting problem in a decentralized manner by decomposing it into a network-wide master problem and BS-specific subproblems. Since the subproblems are convex SDPs, they can be solved by using any standard SDP solver, for example CVX [88]. The master problem is handled by using the projected subgradient method. Decentralized implementation is enabled by having local imperfect CSI at each BS and exchanging scalar information between the BSs via low-rate backhaul links.

Problem approximation and reformulation

The robust SPMin problem (9) is reformulated by introducing auxiliary inter-cell interference power variables $\{\chi_{b,k}\}_{b\in\mathcal{B},k\in\bar{\mathcal{K}}_b}$. The resulting optimization problem is given by

$$\begin{aligned}
\min_{\{\mathbf{m}_k,\boldsymbol{\chi}\}_{k\in\mathcal{K}}} \quad & \sum_{k\in\mathcal{K}} \mathrm{tr}\left(\mathbf{m}_k\mathbf{m}_k^{\mathrm{H}}\right) \\
\text{s. t.} \quad & \left(\hat{\mathbf{h}}_{b_k,k}+\mathbf{u}_{b_k,k}\right)\left(\tfrac{1}{\gamma_k}\mathbf{m}_k\mathbf{m}_k^{\mathrm{H}} - \sum_{i\in\mathcal{K}_{b_k}\setminus\{k\}}\mathbf{m}_i\mathbf{m}_i^{\mathrm{H}}\right)\left(\hat{\mathbf{h}}_{b_k,k}+\mathbf{u}_{b_k,k}\right)^{\mathrm{H}} \\
& \geq N_0 + \sum_{b'\in\mathcal{B}\setminus\{b_k\}} \chi_{b',k}, \forall \mathbf{u}_{b_k,k}\in\mathcal{E}_{b_k,k}, \forall k\in\mathcal{K} \\
& \sum_{i\in\mathcal{K}_b}\left(\hat{\mathbf{h}}_{b,k}+\mathbf{u}_{b,k}\right)\mathbf{m}_i\mathbf{m}_i^{\mathrm{H}}\left(\hat{\mathbf{h}}_{b,k}+\mathbf{u}_{b,k}\right)^{\mathrm{H}} \leq \chi_{b,k}, \\
& \forall \mathbf{u}_{b,k}\in\mathcal{E}_{b,k}, \forall b\in\mathcal{B}, \forall k\in\bar{\mathcal{K}}_b
\end{aligned} \tag{41}$$

Problem (41) is equivalent to the original problem (9) since the added inter-cell interference constraints hold with equality at the optimal solution. In order to turn (9) into a tractable convex form, the principles presented in [89, 125] are followed. First, (9) is approximated as a convex SDP by replacing the rank one matrix $\mathbf{m}_k\mathbf{m}_k^{\mathrm{H}}$ by a semidefinite matrix $\mathbf{Q}_k \succeq 0$, of which rank can be higher than one. However, the constraints are still intractable due to the infinite number of CSI uncertainty realizations. In this respect, the S-Procedure method [81] can be used to obtain an equivalent reformulation of the constraints leading to the tractable convex SDP problem

$$\begin{array}{lll} \underset{\substack{\boldsymbol{\chi},\{\mathbf{Q}_k,\omega_k\}_{k\in\mathcal{K}} \\ \{\beta_{b,k}\}_{b\in\mathcal{B},k\in\bar{\mathcal{K}}_b}}}{\min.} & \sum_{k\in\mathcal{K}} \operatorname{tr}(\mathbf{Q}_k) & \\ \text{s. t.} & \mathbf{Q}_k \succeq 0, \boldsymbol{\Delta}_k \succeq 0, \omega_k \geq 0, \forall k \in \mathcal{K} & \\ & \boldsymbol{\Theta}_{b,k} \succeq 0, \beta_{b,k} \geq 0, \forall b \in \mathcal{B}, \forall k \in \bar{\mathcal{K}}_b. & \end{array} \tag{42}$$

where $\{\omega_k\}_{k\in\mathcal{K}}$ and $\{\beta_{b,k}\}_{b\in\mathcal{B},k\in\bar{\mathcal{K}}_b}$ are slack variables. The matrixes $\boldsymbol{\Delta}_k$ and $\boldsymbol{\Theta}_{b,k}$ are denoted by

$$\boldsymbol{\Delta}_k = \left[\begin{array}{cc} \mathbf{A}_k + \omega_k \mathbf{E}_{b_k,k} & \mathbf{A}_k \hat{\mathbf{h}}_{b_k,k}^{\mathrm{H}} \\ \hat{\mathbf{h}}_{b_k,k}\mathbf{A}_k & \hat{\mathbf{h}}_{b_k,k}\mathbf{A}_k\hat{\mathbf{h}}_{b_k,k}^{\mathrm{H}} - \sum_{b'\in\mathcal{B}\setminus\{b_k\}} \chi_{b',k} - N_0 - \omega_k \end{array}\right] \tag{43}$$

and

$$\boldsymbol{\Theta}_{b,k} = \left[\begin{array}{cc} -\mathbf{B}_b + \beta_{b,k}\mathbf{E}_{b,k} & -\mathbf{B}_b\hat{\mathbf{h}}_{b,k}^{\mathrm{H}} \\ -\hat{\mathbf{h}}_{b,k}\mathbf{B}_b & -\hat{\mathbf{h}}_{b,k}\mathbf{B}_b\hat{\mathbf{h}}_{b,k}^{\mathrm{H}} + \chi_{b,k} - \beta_{b,k} \end{array}\right] \tag{44}$$

where

$$\mathbf{A}_k = \frac{1}{\gamma_k}\mathbf{Q}_k - \sum_{i\in\mathcal{K}_{b_k}\setminus\{k\}} \mathbf{Q}_i, \qquad \mathbf{B}_b = \sum_{i\in\mathcal{K}_b} \mathbf{Q}_i. \tag{45}$$

Due to convexity, (42) can be optimally solved in a centralized manner if having a central controller with global imperfect CSI. The optimal solution of (42) is also globally optimal for the non-convex problem (9) only if the optimal transmit covariance matrices $\{\mathbf{Q}_k\}_{k\in\mathcal{K}}$ are all rank-one. In general, rank-one solutions cannot be guaranteed for (42). However, there are some special cases where rank-one solutions are always guaranteed. It was proved in [160] that rank-one solutions are always achieved for two special cases in a single-cell multi-user MISO system, i.e., the BS has at most two transmit antennas and the spherical/ellipsoidal error region is sufficiently small. In [160], however, the authors remarked that the proposed rank-one bound for the error region may be too conservative since the simulation results demonstrated rank-one solutions also for much larger error regions. In the multi-cell setting, it was shown in [89] that (42) yields always rank-one solutions for three special cases, i.e., single-user per each cell, perfect intra-cell CSI, or a small enough spherical error region. The simulation examples in Section 2.3.2 show that (42) yields rank-one solutions with high probability even when the ellipsoidal error region is relatively large. Similar results were noticed in [125] for a robust cognitive single-cell MISO beamforming case with spherical error regions.

In case (42) yields a higher-rank solution, a feasible rank-one solution can be constructed from the higher-rank solution by using an approximation method. A simple approximation method was proposed for a non-robust cognitive beamforming system in [126]. This approximation method can be extended to the centralized robust multi-cell beamforming problem (42). The idea is to fix beamforming directions by using the principal eigenvectors of the higher rank matrixes, and then optimize the powers to satisfy all the constraints. Specifically, (42) is modified by replacing $\mathbf{Q}_k$ with $\tilde{\mathbf{Q}}_k$ and introducing a set of additional constraints $\tilde{\mathbf{Q}}_k = p_k \tilde{\mathbf{m}}_k \tilde{\mathbf{m}}_k^{\mathrm{H}}, \forall k \in \mathcal{K}$, where $\tilde{\mathbf{m}}_k$ is the dominant eigenvector of $\mathbf{Q}_k$ and the power p_k is an optimization variable. If the resulting approximation problem is infeasible, the robust multi-cell beamforming problem is declared as "infeasible". Then, it is the responsibility of admission control to relax the system requirements, e.g., lower the minimum SINR targets or reduce the number of active users.

BS-specific and network-wide optimization steps

In order to allow a decentralized implementation, (42) is decomposed via primal decomposition into a network-wide master problem and BS-specific subproblems. A similar procedure is followed here as described in Section 2.2.1 where the primal decomposition method was applied to a non-robust SPMin problem with the assumption of perfect CSI. The subproblem at BS b for a fixed $\boldsymbol{\chi}_b$ is a convex SDP:

$$
\begin{aligned}
\min_{\{\mathbf{Q}_k,\omega_k\}_{k\in\mathcal{K}_b},\{\beta_{b,k}\}_{k\in\bar{\mathcal{K}}_b}} \quad & \textstyle\sum_{k\in\mathcal{K}_b} \operatorname{tr}(\mathbf{Q}_k) \\
\text{s. t.} \quad & \mathbf{Q}_k \succeq 0, \boldsymbol{\Delta}_k \succeq 0, \omega_k \geq 0, \forall k \in \mathcal{K}_b \\
& \boldsymbol{\Theta}_{b,k} \succeq 0, \beta_{b,k} \geq 0, \forall k \in \bar{\mathcal{K}}_b.
\end{aligned} \tag{46}
$$

The master problem is given by

$$
\begin{aligned}
\min_{\{\boldsymbol{\chi}_b\}_{b\in\mathcal{B}}} \quad & \sum_{b\in\mathcal{B}} g_b^{\star}(\boldsymbol{\chi}_b) \\
\text{s. t.} \quad & \boldsymbol{\chi}_b \in R_{++}^{N_b}, \forall b \in \mathcal{B}
\end{aligned} \tag{47}
$$

where $g_b^{\star}(\boldsymbol{\chi}_b)$ denotes the optimal objective value of the subproblem (46) for a given $\boldsymbol{\chi}_b$. The master problem (47) is in charge of optimizing each $\chi_{b,k}$ via the iterative updates of the following projected subgradient method

$$\chi_{b,k}^{(r+1)} = P_{++}\left\{\chi_{b,k}^{(r)} - \sigma^{(r)} u_{b,k}^{(r)}\right\} \quad (48)$$

where $\mathcal{P}_{++}$ projects the possible negative values into positive orthant. At iteration r, $\sigma^{(r)}$ and $u_{b,k}^{(r)}$ are the step-size and the subgradient of (15) evaluated at point $\chi_{b,k}^{(r)}$, respectively.

Due to the convexity of (42), strong duality holds, provided that (42) is also strictly feasible. In other words, (42) can be optimally solved via its dual problem. Given this fact, subgradients can be obtained similarly as described in Section 2.2.1. Consequently, the subgradient at point $\chi_{b,k}^{(r)}$ can be written as $u_{b,k}^{(r)} = \lambda_{b,k}^{(r)} - \mu_{b,k}^{(r)}$, where $\lambda_{b,k}^{(r)}$ and $\mu_{b,k}^{(r)}$ are the optimal dual variables with respect to $\chi_{b,k}^{(r)}$ in the b_kth and bth subproblems, respectively. Strong duality also holds for (46) since it is a simplified version of (42). Thus, the optimal dual variables can be solved via the primal problem (46) or the Lagrange dual problem of (46). By solving the primal problem for $\{\mathbf{Q}_k\}_{k\in\mathcal{K}_b}$, the optimal dual variables $\{\lambda_{b,k}\}_{k\in\mathcal{K}_b}$ and $\{\mu_{b,k}\}_{k\in\bar{\mathcal{K}}_b}$ are obtained as side information since when using standard SDP solvers (e.g., CVX [88]), the dual variables are usually provided as a certificate for optimality. By solving the dual problem, the optimal dual variables are achieved explicitly. However, transmit covariance matrixes $\{\mathbf{Q}_k\}_{k\in\mathcal{K}_b}$ still need to be computed via the primal problem. To avoid solving the dual and primal problems separately, we focus solely on the primal one.

With local imperfect CSI and scalar backhaul information exchange between the BSs, the subproblem (46) and the corresponding part of the master problem (47), i.e., the update of $\boldsymbol{\chi}_b$, can be solved independently at BS b for all $b \in \mathcal{B}$ in parallel. The same total amount of backhaul signaling is needed as in the non-robust algorithm in Section 2.2.1, i.e., $2B(B-1)K_b$. The proposed decentralized beamforming design is summarized in *Algorithm 4*. Convergence to the optimal solution of (42) is guaranteed, provided that a proper step-size is selected. The proposed algorithm provides an optimal solution for the original non-convex problem (9), if the optimal transmit covariance matrices are all rank-one. Note that in the case of a higher-rank solution, it may be challenging to apply the known approximation methods, such as proposed in Section 2.3.1 and [34], for the decentralized design. In this case, the optimization problem is usually infeasible when only optimizing the powers, while the beamformers and inter-cell interference variables are fixed. However, to enable decentralized implementation, it is possible to use the principal eigenvectors of $\{\mathbf{Q}_k\}_{k\in\mathcal{K}_b}$ as the transmit beamformers and allow some violation of the rate constraints. The practical features discussed in Section 2.2.1 are also applicable for the proposed robust algorithm.

Algorithm 4 Decentralized robust transmit beamforming design based on primal decomposition for cellular MISO system

---

1: Set $r = 0$. Initialize inter-cell interference variables $\boldsymbol{\chi}_b^{(0)}$.
2: **repeat**
3: Compute transmit covariance matrices $\{\mathbf{Q}_k\}_{k\in\mathcal{K}_b}$ and dual variables $\{\lambda_{b,k}\}_{k\in\mathcal{K}_b}$ and $\{\mu_{b,k}\}_{k\in\bar{\mathcal{K}}_b}$ by solving SDP (46).
4: Communicate $\{\lambda_{b,k}\}_{k\in\mathcal{K}_b}$ and $\{\mu_{b,k}\}_{k\in\bar{\mathcal{K}}_b}$ to the coupled BSs via backhaul.
5: Update inter-cell interference variable $\boldsymbol{\chi}_b^{(r+1)}$ via projected subgradient method (48).
6: Set $r = r + 1$.
7: **until** desired level of convergence

2.3.2 Numerical evaluation

This section provides a performance evaluation of the robust primal decomposition -based decentralized algorithm. The focus is on the convergence behavior and the probabilities of feasible and rank-one solutions. The used simulation model is the same as that in Section 2.2.3. The main system parameters are given by $\{B, K, A_{\mathrm{T}}, A_{\mathrm{R}}\} = \{2, 4, 4, 1\}$. Here, a cell-edge case is modeled by setting the cell separation parameter to 0 dB. For the simulation results presented in *Tables 3* and *4*, the CSI errors are bounded by an ellipsoidal region, i.e., $\mathbf{E}_{b,k} = \mathbf{E} = \left(1/e^2\right)\hat{\mathbf{E}}$, $\forall b \in \mathcal{B}$, $\forall k \in \mathcal{K}$, where $\hat{\mathbf{E}} = \mathrm{diag}(4, 2, 0.5, 0.25)$. For the rest of the simulations, a spherical CSI error modeling is used, i.e., $\mathbf{E}_{b,k} = \mathbf{E} = \left(1/e^2\right)\mathbf{I}_T$, $\forall b \in \mathcal{B}$, $\forall k \in \mathcal{K}$. The rate targets are set equal among the users, i.e., $R_k = R$, $\forall k \in \mathcal{K}$.

In *Table 3* and *Table 4*, the probability of feasible and rank-one solutions for (42) is presented for 50000 channel realizations with various values of the error region radius e and the rate target R. The simulation results show that when e becomes large enough, the problem is infeasible with high probability.

Table 3. Probability that (42) **is feasible ([105] © 2014 IEEE).**

e	0.005	0.01	0.1	0.2	0.4	0.6
$R = 1$ bits/s/Hz	1	1	1	0.9942	0.6441	0.1114
$R = 3.5$ bits/s/Hz	1	0.9996	0.5016	0.0263	0	0
$R = 6.7$ bits/s/Hz	0.9843	0.9221	0	0	0	0

Table 4. Probability that the feasible solution of (42) **is rank-one ([105] © 2014 IEEE).**

e	0.005	0.01	0.1	0.2	0.4	0.6
$R = 1$ bits/s/Hz	1	1	1	0.9998	0.9910	0.9758
$R = 3.5$ bits/s/Hz	0.9997	0.9991	0.9835	0.9711	-	-
$R = 6.7$ bits/s/Hz	0.9673	0.9630	-	-	-	-

In these cases, the system requirements need to be relaxed to obtain a feasible problem. For feasible (42), the probability of achieving rank-one solution is high. Thus, decentralized approaches are mostly applicable. The probability of having rank-one solutions increases with the decreasing e and R.

Fig. 13 shows the normalized sub-optimality of the primal decomposition-based algorithm as a function of iteration r. Convergence behavior is studied for $e = 0.1$ and $e = 0.01$ error region radii with the rate target of $R = 1$ bits/s/Hz. The speed of convergence is shown to be comparable for both cases, and it is relatively fast in general. It was shown in [105] that the proposed primal decomposition-based algorithm has a similar performance with slightly lower computational complexity when compared with that of the ADMM-based approach in [89].

2.4 Summary and discussions

In this chapter, novel decentralized coordinated beamforming algorithms were developed to solve the SPMin problem in multi-cell multi-user MISO systems. The proposed algorithms are based on primal and dual decomposition methods, which turn the reformulated convex optimization problem into two optimization levels by introducing BS-specific subproblems controlled by a network-wide master problem. The subproblems are solved for fixed coupling variables, while the master problem iteratively optimizes the coupling variables via subgradient method that requires some information from the solved subproblems at each it-

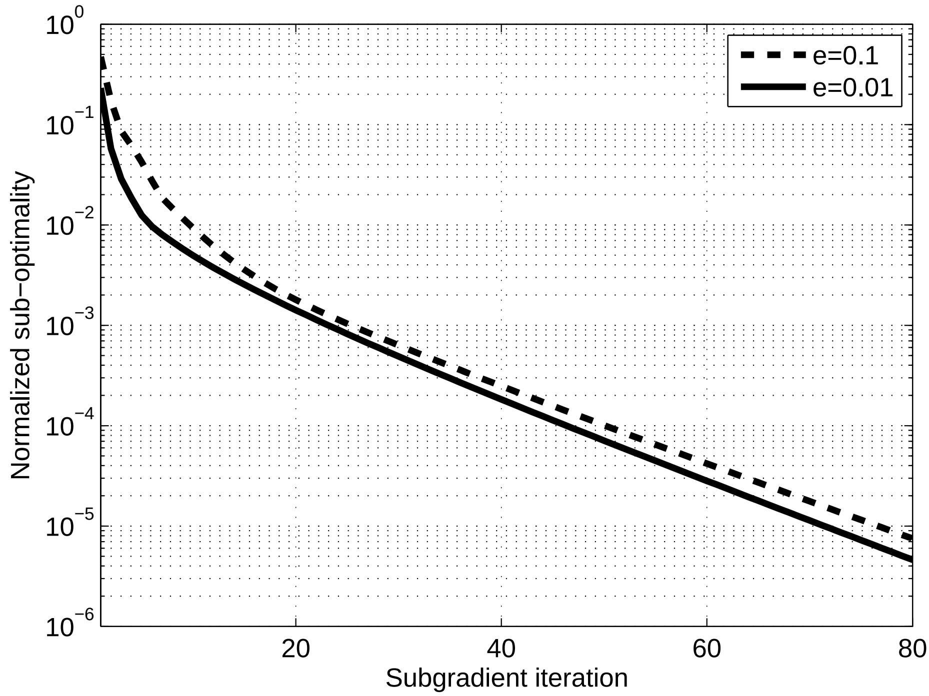

Fig 13. Convergence behavior of primal decomposition-based decentralized algorithm ([105] © 2014 IEEE).

eration. Decentralized implementation is enabled by acquiring local CSI at each BS and allowing scalar information exchange between the coupled BSs via low-rate backhaul links. In the primal decomposition-based algorithm, the coupling variables are inter-cell interference powers, while the exchanged information are the dual variables associated with the fixed inter-cell interference variables. The subproblems can be solved in one shot by using standard convex optimization techniques or alternatively by using an iterative uplink-downlink duality-based method. In the dual decomposition-based algorithm, the coupling variables are the dual variables associated with the local copies of inter-cell interference powers and the exchanged information are the local copies of the inter-cell interference powers. The subproblems are solved by using convex optimization techniques. A detailed discussion on the similarities and differences of the proposed primal and dual decomposition methods were provided.

The proposed decentralized algorithms provide an optimal solution if they are allowed to converge with properly chosen step-sizes. Since the algorithms can provide feasible beamformers at each iteration, delay and signaling overhead can be reduced at the cost of sub-optimal performance by limiting the number of performed iterations. The simulation results demonstrated that performance close to a centralized algorithm is achieved only after a few iterations. Since the signaling load per iteration is relatively small, the signaling overhead can be greatly reduced while achieving near to centralized performance. Further, the proposed algorithms obtained near to centralized performance in time-correlated channel conditions, where the channel and backhaul signaling information is outdated. Simplified designs are allowed to further reduce the signaling and computational load while somewhat increasing the sum power. The promising results provided by the simple two-cell simulator serve as the performance upper bounds for more realistic system-level implementations.

The effect of an imperfect local CSI was also considered, and a primal decomposition-based robust beamforming algorithm was proposed. The original non-convex problem is first approximated and reformulated as a tractable convex problem via the standard SDR and S-procedure methods. The resulting problem is then decomposed via primal decomposition into BS-specific subproblems and a network-wide master problem, which can be solved in a decentralized manner by relying on low-rate backhaul signaling and local imperfect CSI. The proposed algorithm gives an optimal solution for the original non-convex problem, provided that the convex approximation is tight, i.e., the obtained solution is rank-one. The numerical results demonstrated that the probability of achieving rank-one solutions is high. Moreover, the speed of convergence is relatively fast.

Due to its practical nature, the primal decomposition-based decentralized concept is extended to cellular multi-user MIMO and cognitive multi-user MISO networks in Chapters 3 and 4, respectively.

3 Coordinated beamforming in MIMO cellular networks

In this chapter, coordinated beamforming is considered for cellular multi-user MIMO systems. The focus is on designing transmit and receive beamformers for the SPMin problem with per-user rate targets. Both centralized and decentralized beamforming algorithms are proposed.

Section 3.1 presents the multi-cell multi-user MIMO system model and formulates the SPMin problem with perfect CSI assumption. Centralized and decentralized MIMO beamforming designs are developed in Sections 3.2 and 3.3, respectively. Significant performance gains over MISO algorithms and state-of-the-art schemes are demonstrated via a numerical evaluation in Section 3.3.3. Summary and discussion is provided in Section 3.4.

3.1 System model and SPMin problem formulation

The considered multi-cell multi-user MIMO system consists of B BSs, each equipped with A_{T} transmit antennas, and K users with A_{R} receive antennas each. The sets of all BSs and all users are denoted by $\mathcal{B}$ and $\mathcal{K}$, respectively. The number of users served by BS b is given by K_b, and the corresponding set of users is denoted by $\mathcal{K}_b$. The set of users associated with other BSs is denoted by $\bar{\mathcal{K}}_b = \mathcal{K} \setminus \mathcal{K}_b$. User k can receive multiple data streams from its serving BS b_k. The number of spatial data streams allocated to user k is denoted by L_k, and the corresponding set is given by $\mathcal{L}_k$. The lth stream of the kth user is denoted by (k, l). User and beam allocation is assumed to be predefined and fixed. The considered system is illustrated in Fig. 14. The received signal vector of the kth user is given by

$$\mathbf{y}_k = \mathbf{H}_{b_k,k}\mathbf{m}_{k,l}x_{k,l} + \sum_{i\in\mathcal{K}} \sum_{j\in\mathcal{L}_i,(i,j)\neq(k,l)} \mathbf{H}_{b_i,k}\mathbf{m}_{i,j}x_{i,j} + \mathbf{n}_k \qquad (49)$$

where $\mathbf{H}_{b_k,k} \in \mathbb{C}^{A_{\mathrm{R}}\times A_{\mathrm{T}}}$ is the MIMO channel matrix from the b_kth BS to the kth user, $\mathbf{m}_{k,l} \in \mathbb{C}^{A_{\mathrm{T}}\times 1}$ is the unnormalized beamforming vector for the lth stream of user k and $x_{k,l} \in \mathbb{C}$ is the corresponding normalized complex data symbol. The vector $\mathbf{n}_k \sim \mathcal{CN}(\mathbf{0}, N_0\mathbf{I}_{A_{\mathrm{R}}})$ represents the circularly symmetric complex

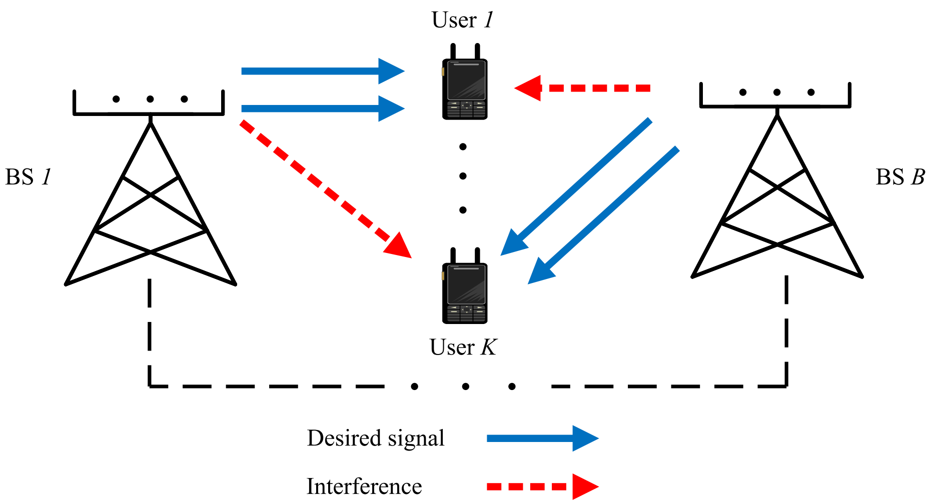

Fig 14. Multi-cell multi-user MIMO system.

white Gaussian noise vector with zero mean and variance N_0 per element. The sum power of the BSs is given by

$$P^{\mathrm{tx}} = \sum_{k\in\mathcal{K}} \sum_{l\in\mathcal{L}_k} \|\mathbf{m}_{k,l}\|_2^2 \tag{50}$$

The rate for user k is expressed as

$$r_k = \sum_{l\in\mathcal{L}_k} \log_2\left(1+\Gamma_{k,l}\right) \tag{51}$$

where $\Gamma_{k,l}$ is the SINR of stream (k,l)

$$\Gamma_{k,l} = \frac{\left|\mathbf{w}_{k,l}^{\mathrm{H}}\mathbf{H}_{b_k,k}\mathbf{m}_{k,l}\right|^2}{N_0\|\mathbf{w}_{k,l}\|_2^2 + \sum\limits_{i\in\mathcal{K}} \sum\limits_{j\in\mathcal{L}_i,(i,j)\neq(k,l)} \left|\mathbf{w}_{k,l}^{\mathrm{H}}\mathbf{H}_{b_i,k}\mathbf{m}_{i,j}\right|^2} \tag{52}$$

The receive beamformer for the lth stream of user k is $\mathbf{w}_{k,l} \in \mathbb{C}^{A_{\mathrm{R}}\times 1}$.

The network optimization problem is to minimize the sum transmission power of the coordinated BSs subject to the user-specific minimum rate constraints $\{R_k\}_{k\in\mathcal{K}}$. This problem is expressed as

$$\begin{aligned} \min_{\{\mathbf{m}_{k,l},\mathbf{w}_{k,l}\}_{k\in\mathcal{K},l\in\mathcal{L}_k}} \quad & \sum_{k\in\mathcal{K}} \sum_{l\in\mathcal{L}_k} \|\mathbf{m}_{k,l}\|_2^2 \\ \text{s. t.} \quad & \sum_{l\in\mathcal{L}_k} \log_2\left(1+\Gamma_{k,l}\right) \geq R_k, \forall k\in\mathcal{K}. \end{aligned} \tag{53}$$

Problem (53) cannot be solved in its current form since is not jointly convex in $\{\mathbf{m}_{k,l}\}_{k\in\mathcal{K},l\in\mathcal{L}_k}$ and $\{\mathbf{w}_{k,l}\}_{k\in\mathcal{K},l\in\mathcal{L}_k}$. Thus, finding efficient approximated (sub-optimal) solutions with convergence of the objective function and tractable computational complexity is of practical interest.

Problem (53) can be solved iteratively, such that the sum power converges by dividing the problem into receive and transmit beamforming optimization steps, which are then alternatingly solved. More precisely, the receive beamformers are optimized while keeping the transmit beamformers fixed, and vice versa. For fixed transmit beamformers, the well-known linear MMSE receiver [161] is optimal in the sense that it maximizes per-stream SINRs, and equivalently the per-user rates. The optimality of the MMSE receiver can also be shown via the Karush-Kuhn-Tucker (KKT) conditions of (53) for the given $\{\mathbf{m}_{k,l}\}_{k\in\mathcal{K},l\in\mathcal{L}_k}$. For user k and stream l, the linear MMSE receiver is given by

$$\begin{aligned}\tilde{\mathbf{w}}_{k,l} &= \left(\sum_{i\in\mathcal{K}}\sum_{j\in\mathcal{L}_k}\mathbf{H}_{b_i,k}\mathbf{m}_{i,j}\mathbf{m}_{i,j}^{\mathrm{H}}\mathbf{H}_{b_i,k}^{\mathrm{H}} + N_0\mathbf{I}_{A_{\mathrm{R}}}\right)^{-1} \\ &\quad \mathbf{H}_{b_k,k}\mathbf{m}_{k,l}. \end{aligned} \tag{54}$$

Since the MMSE receiver is assumed to be used, the relation between the MSE and SINR can be exploited to reformulate the original optimization problem (53). The MSE of stream l of user k is given by

$$\begin{aligned}\epsilon_{k,l} &= \mathrm{E}\left[\left|\mathbf{w}_{k,l}^{\mathrm{H}}\mathbf{y}_k - x_{k,l}\right|^2\right] = \left|1-\mathbf{w}_{k,l}^{\mathrm{H}}\mathbf{H}_{b_k,k}\mathbf{m}_{k,l}\right|^2 + \\ &\quad N_0\|\mathbf{w}_{k,l}\|_2^2 + \sum_{i\in\mathcal{K}}\sum_{j\in\mathcal{L}_i,(i,j)\neq(k,l)}\left|\mathbf{w}_{k,l}^{\mathrm{H}}\mathbf{H}_{b_i,k}\mathbf{m}_{i,j}\right|^2. \end{aligned} \tag{55}$$

Using (54) in (55) yields a well-known relation between the MSE and SINR [162], i.e.,

$$\tilde{\epsilon}_{k,l}^{-1} = 1 + \tilde{\Gamma}_{k,l} \tag{56}$$

where $\tilde{\epsilon}_{k,l}$ and $\tilde{\Gamma}_{k,l}$ are the MSE and SINR assuming that the MMSE receiver $\tilde{\mathbf{w}}_{k,l}$ is used. Using (56) and keeping the MMSE receives fixed, the transmit beamforming optimization part of (53) can be reformulated as

$$\begin{aligned} \min_{\{\mathbf{m}_{k,l}\}_{k\in\mathcal{K},l\in\mathcal{L}_k}} \quad & \sum_{k\in\mathcal{K}}\sum_{l\in\mathcal{L}_k}\left\|\mathbf{m}_{k,l}\right\|_2^2 \\ \text{s. t.} \quad & \sum_{l\in\mathcal{L}_k}\log_2\left(\tilde{\epsilon}_{k,l}^{-1}\right) \geq R_k, \forall k\in\mathcal{K}. \end{aligned} \tag{57}$$

Problem (57) can be reformulated as the difference of convex functions program (DCP) [163] by introducing an additional upper bounding constraint for each MSE term. This procedure follows the idea presented in [71]. The resulting constraint is given by

$$\tilde{\epsilon}_{k,l} \quad \leq \quad \alpha^{-t_{k,l}} \tag{58}$$

where α is fixed and chosen such that $\alpha > 1$. The value of $\alpha = 2$ is used in the numerical examples in Section 3.3.3. Moreover, $t_{k,l}$ is an auxiliary variable with an assumption that $\alpha^{t_{k,l}} \in [1, \infty)$. Thus, the function $\alpha^{-t_{k,l}}$ is convex, and its domain is in the range of possible MSE values, i.e., $(0, 1]$. By applying (58), (57) can be reformulated as

$$\begin{array}{ll} \underset{\{\mathbf{m}_{k,l}, t_{k,l}\}_{k\in\mathcal{K}, l\in\mathcal{L}_k}}{\min.} & \sum_{k\in\mathcal{K}} \sum_{l\in\mathcal{L}_k} \left\|\mathbf{m}_{k,l}\right\|_2^2 \\ \text{s. t.} & \tilde{\epsilon}_{k,l} \leq \alpha^{-t_{k,l}} \forall k \in \mathcal{K}, \forall l \in \mathcal{L}_k \\ & \sum_{l\in\mathcal{L}_k} \log_2\left(\alpha^{t_{k,l}}\right) \geq R_k, \forall k \in \mathcal{K}. \end{array} \tag{59}$$

Constraints in (59) hold with equality at the optimal solution making the relaxation tight. Problem (59) is still non-convex. However, it can be solved efficiently by using an iterative approximation method as described next.

To turn (59) into a computationally tractable form, the non-convex DCP constraints can be approximated as convex ones. By iteratively solving these convex problems one after another, the transmit beamforming problem can be efficiently solved, such that the sum power converges. The procedure, where the approximated convex problem is repeatedly solved, is known as the successive convex approximation (SCA) method [163, 164].

Obtaining the convex approximations of the non-convex DCP constraints, $f(t_{k,l}) = \alpha^{-t_{k,l}}$ can be linearly approximated at a given point $t_{k,l}^{(q)}$ by forming the first-order Taylor series approximation [71, 163], i.e.,

$$\begin{aligned} \bar{f}(t_{k,l}, t_{k,l}^{(q)}) &= f(t_{k,l}^{(q)}) + (t_{k,l} - t_{k,l}^{(q)}) f'_{t_{k,l}}(t_{k,l}^{(q)}) && (60) \\ &= -c_{k,l}^{(q)} t_{k,l} + d_{k,l}^{(q)} && (61) \end{aligned}$$

where q is the iteration index, $f'_{t_{k,l}}(t_{k,l}^{(q)})$ is the first-order partial derivative of f w.r.t. $t_{k,l}$, and

$$c_{k,l}^{(q)} = \log_e(\alpha)\alpha^{-t_{k,l}^{(q)}}, \quad d_{k,l}^{(q)} = \alpha^{-t_{k,l}^{(q)}}\left(1 + \log_e(\alpha) t_{k,l}^{(q)}\right). \tag{62}$$

The resulting optimization problem at the qth iteration for fixed $\{t_{k,l}^{(q)}\}_{k\in\mathcal{K},l\in\mathcal{L}_k}$ is expressed as

$$\begin{array}{ll}\underset{\{\mathbf{m}_{k,l},t_{k,l}\}_{k\in\mathcal{K},l\in\mathcal{L}_k}}{\min.} & \sum_{k\in\mathcal{K}}\sum_{l\in\mathcal{L}_k}\left\|\mathbf{m}_{k,l}\right\|_2^2 \\ \text{s. t.} & \tilde{\epsilon}_{k,l}\leq -c_{k,l}^{(q)}t_{k,l}+d_{k,l}^{(q)}, \forall k\in\mathcal{K},\forall l\in\mathcal{L}_k \\ & \sum_{l\in\mathcal{L}_k} t_{k,l}\geq \hat{R}_k, \forall k\in\mathcal{K}\end{array} \tag{63}$$

where $\hat{R}_k = R_k(\log_2(\alpha))^{-1}$. Note that variable $t_{k,l}$ can be interpreted as a scaled version of the rate of stream l of user k. If α is chosen to be 2, then the scaling factor is 1. Problem (63) is convex since the objective and inequality constraints are all convex. Alternatively, (63) can also be cast as a standard SOCP by following the derivations in [33, 60].

After solving (63) at iteration q, the next point of approximation $t_{k,l}^{(q+1)}$ can be chosen based on the equality of the MSE constraints, i.e.,

$$t_{k,l}^{(q+1)} = -\log_\alpha(\tilde{\epsilon}_{k,l}^{(q+1)}). \tag{64}$$

An alternative option to update $t_{k,l}^{(q+1)}$ is to use a line search method as described in [71], i.e., $t_{k,l}^{(q+1)} = t_{k,l}$. In the SCA method, the objective value converges monotonically since it is improved at each iteration [71] due to the fact that the point of approximation is included in the approximated problem. However, global optimality cannot be guaranteed due to the linear approximations in the iterative optimization process. More details on the properties of the SCA method can be found in [71, 163, 164]. The linear MMSE receiver given in (54) minimizes the per-stream MSE. Thus, (54) is optimal for the approximated problem as well.

Next, a special multi-cell multi-user MIMO problem is considered where the number of spatial data streams per user is limited to one, i.e., $L_k = 1$, $\forall k\in\mathcal{K}$. In this case, the original problem (53) can be reduced to a less complex SPMin problem where the user-specific rate constraints can be directly mapped into SINR constraints. This optimization problem is written as

$$\begin{array}{ll}\underset{\{\mathbf{m}_k,\mathbf{w}_k\}_{k\in\mathcal{K}}}{\min.} & \sum_{k\in\mathcal{K}}\left\|\mathbf{m}_k\right\|_2^2 \\ \text{s. t.} & \dfrac{\left|\mathbf{w}_k^{\mathrm{H}}\mathbf{H}_{b_k,k}\mathbf{m}_k\right|^2}{N_0\|\mathbf{w}_k\|_2^2+\sum_{i\in\mathcal{K}\setminus\{k\}}\left|\mathbf{w}_k^{\mathrm{H}}\mathbf{H}_{b_i,k}\mathbf{m}_i\right|^2}\geq\gamma_k, \forall k\in\mathcal{K}\end{array} \tag{65}$$

where γ_k is the given SINR target for user k. Problem (65) is not jointly convex in $\{\mathbf{m}_k\}_{k\in\mathcal{K}}$ and $\{\mathbf{w}_k\}_{k\in\mathcal{K}}$. The receive and transmit beamforming optimization steps are given by

$$\tilde{\mathbf{w}}_k = \frac{\bar{\mathbf{w}}_k}{\|\bar{\mathbf{w}}_k\|_2}, \forall k \in \mathcal{K}, \tag{66}$$
$$\bar{\mathbf{w}}_k = \left(\sum_{i\in\mathcal{K}} \mathbf{H}_{b_i,k}\mathbf{m}_i\mathbf{m}_i^{\mathrm{H}}\mathbf{H}_{b_i,k}^{\mathrm{H}} + N_0\mathbf{I}_{A_{\mathrm{R}}}\right)^{-1}\mathbf{H}_{b_k,k}\mathbf{m}_k$$

and

$$\begin{aligned} \min_{p^{\mathrm{tx}},\{\mathbf{m}_k\}_{k\in\mathcal{K}}} \quad & p^{\mathrm{tx}} \\ \text{s. t.} \quad & \left\| \begin{matrix} \tilde{\mathbf{w}}_k^{\mathrm{H}}\mathbf{H}_{b_1,k}\mathbf{m}_1 \\ \vdots \\ \tilde{\mathbf{w}}_k^{\mathrm{H}}\mathbf{H}_{b_K,k}\mathbf{m}_K \\ \sqrt{N_0} \end{matrix} \right\|_2 \leq \sqrt{1+\tfrac{1}{\gamma_k}}\tilde{\mathbf{w}}_k^{\mathrm{H}}\mathbf{H}_{b_k,k}\mathbf{m}_k, \forall k \in \mathcal{K} \\ & \left\| \ \bar{\mathbf{m}} \ \right\|_2 \leq p^{\mathrm{tx}}. \end{aligned} \tag{67}$$

In (67), the optimal sum power is $P^{\mathrm{tx}} = (p^{\mathrm{tx}})^2$. Problem (67) is an SOCP, and it is similar to a well-known MISO problem [61]. For the single-stream MIMO case, the MMSE receivers (66) are normalized to avoid additional over-the-air signaling in a decentralized transceiver design as explained in Section 3.3.1.

3.2 Centralized transmit and receive beamforming design

This section considers a centralized transmit and receive beamforming design for single-stream and multi-stream MIMO systems. For centralized processing, global CSI needs to be available at a central controlling unit (or at each BS), which performs the transceiver design by alternating between the transmit and receive beamforming optimization steps. The resulting optimized transmit beamformers are then distributed to the corresponding BSs for data transmission. The linear MMSE receivers are employed at each user for data reception.

The single-stream MIMO problem (65) can be efficiently solved such that the objective function converges by alternatingly computing the receive and transmit beamformers using (66) and (67), respectively. For a convergence proof, see Proposition 5 introduced later in this Section. This optimization procedure follows the idea proposed in [91]. Since (67) is equivalent to a well-studied MISO problem, it can also be solved using any of the existing centralized algorithms, for example the ones proposed in [31, 33, 58]. Centralized transceiver design is summarized in *Algorithm 5.*

Algorithm 5 Centralized transmit and receive beamforming design for cellular single-stream MIMO system

Initialize transmit beamformers $\{\mathbf{m}_k\}_{k\in\mathcal{K}}$.
repeat
  Compute receive beamformers $\{\tilde{\mathbf{w}}_k\}_{k\in\mathcal{K}}$ by using MMSE criterion (66).
  Compute transmit beamformers $\{\mathbf{m}_k\}_{k\in\mathcal{K}}$ by solving SOCP (67).
until desired level of (objective function) convergence

The multi-stream MIMO problem (53) is solved, such that the sum power converges, by alternating between the receive and transmit beamforming designs. The receive beamformers are optimized using the linear MMSE criterion (54). The iterative transmit beamforming optimization is performed by repeatedly computing the linear approximation coefficients using (62), then solving (63) for the transmit beamformers, and updating the auxiliary variables using (64). The proposed centralized design is summarized in *Algorithm 6*.

Algorithm 6 Centralized transmit and receive beamforming design for cellular multi-stream MIMO system

Set $q = 0$. Initialize transmit beamformers and points of approximation $\{\mathbf{m}_{k,l}, t_{k,l}^{(0)}\}_{k\in\mathcal{K},l\in\mathcal{L}_k}$.
repeat
  Compute receive beamformers $\{\tilde{\mathbf{w}}_{k,l}\}_{k\in\mathcal{K},l\in\mathcal{L}_k}$ by using MMSE criterion (54).
  repeat
    Compute SCA coefficients $\{c_{k,l}^{(q)}, d_{k,l}^{(q)}\}_{k\in\mathcal{K},l\in\mathcal{L}_k}$ by using (62).
    Compute transmit beamformers $\{\mathbf{m}_{k,l}, t_{k,l}\}_{k\in\mathcal{K},l\in\mathcal{L}_k}$ by solving convex problem (63).
    Update points of approximation $\{t_{k,l}^{(q+1)}\}_{k\in\mathcal{K},l\in\mathcal{L}_k}$ by using (64).
    Set $q = q + 1$.
  until desired level of (objective function) convergence
until desired level of (objective function) convergence

Proposition 5. *The objective function of the original problem* (53) *converges by performing Algorithm 6.*

Proof. The proof is based on the fact that the objective function is guaranteed to converge if it decreases monotonically at each optimization step, and it is bounded below [95]. Since the original problem (53) and the approximated problem (63) have the same objective function and the optimization variables in (63) satisfy the rate constraints in (53), it is sufficient to show that the sum power of (63) converges by performing *Algorithm 6*. Since the sum power is bounded below (i.e., $P^{\mathrm{tx}} > 0$), it remains to be shown that the sum power is monotonically decreased at each (sum power-related) optimization step of *Algorithm 6*. Note that the sum power remains the same at each receive beamforming update (i.e., step 3 in *Algorithm 6*). However, the receive beamforming update via the MMSE criterion minimizes the per-stream MSE, and thus, less (or equal) transmission power will be needed at the next transmit beamforming update to satisfy the per-stream MSE constraints leading to the decreased sum power. Now, what is left to be proved is that each SCA iteration at the transmit beamforming update phase (i.e., step 6 in *Algorithm 6*) monotonically decreases the sum power. As explained in Section 3.1, the monotonic objective function convergence of the SCA method comes from the fact that the point of approximation is included in the approximated convex problem (63). Consequently, the objective function of (53) is guaranteed to converge by performing *Algorithm 6*. □

Remark 1. *Proposition 5 shows the convergence of the objective function to a limit point of a monotonically decreasing sequence. Since the original problem is non-convex, global optimality of the provided solution cannot be guaranteed. Furthermore, Proposition 5 does not guarantee the convergence of the optimization variables to a KKT-point.*

Nevertheless, the simulation results in Section 3.3.3 demonstrate that *Algorithm 6* provides significant performance gains when compared with the state-of-the-art MISO and single-stream MIMO beamforming approaches.

3.3 Decentralized transmit and receive beamforming design

This section proposes decentralized transceiver designs for single-stream and multi-stream MIMO systems. Solving the SPMin problem using decentralized processing is problematic in general since even if the channels from the BS to the neighboring cells' users are known (i.e., local CSI) via antenna-specific uplink

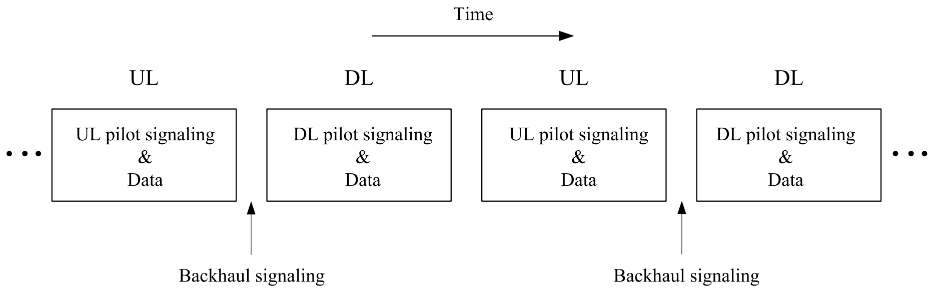

Fig 15. Simplified TDD frame structure with pilot and backhaul signaling ([99] © 2015 IEEE).

pilots, the receivers that these users are employing may not be known. Even in the case of knowing the receivers implicitly via precoded uplink pilots (i.e., local effective CSI), the transmit beamforming design is still coupled between the BSs. In this respect, the network-wide transmit beamforming design can be decoupled into independent BS-level designs by using different decomposition methods. Network-wide optimization via distributed processing is enabled via scalar backhaul information exchange among the neighboring BSs. A pilot and backhaul signaling-based framework is assumed to aid decentralized transceiver processing. The used framework is applicable in TDD-based systems where the reciprocity of downlink and uplink channels can be utilized. The signaling framework with a TDD-based frame structure is depicted in Fig. 15. It is assumed that the uplink pilot signals of each user in the coordinated system can be observed interference free by each BS, i.e., pilots are allocated to the orthogonal resources in time or frequency. A similar assumption is made for the downlink pilots, i.e., each user can observe the pilots of each BS interference free. In Sections 3.3.1 and 3.3.2, two decentralized transmit and receive beamforming algorithms are proposed that are specifically designed for the following uplink pilot strategies.

– *Signaling strategy A*: Precoded uplink pilots are used. Each BS can acquire local effective CSI.
– *Signaling strategy B*: Antenna-specific uplink pilots are used. Each BS can acquire local CSI.

3.3.1 Algorithm with signaling strategy A

Decentralized sum power minimization is obtained using an iterative over-the-air optimization process by repeatedly performing transmit beamforming design at each BS and receive beamforming design at each user. The transmit beamforming design requires local effective CSI acquired from precoded uplink pilots along with scalar over-the-air and backhaul signaling. The receive beamforming design is aided by downlink (precoded) demodulation pilots. The sum power of the system converges by iteratively repeating the aforementioned transmit and receive beamforming updates. In the following subsections, the receive and transmit beamforming designs are first derived. Then, the overall transceiver design is summarized via a step-by-step algorithm. Finally, a simplified algorithm is considered for a single-stream MIMO system.

Receive beamforming design at the user side

Receive beamforming design is straightforward, i.e., the linear MMSE receiver (54) is employed data stream-wise by each user. The computation of the MMSE is aided with the downlink demodulation pilots, which are precoded at the BS similarly as user data is. After the data reception, each user employs its MMSE receivers as precoders for the uplink pilots.

Transmit beamforming design at the BS side

The transmit beamforming design problem (63) is coupled between the BSs in its current form. To enable decentralized implementation, (63) needs to be reformulated such that it decouples at each iteration of the SCA method. Consequently, each BS can independently design the transmit beamformers for its own users. The decoupling procedure can be handled via a primal decomposition method [155], as explained in Section 2.2.1. In order to apply primal decomposition, (63) needs to be reformulated by adding auxiliary inter-cell interference power variables. Inter-cell interference power from BS b to stream l of user k is given by

$$\chi_{b,k,l} = \sum_{i \in \mathcal{K}_b} \sum_{j \in \mathcal{L}_i} \left| \mathbf{e}_{b,k,l} \mathbf{m}_{i,j} \right|^2 \tag{68}$$

where $\mathbf{e}_{b,k,l} = \tilde{\mathbf{w}}_{k,l}^{\mathrm{H}}\mathbf{H}_{b,k}$ is the effective channel of the lth stream of user k as seen by BS b. Note that the SCA-based auxiliary variables $\{t_{k,l}\}_{k\in\mathcal{K},l\in\mathcal{L}_k}$ are naturally decoupled between the BSs. The resulting optimization problem at iteration q of the SCA method is expressed as

$$\begin{aligned}
\min_{\substack{\{\mathbf{m}_{k,l},t_{k,l}\}_{k\in\mathcal{K},l\in\mathcal{L}_k},\\ \{\chi_{b,k,l}\}_{b\in\mathcal{B},k\in\bar{\mathcal{K}}_b,l\in\mathcal{L}_k}}} \quad & \sum_{k\in\mathcal{K}}\sum_{l\in\mathcal{L}_k}\left\|\mathbf{m}_{k,l}\right\|_2^2 \\
\text{s. t.} \quad & \left|1-\mathbf{e}_{b_k,k,l}\mathbf{m}_{k,l}\right|^2 + N_0\|\tilde{\mathbf{w}}_{k,l}\|_2^2 \\
& + \sum_{i\in\mathcal{K}_{b_k}}\sum_{j\in\mathcal{L}_i,(i,j)\neq(k,l)}\left|\mathbf{e}_{b_i,k,l}\mathbf{m}_{i,j}\right|^2 + \sum_{b'\in\mathcal{B}\setminus\{b_k\}}\chi_{b',k,l} \\
& \leq -c_{k,l}^{(q)}t_{k,l} + d_{k,l}^{(q)}, \forall k\in\mathcal{K}, \forall l\in\mathcal{L}_k \\
& \sum_{l\in\mathcal{L}_k} t_{k,l} \geq \hat{R}_k, \forall k\in\mathcal{K} \\
& \sum_{i\in\mathcal{K}_b}\sum_{j\in\mathcal{L}_i}\left|\mathbf{e}_{b,k,l}\mathbf{m}_{i,j}\right|^2 \leq \chi_{b,k,l}, \forall b\in\mathcal{B}, \forall k\in\bar{\mathcal{K}}_b, \forall l\in\mathcal{L}_k.
\end{aligned} \tag{69}$$

In (69), the inter-cell interference power constraints can be relaxed with inequality since they hold with equality at the optimal solution. Problem (69) is convex since the objective and inequality constraints are convex. Alternatively, (69) can also be cast as an SOCP.

By applying the primal decomposition method, (69) is turned into a coupled master problem and multiple decoupled subproblems, one for each BS. Since the original problem is convex, so are the resulting master problem and subproblems [155]. The idea is that the master problem updates the inter-cell interference power terms, using certain information (i.e., subgradients) obtained by solving the subproblems [63]. The resulting subproblem for BS b is given by

$$\begin{aligned}
\min_{\{\mathbf{m}_{k,l},t_{k,l}\}_{k\in\mathcal{K}_b,l\in\mathcal{L}_k}} \quad & \sum_{k\in\mathcal{K}_b}\sum_{l\in\mathcal{L}_k}\left\|\mathbf{m}_{k,l}\right\|_2^2 \\
\text{s. t.} \quad & \left|1-\mathbf{e}_{b_k,k,l}\mathbf{m}_{k,l}\right|^2 + N_0\|\tilde{\mathbf{w}}_{k,l}\|_2^2 \\
& + \sum_{i\in\mathcal{K}_{b_k}}\sum_{j\in\mathcal{L}_i,(i,j)\neq(k,l)}\left|\mathbf{e}_{b_i,k,l}\mathbf{m}_{i,j}\right|^2 + \sum_{b'\in\mathcal{B}\setminus\{b_k\}}\chi_{b',k,l} \\
& \leq -c_{k,l}^{(q)}t_{k,l} + d_{k,l}^{(q)}\forall k\in\mathcal{K}_b, \forall l\in\mathcal{L}_k \\
& \sum_{l\in\mathcal{L}_k} t_{k,l} \geq \hat{R}_k, \forall k\in\mathcal{K}_b \\
& \sum_{i\in\mathcal{K}_b}\sum_{j\in\mathcal{L}_i}\left|\mathbf{e}_{b,k,l}\mathbf{m}_{i,j}\right|^2 \leq \chi_{b,k,l}, \forall k\in\bar{\mathcal{K}}_b, \forall l\in\mathcal{L}_k.
\end{aligned} \tag{70}$$

It is assumed that the effective channels $\{\mathbf{e}_{b,k,l}\}_{k\in\mathcal{K}_b,l\in\mathcal{L}_k}$ are known at BS b by acquiring them from the MMSE-based precoded uplink pilot signals. In addition, user k needs to signal L_k real valued scalars, i.e., $\{\|\tilde{\mathbf{w}}_{k,l}\|_2^2\}_{l\in\mathcal{L}_k}$, to its serving BS b_k. The master problem is written as

$$\begin{aligned}\min_{\{\boldsymbol{\chi}_b\}_{b\in\mathcal{B}}}. \quad & \sum_{b\in\mathcal{B}} g_b^\star(\boldsymbol{\chi}_b) \\ \text{s. t.} \quad & \boldsymbol{\chi}_b \in \mathbb{R}_{++}^{N_b}, \forall b\in\mathcal{B}\end{aligned} \tag{71}$$

where $g_b^\star(\boldsymbol{\chi}_b)$ is the optimal objective value of (70) for given $\boldsymbol{\chi}_b$. The master problem (71) can be solved by updating each $\chi_{b,k,l}$ via projected subgradient method [155], which is given by

$$\chi_{b,k,l}^{(r+1)} = P_{++}\left\{\chi_{b,k,l}^{(r)} - \sigma^{(r)} u_{b,k,l}^{(r)}\right\} \tag{72}$$

where P_{++} is the projection onto the positive real values, r is the iteration index, $\sigma^{(r)}$ is the step-size and $u_{b,k,l}^{(r)}$ is the subgradient of (71) at point $\chi_{b,k,l}^{(r)}$. Due to the convexity of (69), the subgradients can be obtained similarly as described in Section 2.2.1, i.e., $u_{b,k,l}^{(r)} = \lambda_{b_k,k,l}^{(r)} - \mu_{b,k,l}^{(r)}$, where $\lambda_{b_k,k,l}^{(r)}$ and $\mu_{b,k,l}^{(r)}$ are the optimal dual variables with respect to $\chi_{b,k,l}^{(r)}$ in the b_kth and bth subproblems, respectively.

The optimal dual variables can be found by solving the primal subproblem (70) since they are usually provided as a certificate for optimality using a standard convex optimization software package, such as CVX [88]. An alternative way to find the dual variables is to solve the Lagrange dual problem of (70). In this case, transmit beamformers still need to be computed via the primal subproblems or KKT conditions. Here, the focus is on solving the primal subproblems. In order to solve $\boldsymbol{\chi}_b$ independently at BS b, for all $b\in\mathcal{B}$ in parallel, the computed dual variables need to be exchanged between the coupled BSs via backhaul links. The total number of real scalars to be exchanged in the coordinated system at each subgradient iteration is given by $2K_bL_k(B-1)B$, if an equal number of users and streams are assumed at each cell, i.e., $K_b = K/B$, $L_k = L$, $\forall b\in\mathcal{B}$, $\forall k\in\mathcal{K}$. More precisely, BS b signals $\{\lambda_{b,k,l}\}_{k\in\mathcal{K}_b,l\in\mathcal{L}_k}$ and $\{\mu_{b,i,j}\}_{i\in\mathcal{K}_{b'},j\in\mathcal{L}_i}$ to BS b', $\forall b'\in\mathcal{B}\setminus\{b\}, \forall b\in\mathcal{B}$. The projected subgradient method converges to an optimal value for a convex problem provided that the step-size is properly chosen [156]. After solving (69) with the aid of subgradient method at iteration q of the SCA method, the next point of approximation $t_{k,l}^{(q+1)}$ is updated at the corresponding BS according to (64). The outer SCA and inner subgradient methods are repeated until a desired level of convergence is achieved. The proposed decentralized transmit and receive beamforming design is summarized in *Algorithm 7*.

Algorithm 7 Decentralized transmit and receive beamforming design with signaling strategy A for cellular multi-stream MIMO system

---

BS b, $\forall b \in \mathcal{B}$: Set $q = 0$. Initialize inter-cell interference variables $\boldsymbol{\chi}_b$ and transmit beamformers and points of approximation $\{\mathbf{m}_{k,l}, t_{k,l}^{(0)}\}_{k \in \mathcal{K}_b, l \in \mathcal{L}_k}$.
repeat
  BS b, $\forall b \in \mathcal{B}$: Use transmit beamformers $\{\mathbf{m}_{k,l}\}_{k \in \mathcal{K}_b, l \in \mathcal{L}_k}$ to transmit data and downlink pilots.
  User k, $\forall k \in \mathcal{K}$: Compute receive beamformers $\{\tilde{\mathbf{w}}_{k,l}\}_{l \in \mathcal{L}_k}$ by using MMSE criterion (54).
  User k, $\forall k \in \mathcal{K}$: Use MMSE receive beamformers $\{\tilde{\mathbf{w}}_{k,l}\}_{l \in \mathcal{L}_k}$ as precoders for uplink pilots. Signal scalar terms $\{\|\tilde{\mathbf{w}}_{k,l}\|_2^2\}_{l \in \mathcal{L}_k}$ to BS b_k.
  BS b, $\forall b \in \mathcal{B}$: Observe and update effective channels $\{\mathbf{e}_{b,k,l}\}_{k \in \mathcal{K}, l \in \mathcal{L}_k}$.
  repeat
    BS b, $\forall b \in \mathcal{B}$: Compute SCA coefficients $\{c_{k,l}^{(q)}, d_{k,l}^{(q)}\}_{k \in \mathcal{K}_b, l \in \mathcal{L}_k}$ by using (62).
    repeat
      BS b, $\forall b \in \mathcal{B}$: Compute transmit beamformers and dual variables $\{\mathbf{m}_{k,l}, t_{k,l}, \lambda_{b,k,l}\}_{k \in \mathcal{K}_b, l \in \mathcal{L}_k}$, $\{\mu_{b,k,l}\}_{k \in \bar{\mathcal{K}}_b, l \in \mathcal{L}_k}$ by solving convex problem (70).
      BS b, $\forall b \in \mathcal{B}$: Communicate $\{\lambda_{b,k,l}\}_{k \in \mathcal{K}_b, l \in \mathcal{L}_k}$ and $\{\mu_{b,k,l}\}_{k \in \bar{\mathcal{K}}_b, l \in \mathcal{L}_k}$ to the coupled BSs via backhaul.
      BS b, $\forall b \in \mathcal{B}$: Update inter-cell interference variables $\boldsymbol{\chi}_b$ via projected subgradient method (72).
    until desired level of convergence
    BS b, $\forall b \in \mathcal{B}$: Compute transmit beamformers $\{\mathbf{m}_{k,l}, t_{k,l}\}_{k \in \mathcal{K}_b, l \in \mathcal{L}_k}$ by solving convex problem (70).
    BS b, $\forall b \in \mathcal{B}$: Update points of approximation $\{t_{k,l}^{(q+1)}\}_{k \in \mathcal{K}_b, l \in \mathcal{L}_k}$ by using (64).
    Set $q = q + 1$.
  until desired level of (objective function) convergence
until desired level of (objective function) convergence

Following the proof of Proposition 5, the sum power of the original problem (53) is guaranteed to converge by performing *Algorithm 7*, and assuming that the outer SCA and inner subgradient methods (i.e., steps 7-16) are iterated until convergence or until the sum power is improved. At the cost of decreased performance, the number of iterations in the outer SCA and inner subgradient methods can be limited to reduce delay and signaling/computational load.

Simplified algorithm for single-stream MIMO

In this subsection, a decentralized transceiver design is proposed for a single-stream MIMO system. The proposed algorithm has a lower level of complexity compared to *Algorithm 7* since the transmit beamforming problem is convex. At each user, the linear MMSE receivers from (66) are employed. The transmit beamforming problem (67) is first reformulated by defining the effective channels and extracting inter-cell interference power terms as auxiliary variables. Then, the reformulated problem is equivalently turned into B subproblems and a master problem.

Following the derivation in Section 2.2.1, the subproblem for BS b can be expressed as the following SOCP

$$\begin{aligned} \min_{p_b^{\text{tx}},\{\mathbf{m}_k\}_{k\in\mathcal{K}_b}} \quad & p_b^{\text{tx}} \\ \text{s. t.} \quad & \left\| \begin{matrix} \mathbf{M}_b^{\text{H}}\mathbf{e}_{b,k}^{\text{H}} \\ \bar{\boldsymbol{\chi}}_k \\ \sqrt{N_0} \end{matrix} \right\|_2 \leq \sqrt{1+\frac{1}{\gamma_k}}\mathbf{e}_{b,k}\mathbf{m}_k, \forall k \in \mathcal{K}_b, \\ & \left\| \mathbf{M}_b^{\text{H}}\mathbf{e}_{b,k}^{\text{H}} \right\|_2 \leq \bar{\chi}_{b,k}, \forall k \in \bar{\mathcal{K}}_b \\ & \left\| \bar{\mathbf{m}}_b \right\|_2 \leq p_b^{\text{tx}} \end{aligned} \tag{73}$$

Unlike in *Algorithm 7*, the over-the-air signaling of $\{\|\tilde{\mathbf{w}}_k\|_2^2\}_{k\in\mathcal{K}}$ is avoided here since the MMSE receivers in (66) are normalized, i.e., $\|\tilde{\mathbf{w}}_k\|_2 = 1$.

The projected subgradient method for solving the master problem is given by

$$\chi_{b,k}^{(r+1)} = P_{++}\left\{\chi_{b,k}^{(r)} - \sigma^{(r)}\left(\lambda_{b_k,k}^{(r)} - \mu_{b,k}^{(r)}\right)\right\}. \tag{74}$$

The dual variables are found by solving (73) at each BS. By exchanging the dual variables between the coupled BS, $\boldsymbol{\chi}_b$ can be updated at BS b, for all $b \in \mathcal{B}$ in parallel. At each iteration, the total amount of backhaul signaling is $2K_b(B-1)B$. The proposed design is summarized in *Algorithm 8*. The convergence of the sum power can be shown through similar reasoning as described in Section 3.3.1.

Algorithm 8 Decentralized transmit and receive beamforming design with signaling strategy A for cellular single-stream MIMO system

---

BS b, $\forall b \in \mathcal{B}$: Initialize inter-cell interference variables $\boldsymbol{\chi}_b$ and transmit beamformers $\{\mathbf{m}\}_{k\in\mathcal{K}_b}$.
repeat
  BS b, $\forall b \in \mathcal{B}$: Use transmit beamformers $\{\mathbf{m}\}_{k\in\mathcal{K}_b}$ to transmit data and downlink pilots.
  User k, $\forall k \in \mathcal{K}$: Compute receive beamformer $\tilde{\mathbf{w}}_k$ by using MMSE criterion (66).
  User k, $\forall k \in \mathcal{K}$: Use MMSE receive beamformer $\tilde{\mathbf{w}}_k$ as a precoder for uplink pilots.
  BS b, $\forall b \in \mathcal{B}$: Observe and update effective channels $\{\mathbf{e}_{b,k}\}_{k\in\mathcal{K}}$.
  repeat
    BS b, $\forall b \in \mathcal{B}$: Compute transmit beamformers and dual variables $\{\mathbf{m}_k, \lambda_{b,k}\}_{k\in\mathcal{K}_b}$, $\{\mu_{b,k}\}_{k\in\bar{\mathcal{K}}_b}$ by solving SOCP (73).
    BS b, $\forall b \in \mathcal{B}$: Communicate $\{\lambda_{b,k}\}_{k\in\mathcal{K}_b}$ and $\{\mu_{b,k}\}_{k\in\bar{\mathcal{K}}_b}$ to the coupled BSs via backhaul.
    BS b, $\forall b \in \mathcal{B}$: Update inter-cell interference variables $\boldsymbol{\chi}_b$ via projected subgradient method (74)
  until desired level of convergence
until desired level of (objective function) convergence

Practical considerations

The discussion on the practical features in Section 2.2.1 applies also to *Algorithm 7*. In practice, it is important to limit the number of iterations to avoid extra delay and reduce signaling overhead. In this respect, *Algorithm 7* has a valuable property, as it is able to provide feasible beamformers that satisfy the user-specific rate constraints, at intermediate iterations. Hence, *Algorithm 7* can be stopped at any (feasible) iteration leading to reduced delay and signaling overhead. However, the cost here is that the sum power is somewhat increased compared with the centralized algorithm.

Similar to Section 2.2.1, the total backhaul signaling load of *Algorithm 7* is compared with that of the decentralized approach under different system settings in Table 5. With the same assumptions as described in Section 2.2.1, the total backhaul signaling load of the centralized system is given by $2A_\mathrm{R}A_\mathrm{T}K(B-1)B$. The per-iteration signaling overhead of *Algorithm 7* is significantly lower as compared with the centralized algorithm. The difference is increasing with the increasing system size and is even higher than in the MISO system. For example, at each iteration, *Algorithm 7* requires less than 1 % of the signaling load of the centralized algorithm. Therefore, by limiting the number of iterations during the transmit beamforming design, signaling overhead can be significantly reduced. *Algorithm 7* also requires that KL real valued scalars are signaled over-the-air to the serving BS during the uplink transmission phase, i.e., 8, 18 and 32 scalars in the given examples. Note that this procedure is not needed in the single-stream MIMO scheme (i.e., *Algorithm 8*). Thus, to reduce the signaling overhead and computational complexity further, the simpler single-stream MIMO algorithm can be employed.

Table 5. Total backhaul signaling load per iteration ([99] © 2015 IEEE).

	Centr. (Alg. 6)	Decentr. A (Alg. 7)
$\{B,K,A_\mathrm{T},A_\mathrm{R}\}=\{2,4,8,2\}$	256	16 (6.3%)
$\{B,K,A_\mathrm{T},A_\mathrm{R}\}=\{3,6,18,3\}$	3888	72 (1.9%)
$\{B,K,A_\mathrm{T},A_\mathrm{R}\}=\{4,8,32,4\}$	24576	192 (0.7%)

3.3.2 Algorithm with signaling strategy B

Decentralized sum power minimization is achieved by iteratively repeating transmit and receive beamforming updates at each BS, such that the sum power of the system converges. This design requires local CSI acquired from antenna-specific uplink pilots and scalar backhaul information exchange between the BSs. Since there is no information available on the users' receivers at the BS side, a sub-optimal worst case assumption on the receivers is thus made. The resulting modified problem is inherently sub-optimal, but feasible, with respect to the original problem. Thus, the beamformers are feasible for the original problem, i.e., they satisfy the user-specific minimum rate targets, and the converged sum power is sub-optimal. Unlike in strategy A, only one round of over-the-air uplink pilot signaling is needed for the convergence of the local transceiver design at each BS. After the optimization of local transceivers, the resulting transmit beamformers are used for data transmission and downlink pilots. For data reception, each user employs the linear MMSE receiver (54) with the aid of the downlink pilots. In the following subsections, the decentralized transceiver design is derived and presented in detail via a step-by-step algorithm. Lastly, a simplified algorithm is proposed for a single-stream MIMO system.

Transmit and receive beamforming design at the BS side

The derivation of the transmit and receive beamforming design is started by equivalently rewriting the stream-wise inter-cell interference power from BS b to user k as

$$\chi_{b,k,l} = \mathbf{w}_{k,l}^{\mathrm{H}} \left(\sum_{i \in \mathcal{K}_b} \sum_{j \in \mathcal{L}_i} \mathbf{H}_{b,k} \mathbf{m}_{i,j} \mathbf{m}_{i,j}^{\mathrm{H}} \mathbf{H}_{b,k}^{\mathrm{H}} \right) \mathbf{w}_{k,l}. \tag{75}$$

Since the receive beamformers for the kth user are associated with data streams emanating from another BS and only antenna-specific uplink pilot signaling is employed, BS b is unable to deduce what are $\{\mathbf{w}_{k,l}\}_{l \in \mathcal{L}_k}$. In order to remain on the safe side and guarantee the user-specific rate targets, BS b may attempt to prepare for the worst case and maximize the cross term (75) with respect to $\mathbf{w}_{k,l}$. In other words, each BS assumes the (virtual) worst case receivers, which maximize the interference for the other cells' users when designing the transceivers for its own users. The solution of the maximization is straightforward, and the resulting interference power is given by

$$\chi_{b,k,l} = \lambda_{\max} \left(\sum_{i \in \mathcal{K}_b} \sum_{j \in \mathcal{L}_i} \mathbf{H}_{b,k} \mathbf{m}_{i,j} \mathbf{m}_{i,j}^{\mathrm{H}} \mathbf{H}_{b,k}^{\mathrm{H}} \right) \tag{76}$$

where $\lambda_{\max}(\mathbf{X})$ is the maximum eigenvalue of a symmetric matrix $\mathbf{X}$. The receiver $\mathbf{w}_{k,l}$ maximizing the interference from BS b is the eigenvector corresponding to the maximum eigenvalue in (76). For the SPMin problem, (76) can be relaxed with inequality and rewritten as a linear matrix inequality (LMI) constraint: $\sum_{i\in\mathcal{K}_b}\sum_{j\in\mathcal{L}_i}\mathbf{H}_{b,k}\mathbf{m}_{i,j}\mathbf{m}_{i,j}^{\mathrm{H}}\mathbf{H}_{b,k}^{\mathrm{H}} \preceq \chi_{b,k,l}\mathbf{I}_{A_{\mathrm{R}}}$, $\forall l \in \mathcal{L}_k$. Note that this constraint is the same for each stream of user k. Thus, the number of interference variables (and the corresponding dual variables) can be reduced, i.e., $\chi_{b,k,1} = \ldots = \chi_{b,k,L_k} = \chi_{b,k}$. The stream-wise formulation is used here for clarity of presentation. It is worth mentioning also that other types of worst case interference assumptions are also applicable. For example, each eigenvalue of the received signal's covariance matrix can be upper bounded by a separate inter-cell interference power variable. The resulting LMI is given by $\sum_{i\in\mathcal{K}_b}\sum_{j\in\mathcal{L}_i}\mathbf{H}_{b,k}\mathbf{m}_{i,j}\mathbf{m}_{i,j}^{\mathrm{H}}\mathbf{H}_{b,k}^{\mathrm{H}} \preceq \mathrm{diag}\left(\chi_{b,k,1},\ldots,\chi_{b,k,L_k}\right)$. In another example, the interference is upper bounded by the sum of the eigenvalues of the receive covariance matrix. This interference constraint can be reformulated as an SOC constraint: $\|\mathbf{H}_{b,k}\bar{\mathbf{m}}_b\|_2 \leq \bar{\chi}_{b,k,l}$.

In the following, the focus is solely on the maximum eigenvalue-based interference assumption in (76). Since the assumption is sub-optimal, the sum power performance is somewhat degraded when compared with that of the transceiver design with signaling strategy A. However, the positive side is that now each BS can design its transmit beamformers without the explicit or implicit knowledge of the (real) receivers of other cells' users. Thus, there is no need for a similar iterative over-the-air pilot signaling process which is required when using strategy A. Moreover, the overcautious design helps maintain the feasibility of the rate targets in time-varying channel conditions where signaling information and CSI are outdated, as demonstrated via numerical examples in Section 3.3.3. Next, the sum power minimization is divided into transmit and receive beamforming designs that can be repeatedly solved one after another at the corresponding BSs, thus leading to convergence of the sum power.

The receive beamforming design of the cell's own users can be decoupled between the BSs by using the worst case inter-cell interference covariance matrix in the MMSE criterion (54). The corresponding worst case MMSE receiver at

BS b for stream l of user k can be written as

$$\hat{\mathbf{w}}_{k,l} = \left(\sum_{i \in \mathcal{K}_{b_k}} \sum_{j \in \mathcal{L}_j} \mathbf{H}_{b_i,k} \mathbf{m}_{i,j} \mathbf{m}_{i,j}^{\mathrm{H}} \mathbf{H}_{b_i,k}^{\mathrm{H}} + N_0 \mathbf{I}_{A_{\mathrm{R}}} + \sum_{b' \in \mathcal{B} \setminus \{b_k\}} \chi_{b',k,l} \mathbf{I}_{A_{\mathrm{R}}} \right)^{-1} \mathbf{H}_{b_k,k} \mathbf{m}_{k,l}, \forall k \in \mathcal{K}_b, \forall l \in \mathcal{L}_k. \tag{77}$$

For fixed $\{\hat{\mathbf{w}}_{k,l}\}_{k \in \mathcal{K}, l \in \mathcal{L}_k}$, the transmit beamforming optimization problem at the qth iteration of the SCA method can be expressed as

$$\begin{aligned}
\underset{\substack{\{\mathbf{m}_{k,l}, t_{k,l}\}_{k \in \mathcal{K}, l \in \mathcal{L}_k}, \\ \{\chi_{b,k,l}\}_{b \in \mathcal{B}, k \in \bar{\mathcal{K}}_b, l \in \mathcal{L}_k}}}{\min.} \quad & \sum_{k \in \mathcal{K}} \sum_{l \in \mathcal{L}_k} \left\| \mathbf{m}_{k,l} \right\|_2^2 \\
\text{s. t.} \quad & \left| 1 - \hat{\mathbf{w}}_{k,l}^{\mathrm{H}} \mathbf{H}_{b,k} \mathbf{m}_{k,l} \right|^2 + N_0 \|\hat{\mathbf{w}}_{k,l}\|_2^2 + \\
& \sum_{i \in \mathcal{K}_{b_k}} \sum_{j \in \mathcal{L}_i, (i,j) \neq (k,l)} \left| \hat{\mathbf{w}}_{k,l}^{\mathrm{H}} \mathbf{H}_{b_i,k} \mathbf{m}_{i,j} \right|^2 + \\
& \sum_{b' \in \mathcal{B} \setminus \{b_k\}} \chi_{b',k,l} \leq -c_{k,l}^{(q)} t_{k,l} + d_{k,l}^{(q)} \forall k \in \mathcal{K}, \forall l \in \mathcal{L}_k \\
& \sum_{l \in \mathcal{L}_k} t_{k,l} \geq \hat{R}_k, \forall k \in \mathcal{K} \\
& \sum_{i \in \mathcal{K}_b} \sum_{j \in \mathcal{L}_i} \mathbf{H}_{b,k} \mathbf{m}_{i,j} \mathbf{m}_{i,j}^{\mathrm{H}} \mathbf{H}_{b,k}^{\mathrm{H}} \preceq \chi_{b,k,l} \mathbf{I}_{A_{\mathrm{R}}} \\
& \forall b \in \mathcal{B}, \forall k \in \bar{\mathcal{K}}_b, \forall l \in \mathcal{L}_k.
\end{aligned} \tag{78}$$

Problem (78) is non-convex and coupled between the BSs. However, it can be first approximated as an SDP by using the SDR method [81]. The derivation follows the same steps as those described in Section 2.3. The resulting convex transmit beamforming problem can be decoupled between the BSs by using the primal decomposition method and turning it into a master problem and B subproblems. From the results in [81], one can conclude that if the optimal $\{\mathbf{Q}_{k,l}\}_{k \in \mathcal{K}, l \in \mathcal{L}_k}$ are rank-one, i.e., $\mathbf{Q}_{k,l} = \mathbf{m}_{k,l} \mathbf{m}_{k,l}^{\mathrm{H}}$, $\forall k \in \mathcal{K}, l \in \mathcal{L}_k$, then the solution is also optimal for the original non-approximated problem. In general, it cannot be guaranteed that solving an SDR problem yields always a rank-one solution. In case the solution is not rank-one, a simple method described in Section 2.3 can be used to find sub-optimal but feasible rank-one beamformers. However, this simple method is only applicable for centralized systems in practice. Alternatively, it is possible to take the principal eigenvectors of $\{\mathbf{Q}_{k,l}\}_{k \in \mathcal{K}, l \in \mathcal{L}_k}$ as beamformers and allow some violation of the rate constraints to enable a decentralized implementation. Nevertheless, rank-one solutions were always obtained in the numerical examples in Section 3.3.3. Recent works on the SDR problems for different SPMin systems can be found in [89, 125, 160].

After applying primal decomposition, the subproblem at BS b is given by

$$\begin{aligned}
\min_{\{\mathbf{m}_{k,l},t_{k,l},\mathbf{Q}_{k,l}\}_{k\in\mathcal{K}_b,l\in\mathcal{L}_k}} \quad & \sum_{k\in\mathcal{K}_b}\sum_{l\in\mathcal{L}_k} \mathrm{tr}\left(\mathbf{Q}_{k,l}\right) \\
\text{s. t.} \quad & \begin{bmatrix} v_{k,l}\mathbf{I} & \mathbf{f}_{k,l} \\ \mathbf{f}_{k,l}^{\mathrm{H}} & v_{k,l} \end{bmatrix} \succeq 0, \forall k\in\mathcal{K}_b, \forall l \in \mathcal{L}_k \\
& \sum_{l\in\mathcal{L}_k} t_{k,l} \geq \hat{R}_k, \forall k \in \mathcal{K}_b \\
& \sum_{i\in\mathcal{K}_b}\sum_{j\in\mathcal{L}_i} \mathbf{H}_{b,k}\mathbf{Q}_{i,j}\mathbf{H}_{b,k}^{\mathrm{H}} \preceq \chi_{b,k,l}\mathbf{I}_{A_\mathrm{R}} \\
& \forall k\in\bar{\mathcal{K}}_b, \forall l\in\mathcal{L}_k \\
& \mathbf{Q}_{k,l} \succeq 0, \forall k\in\mathcal{K}_b, \forall l\in\mathcal{L}_k \\
& \begin{bmatrix} \mathbf{Q}_{k,l} & \mathbf{m}_{k,l} \\ \mathbf{m}_{k,l}^{\mathrm{H}} & 1 \end{bmatrix} \succeq 0, \forall k\in\mathcal{K}_b, \forall l\in\mathcal{L}_k
\end{aligned} \tag{79}$$

where $v_{k,l} = (1 + c_{k,l}^{(q)} t_{k,l} - d_{k,l}^{(q)})/2$, and

$$\mathbf{f}_{k,l} = \begin{bmatrix} 1 - \hat{\mathbf{w}}_{k,l}^{\mathrm{H}}\mathbf{H}_{b,k}\mathbf{m}_{k,l} \\ \bar{\mathbf{M}}_b^{\mathrm{H}}\mathbf{H}_{b_k,k}^{\mathrm{H}}\hat{\mathbf{w}}_{k,l} \\ \bar{\boldsymbol{\chi}}_{k,l} \\ \sqrt{N_0}\hat{\mathbf{w}}_{k,l} \\ \left(1 - c_{k,l}^{(q)} t_{k,l} + d_{k,l}^{(q)}\right)/2 \end{bmatrix}. \tag{80}$$

The matrix $\bar{\mathbf{M}}_b$ consists of the BS b specific beamformers except the beamformer intended for stream (k,l). In other words, the columns of $\bar{\mathbf{M}}_b$ are taken (in a specific order) from the set $\{\mathbf{m}_{i,j}\}_{i\in\mathcal{K}_b,j\in\mathcal{L}_i,(i,j)\neq(k,l)}$. The elements of $\bar{\boldsymbol{\chi}}_{k,l}$ are taken (in a specific order) from the set $\{\bar{\chi}_{b',k,l}\}_{b'\in\mathcal{B}\setminus\{b\}}$, i.e., $\bar{\boldsymbol{\chi}}_{k,l}$ includes the inter-cell interference experienced by the (k,l)th stream. The master problem is solved iteratively via the following projected subgradient method

$$\chi_{b,k,l}^{(r+1)} = P_{++}\left\{\chi_{b,k,l}^{(r)} - \sigma^{(r)}\left(\lambda_{b_k,k,l}^{(r)} - \mathrm{tr}\left(\boldsymbol{\Lambda}_{b,k,l}^{(r)}\right)\right)\right\} \tag{81}$$

where $\lambda_{b_k,k,l}^{(r)}$ and $\mathrm{tr}(\boldsymbol{\Lambda}_{b,k,l}^{(r)})$ are the optimal dual variables with respect to $\chi_{b,k,l}^{(r)}$ in the b_kth and bth subproblems, respectively. The BS-specific dual variables are found by solving (79). The vector $\boldsymbol{\chi}_b$ is updated at BS b, for all $b \in \mathcal{B}$ in parallel, by exchanging the dual variables between the coupled BSs. The maximum number of scalar variables to be exchanged at each subgradient iteration is $K_b(1 + L_k)(B - 1)B$. This number is less than for *Algorithm 7*. The outer SCA and inner subgradient methods are repeated until a desired level of convergence is reached.

Algorithm 9 Decentralized transmit and receive beamforming design with signaling strategy B for cellular multi-stream MIMO system

BS b, $\forall b \in \mathcal{B}$: Set $q = 0$. Initialize inter-cell interference variables $\boldsymbol{\chi}_b$ and transmit beamformers and points of approximation $\{\mathbf{m}_{k,l}, t_{k,l}^{(0)}\}_{k \in \mathcal{K}_b, l \in \mathcal{L}_k}$.
repeat
  BS b, $\forall b \in \mathcal{B}$: Compute receive beamformers $\{\hat{\mathbf{w}}_{k,l}\}_{k \in \mathcal{K}_b, l \in \mathcal{L}_k}$ by using MMSE criterion (77).
  repeat
    BS b, $\forall b \in \mathcal{B}$: Compute SCA coefficients $\{c_{k,l}^{(q)}, d_{k,l}^{(q)}\}_{k \in \mathcal{K}_b, l \in \mathcal{L}_k}$ by using (62).
    repeat
      BS b, $\forall b \in \mathcal{B}$: Compute transmit beamformers and dual variables $\{\mathbf{m}_{k,l}, t_{k,l}, \lambda_{b,k,l}\}_{k \in \mathcal{K}_b, l \in \mathcal{L}_k}$, $\{\mathrm{tr}(\boldsymbol{\Lambda}_{b,k,l})\}_{k \in \bar{\mathcal{K}}_b, l \in \mathcal{L}_k}$ by solving SDP (79).
      BS b, $\forall b \in \mathcal{B}$: Communicate $\{\lambda_{b,k,l}\}_{k \in \mathcal{K}_b, l \in \mathcal{L}_k}$ and $\{\mathrm{tr}(\boldsymbol{\Lambda}_{b,k,l})\}_{k \in \bar{\mathcal{K}}_b, l \in \mathcal{L}_k}$ to the coupled BSs via backhaul.
      BS b, $\forall b \in \mathcal{B}$: Update inter-cell interference variables $\boldsymbol{\chi}_b$ via projected subgradient method (81).
    until desired level of convergence
    BS b, $\forall b \in \mathcal{B}$: Compute transmit beamformers $\{\mathbf{m}_{k,l}, t_{k,l}\}_{k \in \mathcal{K}_b, l \in \mathcal{L}_k}$ by solving SDP (79).
    BS b, $\forall b \in \mathcal{B}$: Update points of approximation $\{t_{k,l}^{(q+1)}\}_{k \in \mathcal{K}_b, l \in \mathcal{L}_k}$ by using (64).
    Set $q = q + 1$.
  until desired level of (objective function) convergence
until desired level of (objective function) convergence

The overall transceiver design is summarized in *Algorithm 9*. The sum power convergence of the original problem via *Algorithm 9* is guaranteed, based on similar reasoning as given in Section 3.3.1. The practical considerations given in Section 3.3.1 are also valid for *Algorithm 9*. It is worth mentioning that *Algorithm 9* requires less backhaul signaling than *Algorithm 7*. Given the same system settings as in Table 5, *Algorithm 9* requires only 4.7%, 1.2% or 0.5% of the signaling load of the centralized approach.

Simplified algorithm for single-stream MIMO

Here, a decentralized transceiver design is proposed for a single-stream MIMO system. The proposed algorithm is a simplified version of *Algorithm 9* since there is no need for the SCA optimization loop in the transmit beamforming problem. The receive beamforming design is decoupled between the BSs by applying the worst case inter-cell interference covariance matrix $\sum_{b' \in \mathcal{B}\setminus\{b_k\}} \chi_{b',k} \mathbf{I}_{A_\mathrm{R}}$. The (normalized) worst case MMSE receivers for the users assigned to BS b can be written as

$$\begin{aligned}
\hat{\mathbf{w}}_k &= \frac{\check{\mathbf{w}}_k}{\|\check{\mathbf{w}}_k\|_2}, \\
\check{\mathbf{w}}_k &= \left(\sum_{i \in \mathcal{K}_{b_k}\setminus\{k\}} \mathbf{H}_{b_i,k}\mathbf{m}_i\mathbf{m}_i^\mathrm{H}\mathbf{H}_{b_i,k}^\mathrm{H} + \left(N_0 + \sum_{b' \in \mathcal{B}\setminus\{b_k\}} \chi_{b',k} \right) \mathbf{I}_{A_\mathrm{R}} \right)^{-1} \\
&\quad \mathbf{H}_{b_k,k}\mathbf{m}_k, \forall k \in \mathcal{K}_b. \qquad (82)
\end{aligned}$$

The transmit beamforming problem can be approximated and decoupled via SDR and primal decomposition, respectively. The resulting subproblem for BS b is given by

$$\begin{aligned}
\min_{\{\mathbf{Q}_k\}_{k\in\mathcal{K}_b}} \quad & \sum_{k\in\mathcal{K}_b} \mathrm{tr}\left(\mathbf{Q}_k\right) \\
\text{s. t.} \quad & \frac{1}{\gamma_k}\mathrm{tr}\left(\hat{\mathbf{W}}_k\mathbf{H}_{b,k}\mathbf{Q}_k\mathbf{H}_{b,k}^\mathrm{H}\right) - \\
& \sum_{i\in\mathcal{K}_{b_k}\setminus\{k\}} \mathrm{tr}\left(\hat{\mathbf{W}}_k\mathbf{H}_{b,k}\mathbf{Q}_i\mathbf{H}_{b,k}^\mathrm{H}\right) \geq N_0 + \sum_{b'\in\mathcal{B}\setminus\{b_k\}} \chi_{b',k}, \qquad (83) \\
& \forall\ k \in \mathcal{K}_b \\
& \sum_{i\in\mathcal{K}_b} \mathbf{H}_{b,k}\mathbf{Q}_i\mathbf{H}_{b,k}^\mathrm{H} \preceq \chi_{b,k}\mathbf{I}_{A_\mathrm{R}}, \forall b \in \mathcal{B}, \forall k \in \bar{\mathcal{K}}_b \\
& \mathbf{Q}_k \succeq 0, \forall k \in \mathcal{K}_b
\end{aligned}$$

where $\hat{\mathbf{W}}_k = \hat{\mathbf{w}}_k \hat{\mathbf{w}}_k^{\mathrm{H}}$. Problem (83) is an SDP. The following projected subgradient method solves the master problem

$$\chi_{b,k}^{(r+1)} = P_{++} \left\{ \chi_{b,k}^{(r)} - \sigma^{(r)} \left(\lambda_{b_k,k}^{(r)} - \operatorname{tr}\left(\mathbf{\Lambda}_{b,k}^{(r)} \right) \right) \right\}. \tag{84}$$

The vector $\boldsymbol{\chi}_b$ is updated at BS b, for all $b \in \mathcal{B}$ in parallel, after solving (83) for the dual variables and then exchanging them between the coupled BSs. The total amount of backhaul signaling between the BSs per subgradient iteration is $2K_b(B-1)B$. The proposed transceiver design is summarized in *Algorithm 10*. The convergence of the sum power is guaranteed based on the same arguments as those explained in Section 3.3.1.

Algorithm 10 Decentralized transmit and receive beamforming design with signaling strategy B for cellular single-stream MIMO system

BS b, $\forall b \in \mathcal{B}$: Initialize inter-cell interference variables $\boldsymbol{\chi}_b$ and transmit beamformers $\{\mathbf{m}\}_{k \in \mathcal{K}_b}$.
repeat
  BS b, $\forall b \in \mathcal{B}$: Compute receive beamformer $\{\hat{\mathbf{w}}_k\}_{k \in \mathcal{K}_b}$ by using MMSE criterion (82).
  repeat
    BS b, $\forall b \in \mathcal{B}$: Compute transmit beamformers and dual variables $\{\mathbf{m}_k, \lambda_{b,k}\}_{k \in \mathcal{K}_b}$ and $\{\operatorname{tr}(\mathbf{\Lambda}_{b,k})\}_{k \in \bar{\mathcal{K}}_b}$ by solving SDP (83).
    BS b, $\forall b \in \mathcal{B}$: Communicate $\{\lambda_{b,k}\}_{k \in \mathcal{K}_b}$ and $\{\operatorname{tr}(\mathbf{\Lambda}_{b,k})\}_{k \in \bar{\mathcal{K}}_b}$ to the coupled BSs via backhaul.
    BS b, $\forall b \in \mathcal{B}$: Update inter-cell interference variables $\boldsymbol{\chi}_b$ via projected subgradient method (84).
  until desired level of convergence
until desired level of (objective function) convergence

3.3.3 Numerical evaluation

In this section, the performance of the proposed centralized and decentralized algorithms is evaluated via numerical examples. The used simulation model is mostly the same as in Section 2.2.3, i.e., $B = 2$ and $K_1 = K_2 = 2$. The difference now is that each user is equipped with multiple antennas. Unless otherwise stated, the used channel model is based on frequency-flat Rayleigh fading channel conditions with uncorrelated channel coefficients between the antennas. Per-user rate constraints and the number of data streams per user are set equal among the users, i.e., $R_k = R$ and $L_k = L$, $\forall k \in \mathcal{K}$. Moreover, some of the simulation parameters are initialized by setting them equal over the streams and users, i.e., $t_{k,l}^{(0)} = t^{(0)} = R/L$, $\forall k \in \mathcal{K}$, $\forall l \in \mathcal{L}_k$ and $\chi_{b,k,l}^{(0)} = \chi^{(0)} = 0.05$, $\forall b \in \mathcal{B}$, $\forall k \in \bar{\mathcal{K}}_b$, $\forall l \in \mathcal{L}_k$. Transmit beamformers were initialized using the singular vectors of the user-specific channels matrices. Adaptive step-sizes with empirically chosen initial values are used for the projected subgradient methods.

In Figs. 16-17, the average sum power performance of the centralized algorithms is evaluated for various rate targets and cell separation values. The main system parameters are given by $\{B, K, A_{\mathrm{T}}, A_{\mathrm{R}}\} = \{2, 4, 16, 4\}$. The results are achieved by iterating over 20 transmit-receive beamforming steps and averaging over 50 channel realizations. The following centralized schemes are compared

– Multi-stream MIMO (M-MIMO): *Algorithm 6*
– Multi-stream MIMO with worst case receiver (WCRX)
– Multi-stream MIMO with per-stream rate constraints
– Single-stream MIMO (S-MIMO): *Algorithm 5*
– Single-stream MIMO with worst case receiver
– MISO (Chapter 2)

Note that all the centralized results in Figs. 16-17 can be achieved via decentralized processing if the corresponding algorithms are let to converge. Fig. 16 illustrates the sum power as a function of rate target. It can be observed that multi-stream MIMO design (*Algorithm 6*) significantly outperforms other algorithms. The performance gain over the single-stream MIMO design (*Algorithm 5*) is significant, and it is emphasized with the increasing rate target. The results also show that having the worst case receiver assumption in the transceiver design somewhat degrades the performance. This aspect is emphasized near the cell-edge area and with the increasing rate target. In Fig. 17, the sum power is plotted against cell separation. Again, multi-stream MIMO design has superior performance compared with the other algorithms. The performance of all the algorithms improves, as the cell separation increases. The largest improvements in the performance is witnessed for the worst case receiver-based algorithms.

Fig. 18 examines the convergence behavior of the decentralized algorithms

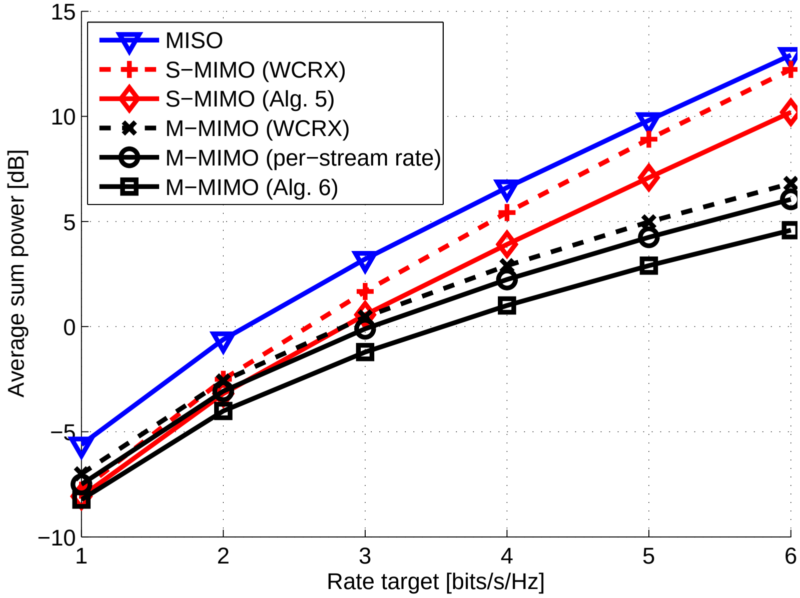

(a) $\eta = 3\text{dB}$

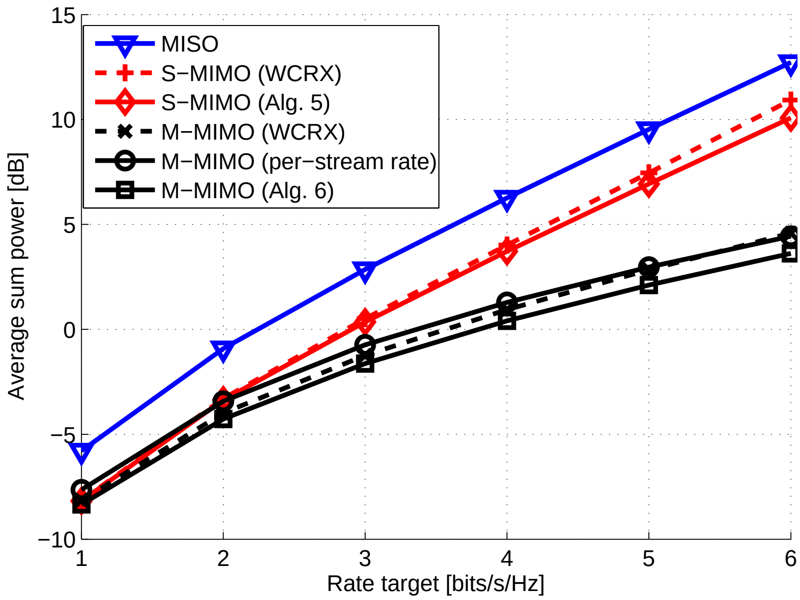

(b) $\eta = 15\text{dB}$

Fig 16. Average sum power versus rate target ([99] © 2015 IEEE).

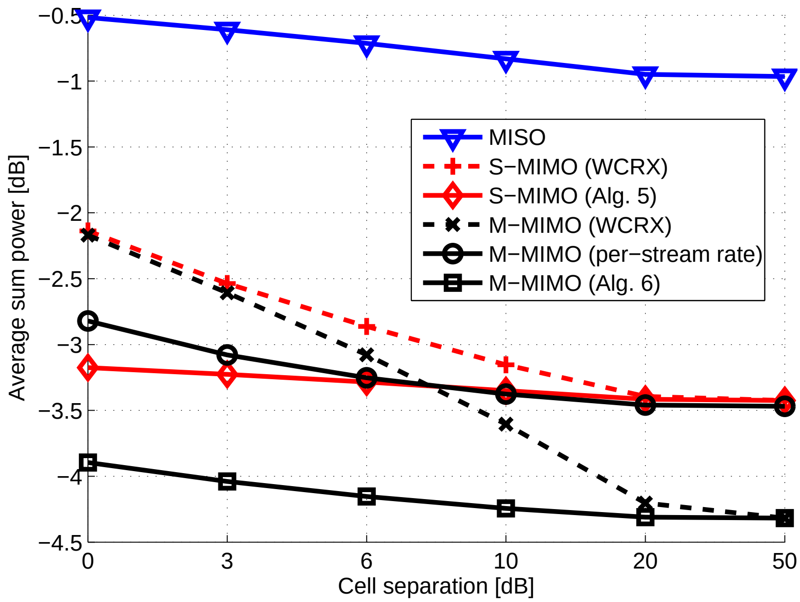

(a) $R = 2$ bits/s/Hz

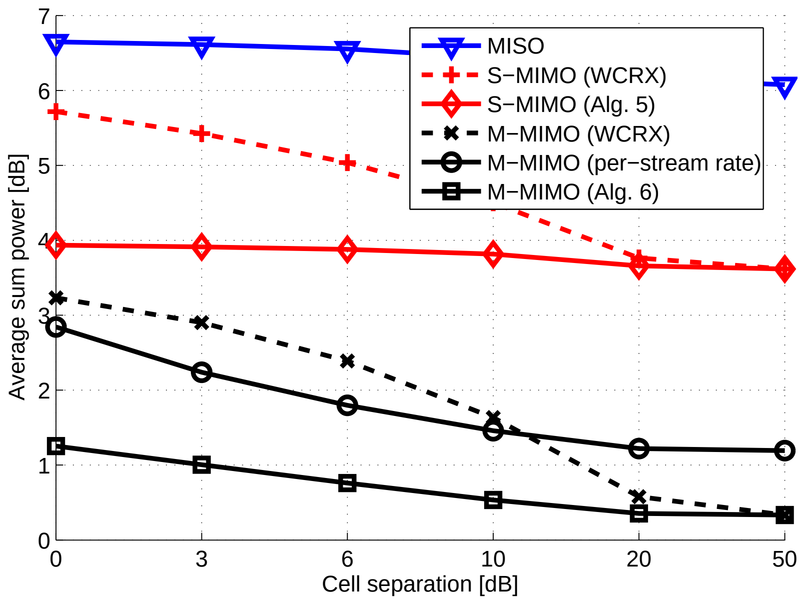

(b) $R = 4$ bits/s/Hz

Fig 17. Average sum power versus cell separation ([99] © 2015 IEEE).

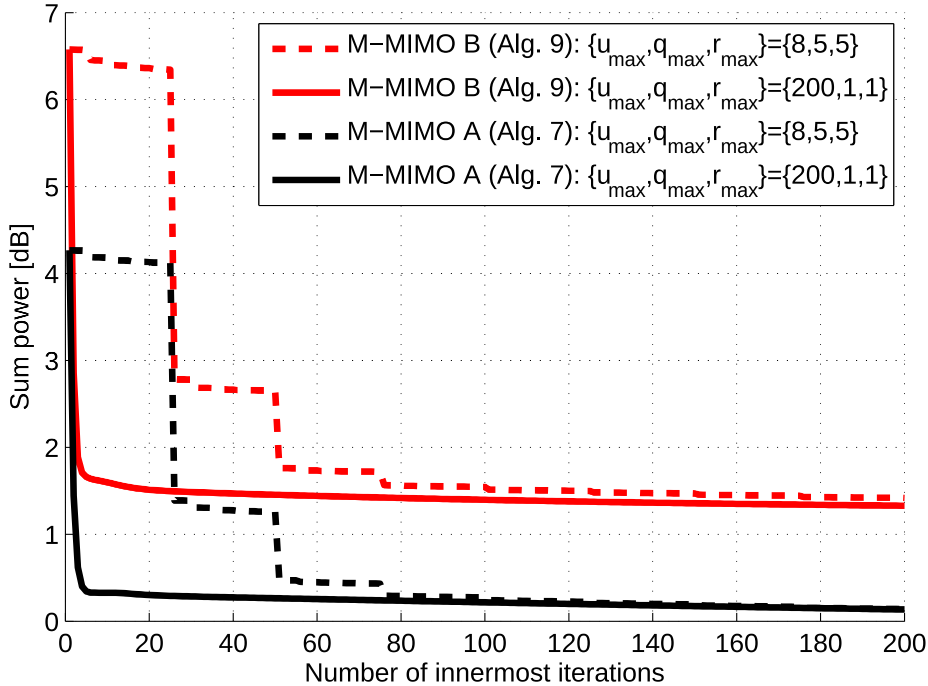

Fig 18. Convergence behavior of decentralized algorithms ([99] © 2015 IEEE).

with signaling strategies A (*Algorithm 7*) and B (*Algorithm 9*). A different number of inner and outer loop iterations are compared. The sum power is plotted as a function of the innermost (subgradient) iteration for a single channel realization. The system parameters are given by $\{B, K, A_{\mathrm{T}}, A_{\mathrm{R}}\} = \{2, 4, 8, 2\}$. The rate target and cell separation are set to 2 bits/s/Hz and 3 dB, respectively, for the rest of the simulations. The symbols $u_{\max}$, $q_{\max}$ and $r_{\max}$ denote the maximum number of iterations in the transmit-receive beamforming, SCA and subgradient optimization steps, respectively. The results demonstrate that even though the algorithms converge to different sum power values, the speed of convergence is comparable. Moreover, the convergence rate is the fastest with one SCA and one subgradient iteration per each transmit beamforming optimization phase in terms of the innermost iterations.

Finally, the performance of *Algorithm 7* and *Algorithm 9* is evaluated in time-correlated flat fading channel conditions with parameters $\{B, K, A_{\mathrm{T}}, A_{\mathrm{R}}\} = \{2, 4, 8, 2\}$. The corresponding channel realizations are generated using Jakes'

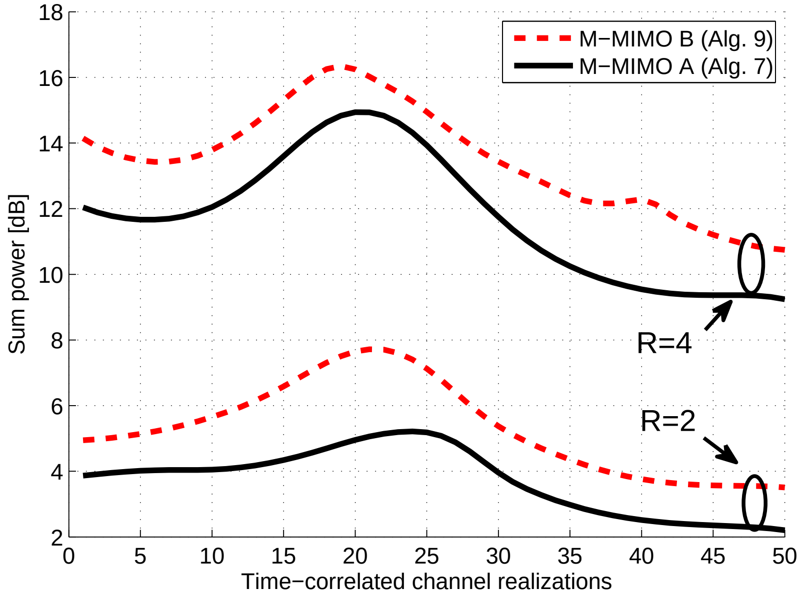

(a) $T_{\mathrm{F}} f_{\mathrm{D}} = 0.005$

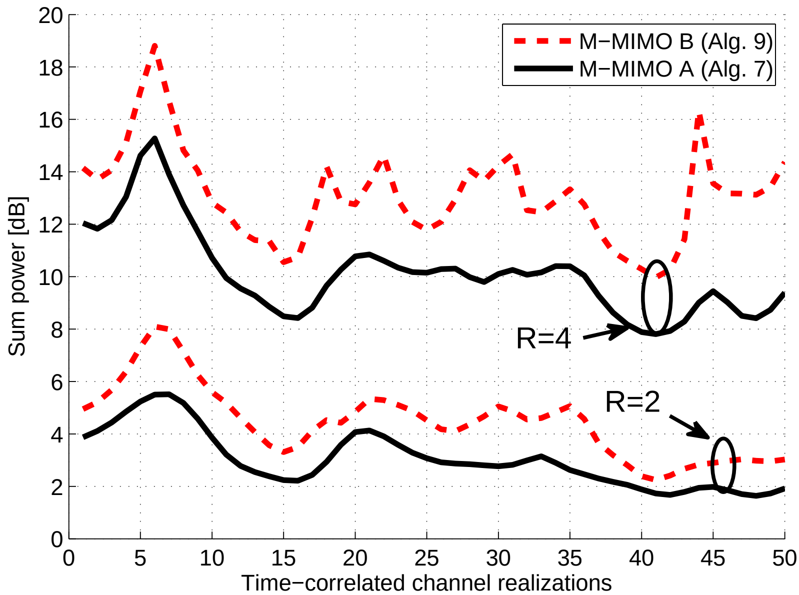

(b) $T_{\mathrm{F}} f_{\mathrm{D}} = 0.02$

Fig 19. Sum power performance in time-correlated channel conditions ([99] © 2015 IEEE).

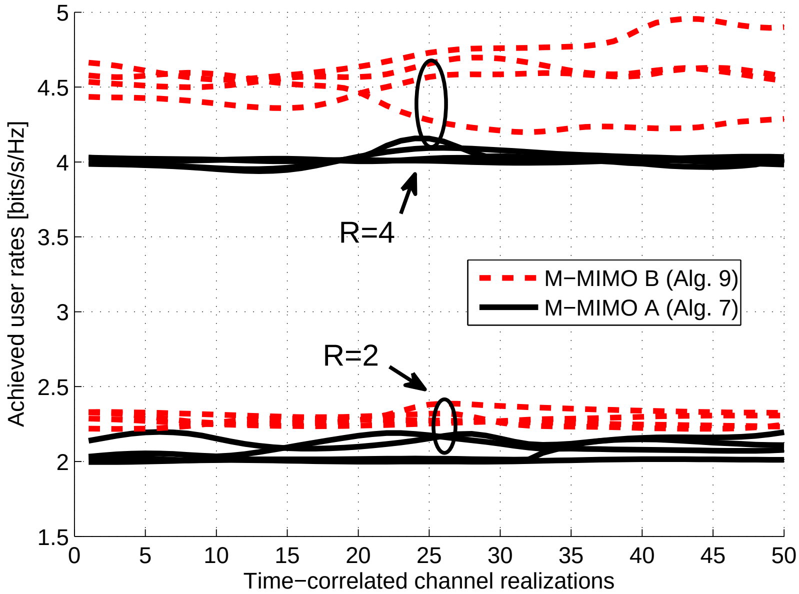

(a) $T_{\mathrm{F}} f_{\mathrm{D}} = 0.005$

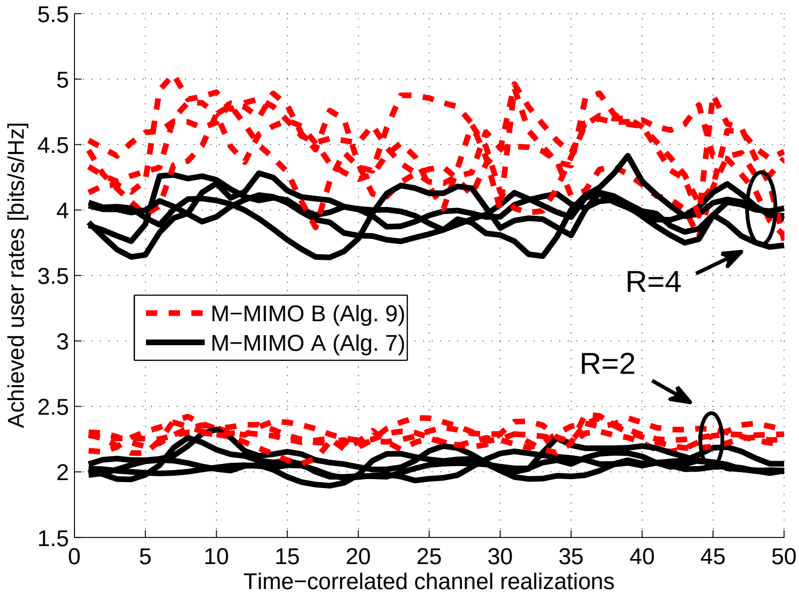

(b) $T_{\mathrm{F}} f_{\mathrm{D}} = 0.02$

Fig 20. Achieved per-user rates in time-correlated channel conditions ([99] © 2015 IEEE).

Doppler spectrum model, as described in Section 2.2.3. The channel variation rate is determined via a normalized user velocity parameter $T_{\mathrm{F}} f_{\mathrm{D}}$, where T_{F} is the duration of each uplink and downlink frame and f_{D} is the maximum Doppler shift. In the simulations, the sum power is measured after each transmit beamforming update phase and the achieved user rates are computed after each receive beamforming phase. Channel conditions are let to change during each uplink and downlink frame. One round of scalar information exchange between the BSs via backhaul is performed after each transmit beamforming design phase. This information will be outdated when used in the next transmit beamforming optimization phase. In Fig. 19, the sum power performance of *Algorithm 7* and *Algorithm 9* is examined for 50 time-correlated channel realizations. In addition, the achieved instantaneous user rates are presented in Fig. 20. Finally, the average rates (over users and iterations) and their ratios to target rate (in percentage) are calculated, and the results are illustrated in *Table 6.* Performance is evaluated for $T_{\mathrm{F}} f_{\mathrm{D}} = 0.005$ and $T_{\mathrm{F}} f_{\mathrm{D}} = 0.02$, which can be considered as 2.7 and 10.8 km/h user velocities if 2 GHz carrier frequency and 1 ms frame duration is assumed. The numerical results show that *Algorithm 7* outperforms *Algorithm 9* with respect to the sum power. However, *Algorithm 9* has higher achieved rates, which implies that it is better protected against outdated information. In most of the numerical examples, the average rates of both algorithms are higher than the target rates.

Table 6. Average rates in time-correlated channel conditions ([99] © 2015 IEEE).

	M-MIMO A (*Alg. 7*)	M-MIMO B (*Alg. 9*)
$T_{\mathrm{F}} f_{\mathrm{D}} = 0.005,\ R = 2$	2.075 (103.8%)	2.281 (114.0%)
$T_{\mathrm{F}} f_{\mathrm{D}} = 0.02,\ R = 2$	2.062 (103.1%)	2.274 (113.7%)
$T_{\mathrm{F}} f_{\mathrm{D}} = 0.005,\ R = 4$	4.015 (100.4%)	4.549 (113.7%)
$T_{\mathrm{F}} f_{\mathrm{D}} = 0.02,\ R = 4$	3.980 (99.50%)	4.450 (111.2%)

3.4 Summary and discussions

In this chapter, novel coordinated beamforming algorithms were proposed for the SPMin problem with user-specific rate targets in a cellular multi-user MIMO system. Centralized MIMO design was derived first, after which two decentralized algorithms were provided. Decentralized processing is enabled by exploiting pilot and backhaul signaling. The used signaling framework is applicable in TDD-based systems since the reciprocity of downlink and uplink channels are exploited. The non-convex original problem is divided into transmit and receive beamforming steps, which are alternately solved such that the objective function (i.e., the sum power) converges. However, global optimality cannot be guaranteed due to the non-convexity of the original problem. In the centralized algorithm, the non-convex transmit beamforming optimization problem is reformulated as a DCP, which can then be approximated and iteratively solved as a series of convex problems, such that the sum power monotonically converges by using the SCA method. The well-known linear MMSE criterion is employed at the receive beamforming optimization step.

In the first decentralized algorithm, sum power is minimized via an iterative over-the-air optimization process where the transmit and receive beamformers are consecutively updated at each BS and user, respectively. BS side processing is aided by local effective CSI, which is acquired from the precoded uplink pilots. In the second decentralized algorithm, the transmit and receive beamformers are iteratively optimized at each BS, requiring only local CSI achieved from one round of antenna-specific uplink pilot signaling. In both algorithms, transmit beamforming design is decoupled among the BSs by applying the primal decomposition method, which allows decentralized processing via scalar backhaul information exchange between the BSs. In addition, simplified decentralized algorithms were developed for a special case of multi-cell MIMO system where the number of data streams per user is limited to one.

The numerical results showed performance gains over the MISO and single-stream MIMO algorithms. The gains are emphasized with the increasing rate target and the number of receive antennas. However, the simpler single-stream MIMO algorithms may be more favorable in the line-of-sight type of channel conditions since the average number of allocated streams per user is close to one. The multi-stream MIMO algorithms were also studied for time-correlated channel conditions where the channel and backhaul information is outdated. In low mobility cases, the achieved instantaneous rates followed the minimum target rates closely while the average rates were even higher than the targets. The MIMO algorithm with effective CSI was superior in terms of sum power performance, whereas the other MIMO scheme with only local CSI achieved higher average rates. This finding implies that the latter algorithm is better protected against outdated channel and backhaul signaling information. Even though the simulation results are promising in a simplified multi-cell environment, further study is needed to reveal the real performance gains of the proposed algorithms by using a more realistic system-level simulator.

It is interesting to notice that the proposed decentralized algorithms may well be applicable to massive MIMO type of systems since the backhaul signaling load does not depend on the number of transmit antennas. Hence, the reduction of signaling overhead, when compared with the centralized algorithm, is emphasized in multi-cell systems with large antenna arrays.

4 Coordinated beamforming in MISO cognitive radio networks

In this chapter, coordinated beamforming is considered in a cognitive radio system where the primary and secondary cells share the same spectrum. The design objective is to minimize the total transmission power of the secondary network while guaranteeing the minimum rate for each SU and keeping the generated interference toward each PU below a predefined threshold. In particular, decentralized coordinated beamforming techniques are developed.

In Section 4.1, the cognitive spectrum sharing multi-user MISO system model is described and the corresponding SPMin problem is formulated with assumptions of perfect and imperfect CSI. Decentralized cognitive beamforming algorithms with perfect and imperfect CSI are developed in Sections 4.2 and 4.3, respectively. The proposed algorithms rely on primal decomposition and ADMM methods to allow decentralized implementations. The performance of the proposed algorithms is evaluated via numerical examples in Sections 4.2.2 and 4.3.2. The chapter is summarized in Section 4.4.

4.1 System model and SPMin problem formulation

Consider a spectrum sharing cognitive radio system where a primary network with P PUs and a secondary network with S SUs coexist. Each PU and SU is equipped with a single antenna. The secondary network consists of T secondary transmitters, each equipped with A_{T} antennas. The considered system is depicted in Fig. 21. For convenience of presentation, the number of primary transmitters is not explicitly presented. Consequently, the term "transmitter" refers to the secondary transmitter unless otherwise stated. The sets of all secondary transmitters, SUs and PUs are denoted by $\mathcal{T}$, $\mathcal{S}$ and $\mathcal{P}$, respectively. Each SU is served by a single secondary transmitter, and each secondary transmitter serves its own set of multiple SUs simultaneously. SU association is assumed to be fixed. The serving transmitter for SU s is denoted by t_s. The set $\mathcal{S}_t$ includes all the SUs served by its respective secondary transmitter s, whereas the set of other secondary cells' users is defined as $\bar{\mathcal{S}}_t = \mathcal{S} \setminus \mathcal{S}_t$. The received signal at SU

s is expressed as

$$y_s \quad = \sum_{s\in\mathcal{S}} \mathbf{h}_{t_s,s}\mathbf{m}_s x_s + \sum_{i\in\mathcal{S}\setminus\{s\}} \mathbf{h}_{t_i,i}\mathbf{m}_i s_i + z_s \tag{85}$$

where $\mathbf{m}_s \in \mathbb{C}^{A_\mathrm{T}\times 1}$ and $x_s \in \mathbb{C}$ denote the unnormalized transmit beamforming vector and the normalized data symbol for SU s. The channel vector from the t_sth secondary transmitter to the sth SU is denoted by $\mathbf{h}_{b_s,s} \in \mathbb{C}^{1\times A_\mathrm{T}}$. The term $z_s \in \mathbb{C}$ with variance Z_0 includes the additive noise and interference from the primary network. The total transmission power of the secondary transmitters is written as

$$P^{\mathrm{tx}} = \sum_{s\in\mathcal{S}} \mathrm{tr}(\mathbf{m}_s\mathbf{m}_s^{\mathrm{H}}) = \sum_{s\in\mathcal{S}} \left\|\mathbf{m}_s\right\|_2^2. \tag{86}$$

The data rate of SU s is given by

$$r_s = \log_2\left(1+\Gamma_s\right) \tag{87}$$

where the SINR is expressed as

$$\Gamma_s = \frac{\left|\mathbf{h}_{t_s,s}\mathbf{m}_s\right|^2}{Z_0 + \sum\limits_{i\in\mathcal{S}\setminus\{s\}} \left|\mathbf{h}_{t_i,s}\mathbf{m}_s\right|^2}. \tag{88}$$

Each PU has a predefined maximum interference power level which the aggregate interference from the secondary network cannot exceed, i.e.,

$$\sum_{t\in\mathcal{T}}\sum_{i\in\mathcal{S}_t} \left|\mathbf{g}_{t,p}\mathbf{m}_i\right|^2 \leq \Phi_p, \forall p\in\mathcal{P} \tag{89}$$

where $\mathbf{g}_{t,p}$ is the channel vector from secondary transmitter s to PU p.

The optimization target is to minimize the sum transmission power of the secondary transmitters, while satisfying the SU-specific minimum rate targets $\{R_s\}_{s\in\mathcal{S}}$ and the PU-specific maximum aggregate interference power constraints $\{\Phi_p\}_{p\in\mathcal{P}}$. Since there is direct mapping between the rate and SINR, the rate targets can be turned into corresponding SINR targets, i.e., $\gamma_s = 2^{R_s} - 1\ \forall s\in\mathcal{S}$. The resulting optimization problem is written as

$$\begin{aligned}
\min_{\{\mathbf{m}_s\}_{s\in\mathcal{S}}}.\quad & \sum_{s\in\mathcal{S}} \left\|\mathbf{m}_s\right\|_2^2 \\
\text{s.t.}\quad & \Gamma_s \geq \gamma_s, \forall s\in\mathcal{S} \\
& \sum_{t\in\mathcal{T}}\sum_{i\in\mathcal{S}_t} \left|\mathbf{g}_{t,p}\mathbf{m}_i\right|^2 \leq \Phi_p, \forall p\in\mathcal{P}.
\end{aligned} \tag{90}$$

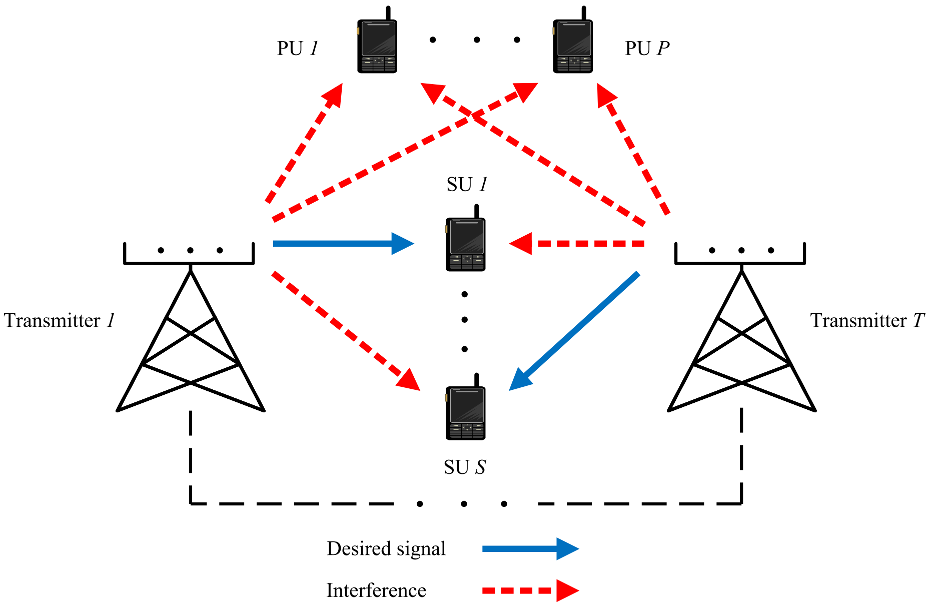

Fig 21. Cognitive multi-cell multi-user MISO system.

In (90), the SINR constraints are met with equality at the optimal solution. However, there may be occasions when the PU-specific interference constraints are inactive, i.e., interference is below a predefined maximum level at the optimal solution. In that case, removing the constraints would not have any impact on solving the problem. In the following mathematical analysis, it is assumed that the aggregate interference constraints are active at the optimal solution. Moreover, (90) is assumed to be strictly feasible, and an optimal solution exists. Feasibility conditions were discussed in [126] for a MISO cognitive radio system with multiple primary and secondary transmitter-receiver pairs. It is worth mentioning that a sufficient condition for (90) to be feasible is when $A_{\mathrm{T}} \geq S+P$, provided that the elements of the channel vectors are independent and random.

Problem (90) can be cast as an SOCP, and solved optimally using standard SOCP solvers assuming that there exists a central controlling unit with access to global CSI. The resulting SOCP is expressed as

$$
\begin{array}{ll}
\underset{p^{\mathrm{tx}},\{\mathbf{m}_s\}_{k\in\mathcal{S}}}{\min.} & p^{\mathrm{tx}} \\
\text{s. t.} & \left\| \bar{\mathbf{m}} \right\|_2 \le p^{\mathrm{tx}} \\
& \left\| \frac{\mathbf{M}^{\mathrm{H}}\mathbf{h}_{t_s,s}^{\mathrm{H}}}{\sqrt{Z_0}} \right\|_2 \le \sqrt{1+\frac{1}{\gamma_s}}\mathbf{h}_{t_s,s}\mathbf{m}_s, \forall s \in \mathcal{S} \\
& \left\| \mathbf{M}^{\mathrm{H}}\mathbf{g}_{t,p}^{\mathrm{H}} \right\|_2 \le \sqrt{\Phi_p}, \forall p \in \mathcal{P}
\end{array}
\tag{91}
$$

where $\bar{\mathbf{m}} = [\mathbf{m}_1^{\mathrm{T}}, \ldots, \mathbf{m}_S^{\mathrm{T}}]^{\mathrm{T}}$ and $\mathbf{M} = [\mathbf{m}_1, \ldots, \mathbf{m}_S]$. The optimal sum transmit power is given by $P^{\mathrm{tx}} = (p^{\mathrm{tx}})^2$. In Section 4.2.1, the coordinated beamforming algorithm is proposed to solve (90) in a decentralized manner.

Next, the assumption of imperfect CSI is considered, and the network design problem is formulated accordingly. The channel vector from transmitter t to SU s is expressed as

$$
\mathbf{h}_{t,s} = \hat{\mathbf{h}}_{t,s} + \mathbf{u}_{t,s}, \forall t \in \mathcal{T}, \forall s \in \mathcal{S} \tag{92}
$$

where $\hat{\mathbf{h}}_{t,s} \in \mathbb{C}^{1\times A_{\mathrm{T}}}$ and $\mathbf{u}_{t,s} \in \mathbb{C}^{1\times A_{\mathrm{T}}}$ are the estimated channel at the transmitter and the CSI error, respectively. It is assumed that the CSI error is bounded by an ellipsoid [103]:

$$
\mathcal{E}_{t,s} = \left\{ \mathbf{u}_{t,s} : \mathbf{u}_{t,s}\mathbf{E}_{t,s}\mathbf{u}_{t,s}^{\mathrm{H}} \le 1 \right\}, \forall t \in \mathcal{T}, \forall s \in \mathcal{S} \tag{93}
$$

where the positive definite matrix $\mathbf{E}_{t,s}$ is known at transmitter t, and it determines the accuracy of the CSI by defining the shape and size of the bounding ellipsoid. The received SINR of the sth SU is given by

$$
\Gamma_k = \frac{\left(\hat{\mathbf{h}}_{t_s,s} + \mathbf{u}_{t_s,s}\right)\left(\mathbf{m}_s\mathbf{m}_s^{\mathrm{H}}\right)\left(\hat{\mathbf{h}}_{t_s,s} + \mathbf{u}_{t_s,s}\right)^{\mathrm{H}}}{Z_0 + \sum\limits_{i\in\mathcal{S}\setminus\{s\}} \left(\hat{\mathbf{h}}_{t_i,s} + \mathbf{u}_{t_i,s}\right)\left(\mathbf{m}_i\mathbf{m}_i^{\mathrm{H}}\right)\left(\hat{\mathbf{h}}_{t_i,s} + \mathbf{u}_{t_i,s}\right)^{\mathrm{H}}} \tag{94}
$$

(95)

The same CSI uncertainty model is also used for the channel vectors from the secondary transmitters to the PUs. In particular, the channel vector from transmitter s to the PU p is given by

$$
\mathbf{g}_{t,p} = \hat{\mathbf{g}}_{t,p} + \mathbf{v}_{t,p}, \forall t \in \mathcal{T}, \forall p \in \mathcal{P} \tag{96}
$$

where $\hat{\mathbf{g}}_{t,p}$ and $\mathbf{v}_{t,p}$ are the estimated channel and the CSI error, respectively. The ellipsoid that bounds CSI uncertainty is given by

$$\mathcal{F}_{t,p} = \left\{ \mathbf{v}_{t,p} : \mathbf{v}_{t,p} \mathbf{F}_{t,p} \mathbf{v}_{t,p}^{\mathrm{H}} \leq 1 \right\}, \forall t \in \mathcal{T}, \forall p \in \mathcal{P} \tag{97}$$

where $\mathbf{F}_{t,p} \succ 0$, and it is known at the transmitter.

The optimization target is to minimize the sum power of secondary transmitters while satisfying the worst case minimum SINR constraints of SUs $\{\gamma_s\}_{s \in \mathcal{S}}$ and the worst case maximum aggregate interference power constraints of PUs $\{\Phi_p\}_{p \in \mathcal{P}}$. This robust problem can be written as

$$\begin{aligned}
\min_{\{\mathbf{m}_s\}_{s\in\mathcal{S}},} \quad & \sum_{k \in \mathcal{K}} \operatorname{tr}\left(\mathbf{m}_k \mathbf{m}_k^{\mathrm{H}}\right) \\
\text{s. t.} \quad & \frac{\left(\hat{\mathbf{h}}_{t_s,s} + \mathbf{u}_{t_s,s}\right)\left(\mathbf{m}_s \mathbf{m}_s^{\mathrm{H}}\right)\left(\hat{\mathbf{h}}_{t_s,s} + \mathbf{u}_{t_s,s}\right)^{\mathrm{H}}}{Z_0 + \sum\limits_{i \in \mathcal{S}\setminus\{s\}} \left(\hat{\mathbf{h}}_{t_i,s} + \mathbf{u}_{t_i,s}\right)\left(\mathbf{m}_i \mathbf{m}_i^{\mathrm{H}}\right)\left(\hat{\mathbf{h}}_{t_i,s} + \mathbf{u}_{t_i,s}\right)^{\mathrm{H}}} \geq \gamma_s \\
& \forall s \in \mathcal{S}, \forall \mathbf{u}_{t_s,s} \in \mathcal{E}_{t_s,s} \\
& \sum_{i \in \mathcal{S}} \left(\hat{\mathbf{g}}_{t,p} + \mathbf{v}_{t,p}\right) \mathbf{m}_i \mathbf{m}_i^{\mathrm{H}} \left(\hat{\mathbf{g}}_{t,p} + \mathbf{v}_{t,p}\right)^{\mathrm{H}} \leq \Phi_p, \forall p \in \mathcal{P}, \forall \mathbf{v}_{t,p} \in \mathcal{F}_{t,p}
\end{aligned} \tag{98}$$

Problem (98) is non-convex and has infinitely many constraints due to the CSI uncertainty. Hence, (98) cannot be solved in its current form. In Section 4.3.1, (98) is approximated and reformulated as a tractable convex problem, and a decentralized robust beamforming algorithm is developed to solve it.

4.2 Decentralized transmit beamforming design

In this section, a primal decomposition-based algorithm is proposed to solve the cognitive SPMin problem (90) in a decentralized manner. The performance of the secondary network is optimized with the assumption that each secondary transmitter knows its local channels to each secondary and primary user in the system, i.e., perfect local CSI is available. The proposed algorithm can be seen as an extension of the cellular algorithm in Section 2.2.1 with an additional set of constraints imposed for the PUs. Since the additional interference constraints are easy to handle, i.e., they can be cast as SOC constraints, the mathematical analysis in Section 2.2.1 applies herein as well. Thorough derivation of the algorithm is given in the following subsections.

4.2.1 Primal decomposition-based algorithm

The primal decomposition method is used to decompose the original problem into network-wide and BS-specific optimizations. The network-wide optimization is solved via the projected subgradient method, whereas the BS-specific optimization relies on either convex optimization techniques or the uplink-downlink duality-based method.

Reformulation of SPMin problem

In order to apply primal decomposition, the original SPMin problem (90) needs to be reformulated by introducing auxiliary variables such that the coupling is transferred from the beamformers into these variables, and by fixing them the problem will decouple. In this respect, two sets of inter-cell interference power variables are introduced, i.e., the interference from each secondary transmitter to each SU and PU. Specifically, the inter-cell interference power from secondary transmitter t to SU s is given by

$$\chi_{t,s} = \sum_{i \in \mathcal{S}_t} \left|\mathbf{h}_{t,s}\mathbf{m}_i\right|^2. \tag{99}$$

Furthermore, the inter-cell interference power from secondary transmitter t to PU p is expressed as

$$\phi_{t,p} = \sum_{i \in \mathcal{S}_t} \left|\mathbf{g}_{t,p}\mathbf{m}_i\right|^2. \tag{100}$$

The reformulated SINR is given by

$$\Gamma_s = \frac{\left|\mathbf{h}_{t_s,s}\mathbf{m}_s\right|^2}{Z_0 + \sum\limits_{t' \in \mathcal{T} \setminus \{t_s\}} \chi_{t',s} + \sum\limits_{i \in \mathcal{S}_t \setminus \{s\}} \left|\mathbf{h}_{t_i,s}\mathbf{m}_i\right|^2}. \tag{101}$$

The resulting problem is expressed as

$$\begin{aligned}
\min_{,\{\mathbf{m}_s\}_{s\in\mathcal{S}},\boldsymbol{\chi},\boldsymbol{\phi}}. \quad & \sum_{s\in\mathcal{S}} \left\|\mathbf{m}_s\right\|_2^2 \\
\text{s.t.} \quad & \widetilde{\Gamma}_s \geq \gamma_s, \forall s \in \mathcal{S} \\
& \sum_{i\in\mathcal{S}_t} \left|\mathbf{h}_{t,s}\mathbf{m}_i\right|^2 \leq \chi_{t,s}, \forall t \in \mathcal{T}, \forall s \in \bar{\mathcal{S}}_t \\
& \sum_{i\in\mathcal{S}_t} \left|\mathbf{g}_{t,p}\mathbf{m}_i\right|^2 \leq \phi_{t,p}, \forall t \in \mathcal{T}, \forall p \in \mathcal{P} \\
& \sum_{i\in\mathcal{S}_t} \left|\mathbf{g}_{t,p}\mathbf{m}_i\right|^2 + \sum_{t'\in\mathcal{T}\setminus\{t\}} \phi_{t',p} \leq \Phi_p, \forall t \in \mathcal{T}, \forall p \in \mathcal{P}
\end{aligned} \tag{102}$$

For notational convenience, all interference variables are gathered into vectors $\boldsymbol{\chi}$ and $\boldsymbol{\phi}$, i.e., the elements of $\boldsymbol{\chi}$ and $\boldsymbol{\phi}$ are taken from the sets $\{\chi_{t,s}\}_{t\in\mathcal{T},s\in\bar{\mathcal{S}}_t}$ and $\{\phi_{t,p}\}_{t\in\mathcal{T},p\in\mathcal{P}}$, respectively. The optimal solution of (90) is equivalent to that of (102) since all the inequality constraints in (102) hold with equality at the optimal point. It is worth mentioning that if a centralized implementation is assumed, the last set of constraints in (102) can be replaced by $\sum_{t\in\mathcal{T}} \phi_{t,p} \leq \Phi_p, \forall t \in \mathcal{T}, \forall p \in \mathcal{P}$. However, the use of the redundant term $\sum_{i\in\mathcal{S}_t} \left|\mathbf{g}_{t,p}\mathbf{m}_i\right|^2$ facilitates decentralized implementation. More details are given in Section 4.2.1.

Based on the derivation in Section 2.2.1, (102) can be cast as an SOCP

$$\begin{aligned}
\min_{p^{\text{tx}},\{\mathbf{m}_s\}_{s\in\mathcal{S}},\boldsymbol{\chi},\boldsymbol{\phi}}. \quad & p^{\text{tx}} \\
\text{s. t.} \quad & \left\| \bar{\mathbf{m}} \right\|_2 \leq p^{\text{tx}} \\
& \left\| \begin{matrix} \mathbf{M}_{t_s}^{\mathrm{H}}\mathbf{h}_{t_s,s}^{\mathrm{H}} \\ \bar{\boldsymbol{\chi}}_s \\ \sqrt{Z_0} \end{matrix} \right\|_2 \leq \sqrt{1+\tfrac{1}{\gamma_s}}\mathbf{h}_{t_s,s}\mathbf{m}_s, \forall s \in \mathcal{S} \\
& \left\| \mathbf{M}_t^{\mathrm{H}}\mathbf{h}_{t,s}^{\mathrm{H}} \right\|_2 \leq \bar{\chi}_{t,s}, \forall t \in \mathcal{T}, \forall s \in \bar{\mathcal{S}}_t \\
& \left\| \mathbf{M}_t^{\mathrm{H}}\mathbf{g}_{t,p}^{\mathrm{H}} \right\|_2 \leq \bar{\phi}_{t,p}, \forall t \in \mathcal{T}, \forall p \in \mathcal{P} \\
& \left\| \begin{matrix} \mathbf{M}_t^{\mathrm{H}}\mathbf{g}_{t,p}^{\mathrm{H}} \\ \bar{\boldsymbol{\phi}}_p \end{matrix} \right\|_2 \leq \sqrt{\Phi_p}, \forall t \in \mathcal{T}, \forall p \in \mathcal{P}
\end{aligned} \tag{103}$$

where $\bar{\chi}_{t,s} = \sqrt{\chi_{t,s}}$, $\bar{\phi}_{t,s} = \sqrt{\phi}_{t,s}$ and $\mathbf{M}_t = [\mathbf{m}_{\mathcal{S}_t(1)}, \ldots, \mathbf{m}_{\mathcal{S}_t(S_t)}]$. The elements of $\bar{\boldsymbol{\chi}}_s$ and $\bar{\boldsymbol{\phi}}_p$ are taken from the set $\{\bar{\chi}_{t',s}\}_{t'\in\mathcal{T}\setminus\{t_s\}}$ and $\{\bar{\phi}_{t',p}\}_{t'\in\mathcal{T}\setminus\{t_s\}}$, respectively. Proposition 1 also holds true herein, and thus, strong duality applies for (103).

Two-level problem structure via primal decomposition

To allow decentralized implementation, primal decomposition is applied to turn (102) into a hierarchical two-level optimization problem. Problem (102) is coupled between the secondary transmitters by the interference variables $\boldsymbol{\chi}$ and $\boldsymbol{\phi}$. Precisely, each element of $\boldsymbol{\chi}$ couples two secondary transmitters, whereas each element of $\boldsymbol{\phi}$ couples all the secondary transmitters. Furthermore, P^{tx} is inherently separable between the secondary transmitters, i.e., $P^{\text{tx}} = \sum_{t\in\mathcal{T}} P_t^{\text{tx}}$, where P_t^{tx} is the transmission power of transmitter t. Hence, (102) will decouple between the secondary transmitters if $\boldsymbol{\chi}$ and $\boldsymbol{\phi}$ are fixed. Thus, primal decomposition is an adequate method to decompose (102) into a network-wide master problem and transmitter-specific subproblems, one for each secondary transmitter. For notational purposes, transmitter-specific interference vectors are introduced, i.e., $\boldsymbol{\chi}_t$ and $\boldsymbol{\phi}_t$, $\forall t \in \mathcal{T}$, which consist of all $\chi_{t,s}$ and $\phi_{t,p}$ that are coupled with transmitter t. Precisely, the elements of $\boldsymbol{\chi}_t$ are taken from the sets $\{\chi_{t,s}\}_{s\in\bar{\mathcal{S}}_t}$ and $\{\chi_{t',s}\}_{t'\in\mathcal{T}\setminus\{t_s\},s\in\mathcal{S}_t}$. The vector $\boldsymbol{\phi}_t$ is defined by $\boldsymbol{\phi}_t = \boldsymbol{\phi}$ since the transmitter t is coupled with each $\phi_{t,p}$.

The lower level subproblem at secondary transmitter t for fixed $\boldsymbol{\chi}_t$ and $\boldsymbol{\phi}_t$ is written as

$$\begin{array}{ll}\underset{P_t^{\text{tx}},\{\mathbf{m}_s\}_{s\in\mathcal{S}_t}}{\text{min.}} & P_t^{\text{tx}} \\ \text{s.t.} & \sum_{s\in\mathcal{S}_t} \left\|\mathbf{m}_s\right\|_2^2 \leq P_t^{\text{tx}} \\ & \widetilde{\Gamma}_s \geq \gamma_s, \forall s \in \mathcal{S}_t \\ & \sum_{i\in\mathcal{S}_t} \left|\mathbf{h}_{t,s}\mathbf{m}_i\right|^2 \leq \chi_{t,s}, \forall k \in \bar{\mathcal{S}}_t \\ & \sum_{i\in\mathcal{S}_t} \left|\mathbf{g}_{t,p}\mathbf{m}_i\right|^2 \leq \phi_{t,p}, \forall p \in \mathcal{P} \\ & \sum_{i\in\mathcal{S}_t} \left|\mathbf{g}_{t,p}\mathbf{m}_i\right|^2 + \sum_{t'\in\mathcal{T}\setminus\{t\}} \phi_{t',p} \leq \Phi_p, \forall p \in \mathcal{P}.\end{array} \tag{104}$$

Strong duality holds for (104) since it is a simplified version of (102).

The network-wide master problem controls the transmitter-specific subproblems by updating the interference variables $\{\boldsymbol{\chi}_t, \boldsymbol{\phi}_t\}_{t\in\mathcal{T}}$. The master problem is expressed as

$$\begin{array}{ll}\underset{\{\boldsymbol{\chi}_t,\boldsymbol{\phi}_t\}_{t\in\mathcal{T}}}{\text{min.}} & \sum_{t\in\mathcal{T}} g_t^\star(\boldsymbol{\chi}_t, \boldsymbol{\phi}_t) \\ \text{subject to} & \boldsymbol{\chi}_t \in \mathbb{R}_{++}^{M_t}, \forall t \in \mathcal{T} \\ & \boldsymbol{\phi}_t \in \mathcal{D}, \forall t \in \mathcal{T}\end{array} \tag{105}$$

where $g_t^\star(\boldsymbol{\chi}_t, \boldsymbol{\phi}_t)$ denotes the optimal objective value of (104) for the given $\boldsymbol{\chi}_t$ and $\boldsymbol{\phi}_t$. The set $\mathcal{D}$ is denoted by $\mathcal{D} = \left\{\boldsymbol{\phi}_t : \phi_{t,p} \in \mathbb{R}_{++}, \sum_{t\in\mathcal{T}} \phi_{t,p} = \Phi_p, \forall p \in \mathcal{P}\right\}$. The problem (105) is convex since its objective and constraint functions are convex.

Master problem: network-wide optimization step

In this section, an outer loop optimization algorithm is derived for the inter-cell interference coordination by iteratively solving the higher level master problem (15). Problem (15) can be solved via a standard projected subgradient method using the following updates of interference power variables:

$$\chi_{t,s}^{(r+1)} = \mathcal{P}_{++}\left\{\chi_{t,s}^{(r)} - \sigma^{(r)}\left(\lambda_{t_s,s}^{(r)} - \mu_{t,s}^{(r)}\right)\right\}, \forall t \in \mathcal{T}, \forall s \in \bar{\mathcal{S}}_t \tag{106}$$

$$\phi_{t,p}^{(r+1)} = \mathcal{P}_{\mathcal{D}}\left\{\phi_{t,p}^{(r)} - \sigma^{(r)}\left(\sum_{t'\in\mathcal{T}\setminus\{t\}} \upsilon_{t',p}^{(r)} - \nu_{t,p}^{(r)}\right)\right\}, \forall t \in \mathcal{T}, \forall p \in \mathcal{P} \tag{107}$$

where $\mathcal{P}_{++}$ and $\mathcal{P}_{\mathcal{D}}$ are the projections onto the sets of positive real numbers and $\mathcal{D}$, respectively. Step-size at iteration t is denoted by $\sigma^{(r)}$. The terms $\lambda_{t_s,s}^{(r)} - \mu_{t,s}^{(r)}$ and $\sum_{t'\in\mathcal{T}\setminus\{t\}} \upsilon_{t',p}^{(r)} - \nu_{t,p}^{(r)}$ are the subgradients of (105) evaluated at the points $\chi_{t,s}^{(r)}$ and $\phi_{t,s}^{(r)}$, respectively. The scalars $\lambda_{t_s,s}^{(r)}$ and $\mu_{t,s}^{(r)}$ are the optimal dual variables associated with $\chi_{t,s}^{(r)}$ in subproblem t_s and t, respectively. Similarly, $\upsilon_{t',p}^{(r)}$ and $\nu_{t,p}^{(r)}$ are the optimal dual variables associated with $\phi_{t,s}^{(r)}$ in t'th and tth subproblems, respectively. The aforementioned subgradients can be found by following the proof of Proposition 2.

It is worth mentioning that the update process of $\phi_{t,p}$ would be different in a decentralized case if the inter-tier interference constraint was equivalently replaced by $\sum_{t\in\mathcal{T}} \phi_{t,p} \le \Phi_p, \forall t \in \mathcal{T}, \forall p \in \mathcal{P}$. In this case, the constraint $\sum_{t\in\mathcal{T}} \phi_{t,p} \le \Phi_p$, $\forall p \in \mathcal{P}$ vanishes in the corresponding subproblem t leading to a subgradient of $-\nu_{t,p}$ at the point $\phi_{t,p}$. The subgradient $-\nu_{t,p}$ depends only on the subproblem t, resulting in an always increasing $\phi_{t,p}$ (before the projection $\mathcal{P}_{\mathcal{D}}$) at each subgradient iteration. By having the term $\sum_{i\in\mathcal{S}_t} \left|\mathbf{g}_{t,p}\mathbf{m}_i\right|^2$ in (90), always increasing $\phi_{t,p}$ can be avoided. Instead, the subgradient in (107) depends on all the subproblems leading to a proper update process of $\phi_{t,p}$.

Since each $\phi_{t,p}$ is projected, such that $\sum_{t\in\mathcal{T}} \phi_{t,p} = \Phi_p$, the last two constraints in (90) must be the same, and thus, their dual variables are also the same, i.e., $\upsilon_{t,p} = \nu_{t,p}$, $\forall t \in \mathcal{T}, \forall p \in \mathcal{P}$. Hence, the term $\sum_{t'\in\mathcal{T}\setminus\{t\}} \upsilon_{t',p}(t)$ in

(107) can be equivalently rewritten as $\sum_{t' \in \mathcal{T} \setminus \{t\}} \nu_{t',p}(t)$. Since the subgradient update is now obtained by solving only $\{\nu_{t,p}\}_{t \in \mathcal{T}}$, the last constraint in (90) can be removed. Thus, (90) can be reformulated accordingly. In the following sections, all the related problems are formulated accordingly.

Subproblems: transmitter-specific optimization step

Two alternative methods are introduced to compute the transmit beamformers and dual variables by solving the subproblem (104) and its dual problem. The first method is based on standard convex optimization techniques, i.e., SOCP and SDP. The second approach exploits uplink-downlink duality by optimizing the downlink transmit beamformers via virtual uplink powers and virtual uplink receive beamformers. The computational complexity of the latter method is generally lower than that of the SOCP and SDP. In the following, the iteration index q is dropped for the sake of clarity.

Convex optimization-based solution

The transmitter-specific subproblem (104) can be cast as an SOCP by following the derivation in Section 2.2.1. The resulting SOCP problem is given by

$$\begin{aligned} \min_{p_t^{\text{tx}}, \{\mathbf{m}_s\}_{s \in \mathcal{S}_t}} \quad & p_t^{\text{tx}} \\ \text{s. t.} \quad & \left\| \bar{\mathbf{m}}_t \right\|_2 \leq p_t^{\text{tx}} \\ & \left\| \begin{matrix} \mathbf{M}_{t_s}^{\text{H}} \mathbf{h}_{t_s,s}^{\text{H}} \\ \bar{\boldsymbol{\chi}}_s \\ \sqrt{Z_0} \end{matrix} \right\|_2 \leq \sqrt{1 + \frac{1}{\gamma_s}} \mathbf{h}_{t_s,s} \mathbf{m}_s, \forall s \in \mathcal{S}_t \\ & \left\| \mathbf{M}_t^{\text{H}} \mathbf{h}_{t,s}^{\text{H}} \right\|_2 \leq \bar{\chi}_{t,s}, \forall s \in \bar{\mathcal{S}}_t \\ & \left\| \mathbf{M}_t^{\text{H}} \mathbf{g}_{t,p}^{\text{H}} \right\|_2 \leq \bar{\phi}_{t,p}, \forall p \in \mathcal{P} \end{aligned} \tag{108}$$

where $\bar{\mathbf{m}}_t = [\mathbf{m}_{\mathcal{S}_t(1)}^{\text{T}}, \ldots, \mathbf{m}_{\mathcal{S}_t(S_t)}^{\text{T}}]^{\text{T}}$ and the optimal per-transmitter power is given by $P_t^{\text{tx}} = (p_t^{\text{tx}})^2$. As discussed in Section 2.2.1, some standard solvers, such as CVX [88], cannot provide the dual variables by solving the primal problems that are formulated as SOCP problems. Since strong duality holds for (14), the optimal dual variables can be found by solving the Lagrange dual problem of

(14). The dual problem is given by

$$\begin{aligned}
\max_{\boldsymbol{\lambda}_t,\boldsymbol{\mu}_t,\boldsymbol{\nu}_t}. \quad & \sum_{s\in\mathcal{S}_t} \lambda_{t,s} \left(Z_0 + \sum_{t'\in\mathcal{T}\setminus\{t_s\}} \chi_{t',s} \right) - \sum_{s\in\bar{\mathcal{S}}_t} \mu_{t,s}\chi_{t,s} - \sum_{p\in\mathcal{P}} \nu_{t,p}\phi_{t,p} \\
\text{s. t.} \quad & \mathbf{I} + \sum_{i\in\mathcal{S}_t} \lambda_{t,i}\mathbf{h}_{t_s,i}^{\mathrm{H}}\mathbf{h}_{t_s,i} + \sum_{j\in\bar{\mathcal{S}}_b} \mu_{t,j}\mathbf{h}_{t_s,j}^{\mathrm{H}}\mathbf{h}_{t_s,j} - \left(1+\tfrac{1}{\gamma_s}\right)\lambda_{t,s}\mathbf{h}_{t_s,s}^{\mathrm{H}}\mathbf{h}_{t_s,s} \\
& + \sum_{p\in\mathcal{P}} \nu_{t,p}\mathbf{g}_{t_s,p}^{\mathrm{H}}\mathbf{g}_{t_s,p} \succeq 0, \forall\ s\in\mathcal{S}_t \\
& \boldsymbol{\lambda}_t \succeq 0, \boldsymbol{\mu}_t \succeq 0, \boldsymbol{\nu}_t \succeq 0
\end{aligned} \tag{109}$$

where $\boldsymbol{\lambda}_t = [\lambda_{t,1},\ldots,\lambda_{t,S_t}]^{\mathrm{T}}$, $\boldsymbol{\mu}_t = [\mu_{t,1},\ldots,\mu_{t,|\bar{\mathcal{S}}_t|}]^{\mathrm{T}}$ and $\boldsymbol{\nu}_t = [\nu_{t,1},\ldots,\nu_{t,P}]^{\mathrm{T}}$. Problem (109) can be optimally solved by using SDP solvers since it can be reformulated as a standard form SDP by turning the maximization into minimization and changing the sign of the objective function.

Uplink-downlink duality-based solution

Uplink-downlink SINR duality can be exploited to solve the transmitter-specific subproblem (104) without relying on convex optimization techniques. Instead, the downlink transmit beamformers can be computed with the aid of the MMSE-based uplink receive beamformers and the uplink powers, which can be found by solving a virtual uplink SPMin problem via a simple projected subgradient and fixed-point iteration methods. A detailed derivation of the uplink-downlink duality-based approach is given as follows.

First, the dual problem (109) is split into an outer maximization on $\boldsymbol{\mu}_t$ and $\boldsymbol{\nu}_t$ and an inner maximization on $\boldsymbol{\lambda}_t$. The vectors $\boldsymbol{\mu}_t$ and $\boldsymbol{\lambda}_t$ consist of the dual variables associated with the inter-cell interference and SINR constraints, respectively. Since (19) is concave, both the outer and inner problems are also concave.

The outer maximization can be expressed as

$$\begin{aligned}
\max_{\boldsymbol{\mu}_t,\boldsymbol{\nu}_t}. \quad & \bar{g}_t^{\star}(\boldsymbol{\mu}_t,\boldsymbol{\nu}_t) \\
\text{subject to} \quad & \boldsymbol{\mu}_t \in \mathbb{R}_+^{S_t}, \boldsymbol{\nu}_t \in \mathbb{R}_+^{P}
\end{aligned} \tag{110}$$

where $\bar{g}_t^{\star}(\boldsymbol{\mu}_t,\boldsymbol{\nu}_t)$ is the optimal objective value of the inner maximization on $\boldsymbol{\lambda}_t$ for given $\boldsymbol{\mu}_t$ and $\boldsymbol{\nu}_t$. The projected subgradient method is used to optimally solve the outer maximization problem (20) for $\boldsymbol{\mu}_t$ and $\boldsymbol{\nu}_t$. Projected subgradient updates are given by

$$\boldsymbol{\mu}_{t,s}^{(n+1)} = \mathcal{P}_{++}\left\{\mu_{t,s}^{(n)} + \sigma^{(n)}u_{t,s}^{(n)}\right\}, \forall s \in \bar{\mathcal{S}}_t \tag{111}$$

$$\boldsymbol{\nu}_{t,p}^{(n+1)} = \mathcal{P}_{+}\left\{\nu_{t,p}^{(n)} + \sigma^{(n)}\tilde{u}_{t,p}^{(n)}\right\}, \forall p \in \mathcal{P} \tag{112}$$

where $\mathcal{P}_+$ is the projection onto the real non-negative values. At iteration n, the step-size is denoted by $\sigma^{(n)}$. Based on Proposition 2, subgradients $u_{t,s}^{(n)}$ and $\tilde{u}_{t,p}^{(n)}$ at points $\mu_{t,s}^{(n)}$ and $\nu_{t,p}^{(n)}$ can be expressed as

$$u_{t,s}^{(n)} = \textstyle\sum_{i\in\mathcal{S}_t} |\mathbf{h}_{t,s}\mathbf{m}_i|^2 - \chi_{t,s}, \forall s \in \bar{\mathcal{S}}_t \tag{113}$$

$$\tilde{u}_{t,p}^{(n)} = \textstyle\sum_{i\in\mathcal{S}_t} |\mathbf{g}_{t,p}\mathbf{m}_i|^2 - \phi_{t,p}, \forall p \in \mathcal{P}. \tag{114}$$

In order to solve (113), the optimal beamformers $\{\mathbf{m}_s\}_{s\in\mathcal{S}_t}$ need to be found at each iteration n. For ease of presentation, the iteration index n is omitted in the following.

The inner optimization problem on $\boldsymbol{\lambda}_t$ is expressed as

$$\begin{aligned} \max_{\boldsymbol{\lambda}_t}.\ & \sum_{s\in\mathcal{S}_t} \lambda_{t,s}\left(Z_0 + \sum_{t'\in\mathcal{T}\setminus\{t\}} \chi_{t',s}\right) \\ \text{s. t. } & \mathbf{I} + \sum_{i\in\mathcal{S}_t} \lambda_{t,i}\mathbf{h}_{t_s,i}^{\mathrm{H}}\mathbf{h}_{t_s,i} + \sum_{j\in\bar{\mathcal{S}}_t} \mu_{t,j}\mathbf{h}_{t_s,j}^{\mathrm{H}}\mathbf{h}_{t_s,j} \\ & + \sum_{p\in\mathcal{P}} \nu_{t,p}\mathbf{g}_{t_s,p}^{\mathrm{H}}\mathbf{g}_{t_s,p} - \left(1+\tfrac{1}{\gamma_s}\right)\lambda_{t,s}\mathbf{h}_{t_s,s}^{\mathrm{H}}\mathbf{h}_{t_s,s} \succeq 0, \forall\ s\in\mathcal{S}_t \\ & \boldsymbol{\lambda}_t \succeq 0. \end{aligned} \tag{115}$$

Note that the term $\sum_{s\in\bar{\mathcal{S}}_t} \mu_{t,s}\chi_{t,s} - \sum_{p\in\mathcal{P}} \nu_{t,p}\phi_{t,p}$ from (109) is now fixed, and it can be omitted from the objective since it does not have any impact on finding the optimal $\boldsymbol{\lambda}_t$. Optimal $\boldsymbol{\lambda}_t$ and $\{\mathbf{m}_s\}_{s\in\mathcal{S}_t}$ can be found with the aid of uplink-downlink duality by first formulating a virtual uplink problem, and then solving it using simple methods. Based on the proof of Theorem 1, it can be shown that (115) is equivalent to the following problem:

$$\begin{aligned} \min_{\boldsymbol{\lambda}_t,\{\mathbf{w}_s\}_{s\in\mathcal{S}_t}}.\ & \sum_{s\in\mathcal{S}_t} \lambda_{t,s}\left(Z_0 + \sum_{t'\in\mathcal{T}\setminus\{t\}} \chi_{t',s}\right) \\ \text{s. t. } & \tfrac{1}{\gamma_s}\lambda_{t,s}\left|\mathbf{w}_s^{\mathrm{H}}\mathbf{h}_{t_s,s}\right|^2 - \sum_{i\in\mathcal{S}_{t_s}\setminus\{s\}} \lambda_{t,i}\left|\mathbf{w}_s^{\mathrm{H}}\mathbf{h}_{t_i,i}\right|^2 \\ & \geq \sum_{j\in\bar{\mathcal{S}}_t} \mu_{t,j}\left|\mathbf{w}_s^{\mathrm{H}}\mathbf{h}_{t_s,j}\right|^2 + \sum_{p\in\mathcal{P}} \nu_{t,p}\left|\mathbf{w}_s^{\mathrm{H}}\mathbf{g}_{t_s,p}\right|^2 \\ & + \mathbf{w}_s^{\mathrm{H}}\mathbf{I}\mathbf{w}_s, \forall\ s\in\mathcal{S}_t \\ & \boldsymbol{\lambda}_t \succeq 0. \end{aligned} \tag{116}$$

where $\mathbf{w}_s \in \mathbb{C}^{A_{\mathrm{T}} \times 1}$ is a virtual uplink receive beamformer for SU s. Problem (116) can be interpreted as a virtual dual uplink (weighted) SPMin problem for a cognitive multi-user MISO system where the SU-specific SINR constraints remain the same as in the downlink. Precisely, the vectors $\boldsymbol{\lambda}_t$, $\boldsymbol{\mu}_t$ and $\boldsymbol{\nu}_t$ can be interpreted as the virtual dual uplink powers for the SUs at the serving cell, SUs at the other cells and PUs, respectively. Moreover, the virtual uplink power of SU s is scaled in the objective by a constant that is the sum of the noise and fixed interference powers experienced by SU s in the downlink.

Following the proof of Proposition 3, (116) can be optimally solved for $\boldsymbol{\lambda}_t$ via the following fixed point iteration:

$$\lambda_{t,s}^{(m+1)} = \frac{1}{\left(1 + \frac{1}{\gamma_s}\right) \mathbf{h}_{t_s,s} \left(\boldsymbol{\Omega}_t^{(m)}\right)^{-1} \mathbf{h}_{t_s,s}^{\mathrm{H}}}, \forall s \in \mathcal{S}_t \tag{117}$$

where

$$\begin{aligned} \boldsymbol{\Omega}_t^{(m)} &= \mathbf{I} + \sum_{i \in \mathcal{S}_t} \lambda_{t,i}^{(m)} \mathbf{h}_{t_s,i}^{\mathrm{H}} \mathbf{h}_{t_s,i} \\ &+ \sum_{j \in \bar{\mathcal{S}}_t} \mu_{t,j} \mathbf{h}_{t_s,j}^{\mathrm{H}} \mathbf{h}_{t_s,j} + \sum_{p \in \mathcal{P}} \nu_{t,p} \mathbf{g}_{t_s,p}^{\mathrm{H}} \mathbf{g}_{t_s,p}. \end{aligned} \tag{118}$$

For fixed (optimal) $\boldsymbol{\lambda}_t$, the optimal virtual uplink receive beamformers $\{\acute{\mathbf{w}}_s\}_{s \in \mathcal{S}_t}$ can be computed using the following linear MMSE receiver

$$\begin{aligned} \acute{\mathbf{w}}_s = \frac{\grave{\mathbf{w}}_s}{||\grave{\mathbf{w}}_s||_2}, \grave{\mathbf{w}}_s = \Bigg(&\sum_{i \in \mathcal{S}_t} \lambda_{t,i} \mathbf{h}_{t_s,i}^{\mathrm{H}} \mathbf{h}_{t_s,i} + \sum_{j \in \bar{\mathcal{S}}_t} \mu_{t,j} \\ \mathbf{h}_{t_s,j}^{\mathrm{H}} \mathbf{h}_{t_s,j} + \sum_{p \in \mathcal{P}} \nu_{t,p} \mathbf{g}_{t_s,p}^{\mathrm{H}} \mathbf{g}_{t_s,p} + \mathbf{I} &\Bigg)^{-1} \mathbf{h}_{t_s,s}, \forall s \in \mathcal{S}_t. \end{aligned} \tag{119}$$

Based on the proof of Proposition 4, it can be shown that the optimal downlink transmit beamformers $\{\mathbf{m}_s\}_{s \in \mathcal{S}_t}$ are found via the optimal virtual uplink beamformers $\{\acute{\mathbf{w}}_s\}_{s \in \mathcal{S}_t}$ by scaling, i.e.,

$$\mathbf{m}_s = \sqrt{\varepsilon_s} \acute{\mathbf{w}}_s, \forall s \in \mathcal{S}_t. \tag{120}$$

The scaling factors $\{\varepsilon_s\}_{s \in \mathcal{S}_t}$ are solved via the matrix equation:

$$[\varepsilon_1, \ldots, \varepsilon_{S_t}]^{\mathrm{T}} = \mathbf{A}^{-1} \mathbf{b} \tag{121}$$

where the (i,j)-th and sth elements of the matrix $\mathbf{A}$ and the vector $\mathbf{b}$ are given by

$$[\mathbf{A}]_{ij} = \begin{cases} (1/\gamma_i)|\mathbf{h}_{t_i,i}\acute{\mathbf{w}}_i|^2, & \text{if} \quad i = j \\ -|\mathbf{h}_{t_i,i}\acute{\mathbf{w}}_j|^2, & \text{if} \quad i \neq j \end{cases}, \forall i, j \in \mathcal{S}_t \tag{122}$$

and $[\mathbf{b}]_s = \sum_{t' \in \mathcal{T} \setminus \{t_s\}} \chi_{t',s} + Z_0$, $\forall s \in \mathcal{S}_t$, respectively.

In conclusion, the optimal objective value of the downlink problem (104) is the same as the optimal objective value obtained by solving the outer maximization (110) via the projected subgradient method (111)-(112) and the inner minimization via the virtual uplink problem (116). Consequently, the achieved downlink beamformers and the dual variables are optimal. These optimization steps can be solved independently at secondary transmitter t, for all $t \in \mathcal{T}$ in parallel. The proposed transmitter-level optimization is summarized in *Algorithm 11.*

Algorithm 11 Transmitter-specific optimization via uplink-downlink duality

```
Set m = 0 and n = 0. Initialize λ_t^(0), μ_t^(0) and ν_t^(0).
repeat
    repeat
        Update virtual uplink powers λ_t^(m+1) via fixed-point iteration (117).
        Set m = m + 1.
    until desired level of convergence
    Compute virtual uplink receive beamformers {ẃ_s}_{s∈S_t} via MMSE criterion (119).
    Compute downlink transmit beamformers {m_s}_{s∈S_t} via scaling (120).
    Update dual variables μ_t^(n+1) and ν_t^(n+1) via projected subgradient
    method (111) and (112), respectively.
    Set n = n + 1.
until desired level of convergence
```

Decentralized implementation

Decentralized implementation is enabled by having local CSI at each transmitter and allowing the exchange of the BS-specific subgradients between the coupled BSs via low-rate backhaul links. Local CSI can be acquired by each transmitter via antenna-specific uplink pilots if a TDD-based system is assumed since the uplink and downlink channels are reciprocal. After having the local CSI, the subproblem t in (104) and the corresponding part of the master problem in (105), i.e., the update of $\boldsymbol{\chi}_t$ and $\boldsymbol{\phi}_t$, can be solved independently at transmitter t, for all $t \in \mathcal{T}$ in parallel. At subgradient iteration r, the backhaul information exchange is performed by transmitter t as follows. Transmitter t signals the dual variables associated with the SINR constraints, i.e., $\{\lambda_{t,s}\}_{s\in\mathcal{S}_t}$, to all the interfering transmitters. Whereas the dual variables associated with the inter-cell interference constraints, i.e., $\{\mu_{t,s}\}_{s\in\bar{\mathcal{S}}_t}$, are signaled to the transmitter of which user is being interfered by transmitter t. In addition, transmitter t signals the dual variables associated with $\boldsymbol{\phi}_t$, i.e., $\{\nu_{t,p}\}_{p\in\mathcal{P}}$, to all other transmitters. The total amount of the required backhaul signaling at each network-wide subgradient iteration t is the sum of the real-valued terms exchanged between the coupled transmitters, i.e., $2T(T-1)S_t$ for $\boldsymbol{\chi}$ optimization and $T(T-1)P$ for $\boldsymbol{\phi}$ optimization. The primal decomposition-based decentralized coordinated beamforming design is summarized in *Algorithm 12*. All the calculations in *Algorithm 12* are performed at transmitter t, for all $t \in \mathcal{T}$ in parallel. In conclusion, *Algorithm 12* converges to the optimal solution if the step-sizes are properly chosen and the iterates are feasible.

Algorithm 12 Decentralized transmit beamforming design based on primal decomposition method for cognitive MISO system

1: Set $t = 0$. Initialize interference variables $\boldsymbol{\chi}_t^{(0)}$ and $\boldsymbol{\phi}_t^{(0)}$.
2: **repeat**
3: Compute transmit beamformers and dual variables $\{\mathbf{m}_s, \lambda_{t,s}\}_{s\in\mathcal{S}_t}$, $\{\mu_{t,s}\}_{s\in\bar{\mathcal{S}}_t}$, $\{\nu_{t,p}\}_{p\in\mathcal{P}}$ by solving SOCP (108) and SDP (109), respectively, or alternatively by using uplink-downlink duality-based *Algorithm 11.*
4: Communicate $\{\lambda_{t,s}\}_{s\in\mathcal{S}_t}$, $\{\mu_{t,s}\}_{s\in\bar{\mathcal{S}}_b}$ and $\{\nu_{t,p}\}_{p\in\mathcal{P}}$ to the coupled transmitters via backhaul.
5: Update interference variables $\boldsymbol{\chi}_t^{(r+1)}$ and $\boldsymbol{\phi}_t^{(r+1)}$ via projected subgradient method (111) and (112), respectively.
6: Set $r = r + 1$.
7: **until** desired level of convergence

Practical considerations and alternative algorithms

At the cost of sub-optimal performance, *Algorithm 12* can be stopped after a limited number of iterations since feasible beamformers can be provided at intermediate iterations. This practical property can be used to avoid extra delay and reduce backhaul signaling overhead. Furthermore, *Algorithm 12* allows for some special design cases where the number of coupled optimization variables is decreased leading to reduced computational and backhaul signaling loads. Some lower complexity design cases are given below

- Common SU-specific interference constraints: $\chi_{t,s} = \chi, \forall t \in \mathcal{T}, \forall s \in \bar{\mathcal{S}}_t$.
- Fixed SU-specific interference constraints: $\chi_{t,s} = c_{t,s}$, $\forall t \in \mathcal{T}, \forall s \in \bar{\mathcal{S}}_t$, where $c_{t,s}$ is a predefined constant.
- Fixed PU-specific per-BS interference constraints: $\phi_{t,p} = \frac{\Phi_p}{T}$, $\forall t \in \mathcal{T}, \forall p \in \mathcal{P}$.
- ZF beamforming for all interference: $\chi_{t,s} = 0$ and $\phi_{t,p} = 0$, $\forall t \in \mathcal{T}, \forall s \in \bar{\mathcal{S}}_t, \forall p \in \mathcal{P}$.

Problem (105) can also be solved using a hierarchical two-level primal-primal decomposition approach where one set of coupling variables, e.g. $\boldsymbol{\phi}$, is decomposed at a higher level and the other set, i.e. $\boldsymbol{\chi}$, at a lower level. Primal-primal decomposition approach converges if the lower level master problem is solved on a faster timescale than the higher level master problem. See [155] for more details on solving problems with variables optimized for different timescales. There are also other options to reformulate (90) and achieve decentralized beamforming designs, i.e., using dual decomposition [155] or ADMM [165]. Both approaches lead to the optimal solution. Note that (90) can also be solved in a decentralized way via its dual problem and with the aid of the uplink-downlink duality using a similar idea as presented in [126]. However, intermediate iterates are not necessarily feasible. If the algorithm cannot provide feasible beamformers with a limited number of iterations, it may cause extra delay and increase the signaling overhead.

4.2.2 Numerical evaluation

In this section, the performance of the proposed primal decomposition beamforming algorithm is examined in a simplified cognitive multi-cell environment. The simulation model consists of $T = 2$ secondary transmitters and a single primary transmitter. Each secondary transmitter serves its own set of two single antenna SUs, i.e., $S_1 = S_2 = 2$. In addition, $P = 2$ PUs are served by the primary transmitter. Each user is equipped with a single antenna, and each transmitter with $A_{\mathrm{T}} = 8$ antennas.

The pathloss between a secondary transmitter and its served users is 0 dB, i.e., the path gain to noise ratio is 1. A network separation parameter is introduced as the path loss between a secondary transmitter and a PU. In other words, the interfering signal from the secondary transmitter to the PU is attenuated by the value of $\bar{\eta}$. A cell-edge scenario, where all the SUs and PUs are at the cell-edge, can be modeled by setting the network separation parameter to 0 dB. In this case, the path loss is the same between each transmitter and each user, i.e., 0 dB. On the other hand, by increasing the value of $\bar{\eta}$, the secondary and primary networks become more isolated from each other. In the extreme case, i.e., $\bar{\eta} = \infty$, the secondary and primary networks do not interfere with each other at all.

Simulations are run by using frequency-flat Rayleigh fading channel conditions with uncorrelated channel coefficients between the antennas. It is assumed that the primary transmitter employs the optimal minimum power beamforming for serving its PUs without being concerned on the caused interference to the SUs. Each PU has a rate target of 1 bits/s/Hz. Interference from the primary transmitter to SU s is denoted by θ_s, which is assumed to be known at the serving secondary transmitter t_s. Since the primary network interference is explicitly known, the interference plus noise variance is reduced to include only noise, i.e., $Z_0 = N_0 = 1$. The rate and interference constraints are set equal among the users, i.e., $R_s = R$ and $\Phi_s = \Phi$. In addition, the initialization of interference power levels are given by $\chi_{t,s}^{(0)} = \chi^{(0)}$ and $\phi_{t,p}^{(0)} = \frac{\Phi_p}{S}$, $\forall t \in \mathcal{T}, \forall s \in \bar{\mathcal{S}}_t, \forall p \in \mathcal{P}$, where $\chi^{(0)}$ is selected empirically. Adaptive step-sizes are used in the projected sub-gradient methods, as explained in Section 2.2.3.

In Figs. 22-24, the performance of optimal coordinated beamforming and ZF beamforming (for all interference) is compared. The results are obtained by averaging over 100 channel realizations. Optimal coordinated beamforming results are achieved via centralized processing in the simulation examples. However, optimal performance can be also obtained via the proposed decentralized algorithm (i.e.,*Algorithm 12*) by allowing it to converge.

Fig. 22 shows the average sum power versus rate target for different values of network separation. One can see that coordinated beamforming significantly

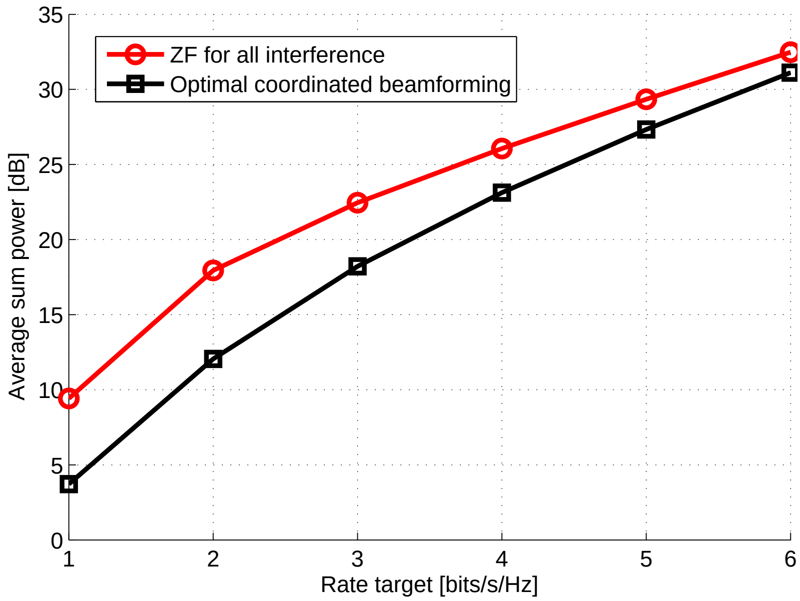

(a) $\bar{\eta} = 0\text{dB}$

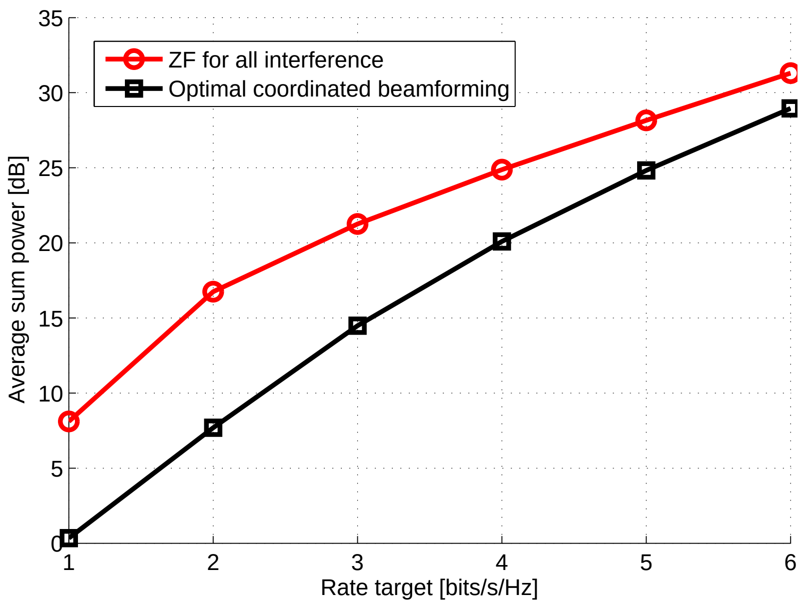

(b) $\bar{\eta} = 10\text{dB}$

Fig 22. Average sum power versus rate target.

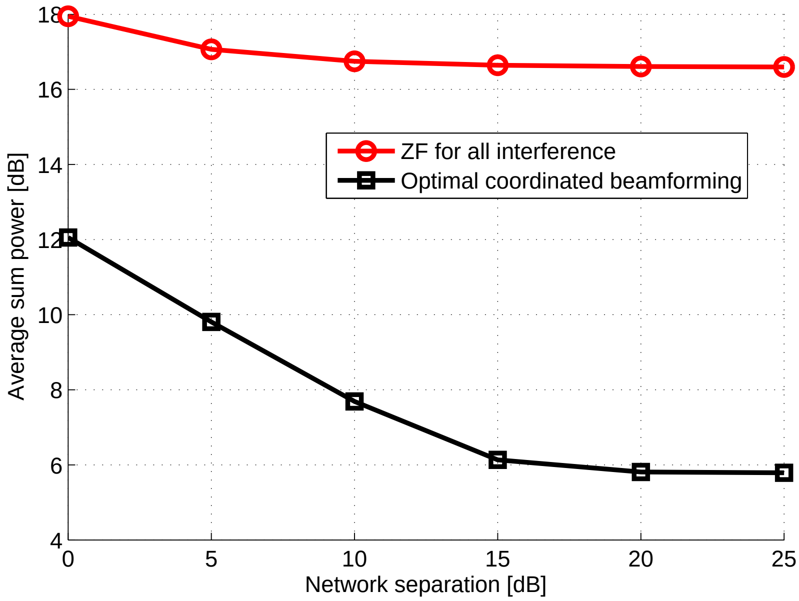

(a) $R = 2$ bits/s/Hz

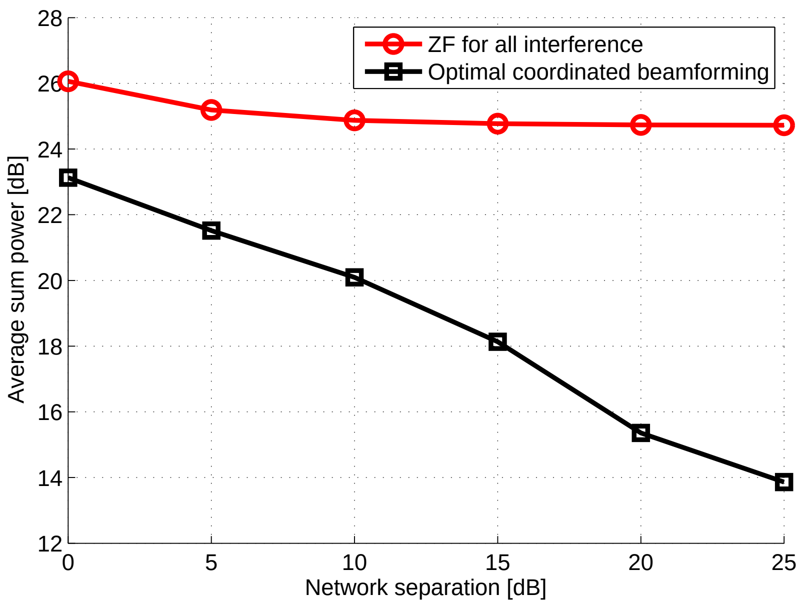

(b) $R = 4$ bits/s/Hz

Fig 23. Average sum power versus network separation.

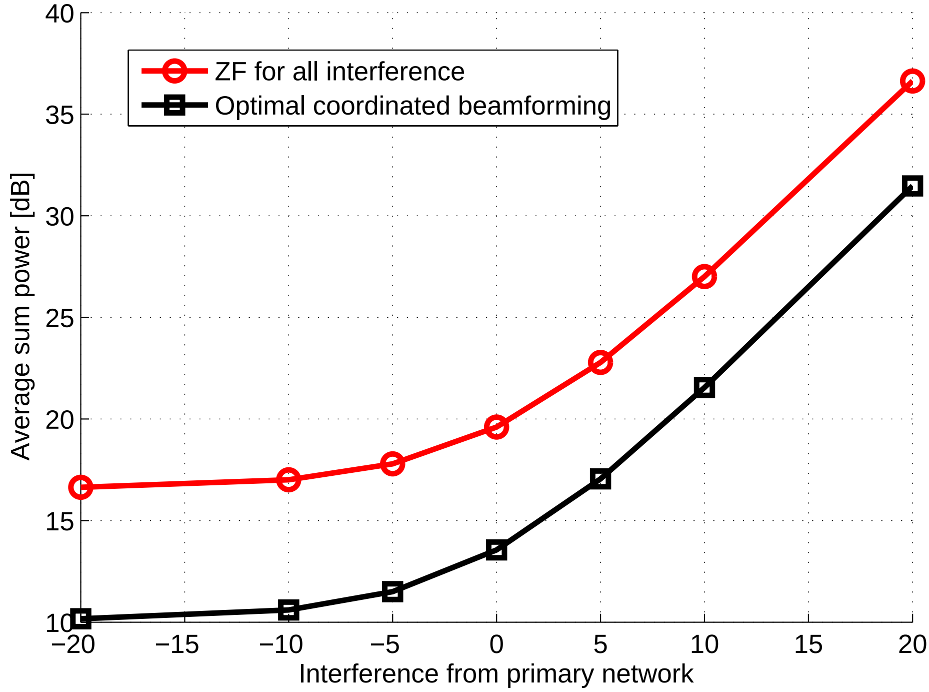

Fig 24. Average sum power versus primary network interference.

outperforms the ZF strategy, especially at low and medium rate targets. The results also imply that the performance gain increases with the increasing value of network separation and decreases as the rate target increases. In Fig. 23, the sum power is presented as a function of network separation for different rate targets. As expected, coordinated beamforming has superior performance compared with the ZF scheme. The performance gain is increased, as the secondary and primary networks become more separated and as the rate target increases.

For the rest of the simulation examples, the rate target and network separation values are set to 2 bits/s/Hz and 0 dB, respectively. Fig. 24 illustrates the average sum power versus primary network interference θ. The results demonstrate that in both strategies the sum power starts increasing heavily after the interference power levels exceeds -5 dB. This result implies that the primary network transmissions have significant impact on the performance of the secondary network. Fig. 25 shows the average transmit powers of both the secondary and primary networks as a function of the maximum aggregate interference power

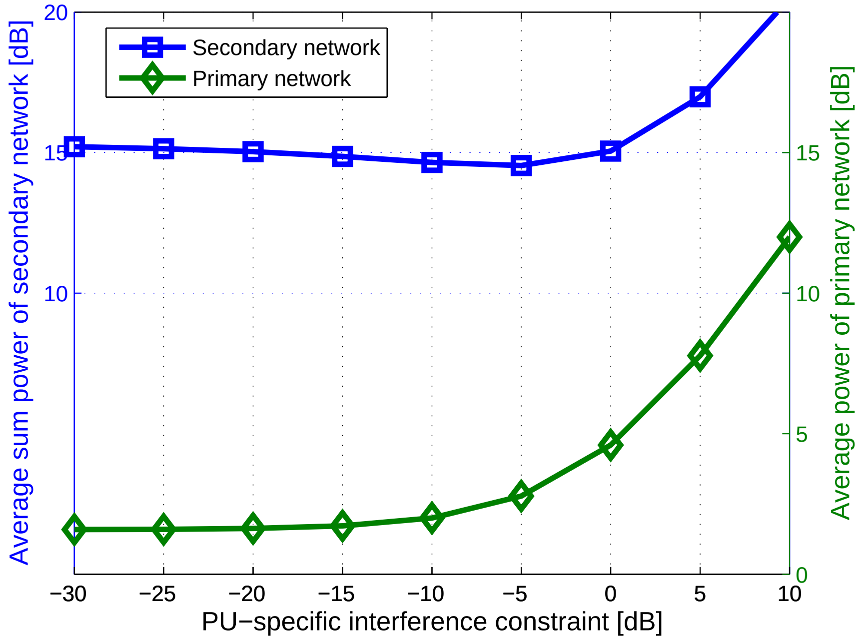

Fig 25. Average sum powers of secondary and primary networks versus PU-specific aggregate interference constraint.

level Φ. It can be seen that the performance of the primary network starts to decrease rapidly after the interference constraint Φ goes above -5 dB. The performance of the secondary network remains almost the same when Φ gets values from -30 to -5 dB, and starts to decrease significantly for larger values of Φ. The reason for this behavior is that Φ being large, the secondary transmissions cause severe interference for the PUs, which leads the primary transmitter to increase its power to satisfy the PUs' rate targets. This again causes severe interference to the SUs, and thus, the secondary transmitters have to raise their powers to satisfy the SINR targets of the SUs. The results imply that the PU interference constraint should be set to a fairly low value.

The convergence behavior of the primal decomposition-based algorithm (*Algorithm 12*) is examined next. Fig. 26 presents the normalized sub-optimality of *Algorithm 12* as a function of the subgradient iteration number r. Normalized sub-optimality is defined in (40). The simulation results demonstrate that the speed of convergence is somewhat slower for the higher value of Φ.

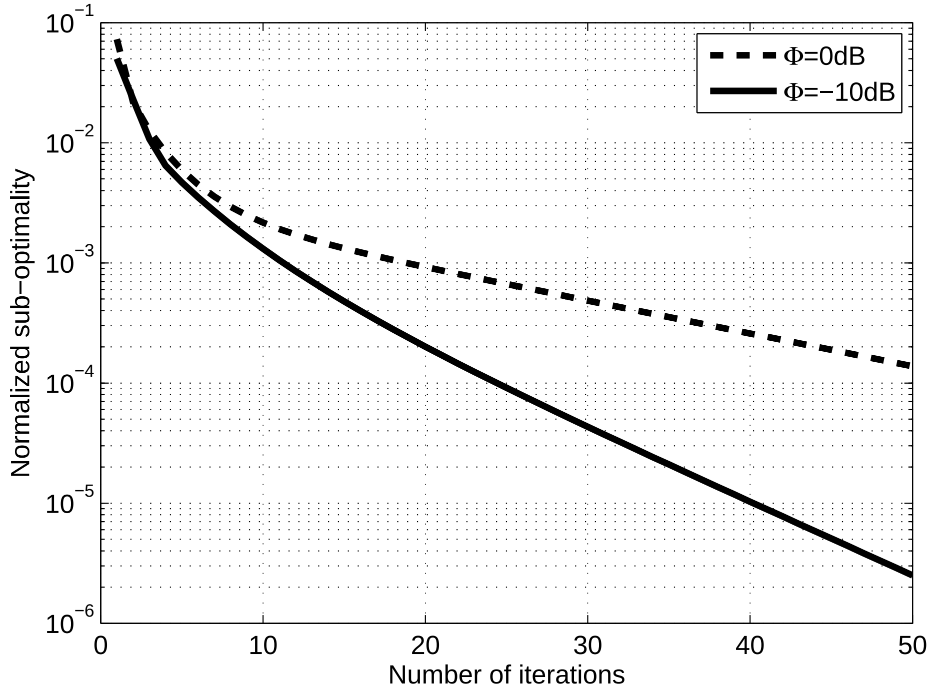

Fig 26. Converge behavior of primal decomposition-based decentralized algorithm.

In Fig. 27, the sum power is presented for 25 independent channel realizations. The performance of *Algorithm 12* is compared with that of the ZF and centralized coordinated beamforming strategies. As can be observed, *Algorithm 12* obtains close to optimal performance after a few iterations. Moreover, the ZF beamforming scheme is outperformed significantly.

4.3 Decentralized transmit beamforming design with imperfect CSI

In this section, an ADMM-based decentralized beamforming design is proposed to solve the robust SPMin problem in a cognitive multi-cell multi-user MISO system, where CSI is assumed to be imperfect. The original non-convex problem needs to be approximated and reformulated as a tractable convex problem. The ADMM method can then be applied to solve the resulting problem in a decentralized manner by relying on local imperfect CSI and low-rate backhaul signaling between the secondary transmitters. The proposed algorithm provides an opti-

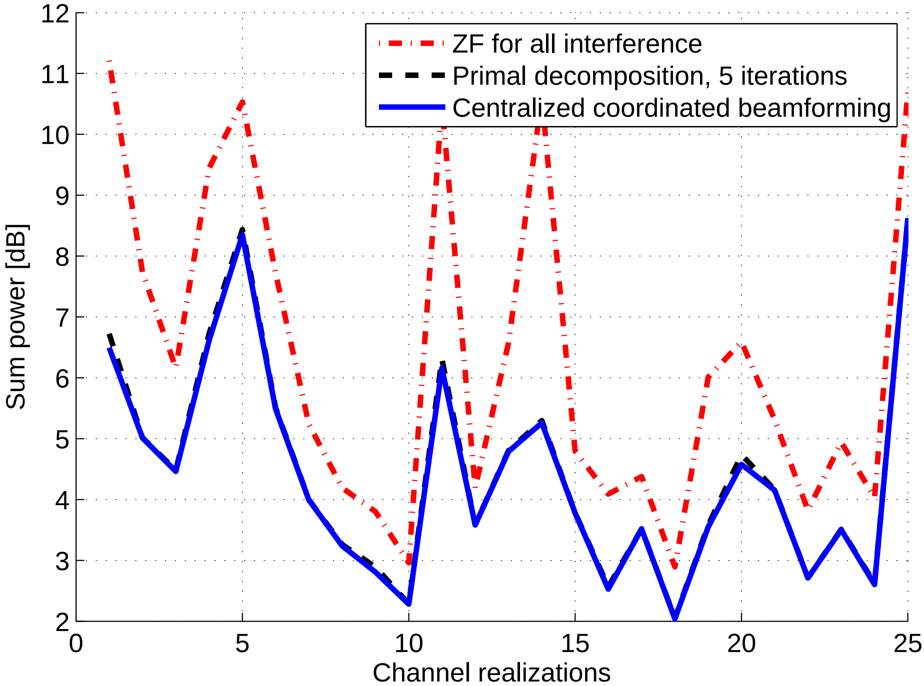

Fig 27. Sum power performance in quasi-static channel conditions.

mal solution for the original non-convex problem, if the convex approximation is tight.

4.3.1 ADMM-based algorithm

First, the original problem is equivalently rewritten as a form of combined consensus and sharing problem [165]. This is a key step for achieving a decentralized algorithm. Then, the resulting problem is approximated as a tractable convex problem via the SDR [81, 103] and S-procedure [81] methods. Finally, the problem is solved in a decentralized manner via the ADMM method. A detailed derivation of the decentralized algorithm is given in the following subsections.

Reformulation and approximation of robust SPMin problem

First, auxiliary interference variables are introduced, i.e., $\tilde{\chi}^{t'}_{t,s}$ and $\tilde{\phi}_{t',p}$ are the local copies of the SU-specific interference variable $\chi_{t,s}$ and the PU-specific interference variable $\phi_{t',p}$ at the transmitter t', respectively. Note that each $\chi_{t,s}$ couples exactly two transmitters, i.e., the serving transmitter t_s and the interfering transmitter t. Whereas, each $\phi_{t,p}$ couples all the transmitters. Consequently, the aim of the reformulated problem is to enforce a consensus between each pair of transmitter-level copies of $\tilde{\chi}_{t,s}^{t}$ and $\tilde{\chi}_{t,s}^{t_s}$, as well as, optimally share resources $\{\tilde{\phi}_{t,p}\}_{t\in\mathcal{T},p\in\mathcal{P}}$ between the transmitters. The resulting problem is expressed as

$$\begin{aligned}
\min_{\substack{\{\mathbf{m}_s\}_{s\in\mathcal{S}},\\ \{\chi_{t,s}\}_{t\in\mathcal{T},s\in\bar{\mathcal{S}}_t},\\ \{\phi_{t,p},\tilde{\phi}_{t,p}\}_{t\in\mathcal{T},p\in\mathcal{P}},\\ \{\tilde{\chi}_{t,s}^{t'}\}_{t\in\mathcal{T},s\in\bar{\mathcal{S}}_t,\forall t'\in\{t_s,t\}}}} \quad & \sum_{t\in\mathcal{T}}\sum_{s\in\mathcal{S}_t} \operatorname{tr}\left(\mathbf{m}_s\mathbf{m}_s^{\mathrm{H}}\right) \\
\text{s. t.} \quad & \left(\hat{\mathbf{h}}_{t_s,s}+\mathbf{u}_{t_s,s}\right)\left(\tfrac{1}{\gamma_s}\mathbf{m}_s\mathbf{m}_s^{\mathrm{H}}-\textstyle\sum_{i\in\mathcal{S}_{t_s}\setminus\{s\}}\mathbf{m}_i\mathbf{m}_i^{\mathrm{H}}\right) \\
& \left(\hat{\mathbf{h}}_{t_s,s}+\mathbf{u}_{t_s,s}\right)^{\mathrm{H}} \geq Z_0+\textstyle\sum_{t\in\mathcal{T}\setminus\{t_s\}}\tilde{\chi}_{t,s}^{t_s}, \\
& \forall s\in\mathcal{S}, \forall\mathbf{u}_{t_s,s}\in\mathcal{E}_{t_s,s} \\
& \textstyle\sum_{i\in\mathcal{S}_t}\left(\hat{\mathbf{h}}_{t,s}+\mathbf{u}_{t,s}\right)\mathbf{m}_i\mathbf{m}_i^{\mathrm{H}}\left(\hat{\mathbf{h}}_{t,s}+\mathbf{u}_{t,s}\right)^{\mathrm{H}} \leq \tilde{\chi}_{t,s}^{t}, \\
& \forall t\in\mathcal{T}, \forall s\in\bar{\mathcal{S}}_t, \forall\mathbf{u}_{t,s}\in\mathcal{E}_{t,s} \\
& \textstyle\sum_{i\in\mathcal{S}_t}\left(\hat{\mathbf{g}}_{t,p}+\mathbf{v}_{t,p}\right)\mathbf{m}_i\mathbf{m}_i^{\mathrm{H}}\left(\hat{\mathbf{g}}_{t,p}+\mathbf{v}_{t,p}\right)^{\mathrm{H}} \leq \tilde{\phi}_{t,p}, \\
& \forall t\in\mathcal{T}, \forall p\in\mathcal{P}, \forall\mathbf{v}_{t,p}\in\mathcal{F}_{t,p} \\
& \textstyle\sum_{t\in\mathcal{T}}\phi_{t,p}\leq\Phi_p, \forall p\in\mathcal{P} \\
& \tilde{\chi}_{t,s}^{t'}=\chi_{t,s}, \forall t\in\mathcal{T}, \forall s\in\bar{\mathcal{S}}_t, \forall t'\in\{t_s,t\} \\
& \tilde{\phi}_{t,p}=\phi_{t,p}, \forall t\in\mathcal{T}, \forall p\in\mathcal{P}.
\end{aligned} \tag{123}$$

The problem (123) can be turned into a tractable convex form by using the standard SDR and S-procedure methods [89, 103, 133]. Using the SDR [103], (123) is approximated as an SDP by replacing the rank-one matrix $\mathbf{m}_s\mathbf{m}_s^{\mathrm{H}}$ by a semidefinite matrix $\mathbf{Q}_s$ without a rank-one constraint. The resulting problem is still intractable due to the infinite number of constraints. Since the constraints are quadratic w.r.t. the corresponding CSI error vectors, the S-Procedure [81] can be applied to equivalently reformulate these constraints as linear matrix inequalities (LMIs) [133]. Further details on this derivation can be found in

[133]. The resulting problem is a tractable convex SDP

$$\begin{aligned}
\min_{\substack{\{\mathbf{Q}_s,\omega_s\}_{s\in\mathcal{S}},\\ \{\chi_{t,s},\beta_{t,s}\}_{t\in\mathcal{T},s\in\bar{\mathcal{S}}_t},\\ \{\phi_{t,p},\tilde{\phi}_{t,p},\varphi_{t,p}\}_{t\in\mathcal{T},p\in\mathcal{P}},\\ \{\tilde{\chi}_{t,s}^{t'}\}_{t\in\mathcal{T},s\in\bar{\mathcal{S}}_t,\forall t'\in\{t_s,t\}}}} \quad & \sum_{t\in\mathcal{T}}\sum_{s\in\mathcal{S}_t}\mathrm{tr}\left(\mathbf{Q}_s\right)\\
\text{s. t.} \quad & \mathbf{Q}_s\succeq 0, \boldsymbol{\Delta}_s\succeq 0, \omega_s\geq 0, \forall t\in\mathcal{T}, \forall s\in\mathcal{S}_t\\
& \boldsymbol{\Theta}_{t,s}\succeq 0, \beta_{t,s}\geq 0, \forall t\in\mathcal{T}, \forall s\in\bar{\mathcal{S}}_t\\
& \boldsymbol{\Lambda}_{t,p}\succeq 0, \varphi_{t,p}\geq 0, \forall t\in\mathcal{T}, \forall p\in\mathcal{P}\\
& \textstyle\sum_{t\in\mathcal{T}}\phi_{t,p}\leq \Phi_p, \forall p\in\mathcal{P}\\
& \tilde{\chi}_{t,s}^{t'}=\chi_{t,s}, \forall t\in\mathcal{T}, \forall s\in\bar{\mathcal{S}}_t, \forall t'\in\{t_s,t\}\\
& \tilde{\phi}_{t,p}=\phi_{t,p}, \forall t\in\mathcal{T}, \forall p\in\mathcal{P}
\end{aligned} \tag{124}$$

where the matrixes $\boldsymbol{\Delta}_s$, $\boldsymbol{\Theta}_{t,s}$ and $\boldsymbol{\Lambda}_{t,p}$ are denoted by

$$\boldsymbol{\Delta}_s = \begin{bmatrix} \mathbf{A}_s+\omega_s\mathbf{E}_{t_s,s} & \mathbf{A}_s\hat{\mathbf{h}}_{t_s,s}^{\mathrm{H}}\\ \hat{\mathbf{h}}_{t_s,s}\mathbf{A}_s & \hat{\mathbf{h}}_{t_s,s}\mathbf{A}_s\hat{\mathbf{h}}_{t_s,s}^{\mathrm{H}}-\sum\limits_{t'\in\mathcal{T}\backslash t_s}\tilde{\chi}_{t',s}^{t_s}-Z_0-\omega_s \end{bmatrix} \tag{125}$$

$$\boldsymbol{\Theta}_{t,s} = \begin{bmatrix} -\mathbf{B}_t+\beta_{t,s}\mathbf{E}_{t,s} & -\mathbf{B}_t\hat{\mathbf{h}}_{t,s}^{\mathrm{H}}\\ -\hat{\mathbf{h}}_{t,s}\mathbf{B}_t & -\hat{\mathbf{h}}_{t,s}\mathbf{B}_t\hat{\mathbf{h}}_{t,s}^{\mathrm{H}}+\tilde{\chi}_{t,s}^{t}-\beta_{t,s} \end{bmatrix} \tag{126}$$

$$\boldsymbol{\Lambda}_{t,p} = \begin{bmatrix} -\mathbf{B}_t+\varphi_{t,p}\mathbf{F}_{t,p} & -\mathbf{B}_t\hat{\mathbf{g}}_{t,p}^{\mathrm{H}}\\ -\hat{\mathbf{g}}_{t,p}\mathbf{B}_t & -\hat{\mathbf{g}}_{t,p}\mathbf{B}_t\hat{\mathbf{g}}_{t,p}^{\mathrm{H}}+\tilde{\phi}_{t,p}-\varphi_{t,p} \end{bmatrix} \tag{127}$$

where $\mathbf{A}_s = \frac{1}{\gamma_s}\mathbf{Q}_s - \sum_{i\in\mathcal{S}_{t_s}\backslash\{s\}}\mathbf{Q}_i$ and $\mathbf{B}_t = \sum_{i\in\mathcal{S}_t}\mathbf{Q}_i$. The sets $\{\omega_s\}_{s\in\mathcal{S}}$, $\{\beta_{t,s}\}_{t\in\mathcal{T},s\in\bar{\mathcal{S}}_t}$ and $\{\varphi_{t,p}\}_{t\in\mathcal{T},p\in\mathcal{P}}$ consist of slack variables. If global imperfect CSI is available, (124) can be optimally solved using an SDP solver. If the optimal $\{\mathbf{Q}_s\}_{s\in\mathcal{S}}$ are all rank-one (i.e., the SDR is tight), then the solution of the relaxed problem (124) is also globally optimal for the original non-convex problem (123). In general, the solution of (124) cannot be guaranteed to be rank-one. However, it was shown in [133] that rank-one solutions can always be achieved in a cognitive interference channel, where each of the multiple transmitters serves only a single user. In case the solution of (124) is higher-rank, a feasible rank-one solution may be achieved via approximation methods [89]. For example, a simple approximation method in [126] can be extended for (124). In the rest of the paper, only the local imperfect CSI is assumed to be available.

An ADMM-based decentralized algorithm is proposed next to solve the combined consensus and sharing problem (124). In general, ADMM can combine the decomposability of dual decomposition and the convergence properties of the method of multipliers [165]. In particular, ADMM can converge under more general conditions than dual decomposition can, e.g., without the requirements of strict convexity or finiteness of the objective function [165].

For simplicity of notation, (124) is first rewritten in a compact form:

$$\begin{array}{ll} \underset{\{\hat{\mathbf{Q}}_t,\tilde{\boldsymbol{\chi}}_t,\tilde{\boldsymbol{\phi}}_t,\mathbf{D}_t,\boldsymbol{\chi}_t,\boldsymbol{\phi}_t\}_{t\in\mathcal{T}}}{\min.} & \sum_{t\in\mathcal{T}} f_t\left(\hat{\mathbf{Q}}_t,\tilde{\boldsymbol{\chi}}_t,\tilde{\boldsymbol{\phi}}_t,\mathbf{D}_t\right) \\ \text{s. t.} & \tilde{\boldsymbol{\chi}}_t=\boldsymbol{\chi}_t, \forall t\in\mathcal{T} \\ & \tilde{\boldsymbol{\phi}}_t=\boldsymbol{\phi}_t, \forall t\in\mathcal{T} \\ & \sum_{t\in\mathcal{T}}\phi_{t,p}\leq\Phi_p, \forall p\in\mathcal{P}. \end{array} \tag{128}$$

All the optimization variables are collected into transmitter t specific matrixes and vectors: $\hat{\mathbf{Q}}_t = [\mathbf{Q}_{\mathcal{S}_t(1)},\ldots,\mathbf{Q}_{\mathcal{S}_t(S_t)}]$, $\tilde{\boldsymbol{\phi}}_t = [\tilde{\phi}_{t,\mathcal{P}(1)},\ldots,\tilde{\phi}_{t,\mathcal{P}(P)}]^{\mathrm{T}}$, $\boldsymbol{\phi}_t = [\phi_{t,\mathcal{P}(1)},\ldots,\phi_{t,\mathcal{P}(P)}]^{\mathrm{T}}$, $\mathbf{D}_t=[\boldsymbol{\omega}_t,\boldsymbol{\beta}_t,\boldsymbol{\varphi}_t]$, $\boldsymbol{\omega}_t=[\omega_{\mathcal{S}_t(1)},\ldots,\omega_{\mathcal{S}_t(S_t)}]^{\mathrm{T}}$, $\boldsymbol{\beta}_t=[\beta_{t,\bar{\mathcal{S}}_t(1)},\ldots,\beta_{t,\bar{\mathcal{S}}_t(|\bar{\mathcal{S}}_t|)}]^{\mathrm{T}}$, $\boldsymbol{\varphi}_t=[\varphi_{t,\mathcal{P}(1)},\ldots,\varphi_{t,\mathcal{P}(P)}]^{\mathrm{T}}$. The elements of the vector $\tilde{\boldsymbol{\chi}}_t$ are taken from the sets $\{\tilde{\chi}^t_{t',s}\}_{t'\in\mathcal{T}\setminus\{t_s\},s\in\mathcal{S}_t}$ and $\{\tilde{\chi}^t_{t,s}\}_{s\in\bar{\mathcal{S}}_t}$ in a specific order. Similarly, the vector $\boldsymbol{\chi}_t$ is composed of the sets $\{\chi_{t',s}\}_{t'\in\mathcal{T}\setminus\{t_s\},s\in\mathcal{S}_t}$ and $\{\chi_{t,s}\}_{s\in\bar{\mathcal{S}}_t}$ using the same ordering. The function f_t is defined as

$$f_t\left(\hat{\mathbf{Q}}_t,\tilde{\boldsymbol{\chi}}_t,\tilde{\boldsymbol{\phi}}_t,\mathbf{D}_t\right)=\begin{cases}\sum_{s\in\mathcal{S}_t}\mathrm{tr}\left(\mathbf{Q}_s\right), & \left(\hat{\mathbf{Q}}_t,\tilde{\boldsymbol{\chi}}_t,\tilde{\boldsymbol{\phi}}_t,\mathbf{D}_t\right)\in\mathcal{C}_t \\ \infty, & \text{otherwise.}\end{cases} \tag{129}$$

The set $\mathcal{C}_t$ is defined as

$$\mathcal{C}_t = \left\{\hat{\mathbf{Q}}_t,\tilde{\boldsymbol{\chi}}_t,\tilde{\boldsymbol{\phi}}_t,\mathbf{D}_t \;\middle|\; \begin{array}{l}\mathbf{Q}_s\succeq 0,\boldsymbol{\Delta}_s\succeq 0,\omega_s\geq 0,\\ \forall s\in\mathcal{S}_t\\ \boldsymbol{\Theta}_{t,s}\succeq 0,\beta_{t,s}\geq 0,\forall s\in\bar{\mathcal{S}}_t\\ \boldsymbol{\Lambda}_{t,p}\succeq 0,\varphi_{t,p}\geq 0,\forall p\in\mathcal{P}\end{array}\right\}. \tag{130}$$

The first step in ADMM is to write the augmented Lagrangian [165]. The (partial) augmented Lagrangian for (128) is given by

$$\begin{aligned} & P_\rho\left(\left\{\hat{\mathbf{Q}}_t, \tilde{\boldsymbol{\chi}}_t, \tilde{\boldsymbol{\phi}}_t, \mathbf{D}_t, \boldsymbol{\chi}_t, \boldsymbol{\phi}_t, \boldsymbol{\mu}_t, \boldsymbol{\nu}_t\right\}_{t\in\mathcal{T}}\right) \\ & = \textstyle\sum_{t\in\mathcal{T}}\Big(f_t(\hat{\mathbf{Q}}_t, \tilde{\boldsymbol{\chi}}_t, \tilde{\boldsymbol{\phi}}_t, \mathbf{D}_t) + \boldsymbol{\mu}_t^{\mathrm{T}}(\tilde{\boldsymbol{\chi}}_t - \boldsymbol{\chi}_t) \\ & + \boldsymbol{\nu}_t^{\mathrm{T}}(\tilde{\boldsymbol{\phi}}_t - \boldsymbol{\phi}_t) + \frac{\rho}{2}\|\tilde{\boldsymbol{\chi}}_t - \boldsymbol{\chi}_t\|_2^2 + \frac{\rho}{2}\|\tilde{\boldsymbol{\phi}}_t - \boldsymbol{\phi}_t\|_2^2\Big) \end{aligned} \tag{131}$$

where $\boldsymbol{\mu}_t$ and $\boldsymbol{\nu}_t$ are the dual variables associated with the interference equality constraints of (128). The last two terms of (131) are quadratic penalty terms with a penalty parameter $\rho > 0$, and they penalize for violation of the equality constraints of (128). The augmented Lagrangian (131) can be seen as a standard Lagrangian of (128) where the quadratic penalty terms are added to the objective function. Due to the added penalty terms, ADMM is able to converge without the need of strict convexity or the finiteness of the original objective function of (128). ADMM operates iteratively via the following steps: 1) update of local primal variables, 2) update of global primal variables and 3) update of local dual variables. At iteration $r+1$, these steps are given by

$$\begin{aligned} & \hat{\mathbf{Q}}_t^{(r+1)}, \tilde{\boldsymbol{\chi}}_t^{(r+1)}, \tilde{\boldsymbol{\phi}}_t^{(r+1)}, \mathbf{D}_t^{(r+1)} \\ & = \underset{\hat{\mathbf{Q}}_t, \tilde{\boldsymbol{\chi}}_t, \tilde{\boldsymbol{\phi}}_t, \mathbf{D}_t}{\operatorname{argmin}}\ P_\rho\left(\hat{\mathbf{Q}}_t, \tilde{\boldsymbol{\chi}}_t, \tilde{\boldsymbol{\phi}}_t, \mathbf{D}_t, \boldsymbol{\chi}_t^{(r)}, \boldsymbol{\phi}_t^{(r)}, \boldsymbol{\mu}_t^{(r)}, \boldsymbol{\nu}_t^{(r)}\right), \forall t\in\mathcal{T} \end{aligned} \tag{132}$$

$$\begin{aligned} & \{\boldsymbol{\chi}_t^{(r+1)}, \boldsymbol{\phi}_t^{(r+1)}\}_{t\in\mathcal{T}} \\ & = \underset{\{\boldsymbol{\chi}_t, \boldsymbol{\phi}_t\}_{t\in\mathcal{T}}}{\operatorname{argmin}}\ P_\rho\left(\left(\{\hat{\mathbf{Q}}_t^{(r+1)}, \tilde{\boldsymbol{\chi}}_t^{(r+1)}, \tilde{\boldsymbol{\phi}}_t^{(r+1)}, \mathbf{D}_t^{(r+1)}, \boldsymbol{\chi}_t, \boldsymbol{\phi}_t, \boldsymbol{\mu}_t^{(r)}, \boldsymbol{\nu}_t^{(r)}\right\}_{t\in\mathcal{T}}\right) \end{aligned} \tag{133}$$

$$\boldsymbol{\mu}_t^{(r+1)} = \boldsymbol{\mu}_t + \rho\left(\tilde{\boldsymbol{\chi}}_t^{(r+1)} - \boldsymbol{\chi}_t^{(r+1)}\right), \forall t\in\mathcal{T} \tag{134}$$

$$\boldsymbol{\nu}_t^{(r+1)} = \boldsymbol{\nu}_t + \rho\left(\tilde{\boldsymbol{\phi}}_t^{(r+1)} - \boldsymbol{\phi}_t^{(r+1)}\right), \forall t\in\mathcal{T}. \tag{135}$$

The steps (132), (134) and (135) are separable between transmitters, and thus, they can be solved independently in parallel at each transmitter. The step (133) needs network-level coordination, i.e., information exchange between transmitters via backhaul. In particular, transmitter t signals the local copies $\tilde{\boldsymbol{\chi}}_t^{(r+1)}$ and $\tilde{\boldsymbol{\phi}}_t^{(r+1)}$ to the coupled transmitters. Next, how to optimally solve the steps (132) and (133) is explained.

The local primal variables in (132) are updated by solving the following problem

$$\begin{aligned} \min_{\hat{\mathbf{Q}}_t,\tilde{\boldsymbol{\chi}}_t,\tilde{\boldsymbol{\phi}}_t,\mathbf{D}_t} \quad & f_t(\hat{\mathbf{Q}}_t,\tilde{\boldsymbol{\chi}}_t,\tilde{\boldsymbol{\phi}}_t,\mathbf{D}_t)+\frac{\rho}{2}\|\tilde{\boldsymbol{\chi}}_t-\boldsymbol{\chi}_t^{(r)}+\tilde{\boldsymbol{\mu}}_t^{(r)}\|_2^2 \\ & +\frac{\rho}{2}\|\tilde{\boldsymbol{\phi}}_t-\boldsymbol{\phi}_t^{(r)}+\tilde{\boldsymbol{\nu}}_t^{(r)}\|_2^2. \end{aligned} \tag{136}$$

For simplicity of presentation, the scaled ADMM formulation [165] is used in (136) by combining the linear and quadratic terms of (131):

$$(\boldsymbol{\mu}_t^{(r)})^{\mathrm{T}}(\tilde{\boldsymbol{\chi}}_t-\boldsymbol{\chi}_t^{(r)})+\frac{\rho}{2}\|\tilde{\boldsymbol{\chi}}_t-\boldsymbol{\chi}_t^{(r)}\|_2^2=\frac{\rho}{2}\|\tilde{\boldsymbol{\chi}}_t-\boldsymbol{\chi}_t^{(r)}+\hat{\boldsymbol{\mu}}_t^{(r)}\|_2^2-\frac{\rho}{2}\|\hat{\boldsymbol{\mu}}_t^{(r)}\|_2^2 \tag{137}$$

and

$$(\boldsymbol{\nu}_t^{(r)})^{\mathrm{T}}(\tilde{\boldsymbol{\phi}}_t-\boldsymbol{\phi}_t^{(r)})+\frac{\rho}{2}\|\tilde{\boldsymbol{\phi}}_t-\boldsymbol{\phi}_t^{(r)}\|_2^2=\frac{\rho}{2}\|\tilde{\boldsymbol{\phi}}_t-\boldsymbol{\phi}_t^{(r)}+\hat{\boldsymbol{\nu}}_t^{(r)}\|_2^2-\frac{\rho}{2}\|\hat{\boldsymbol{\nu}}_t^{(r)}\|_2^2 \tag{138}$$

where $\hat{\boldsymbol{\mu}}_t^{(r)}=\frac{1}{\rho}\boldsymbol{\mu}_t^{(r)}$ and $\hat{\boldsymbol{\nu}}_t^{(r)}=\frac{1}{\rho}\boldsymbol{\nu}_t^{(r)}$. The last constant terms were dropped from (136) since they do not impact finding the optimal points. The problem (136) can be recast as an SDP via the following steps. After writing (136) in epigraph form [81], the resulting quadratic constraint

$$\sum_{s\in\mathcal{S}_t}\mathrm{tr}\,(\mathbf{Q}_s)+\frac{\rho}{2}\|\tilde{\boldsymbol{\chi}}_t-\boldsymbol{\chi}_t^{(r)}+\hat{\boldsymbol{\mu}}_t^{(r)}\|_2^2+\frac{\rho}{2}\|\tilde{\boldsymbol{\phi}}_t-\boldsymbol{\phi}_t^{(r)}+\hat{\boldsymbol{\nu}}_t^{(r)}\|_2^2-a_t\le 0 \tag{139}$$

can be reformulated as an SOC constraint [60]: $\|\mathbf{y}_t\|_2\le x_t$, where

$$\mathbf{y}_t = \\ [(1+(\sum_{s\in\mathcal{S}_t}\mathrm{tr}\,(\mathbf{Q}_s)-a_t))/2,\sqrt{\frac{\rho}{2}}(\tilde{\boldsymbol{\chi}}_t-\boldsymbol{\chi}_t^{(r)}+\hat{\boldsymbol{\mu}}_t^{(r)})^{\mathrm{T}},\sqrt{\frac{\rho}{2}}(\tilde{\boldsymbol{\phi}}_t-\boldsymbol{\phi}_t^{(r)}+\hat{\boldsymbol{\nu}}_t^{(r)})^{\mathrm{T}}]^{\mathrm{T}}$$

and

$$x_t=(1-(\sum_{s\in\mathcal{S}_t}\mathrm{tr}\,(\mathbf{Q}_s)-a_t))/2 \tag{140}$$

Now the SOC constraint can be written in the form of LMI [33]. The optimal points $\hat{\mathbf{Q}}_t^{\star}$, $\tilde{\boldsymbol{\chi}}_t^{\star}$ and $\tilde{\boldsymbol{\phi}}_t^{\star}$ are found by solving the resulting SDP

$$\begin{aligned} \min_{\hat{\mathbf{Q}}_t,\tilde{\boldsymbol{\chi}}_t,\tilde{\boldsymbol{\phi}}_t,\mathbf{D}_t,a_t} \quad & a_t \\ \text{s. t.} \quad & \begin{bmatrix} x_t & \mathbf{y}_t^{\mathrm{H}} \\ \mathbf{y}_t & x_t\mathbf{I} \end{bmatrix}\succeq 0,\forall s\in\mathcal{S}_t \\ & \mathbf{Q}_s\succeq 0,\boldsymbol{\Delta}_s\succeq 0,\omega_s\ge 0,\forall s\in\mathcal{S}_t \\ & \boldsymbol{\Theta}_{t,s}\succeq 0,\beta_{t,s}\ge 0,\forall s\in\bar{\mathcal{S}}_t \\ & \boldsymbol{\Lambda}_{t,p}\succeq 0,\varphi_{t,p}\ge 0,\forall p\in\mathcal{P}. \end{aligned} \tag{141}$$

Now the local primal variables can be updated: $\hat{\mathbf{Q}}_t^{(r+1)} = \hat{\mathbf{Q}}_t^\star$, $\tilde{\boldsymbol{\chi}}_t^{(r+1)} = \tilde{\boldsymbol{\chi}}_t^\star$ and $\tilde{\boldsymbol{\phi}}_t^{(r+1)} = \tilde{\boldsymbol{\phi}}_t^\star$.

The global primal variables in (133) are updated with the optimal points of the following problem

$$\begin{array}{ll} \underset{\{\boldsymbol{\chi}_t, \boldsymbol{\phi}_t\}_{t\in\mathcal{T}}}{\min.} & \sum_{t\in\mathcal{T}} \Big((\boldsymbol{\mu}_t^{(r)})^{\mathrm{T}} (\tilde{\boldsymbol{\chi}}_t^{(r+1)} - \boldsymbol{\chi}_t) + \frac{\rho}{2} \|\tilde{\boldsymbol{\chi}}_t^{(r+1)} - \boldsymbol{\chi}_t\|_2^2 \\ & + (\boldsymbol{\nu}_t^{(r)})^{\mathrm{T}} (\tilde{\boldsymbol{\phi}}_t^{(r+1)} - \boldsymbol{\phi}_t) + \dfrac{\rho}{2} \|\tilde{\boldsymbol{\phi}}_t^{(r+1)} - \boldsymbol{\phi}_t\|_2^2 \Big) \\ \text{s. t.} & \sum_{t\in\mathcal{T}^{\mathrm{S}}} \phi_{t,p} \leq \Phi_p, \forall p \in \mathcal{P}. \end{array} \tag{142}$$

Since the objective and constraint functions of (142) are separable in $\boldsymbol{\chi}_t$ and $\boldsymbol{\phi}_t$, these variables can be solved independently. Since the optimization problem is unconstrained and quadratic in $\boldsymbol{\chi}_t$, the optimal point $\boldsymbol{\chi}_t^\star$ is found by setting the gradient of (142) w.r.t. $\boldsymbol{\chi}_t$ to zero. The resulting solution is expressed in component wise as

$$\chi_{t,s}^\star = \frac{1}{2} \left(\tilde{\chi}_{t,s}^{t,(r+1)} + \tilde{\chi}_{t,s}^{t_s,(r+1)} + \frac{1}{\rho} (\mu_{t,s}^{t,(r)} + \mu_{t,s}^{t_s,(r)}) \right) \tag{143}$$

and the update is $\chi_{t,s}^{(r+1)} = \chi_{t,s}^\star$. Note that $\mu_{t,s}^{t,(r)} + \mu_{t,s}^{t_s,(r)} = 0$ by substituting $\chi_{t,s}^{(r+1)}$ in (134). Hence, $\chi_{t,s}^{(r+1)}$-update simplifies to $\chi_{t,s}^{(r+1)} = 1/2(\tilde{\chi}_{t,s}^{t,(r+1)} + \tilde{\chi}_{t,s}^{t_s,(r+1)})$. The optimal point $\boldsymbol{\phi}_t^\star$ is found by solving the following convex quadratic optimization problem

$$\begin{array}{ll} \underset{\{\boldsymbol{\phi}_t\}_{t\in\mathcal{T}}}{\min.} & \sum_{t\in\mathcal{T}} \Big((\boldsymbol{\nu}_t^{(r)})^{\mathrm{T}} (\tilde{\boldsymbol{\phi}}_t^{(r+1)} - \boldsymbol{\phi}_t) + \frac{\rho}{2} \|\tilde{\boldsymbol{\phi}}_t^{(r+1)} - \boldsymbol{\phi}_t\|_2^2 \Big) \\ \text{s. t.} & \sum_{t\in\mathcal{T}} \phi_{t,p} \leq \Phi_p, \forall p \in \mathcal{P}. \end{array} \tag{144}$$

The update is $\boldsymbol{\phi}_t^{(r+1)} = \boldsymbol{\phi}_t^\star$. Using the updated primal variables, the local dual variables can be updated as presented in (134) and (135). Finally, the proposed decentralized ADMM-based beamforming approach is summarized in *Algorithm 13*.

With the standard assumptions for ADMM [165], *Algorithm 13* converges to the optimal solution of (128). Note that *Algorithm 13* does not necessarily provide a feasible beamforming solution for the original primal problem (128) at intermediate iterations. This is due to an inherent characteristic of the ADMM that the local copies of the optimization variables, i.e., the interference terms, are not necessarily required to be equal at intermediate iterations leading to a violation of the QoS constraints. However, a feasible set of beamformers may be achieved at each iteration by enforcing consistency between the local interference values. This can be done by fixing $\tilde{\boldsymbol{\chi}}_t = \boldsymbol{\chi}_t$ and $\tilde{\boldsymbol{\phi}}_t = \boldsymbol{\phi}_t$, and solving (141) at the transmitter t, $\forall t \in \mathcal{T}$. At a cost of sub-optimal performance, *Algorithm 13* can be stopped at any (primal) feasible iterate to reduce delay and signaling/computational load. If the optimal solution of *Algorithm 13* is rank-one, it is also globally optimal for the original non-convex problem (123). The special case designs described in Section 4.2.1 are also applicable to *Algorithm 13*.

Algorithm 13 Decentralized robust transmit beamforming design based on ADMM for cognitive MISO system

1: Set $r = 0$. Initialize $\boldsymbol{\mu}_t^{(0)}$, $\boldsymbol{\chi}_t^{(0)}$, $\boldsymbol{\nu}_t^{(0)}$ and $\boldsymbol{\phi}_t^{(0)}$.
2: **repeat**
3: Compute transmitter-specific transmit covariance matrices and interference variables $\hat{\mathbf{Q}}_t^{(r+1)}$, $\tilde{\boldsymbol{\chi}}_t^{(r+1)}$ and $\tilde{\boldsymbol{\phi}}_t^{(r+1)}$ by solving SDP (141).
4: Communicate the elements of $\tilde{\boldsymbol{\chi}}_t^{(r+1)}$ and $\tilde{\boldsymbol{\phi}}_t^{(r+1)}$ to the coupled transmitters via backhaul.
5: Compute network-wide interference variables $\boldsymbol{\chi}_t^{(r+1)}$ and $\boldsymbol{\phi}_t^{(r+1)}$ by solving equation (143) and convex problem (144), respectively.
6: Update transmitter-specific dual variables $\boldsymbol{\mu}_t^{(r+1)}$ and $\boldsymbol{\nu}_t^{(r+1)}$ by solving equations (134) and (135), respectively.
7: Set $r = r + 1$.
8: **until** desired level of convergence

4.3.2 Numerical evaluation

In this section, the convergence behavior of the ADMM-based decentralized scheme (*Algorithm 13*) is evaluated via numerical examples. The used simulation model is the same as used in Section 4.2.2. The main parameters are given by $\{T, S, P, A_{\mathrm{T}}, A_{\mathrm{R}}\} = \{2, 4, 2, 8, 1\}$. The CSI errors are bounded by spherical regions, i.e., $\mathbf{E}_{t,s} = \left(1/e^2\right)\mathbf{I}_T$ and $\mathbf{F}_{t,p} = \left(1/e^2\right)\mathbf{I}_{A_{\mathrm{T}}}$, $\forall t \in \mathcal{T}$, $\forall s \in \mathcal{S}$, $\forall p \in \mathcal{P}$, and $e = 0.1$. The rate and interference constraints are set to $R_s = R = 1$ bits/s/Hz, $\forall s \in \mathcal{S}$ and $\Phi_p = \Phi = -10$ dB, $\forall p \in \mathcal{P}$. The power of noise plus primary network interference is set to 1, i.e., $Z_0 = 1$. A cell-edge case is modeled by setting the network separation parameter to 0 dB.

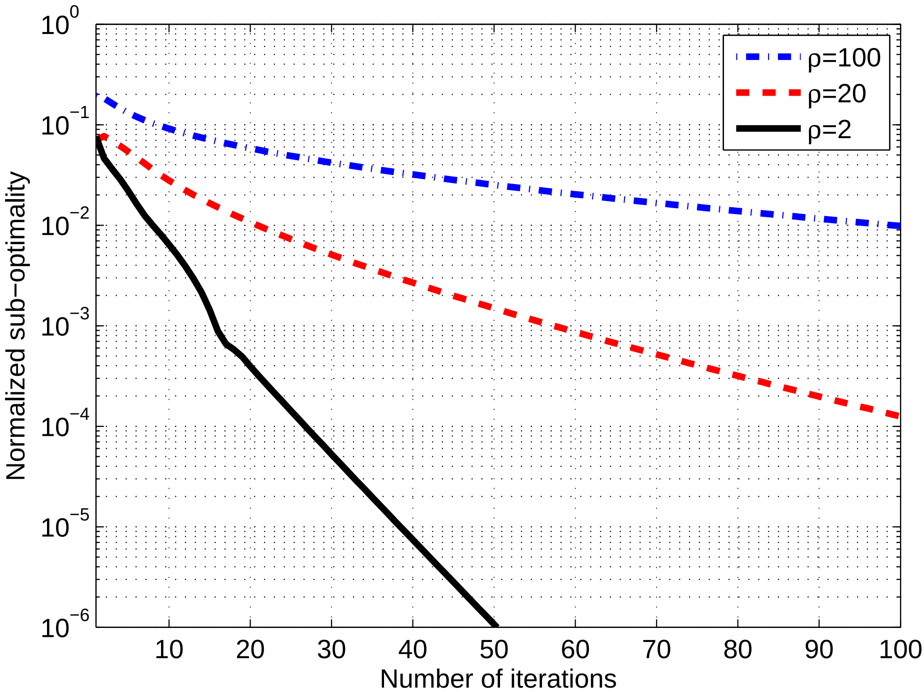

Fig 28. Convergence behavior of ADMM-based decentralized algorithm ([134] © 2014 IEEE).

Fig. 28 illustrates the normalized sub-optimality of *Algorithm 13* as a function of iteration r. The sub-optimality is defined as the normalized difference between the value of the objective function at iteration r in *Algorithm 13* and the optimal objective value achieved by solving the centralized problem (124). The results demonstrate that the speed of convergence depends on the choice of penalty parameter ρ. One can see that with properly chosen ρ the convergence is fast. In Fig. 28, all the converged optimal solutions are rank-one. Therefore, they are also optimal for the original problem (123).

4.4 Summary and discussions

In this chapter, coordinated beamforming was considered in a cognitive radio system where the primary and secondary networks share the same spectrum. The aim was to optimize the performance of the secondary network while keeping the generated interference toward each PU below a predefined level. Specifically, the considered system optimization objective was to minimize the total transmission power of the secondary network while guaranteeing the minimum rate target for each SU and satisfying the maximum aggregate interference constraint for each PU. This problem can be seen as an extension of the SPMin problem in a cellular multi-user MISO system in Section 2. A primal decomposition-based algorithm was proposed where decentralized implementation is achieved by decomposing the problem into network-level and transmitter-level optimization steps. The network-level optimization is solved via a projected subgradient method relying on scalar backhaul information exchange between the secondary transmitters. Each secondary transmitter-specific optimization is solved by using standard convex optimization techniques or the uplink-downlink duality-based method with the knowledge of local CSI at each transmitter. The proposed algorithm provides an optimal solution if the step-size is properly chosen, and the algorithm is allowed to converge. The numerical results showed significant gains over the ZF beamforming strategy and close to optimal performance even after a few subgradient iterations. It is also worth mentioning that the results can be seen as performance upper bounds in cognitive radio systems since the interference generated by the primary network is assumed to be known at the secondary transmitters. The proposed algorithm allows for some special case designs where the number of optimization variables is decreased, leading to reduced computational load and signaling overhead.

In addition, a practical assumption of erroneous CSI was also considered, and an ADMM-based decentralized algorithm was developed. Similarly as in Section 2, SDR and S-procedure methods were first applied in order to turn the original non-convex problem into a convex and tractable form. The resulting problem was then decomposed via ADMM into network-wide and transmitter-specific optimization steps that can be solved in a decentralized manner by relying on local imperfect CSI and low-rate backhaul signaling. The proposed algorithm provides an optimal solution to the original problem if the convex approximation is tight. The simulation results demonstrated that the algorithm converges relatively fast if the penalty parameter is properly chosen.

5 Conclusions and future work

The focus of this thesis was to design coordinated beamforming techniques for cellular and cognitive radio networks with the system design objective of sum power minimization subject to user-specific rate constraints. In particular, decentralized algorithms were developed. The proposed algorithms are based on the assumptions that each BS has local CSI and all the BSs can exchange scalar information between each other via low-rate backhaul links. In TDD-mode, uplink pilots can be used to aid the acquisition of the local CSI since the reciprocity of the uplink and downlink channels applies. The thesis aims to bring optimization-oriented coordinated beamforming designs closer to practical implementation, thus bridging the gap between reality and the theoretical studies in the literature. Due to the practical nature of the proposed decentralized concepts, this thesis paves the way for advanced MIMO and interference coordination strategies for 5G and beyond.

Chapter 1 highlighted the motivation for the research, and introduced the concept of coordinated beamforming. Chapter 1 also presented a detailed literature review of coordinated beamforming techniques designed in particular for cellular and cognitive radio systems.

In Chapter 2, decentralized coordinated beamforming schemes were developed for cellular multi-user MISO networks. In the proposed algorithms, the original convex SPMin optimization problem is divided into two optimization levels, i.e., BS-specific subproblems and a network-wide master problem, using the primal or dual decomposition method. In the primal decomposition-based algorithm, each BS optimizes its transmit beamformers for the given limits of experienced and generated inter-cell interference powers, and the corresponding dual variables by solving the corresponding subproblem using convex optimization techniques or the uplink-downlink duality-based method. The master problem iteratively optimizes the inter-cell interference power limits by using the projected subgradient method and given the dual variables provided by the subproblems. Each BS can solve its part of the master problem by exchanging the obtained dual variables between the coupled BSs at each iteration of the subgradient method. In addition, a dual decomposition-based algorithm was described where the convex subproblems are solved for the transmit beamformers and the local copies of inter-cell interference levels with fixed prices (i.e., the dual variables). The master problem is in charge of iteratively updating the prices via the subgradient method requiring the exchange of local inter-cell interference values between the BSs. For both algorithms, decentralized implementation is enabled if BSs acquire local CSI and exchange scalar information via low-rate backhaul links. The effect of imperfect CSI was also studied, and a primal decomposition-based robust beamforming design was proposed.

Optimal beamformers are obtained if the algorithms are allowed to converge. However, aiming for optimal solution is impractical since the more iterations are run, the higher the signaling/computational load and the longer the caused delay. Unlike the existing approaches, the proposed algorithms are able to provide feasible beamformers, which satisfy the minimum rate targets of active users, at intermediate iterations. Thus, the algorithms can be stopped after a limited number of iterations to reduce delay and backhaul signaling overhead. This valuable property makes the algorithms attractive for practical implementation since the delay and backhaul signaling overhead can be controlled and minimized on demand. The simulation results show that the decentralized algorithms provide performance close to a centralized scheme after a few iterations with significantly reduced signaling overhead. The capacity requirements of the backhaul links are also relaxed. To further reduce the signaling load, special designs are allowed. At the extreme case, there is no need for backhaul signaling at all. Due to its practical nature, the proposed decentralized concept was extended to cellular MIMO and cognitive MISO networks in Chapters 3 and 4, respectively.

Chapter 3 considered cellular multi-user MIMO systems. The non-convex SPMin problem was divided into transmit and receive beamforming optimization steps that can be solved in a centralized way by alternating between the SCA method and the MMSE criterion, respectively, until the desired level of sum power convergence is achieved. In addition, two decentralized primal decomposition -based algorithms were developed where the transmit and receive beamforming designs are aided by a combination of over-the-air pilot signaling and low-rate backhaul information exchange. In the first algorithm, sum power is minimized via an iterative over-the-air optimization process where the transmit beamformers are optimized at the BS side by using convex optimization techniques and the receive beamformers are computed at the user side via the

MMSE criterion. The BS and user side processing is aided by effective CSI acquired from precoded uplink and downlink pilots, respectively. In the second algorithm, the transmit and receive beamformers are iteratively optimized at each BS requiring only local CSI achieved from one round of antenna-specific uplink pilot signaling. In both algorithms, decentralized transmit beamforming design is enabled by applying the primal decomposition-based concept with low-rate backhaul signaling from Chapter 2. In addition, simplified decentralized algorithms were developed for single-stream MIMO systems. The numerical results showed that the proposed MIMO algorithms significantly outperform the simpler single-stream MIMO and MISO schemes. However, the computational complexity is higher with increased signaling overhead. The performance gains are emphasized, as the rate targets and number of receive antennas increase. Furthermore, the decentralized algorithms perform relatively well in low mobility time-correlated channel conditions, where the channel and signaling information are outdated. The instantaneous rates follow the minimum rate targets closely, whereas the average rates are higher than the targets.

In Chapter 4, the concept of coordinated beamforming was extended to underlay cognitive radio systems where the primary and secondary networks share the same spectrum. The aim was to optimize the secondary network performance with given additional constraints on the maximum allowed interference levels experienced by the PUs. A primal decomposition-based decentralized algorithm was derived. The practical properties discussed in Chapter 2 also apply here. The simulation results demonstrated notable gains over the interference nulling strategy and near to optimal performance after a few subgradient iterations. The proposed algorithm allows for some special designs where the computational and signaling loads are reduced at the cost of sub-optimal performance. In addition, the effect of imperfect CSI was examined, and an ADMM-based decentralized algorithm was proposed.

A coherent future work is to extend the cellular MIMO algorithms in Chapter 3 to a cognitive radio network with multi-antenna users. Specifically, the sum power is minimized for the secondary network with minimum rate targets for multi-antenna SUs while keeping the generated interference towards multi-antenna PUs below a predefined level. The effect of imperfect CSI could be also taken into consideration. Furthermore, the proposed algorithms are well applicable to heterogeneous networks, where the networks are comprised of lower and higher level tiers with some level of intra-tier and inter-tier coordination. An example is a network of small cells underlaying a macro cell network.

Theoretically, all the proposed coordinated beamforming algorithms can be applied to any size of the network. For large networks, however, the signaling overhead may become overly high. To avoid this issue, clustering, i.e., forming small clusters of BSs, can be applied in practice. If the clusters are of a limited size, the signaling overhead remains reasonable inside each cluster. However, system performance may be degraded if inter-cluster interference is not taken into account in the system design. Studying the effect of clustering is thus a practical topic for future research.

The simplified multi-cell environment used in the numerical evaluation is useful to demonstrate preliminary performance gains, which can serve as upper bounds for more realistic performance. In further studies, it would be also worthwhile to evaluate practical gains by employing a realistic wrap-around system-level simulation environment with more practical assumptions, such as multicarrier communication, pilot contamination, scheduling, clustering, delayed and erroneous channel/signaling information and practical modulation/coding schemes. For example, realistic system-level performance results were produced in [84, 151] for joint processing COMP with the block-diagonalization beamforming method. In such a practical environment, it may be challenging to guarantee instantaneous minimum rate targets for all active users. A straightforward solution is to introduce a protection margin, which sets the minimum target rates somewhat higher than ideally needed, possibly based on a heuristic metric.

Another interesting future research direction is to consider coordinated beamforming in the massive MIMO type of setting, where large antenna arrays are used at the transmitter side. Recent studies have shown that massive MIMO can provide high data rates by using low-complexity transmission strategies in a special setting where the number of transmit antennas is significantly larger than the number of users [166, 167]. However, better performance is obtained via coordinated beamforming in a practical multi-cell scenario, where large antenna arrays are used and the imbalance between the number of antennas and users is moderate. Due to the large number of antennas, the size of the channel matrices is large, thus leading to overly high signaling overhead for centralized designs. By applying the decentralized concept proposed in Chapter 2, backhaul signaling overhead does not increase with the number of transmit antennas, but only with the number of users and allocated data streams. Hence, the reduction of signaling overhead is emphasized as the number of transmit antennas increases. Therefore, decentralized designs become increasingly valuable for multi-cell systems with large antenna arrays. A recent study in [168] showed that signaling overhead can be even further reduced by exploiting large system analysis via random matrix theory in combination with the primal decomposition concept in Chapter 2.

Another promising future topic is dynamic TDD, which has been recently recognized as a potential concept to substantially improve the overall resource utilization in a multi-cell network. In dynamic TDD systems, each cell is operating either in uplink or downlink mode based on its instantaneous traffic demand. As a result, additional types of interference are present, i.e., user-to-user and BS-to-BS interference. Even a centralized design is difficult to implement due to the unavailability of the cross-user channels. However, decentralized implementation could be possible by adapting the MIMO design in Chapter 3 to dynamic TDD systems with bi-directional over-the-air signaling concept [169]. Moreover, the resulting decentralized framework would be directly applicable to a network assisted device-to-device (D2D) communication system, where both uplink and downlink resources can be used for direct D2D communication.

References

1. Olsson M, Cavdar C, Frenger P, Tombaz S, Sabella D & Jäntti R (2013) 5GrEEn: Towards green 5G mobile networks. In: Proc. IEEE Int. Conf. Wireless Mobile Comp., Netw. and Commun., pp. 212–216. Lyon, France.
2. Li Q, Niu H, Papathanassiou A & Wu G (2014) 5G network capacity: Key elements and technologies. IEEE Veh. Technol. Mag. 9(1): 71–78.
3. Wang CX, Haider F, Gao X, You XH, Yang Y, Yuan D, Aggoune H, Haas H, Fletcher S & Hepsaydir E (2014) Cellular architecture and key technologies for 5G wireless communication networks. IEEE Commun. Mag. 52(2): 122–130.
4. Fettweis G & Alamouti S (2014) Personal mobile internet beyond what cellular did to telephony. IEEE Commun. Mag. 52(2): 140–145.
5. Andrews J, Buzzi S, Wan C, Hanly SV, Lozano A, Soong ACK & Zhang JC (2014) What will 5G be? IEEE J. Select. Areas Commun. 32(6): 1065–1082.
6. Jungnickel V, Manolakis K, Zirwas W, Panzner B, Braun V, Lossow M, Sternad M, Apelfröjd R & Svensson T (2014) The role of small cells, coordinated multipoint, and massive MIMO in 5G. IEEE Commun. Mag. 52(5): 44–51.
7. Gozalvez J (2015) 5G tests and demonstrations. IEEE Veh. Technol. Mag. 10(2): 16–25.
8. Gupta A & Jha RK (2015) A survey of 5G network: Architecture and emerging technologies. IEEE Access 3(1): 1206–1232.
9. Hossain E & Hasan M (2015) 5G cellular: Key enabling technologies and research challenges. IEEE Instrumentation and Measument Mag. 18(3): 11–21.
10. 3GPP (2013) Overall description. TS 36.300 v11.5.0, 3rd Generation Partnership Project (3GPP); Technical Specification Group Radio Access Network.
11. 3GPP (2010) Further Advancements for E-UTRA Physical Layer Aspects. TR 36.814 v9.0.0, 3rd Generation Partnership Project (3GPP); Technical Specification Group Radio Access Network.
12. Gesbert D, Hanly S, Huang H, Shamai S, Simeone O & Yu W (2010) Multi-cell MIMO cooperative networks: A new look at interference. IEEE J. Select. Areas Commun. 28(9): 1–29.
13. 3GPP (2011) Coordinated multi-point operation for LTE physical layer aspects. Technical report, 3GPP TR 36.819 V11.0.0.
14. Goldsmith A, Jafar S, Jindal N & Vishwanath S (2003) Capacity limits of MIMO channels. IEEE J. Select. Areas Commun. 21(5): 684–702.
15. Gesbert D, Kountouris M, Heath RW, Chae CB & Salzer T (2007) Shifting the MIMO paradigm. IEEE Signal Processing Mag. 24(5): 36–46.
16. Winters J (1987) On the capacity of radio communication systems with diversity in a rayleigh fading environment. IEEE J. Select. Areas Commun. 5(5): 871–878.
17. Foschini GJ (1996) Layered space-time architecture for wireless communication in a fading environment when using multi-element antennas. Bell Labs Technical Journal 1(2): 41–59.
18. Telatar E (1999) Capacity of multi-antenna Gaussian channels. European Trans. Telecommun. 10(6): 585–595.

19. Alamouti S (1998) A simple transmit diversity technique for wireless communications. IEEE J. Select. Areas Commun. 16(8): 1451–1458.
20. Hochwald BM & Marzetta TL (2000) Unitary space-time modulation for multiple-antenna communications in Rayleigh flat fading. IEEE Trans. Inform. Theory 46(2): 543–563.
21. Biglieri E, Taricco G & Tulino A (2002) Decoding space-time codes with BLAST architectures. IEEE Trans. Signal Processing 50(10): 2547–2552.
22. Zheng L & Tse DNC (2003) Diversity and multiplexing: A fundamental tradeoff in multiple-antenna channels. IEEE Trans. Inform. Theory 49(5): 1073–1096.
23. Costa MHM (1983) Writing on dirty paper. IEEE Trans. Inform. Theory 29(3): 439–441.
24. Caire G & Shamai S (2003) On the achievable throughput of a multiantenna Gaussian broadcast channel. IEEE Trans. Inform. Theory 49(7): 1691–1706.
25. Weingarten H, Steinberg Y & Shamai S (2006) The capacity region of the Gaussian multiple-input multiple-output broadcast channel. IEEE Trans. Inform. Theory 52(9): 3936–3964.
26. Peel CB, Hochwald BM & Swindlehurst AL (2005) A vector-perturbation technique for near-capacity multiantenna multiuser communication - Part I: Channel inversion and regularization. IEEE Trans. Commun. 53(1): 195–202.
27. Spencer QH & Haardt M (2002) Capacity and downlink transmission algorithms for a multi-user MIMO channel. In: Proc. Annual Asilomar Conf. Signals, Syst. and Comp., pp. 1384–1388. Pacific Grove, CA, USA.
28. Peel CB, Swindlehurst AL & Haardt M (2004) Zero-forcing methods for downlink spatial multiplexing in multiuser MIMO channels. IEEE Trans. Signal Processing 52(2): 461–471.
29. Choi LU & Murch RD (2004) A transmit preprocessing technique for multiuser MIMO systems using a decomposition approach. IEEE Trans. Communications 3(1): 20–24.
30. Yoo T & Goldsmith A (2006) On the optimality of multiantenna broadcast scheduling using zero-forcing beamforming. IEEE J. Select. Areas Commun. 24(3): 528–541.
31. Bengtsson M & Ottersten B (1999) Optimal downlink beamforming using semidefinite optimization. In: Proc. Annu. Allerton Conf. Communic., Contr. and Comp., pp. 987–996. IL, USA.
32. Bengtsson M & Ottersten B (2001) Optimal and suboptimal transmit beamforming. In Handbook of Antennas in Wireless Commincations. Boca Raton, FL, USA: L. C. Godara, Ed. CRC Press.
33. Wiesel A, Eldar C & Shamai S (2006) Linear precoding via conic optimization for fixed MIMO receivers. IEEE Trans. Signal Processing 54(1): 161–176.
34. Sidiropoulos ND, Davidson TN & Luo ZQ (2006) Transmit beamforming for physical-layer multicasting. IEEE Trans. Signal Processing 54(6): 2239–2251.
35. Yu W & Lan T (2007) Transmitter optimization for the multi-antenna downlink with per-antenna power constraints. IEEE Trans. Signal Processing 55(6): 2646–2660.
36. Gershman AB, Sidiropoulos ND, Shahbazpanahi S, Bengtsson M & Ottersten B (2010) Convex optimization-based beamforming. IEEE Signal Processing Mag.

27(3): 62–75.
37. Wagner S & Slock DTM (2011) Weighted sum rate maximization of correlated MISO broadcast channels under linear precoding: A large system analysis. In: Proc. IEEE Int. Workshop Signal Processing Adv. Wireless Commun., pp. 411–415. San Francisco, CA, USA.
38. Bogale TE, Chalise BK & Vandendorpe V (2012) Robust transceiver optimization for downlink multiuser MIMO systems. IEEE Trans. Signal Processing 59(1): 446–453.
39. Bogale TE & Vandendorpe V (2012) Weighted sum rate optimization for downlink multiuser MIMO systems with per antenna power constraint: Downlink-uplink duality approach. In: Proc. Int. Conf. Acoust., Speech, Signal Processing, pp. 3245–3248. Kioto, Japan.
40. Christopoulos D, Chatzinotas S & Ottersten B (2014) Weighted fair multicast multigroup beamforming under per-antenna power constraints. IEEE Trans. Signal Processing 62(19): 5132–5142.
41. Huang Y, He S, Jin S, Wang H & Yang L (2014) Duality based energy-efficient beamforming design for multiuser downlink systems. IEEE Wireless Commun. Letters 3(4): 409–412.
42. Tervo O, Tran LN & Juntti M (2015) Optimal energy-efficient transmit beamforming for multi-user MISO downlink. IEEE Trans. Signal Processing 63(99).
43. Luo ZQ & Yu W (2006) An introduction to convex optimization for communications and signal processing. IEEE J. Select. Areas Commun. 24(8): 1426–1438.
44. Luo ZQ, Ma WK, So AMC, Ye Y & Zhang S (2010) Semidefinite relaxation of quadratic optimization problems. IEEE Signal Processing Mag. 27(3): 20–34.
45. Dawod NH, Marsland ID & Hafez RHM (2006) Improved transmit null steering for MIMO-OFDM downlinks with distributed base station antenna arrays. IEEE J. Select. Areas Commun. 24(3): 419–426.
46. Foschini GJ, Huang HC, Karakayali K, Valenzuela RA & Venkatesan S (2005) The value of coherent base station coordination. In: Proc. Conf. Inform. Sciences and Systems. vol. 3. Baltimore, Maryland, USA.
47. Karakayali MK, Foschini GJ & Valenzuela RA (2006) Network coordination for spectrally efficient communications in cellular systems. IEEE Wireless Commun. Mag. 3(14): 56–61.
48. Karakayali MK, Foschini GJ, Valenzuela RA & Yates RD (2006) On the maximum common rate achievable in a coordinated network. In: Proc. IEEE Int. Conf. Commun., pp. 4333–4338. Istanbul, Turkey.
49. Shamai S & Zaidel B (2001) Enhancing the cellular downlink capacity via co-processing at the transmitting. In: Proc. IEEE Veh. Technol. Conf., pp. 1745–1749. Rhodes, Greece.
50. Shamai S, Zaidel B & Verdu S (2002) On information theoretic aspects of multi-cell wireless systems. In: Proc. Int. ITG Conf. Source and Channel Coding. vol. 4. Berlin, Germany.
51. Somekh O, Simeone O & Haimovich YBN (2006) Distributed multi-cell zero-forcing beamforming in cellular downlink channels. In: Proc. IEEE Global Telecommun. Conf., pp. 1–5. San Francisco, CA, USA.
52. Tölli A, Codreanu M & Juntti M (2008) Cooperative MIMO-OFDM cellular sys-

tem with soft handover between distributed base station antennas. IEEE Trans. Wireless Commun. 7(4): 1428–1440.
53. Zakhour R & Gesbert D (2010) Distributed multicell-MISO precoding using the layered virtual sinr framework. IEEE Wireless Commun. 9(8): 2444–2448.
54. Björnson E, Zakhour R, Gesbert D & Ottersten B (2010) Cooperative multicell precoding: rate region characterization and distributed strategies with instantaneous and statistical CSI. IEEE Trans. Signal Processing 58(8): 4298–4310.
55. Björnson E, Jalden N, Bengtsson M & Ottersten B (2011) Optimality properties, distributed strategies, and measurement-based evaluation of coordinated multicell OFDMA transmission. IEEE Trans. Signal Processing 59(12): 6086–6101.
56. Komulainen P, Tölli A & Juntti M (2013) Effective CSI signaling and decentralized beam coordination in TDD multi-cell MIMO systems. IEEE Trans. Signal Processing 61(9): 2204–2218.
57. Kobayashi M, Jindal N & Caire G (2011) Training and feedback optimization for multiuser MIMO downlink. IEEE Trans. Commun. 59(8): 2228–2240.
58. Rashid-Farrokhi F, Liu K & Tassiulas L (1998) Transmit beamforming and power control for cellular wireless systems. IEEE J. Select. Areas Commun. 16(8): 1437–1450.
59. Dahrouj H & Yu W (2010) Coordinated beamforming for the multicell multi-antenna wireless system. IEEE Trans. Wireless Commun. 9(5): 1748–1759.
60. Tölli A, Pennanen H & Komulainen P (2011) Decentralized minimum power multi-cell beamforming with limited backhaul signaling. IEEE Trans. Wireless Commun. 10(2): 570–580.
61. Pennanen H, Tölli A & Latva-aho M (2011) Decentralized coordinated downlink beamforming via primal decomposition. IEEE Signal Processing Letters 18(11): 647–650.
62. Hellings C, Joham M & Utschick W (2012) Gradient-based power minimization in MIMO broadcast channels with linear precoding. IEEE Trans. Signal Processing 60(2): 877–890.
63. Pennanen H, Tölli A & Latva-aho M (2014) Multi-cell beamforming with decentralized coordination in cognitive and cellular networks. IEEE Trans. Signal Processing 62(2): 295–308.
64. Negro F, Cardone M, Ghauri I & Slock DTM (2011) SINR balancing and beamforming for the MISO interference channel. In: Proc. Int. Symp. Pers., Indoor, Mobile Radio Commun., pp. 1552–1556. Toronto, Canada.
65. Huang Y, Zheng G, Bengtsson M, Wong KK, Yang L & Ottersten B (2012) Distributed multicell beamforming design approaching pareto boundary with max-min fairness. IEEE Trans. Wireless Commun. 11(8): 2921–2933.
66. Liu YF, Dai YH & Luo ZQ (2013) Max-min fairness linear transceiver design for a multi-user MIMO interference channel. IEEE Trans. Signal Processing 61(9): 2413–2423.
67. Negro F, Shenoy SP, Ghauri I & Slock DTM (2010) Weighted sum rate maximization in the MIMO interference channel. In: Proc. Int. Symp. Pers., Indoor, Mobile Radio Commun., pp. 684–689. Istanbul, Turkey.
68. Shi Q, Razaviyayn M, Luo Z & He C (2011) An iteratively weighted MMSE approach to distributed sum-utility maximization for a MIMO interfering broadcast

channel. IEEE Trans. Signal Processing 9(4): 4331–4340.
69. Bogale TE & Vandendorpe V (2012) Weighted sum rate optimization for downlink multiuser MIMO coordinated base station systems: Centralized and distributed algorithms. IEEE Trans. Signal Processing 60(4): 1876–1889.
70. Negro F, Ghauri I & Slock DTM (2012) Sum rate maximization in the noisy MIMO interfering broadcast channel with partial CSIT via the expected weighted MSE. In: Proc. Int. Symp. Wireless Commun. Syst., pp. 576–580. Paris, France.
71. Kaleva J, Tölli A & Juntti M (2012) Weighted sum rate maximization for interfering broadcast channel via successive convex approximation. In: Proc. IEEE Global Telecommun. Conf., pp. 3838–3843. Anaheim, CA, USA.
72. He S, Huang Y, Jin S & Yang L (2013) Coordinated beamforming for energy efficient transmission in multicell multiuser systems. IEEE Trans. Commun. 61(12): 4961–4971.
73. Huang Y, He S, Jin S & Chen W (2014) Decentralized energy efficient coordinated beamforming for multicell systems. IEEE Trans. Veh. Technol. 63(9): 4302–4314.
74. He S, Huang Y, Yang L & Ottersten B (2014) Coordinated multicell multiuser precoding for maximizing weighted sum energy efficiency. IEEE Trans. Signal Processing 62(3): 741–751.
75. He S, Huang Y, Jin S & Yang L (2015) Energy efficient coordinated beamforming design in multi-cell multicast networks. IEEE Commun. Letters 19(6): 985–988.
76. Vucic N, Boche H & Shi S (2009) Robust transceiver optimization in downlink multiuser MIMO systems. IEEE Trans. Signal Processing 57(9): 3576–3587.
77. Bogale TE & Vandendorpe V (2012) Robust sum MSE optimization for downlink multiuser MIMO systems with arbitrary power constraint: Generalized duality approach. IEEE Trans. Signal Processing 60(4): 1862–1875.
78. Bogale TE & Vandendorpe V (2012) Robust transceiver optimization for downlink coordinated base station systems: Distributed algorithm. IEEE Trans. Signal Processing 60(1): 337–350.
79. Bogale TE & Vandendorpe V (2013) Linear transceiver design for downlink multiuser MIMO systems: Downlink-interference duality approach. IEEE Trans. Signal Processing 61(19): 4686–4700.
80. Schmidt DA, Changxin S, Berry RA, Honig ML & Utschick W (2013) Comparison of distributed beamforming algorithms for MIMO interference networks. IEEE Trans. Signal Processing 61(13): 3476–3489.
81. Boyd S & Vandenberghe L (2004) Convex Optimization. Cambridge, UK: Cambridge University Press.
82. Tölli A, Codreanu M & Juntti M (2008) Linear multiuser MIMO transceiver design with quality of service and per-antenna power constraints. IEEE Trans. Signal Processing 56(7): 3049–3055.
83. Stridh R, Bengtsson M & Ottersten B (2006) System evaluation of optimal downlink beamforming with congestion control in wireless communication. IEEE Trans. Wireless Commun. 5(4): 743–751.
84. Haataja T, Pennanen H, Leinonen J, Tölli A & Latva-aho M (2011) Space-frequency scheduling in TDD based LTE-advanced MIMO-OFDMA systems. In: Proc. IEEE Veh. Technol. Conf., pp. 1–5. Budabest, Hungary.
85. Weeraddana PC, Codreanu M, Latva-Aho M & Ephremides A (2013) Multicell

MISO downlink weighted sum-rate maximization: A distributed approach. IEEE Trans. Signal Processing 61(3): 556–570.
86. Visotsky E & Madhow U (1999) Optimum beamforming using transmit antenna arrays. In: Proc. IEEE Veh. Technol. Conf., volume 1, pp. 851–856.
87. Schubert M & Boche H (2004) Solution of the multiuser downlink beamforming problem with individual SINR constraints. IEEE Trans. Veh. Technol. 53(1): 18–28.
88. Grant M & Boyd S (2013). CVX: Matlab software for disciplined convex programming, version 2.0 beta. http://cvxr.com/cvx.
89. Shen C, Chang TH, Wang KY, Qiu Z & Chi CY (2012) Distributed robust multicell coordinated beamforming with imperfect CSI: An ADMM approach. IEEE Trans. Signal Processing 60(6): 2988–3003.
90. Joshi S, Codreanu M & Latva-aho M (2014) Distributed resource allocation for MISO downlink systems via the alternating direction method of multipliers. EURASIP J. Wireless Comm. and Netw. 1(1): 1–19.
91. Bengtsson M (2002) A pragmatic approach to multi-user spatial multiplexing. In: Proc. IEEE Sensor Array and Multichannel Signal Processing Workshop, pp. 130–134. Washington, USA.
92. Khachan AM, Tenenbaum AJ & Adve RS (2006) Linear processing for the downlink in multiuser MIMO systems with multiple data streams. In: Proc. IEEE Int. Conf. Commun., pp. 4113–4118. Istanbul, Turkey.
93. Mezghani A, Joham M, Hunger R & Utschick W (2006) Transceiver design for multi-user MIMO systems. In: Proc. Int. ITG Workshop on Smart Antennas, pp. 1–9. Ulm, Germany.
94. Ma K, Wang W, Zhao X & Zheng K (2008) Joint transmitter-receiver design for the downlink multiuser spatial multiplexing MIMO system. In: Proc. IEEE Int. Conf. Commun., pp. 3526–3530. Beijing, China.
95. Shi S, Schubert M & Boche H (2008) Rate optimization for multiuser MIMO systems with linear processing. IEEE Trans. Signal Processing 56(8): 4020–4030.
96. Chang JH, Tassiulas L & Rashid-Farrokhi F (2002) Joint transmitter receiver diversity for efficient space division multiaccess. IEEE Trans. Wireless Commun. 2(1): 16–27.
97. Schubert M, Shi S & Boche H (2006) Iterative transceiver optimization for linear multiuser MIMO channels with per-user MMSE requirements. In: Proc. European Signal Processing Conf., pp. 1–5. Florence, Italy.
98. Shi S, Schubert M & Boche H (2006) Computational efficient transceiver optimization for multiuser MIMO systems: Power minimization with user-MMSE requirements. In: Proc. Annual Asilomar Conf. Signals, Syst. and Comp., pp. 1247–1251. Pasific Grove, CA, USA.
99. Pennanen H, Tölli A, Kaleva J, Komulainen P & Latva-aho M (2015, submitted) Decentralized linear transceiver design and signaling strategies for sum power minimization in multi-cell MIMO systems. IEEE Trans. Signal Processing .
100. Shenouda MB & Davidson TN (2007) Convex conic formulations of robust downlink precoder designs with quality of service constraints. IEEE J. Select. Topics Signal Processing 1: 714–724.
101. Vucic N & Boche H (2009) Robust QoS-constrained optimization of downlink

multiuser MISO systems. IEEE Trans. Signal Processing 57(2): 714–725.
102. Tajer A, Prasad N & Wang X (2011) Robust linear precoder design for multi-cell downlink transmission. IEEE Trans. Signal Processing 59(1): 235–251.
103. Zheng G, Wong KK & Ng TS (2008) Robust linear MIMO in the downlink: A worst-case optimization with ellipsoidal uncertainty regions. EURASIP J. Adv. Signal Processing pp. 1–15.
104. Song E, Shi Q, Sanjabi M, Sun R & Luo ZQ (2011) Robust SINR constrained MISO downlink beamforming: When is semidefinite programming relaxation tight? In: Proc. IEEE Int. Conf. Acoustics, Speech and Signal Processing, pp. 3096 – 3099. Prague, Czech.
105. Pennanen H, Tölli A & Latva-aho M (2014) Decentralized robust beamforming for coordinated multi-cell MISO networks. IEEE Signal Processing Letters 21(3): 334–338.
106. Mitola J & Maguire GQ (1999) Cognitive radio: Making software radios more personal. IEEE Personal Commun. 6(6): 13–18.
107. Haykin S (2005) Cognitive radio: Brain-empowered wireless communications. IEEE J. Select. Areas Commun. 23(2): 201–220.
108. Tragos E, Zeadally S, Fragkiadakis A & Siris V (2013) Spectrum assignment in cognitive radio networks: A comprehensive survey. IEEE Commun. Surveys and Tutorials 15(3): 1108–1135.
109. Zhao Q & Sadler M (2007) A survey of dynamic spectrum access. IEEE Signal Processing Mag. 24(3): 79–89.
110. Devroye N, Vu M & Tarokh V (2008) Cognitive radio networks. IEEE Signal Processing Mag. 25(6): 12–23.
111. Zhang R & Liang YC (2008) Exploiting multi-antennas for opportunistic spectrum sharing in cognitive radio networks. IEEE J. Select. Areas Commun. 2(1): 88–102.
112. Islam MH, Liang YC & Hoang AT (2007) Joint beamforming and power control in the downlink of cognitive radio networks. In: Proc. IEEE Wireless Commun. and Netw. Conf., pp. 21–26. Hong Kong.
113. Xiao F, Wang J & Li S (2009) Joint power management and beamforming for base stations in cognitive radio systems. In: Proc. IEEE Int. Symp. Wireless Commun. Syst., pp. 403 – 407. Tuscany, Italy.
114. Phan KT, Vorobyov SA, Sidiropoulos ND & Tellambura C (2009) Spectrum sharing in wireless networks via QoS-aware secondary multicast beamforming. IEEE Trans. Signal Processing 57(6): 2323–2335.
115. Pesavento M, Ciochina D & Gershman AB (2010) Iterative dual downlink beamforming for cognitive radio networks. In: Proc. Int. Conf. Cognitive Radio Oriented Wireless Netw. and Commun., pp. 1–5. Cannes, France.
116. Negro F, Ghauri I & Slock DTM (2010) Beamforming for the underlay cognitive MISO interference channel via UL-DL duality. In: Proc. Int. Conf. Cognitive Radio Oriented Wireless Netw. and Commun., pp. 1–5. Cannes, France.
117. Gharavol EA, Liang YC & Mouthaan K (2010) Robust downlink beamforming in multiuser MISO cognitive radio networks with imperfect channel-state information. IEEE Trans. Veh. Technol. 59(6): 2852–2860.
118. Wajid I, Pesavento M, Eldar YC & Gershman A (2010) Robust downlink beam-

forming for cognitive radio networks. In: Proc. IEEE Global Telecommun. Conf., pp. 1–5. Miami, FL, USA.
119. Ramamonjison R & Bhargava VK (2012) Distributed beamforming in cognitive multi-cell wireless systems by fast interference coordination. In: Proc. IEEE Int. Symp. Pers. Indoor and Mobile Radio Commun., pp. 2208–2213. Sydney, Australia.
120. Du H, Ratnarajah T, Pesavento M & Papadias C (2012) Joint transceiver beamforming in MIMO cognitive radio network via second-order cone programming. IEEE Trans. Signal Processing 60(2): 781–792.
121. Kim SJ & Giannakis G (2008) Optimal resource allocation for MIMO ad hoc cognitive radio networks. In: Proc. Annu. Allerton Conf. Commun., Control and Comp., pp. 39 – 45. Urbana-Champaign, IL.
122. Scutari G & Palomar DP (2009) Competitive optimization of cognitive radio MIMO systems via game theory. In: Proc. Int. Conf. Game Theory for Netw., pp. 452 – 461. Istanbul, Turkey.
123. Zhang R, Liang YC, Xin Y & Poor HV (2009) Robust cognitive beamforming with partial channel state information. IEEE Trans. Wireless Commun. 8(8): 4143–4153.
124. Gallo L, Negro F, Ghauri I & Slock DTM (2011) Weighted sum rate maximization in the underlay cognitive MISO interference channel. In: Proc. Int. Symp. Pers., Indoor, Mobile Radio Commun., pp. 661–665. Toronto, Canada.
125. Zheng G, Wong KK & Ottersten B (2009) Robust cognitive beamforming with bounded channel uncertainties. IEEE Trans. Signal Processing 57(12): 4871–4881.
126. Tajer A, Prasad N & Wang X (2010) Beamforming and rate allocation in MISO cognitive radio networks. IEEE Trans. Signal Processing 58(1): 362–377.
127. Cumanan K, Musavian L, Lambotharan S & Gersham AB (2010) SINR balancing technique for downlink beamforming in cognitive radio networks. IEEE Signal Processing Letters 17(2): 133–136.
128. Zheng G, Ma S, Wong KK & Ng TS (2010) Robust beamforming in cognitive radio. IEEE Trans. Wireless Commun. 9(2): 570–576.
129. Gharavol EA, Liang YC & Mouthaan K (2011) Robust linear transceiver design in MIMO ad hoc cognitive radio networks with imperfect channel state information. IEEE Trans. Wireless Commun. 10(5): 1448–1457.
130. Wang F & Wang W (2010) Robust beamforming and power control for multiuser cognitive radio network. In: Proc. IEEE Global Telecommun. Conf., pp. 1 – 5. Miami, FL.
131. Hanif M, Smith P & Alouini M (2010) SINR balancing in the downlink of cognitive radio networks with imperfect channel knowledge. In: Proc. Int. Conf. Cognitive Radio Oriented Wireless Netw. and Commun., pp. 1 – 5. Cannes, France.
132. Zhang Y, Dall'Anese E & Giannakis B (2012) Distributed optimal beamformers for cognitive radios robust to channel uncertainties. IEEE Trans. Signal Processing 60(12): 6495–6508.
133. Wijewardhana UL, Codreanu M & Latva-aho M (2013) Robust beamformer design for underlay cognitive radio network using worst case optimization. In: Proc. Int. Symp. Modeling and Optimization in Mobile, Ad Hoc Wireless Netw., pp. 404 – 411. Tsukuba, Japan.

134. Pennanen H, Tölli A & Latva-aho M (2014) Robust beamforming with decentralized interference coordination in cognitive radio networks. In: Proc. IEEE Int. Conf. Acoustics, Speech and Signal Processing, pp. 7308–7312. Florence, Italy.
135. Pennanen H, Tölli A & Latva-aho M (2011) Decentralized coordinated downlink beamforming for cognitive radio networks. In: Proc. IEEE Int. Symp. Pers. Indoor and Mobile Radio Commun., pp. 566–571. Toronto, Canada.
136. Pennanen H, Tölli A & Latva-aho M (2011) Decentralized multi-cell beamforming coordination for multiuser MISO systems. In: Proc. Annual Asilomar Conf. Signals, Syst. and Comp., pp. 1376–1380. Pasific Grove, CA, USA.
137. Pennanen H, Tölli A & Latva-aho M (2012) Decentralized linear transceiver design in coordinated multi-cell multiuser MIMO systems. In: Proc. IEEE Global Commun. Conf., pp. 4338–4343. Anaheim, CA, USA.
138. Pennanen H, Tölli A & Latva-aho M (2012) Pragmatic multi-cell MIMO beamforming with decentralized coordination. In: Proc. Annual Asilomar Conf. Signals, Syst. and Comp., pp. 1996–2000. Pasific Grove, CA, USA.
139. Alatossava M, Pennanen H, Holappa V & Yli-talo J (2007) The impact of noise threshold setting on estimated radio channel parameters and BER. In: Proc. IEEE Int. Symp. Wireless Pers. Multimedia Commun., pp. 1–4. Jaipur, India.
140. Pennanen H, Leinonen J & Ylitalo J (2007) Transmission adaptation for broadband wireless MIMO-OFDM systems with limited feedback. In: Proc. Finnish Signal Processing Symp., pp. 1–5. Oulu, Finland.
141. Pennanen H, Leinonen J, Skowron M & Latva-aho M (2008) Enhanced link adaptation techniques for MIMO-OFDM systems with limited feedback - A channel measurement based evaluation. In: Proc. IEEE Int. Symp. Wireless Pers. Multimedia Commun., pp. 1–6. Saariselkä, Finland.
142. Pennanen H, Leinonen J, Lu X, Skowron M & Latva-aho M (2008) Performance evaluation of adaptive MIMO-OFDM systems with imperfect feedback in measurement based channels. In: Proc. Annual Asilomar Conf. Signals, Syst. and Comp., pp. 923–927. Pasific Grove, CA, USA.
143. Tölli A, Pennanen H & Komulainen P (2009) Distributed coordinated multi-cell transmission based on dual decomposition. In: Proc. IEEE Global Commun. Conf., pp. 1–6. Honolulu, HI, USA.
144. Tölli A, Pennanen H & Komulainen P (2009) Distributed implementation of coordinated multi-cell beamforming. In: Proc. IEEE Int. Symp. Pers. Indoor and Mobile Radio Commun., pp. 818–822. Tokyo, Japan.
145. Tölli A, Pennanen H & Komulainen P (2009) On the value of coherent and coordinated multi-cell transmission. In: Proc. Int. Workshop on LTE Evolution, pp. 1–5. Dresden, Germany.
146. Tölli A, Pennanen H & Komulainen P (2009) Beamformer design and resource allocation for centralised and distributed coordinated multi-point transmission. In: Proc. IEEE Int. Symp. Wireless Pers. Multimedia Commun., pp. 1–7. Sendai, Japan.
147. Tölli A, Pennanen H & Komulainen P (2009) SINR balancing with coordinated multi-cell transmission. In: Proc. IEEE Wireless Commun. and Netw. Conf., pp. 1–6. Budabest, Hungary.
148. Boldi M, Komulainen P, Olsson M, Pennanen H, Seifi N, Svensson T, Tölli A &

Wild T (2009) Coordinated multipoint systems for IMT-advanced in the framework of the WINNER+ project. In: Proc. ICT Mobile and Wireless Communications Summit, pp. 1–8. Santander, Spain.
149. Boldi M, Hardouin E, Olsson M, Pennanen H & Tölli A (2010) Coordinated beamforming for IMT-advanced in the framework of WINNER+ project. In: Proc. Future Network and Mobile Summit, pp. 1–8. Florence, Italy.
150. Pennanen H, Tölli A & Latva-aho M (2010) Decentralized base station assignment in combination with downlink beamforming. In: Proc. IEEE Int. Workshop Signal Processing Adv. Wireless Commun., pp. 1–5. Marrakach, Morocco.
151. Pennanen H, Haataja T, Leinonen J, Tölli A & Latva-aho M (2010) System level evaluation of TDD based LTE-advanced MIMO-OFDMA systems. In: Proc. IEEE Broadband Wireless Access Workshop, pp. 809–813. Miami, FL, USA.
152. Pennanen H, Alatossava M, Leinonen J & Latva-aho M (2011) Performance evaluation of adaptive MIMO-OFDM systems with limited feedback using measurement based channels. Int. J. Wireless Information Netw. 18(1): 1–10.
153. Ghazanfari A, Tölli & Pennanen H (2014) Sum power minimization for cellular systems with underlay D2D communications. In: Proc. Int. Conf. Cognitive Radio Oriented Wireless Netw. and Commun., pp. 45–50. Oulu, Finland.
154. Laiyemo A, Pennanen H, Pirinen P & Latva-aho M (2015, to be submitted) Transmission strategies for throughput maximization in high speed train communications: From theoretical analysis to practical design. IEEE Trans. Veh. Technol .
155. Palomar DP & Chiang M (2006) A tutorial on decomposition methods for network utility maximization. IEEE J. Select. Areas Commun. 24(8): 1439–1451.
156. Bertsekas DP, Nedic A & Ozdaglar AE (2003) Convex Analysis and Optimization. Belmont, MA, USA: Athena Scientific.
157. Boyd S, Xiao L, Mutapic A & Mattingley J (2007) Subgradient methods. In: Notes for EE364b, Stanford University, Available online: http://ww.stanford.edu/class/ee364b/.
158. Lobo M, Vandenberghe L, Boyd S & Lebret H (1998) Applications of second-order cone programming. Linear algebra and its applications 284(1): 193–228.
159. Vandenberghe L & Boyd S (1996) Semidefinite programming. SIAM review 38(1): 49–95.
160. Song E, Shi Q, Sanjabi M, Sun R & Luo ZQ (2012) Robust SINR constrained MISO downlink beamforming: When is semidefinite programming relaxation tight? EURASIP J. Wireless Communun. and Netw. 2012(1): 1–11.
161. Kay SM (1993) Fundamentals of Statistical Signal Processing: Estimation Theory. Englewood Cliffs, NJ, USA: Prentice-Hall.
162. Hunger C, Joham M & Utschick W (2009) On the MSE-duality of the broadcast channel and the multiple access channel. IEEE Trans. Signal Processing 57(2): 698–713.
163. Boyd S, Xiao L, Mutapic A & Mattingley J (2007) Sequential convex programming. In: Notes for EE364b, Stanford University, Available online: http://ww.stanford.edu/class/ee364b/.
164. Marks B & Wright G (1978) A general inner approximation algorithm for nonconvex mathematical programs. Journal of the Operations Research Society of

America 26(4): 681–683.
165. Boyd N S Parikh, Chu E, Peleato P & Eckstein J (2011) Distributed optimization and statistical learning via the alternating direction method of multipliers. Foundations and Trends in Machine Learning 3(1): 1–122.
166. Marzetta T (2010) Noncooperative cellular wireless with unlimited numbers of base station antennas. IEEE Trans. Wireless Commun. 9(11): 3590–3600.
167. Rusek F, Persson D, Lau BK, Larsson EG, Marzetta T, Edfors O & Tufvesson F (2013) Scaling up MIMO: Opportunities and challenges with very large arrays. IEEE Signal Processing Mag. 30(1): 40–60.
168. Asgharimoghaddam H, Tölli A & Rajatheva N (2014) Decentralizing the optimal multi-cell beamforming via large system analysis. In: Proc. IEEE Int. Conf. Commun., pp. 1–5. Sydney, Australia.
169. Jayasinghe P, Tölli A, Kaleva J & Latva-aho M (2015) Bi-directional signaling for dynamic TDD with decentralized beamforming. In: IEEE Workshop on Small Cell and 5G Netw., pp. 185–190. London, UK.
170. Yates R (1995) A framework for uplink power control in cellular radio systems. IEEE J. Select. Areas Commun. 13(7): 1341–1347.

Appendix 1 Proof of Proposition 1

In this appendix, it is proved that strong duality holds for (12). It is known that strong duality holds for convex problems that are strictly feasible, i.e, Slater's conditions hold [81]. Hence, strong duality holds for the reformulated convex SOCP problem (13). Given the fact that equivalent optimization problems, such as (12) and (13), may have different Lagrange dual problems [81], it needs to be shown that the Lagrangians of (12) and (13) are the same. Therefore, the dual problems also must be the same. First, the Lagrangians of (12) and (13) are formulated as follows

$$\begin{aligned}
&L\left(P^{\mathrm{tx}}, \mathbf{M}, \boldsymbol{\chi}, \omega, \boldsymbol{\lambda}, \boldsymbol{\mu}\right) \\
&= (1-\omega)P^{\mathrm{tx}} + \sum_{k\in\mathcal{K}} \lambda_{b,k}\left(N_0 + \sum_{b'\in\bar{\mathcal{B}}\setminus\{b_k\}} \chi_{b',k}\right) - \sum_{b\in\mathcal{B}}\sum_{k\in\bar{\mathcal{K}}_b} \mu_{b,k}\chi_{b,k} \\
&+ \sum_{k\in\mathcal{K}} \mathbf{m}_k^{\mathrm{H}} \left\{ \omega\mathbf{I} + \sum_{i\in\mathcal{K}_b} \lambda_{b,i}\mathbf{h}_{b_k,i}^{\mathrm{H}}\mathbf{h}_{b_k,i} + \sum_{j\in\bar{\mathcal{K}}_b} \mu_{b,j}\mathbf{h}_{b_k,j}^{\mathrm{H}}\mathbf{h}_{b_k,j} \right. \\
&\left. - \left(1+\frac{1}{\gamma_k}\right)\lambda_{b,k}\mathbf{h}_{b_k,k}^{\mathrm{H}}\mathbf{h}_{b_k,k} \right\} \mathbf{m}_k
\end{aligned} \tag{145}$$

and

$$\begin{aligned}
&L\left(p^{\mathrm{tx}}, \mathbf{M}, \bar{\boldsymbol{\chi}}, a, \mathbf{b}, \mathbf{c}\right) = \\
&p^{\mathrm{tx}} + a\left(\|\bar{\mathbf{m}}\|_2 - p^{\mathrm{tx}}\right) - \sum_{k\in\mathcal{K}} b_{b,k}\left(\sqrt{1+\frac{1}{\gamma_k}}\mathbf{h}_{b_k,k}\mathbf{m}_k - \left\| \begin{matrix} \mathbf{M}_{b_k}^{\mathrm{H}}\mathbf{h}_{b_k,k}^{\mathrm{H}} \\ \bar{\boldsymbol{\chi}}_k \\ \sqrt{N_0} \end{matrix} \right\|_2\right) \\
&- \sum_{b\in\mathcal{B}}\sum_{k\in\bar{\mathcal{K}}_b} b_{b,k}\left(\chi_{b,k} - \left\| \mathbf{M}_b^{\mathrm{H}}\mathbf{h}_{b,k}^{\mathrm{H}} \right\|_2\right)
\end{aligned} \tag{146}$$

Next, a similar derivation as in [35] is used to reformulate (146). It can be written that

$$\tilde{a} = \|\bar{\mathbf{m}}\|_2, \tag{147}$$

$$\tilde{b}_{b,k} = \sqrt{1+\tfrac{1}{\gamma_k^{\mathrm{S}}}}\mathbf{h}_{b_k,k}\mathbf{m}_k + \left\| \begin{matrix} \mathbf{M}_{b_k}^{\mathrm{H}}\mathbf{h}_{b_k,k}^{\mathrm{H}} \\ \bar{\boldsymbol{\chi}}_k \\ \sqrt{N_0} \end{matrix} \right\|_2, \tag{148}$$

$$\tilde{c}_{b,k} = \chi_{b,k} + \left\| \ \mathbf{M}_b^{\mathrm{H}} \mathbf{h}_{b,k}^{\mathrm{H}} \ \right\|_2 . \tag{149}$$

By substituting these terms into (146), the following formulation is obtained

$$\begin{aligned}
&L\left(P^{\mathrm{tx}}, \mathbf{M}, \boldsymbol{\chi}, a, \mathbf{b}, \mathbf{c}\right) = \\
&(1-\frac{a}{\tilde{a}})P^{\mathrm{tx}} + \sum_{k\in\mathcal{K}} \frac{b_{b,k}}{\tilde{b}_{b,k}} \left(N_0 + \sum_{b'\in\mathcal{B}\setminus\{b_k\}} \chi_{b',k} \right) - \sum_{b\in\mathcal{B}} \sum_{k\in\bar{\mathcal{K}}_b} \frac{c_{b,k}}{\tilde{c}_{b,k}} \chi_{b_k,k} \\
&+ \sum_{k\in\mathcal{K}} \mathbf{m}_k^{\mathrm{H}} \left\{ \frac{a}{\tilde{a}} \mathbf{I} + \sum_{i\in\mathcal{K}_b} \frac{b_{b,i}}{\tilde{b}_{b,i}} \mathbf{h}_{b_k,i}^{\mathrm{H}} \mathbf{h}_{b_k,i} + \sum_{j\in\bar{\mathcal{K}}_b} \frac{c_{b,i}}{\tilde{c}_{b,i}} \mathbf{h}_{b_k,j}^{\mathrm{H}} \mathbf{h}_{b_k,j} \right. \\
&\left. - \left(1+\frac{1}{\gamma_k}\right) \frac{b_{b,k}}{\tilde{b}_{b,k}} \mathbf{h}_{b_k,k}^{\mathrm{H}} \mathbf{h}_{b_k,k} \right\} \mathbf{m}_k
\end{aligned} \tag{150}$$

Due to strict positivity of $\tilde{a}$, $\tilde{b}_{b,k}$ and $\tilde{c}_{b,k}$, the optimization variables can be changed in (150), i.e., $\omega = a/\tilde{a}$, $\lambda_{b,k} = b_{b,k}/\tilde{b}_{b,k}$ and $\mu_{b,k} = c_{b,k}/\tilde{c}_{b,k}$. Thus, the Lagrangians of the original problem and the SOCP problem, i.e., (145) and (150), are exactly the same, thus leading to the same dual problem.

Appendix 2 Proof of Proposition 2

It is shown here that (17) is a valid subgradient of (15) at point $\chi_{b,k}$. The proof is inspired by the result in [35]. First, the objective value of (15) is rewritten by $g^\star(\boldsymbol{\chi})$, where $g^\star(\boldsymbol{\chi})$ is the optimal objective value of (12) at point $\boldsymbol{\chi}$. Since strong duality holds for (12), $g^\star(\boldsymbol{\chi})$ can be achieved by solving the Lagrange dual problem of (12) at point $\boldsymbol{\chi}$. This can be expressed as

$$\begin{aligned}
\max_{\boldsymbol{\lambda},\boldsymbol{\mu}}.\quad & \sum_{b\in\mathcal{B}}\sum_{k\in\mathcal{K}_b}\lambda_{b,k}\left(N_0+\sum_{b'\in\mathcal{B}\setminus\{b_k\}}\chi_{b',k}\right)-\sum_{b\in\mathcal{B}}\sum_{k\in\bar{\mathcal{K}}_b}\mu_{b,k}\chi_{b_k,k}\\
\text{s. t.}\quad & \mathbf{I}+\sum_{i\in\mathcal{K}_b}\lambda_{b,i}\mathbf{h}^{\mathrm{H}}_{b_k,i}\mathbf{h}_{b_k,i}+\sum_{j\in\bar{\mathcal{K}}_b}\mu_{b,j}\mathbf{h}^{\mathrm{H}}_{b_k,j}\mathbf{h}_{b_k,j}\\
& -\left(1+\tfrac{1}{\gamma_k^{\mathrm{S}}}\right)\lambda_{b,k}\mathbf{h}^{\mathrm{H}}_{b_k,k}\mathbf{h}_{b_k,k}\succeq 0,\forall b\in\mathcal{B},\forall k\in\mathcal{K}_b\\
& \boldsymbol{\lambda}\succeq 0,\boldsymbol{\mu}\succeq 0
\end{aligned}\tag{151}$$

where the vectors $\boldsymbol{\lambda}$ and $\boldsymbol{\mu}$ consist of the elements of the sets $\{\lambda_{b,k}\}_{b\in\mathcal{B},k\in\mathcal{K}_b}$ and $\{\mu_{b,k}\}_{b\in\mathcal{B},k\in\bar{\mathcal{K}}_b}$, respectively.

Since the dual problem (151) is concave, a subgradient of $g^\star$ at the point $\boldsymbol{\chi}$ can be defined as any vector $\mathbf{z}$, which satisfies the following [157]: $g^\star(\tilde{\boldsymbol{\chi}})-g^\star(\boldsymbol{\chi})\leq\mathbf{z}^{\mathrm{T}}(\tilde{\boldsymbol{\chi}}-\boldsymbol{\chi})$, for all $\tilde{\boldsymbol{\chi}}$. Next, it is assumed that $\tilde{\boldsymbol{\tau}}$ and $\boldsymbol{\tau}$ are the optimal dual variable vectors at the points $\tilde{\boldsymbol{\chi}}$ and $\boldsymbol{\chi}$, respectively. Replacing $\tilde{\boldsymbol{\tau}}$ with $\boldsymbol{\tau}$ in the dual objective expression of $g^\star(\tilde{\boldsymbol{\chi}})$, it can be written that

$$\begin{aligned}
g^\star(\tilde{\boldsymbol{\chi}})-g^\star(\boldsymbol{\chi}) \quad\leq\quad & \boldsymbol{\tau}^{\mathrm{T}}\tilde{\boldsymbol{\chi}}-\boldsymbol{\tau}^{\mathrm{T}}\boldsymbol{\chi}=\boldsymbol{\tau}^{\mathrm{T}}(\tilde{\boldsymbol{\chi}}-\boldsymbol{\chi})\\
& =\sum_{b\in\mathcal{B}}\sum_{k\in\bar{\mathcal{K}}_b}(\lambda_{b_k,k}-\mu_{b,k})(\tilde{\chi}_{b,k}-\chi_{b,k})
\end{aligned}\tag{152}$$

Based on the subgradient definition, one can see that $\lambda_{b_k,k}-\mu_{b,k}$ is the subgradient of $g^\star$ at the point $\chi_{b,k}$.

Appendix 3 Proof of Theorem 1

The proof is a modification of uplink-downlink duality results proposed in [35]. First, a virtual dual uplink problem is formulated, where the user-specific SINR constraints are the same as in the downlink problem. This is expressed as

$$\begin{aligned} \min_{\{\tilde{P}_k^{\mathrm{tx}},\mathbf{w}_k\}_{k\in\mathcal{K}_b}} \quad & \sum_{k\in\mathcal{K}_b} \upsilon_k \tilde{P}_k^{\mathrm{tx}} \\ \text{s. t.} \quad & \frac{\tilde{P}_k^{\mathrm{tx}}\left|\mathbf{w}_k^{\mathrm{H}}\mathbf{h}_{b_k,k}\right|^2}{\sum_{i=1,i\neq k}^{K}\tilde{P}_i^{\mathrm{tx}}\left|\mathbf{w}_k^{\mathrm{H}}\mathbf{h}_{b_k,i}\right|^2+\mathbf{w}_k^{\mathrm{H}}\mathbf{I}\mathbf{w}_k} \geq \gamma_k, \forall k\in\mathcal{K}_b \end{aligned} \tag{153}$$

where $\tilde{P}_k^{\mathrm{tx}}$ and υ_k denote the virtual uplink power and its (constant) scaler for user k , respectively. One can observe that (153) is exactly the same as (24) if it is denoted that $\upsilon_k = N_0 + \sum_{b'\in\mathcal{B}\setminus\{b_k\}}\chi_{b',k}$, $\tilde{P}_k^{\mathrm{tx}} = \lambda_{b,k}$, $\tilde{P}_i^{\mathrm{tx}} = \mu_{b,i}$, $\forall k\in\mathcal{K}_b$, $\forall i\in\bar{\mathcal{K}}_b$. The vectors $\boldsymbol{\lambda}_b$ and $\boldsymbol{\mu}_b$ can be interpreted as the virtual dual uplink powers for the users at the serving cell and the users at the other cells, respectively. Moreover, the virtual uplink power of user k is scaled in the objective by the constant υ_k that is a sum of the noise and fixed interference powers experienced by user k in downlink.

When $\boldsymbol{\lambda}_b$ is fixed, an explicit optimal solution to (24) is found by using the MMSE receiver, which maximizes the SINR. The MMSE receiver is given by

$$\begin{aligned} \acute{\mathbf{w}}_k &= \frac{\grave{\mathbf{w}}_k}{||\grave{\mathbf{w}}_k||_2}, \\ \grave{\mathbf{w}}_k &= \left(\sum_{i\in\mathcal{K}_b}\lambda_{b,i}\mathbf{h}_{b_k,i}^{\mathrm{H}}\mathbf{h}_{b_k,i} + \sum_{j\in\bar{\mathcal{K}}_b}\mu_{b,j}\mathbf{h}_{b_k,j}^{\mathrm{H}}\mathbf{h}_{b_k,j} + \mathbf{I}\right)^{-1}\mathbf{h}_{b_k,k}, \forall k\in\mathcal{K}_b. \end{aligned} \tag{154}$$

By substituting $\{\mathbf{w}_k\}_{k\in\mathcal{K}_b}$ into (24) and using Lemma 1 from [35], the SINR constraints in (24) can be expressed as

$$\begin{aligned} &\mathbf{I} + \sum_{i\in\mathcal{K}_b}\lambda_{b,i}\mathbf{h}_{b_k,i}^{\mathrm{H}}\mathbf{h}_{b_k,i} + \sum_{j\in\bar{\mathcal{K}}_b}\mu_{b,j}\mathbf{h}_{b_k,j}^{\mathrm{H}}\mathbf{h}_{b_k,j} - \left(1+\tfrac{1}{\gamma_k}\right)\lambda_{b,k}\mathbf{h}_{b_k,k}^{\mathrm{H}}\mathbf{h}_{b_k,k} \preceq 0, \\ &\forall k\in\mathcal{K}_b. \end{aligned} \tag{155}$$

These constraints are the same as in (23) except that they are reversed. If the minimization is changed into the maximization and the SINR constraints in

(24) are reversed, the resulting problem is exactly (23). The reversing does not change the optimal value of the problem since the SINR constraints are met with equality in the optimal solution. Thus, (23) and (24) are equivalent problems with identical solutions.

Appendix 4 Proof of Proposition 3

In the following, it is proved that $\boldsymbol{\lambda}_b$ is optimally solved using (25). This proof is inspired by the prior work in [33, 59, 170]. First, the gradient of the Lagrangian of (14) with respect to $\{\mathbf{m}_k\}_{k\in\mathcal{K}_b}$ is set to zero. This is expressed as

$$\left\{\mathbf{I}+\sum_{i\in\mathcal{K}_b}\lambda_{b,i}\mathbf{h}_{b_k,i}^{\mathrm{H}}\mathbf{h}_{b_k,i}+\sum_{j\in\bar{\mathcal{K}}_b}\lambda_{b,j}\mathbf{h}_{b_k,j}^{\mathrm{H}}\mathbf{h}_{b_k,j}-\left(1+\frac{1}{\gamma_k}\right)\lambda_{b,k}\mathbf{h}_{b_k,k}^{\mathrm{H}}\mathbf{h}_{b_k,k}\right\}\mathbf{m}_k = 0, \forall k\in\mathcal{K}_b. \tag{156}$$

After rearranging, similar to that in [59], the function (25) is obtained. We can rewrite (25) as follows: $\lambda_{b,k}^{(m+1)} = g_{b,k}(\boldsymbol{\lambda}_b^{(m)})$, $\forall k \in \mathcal{K}_b$. The function $g_{b,k}$ is a standard function if it satisfies the properties of 1) positivity, 2) monotonicity and 3) scalability, i.e.,

1) If $\lambda_{b,k} \geq 0$, $\forall k \in \mathcal{K}_b$, then $g_{b,k}(\boldsymbol{\lambda}_b) > 0$, $\forall k \in \mathcal{K}_b$.
2) If $\lambda_{b,k} \geq \tilde{\lambda}_{b,k}$, $\forall k \in \mathcal{K}_b$, then $g_{b,k}(\boldsymbol{\lambda}_b) \geq g_{b,k}(\tilde{\boldsymbol{\lambda}}_b)$, $\forall k \in \mathcal{K}_b$.
3) For $\varphi > 1$, $\varphi g_{b,k}(\boldsymbol{\lambda}_b) > g_{b,k}(\varphi\boldsymbol{\lambda}_b)$, $\forall k \in \mathcal{K}_b$.

The proof, which shows that these properties are satisfied by (25), is omitted since it follows the principles in [33]. Since the standard function always converges to a unique fixed point for any initial value [170], the obtained $\boldsymbol{\lambda}_b$ is optimal.

Appendix 5 Proof of Proposition 4

In this appendix, it is shown that the optimal downlink transmit beamformers can be solved via the optimal virtual uplink receive beamformers by scaling. The proof is a modification of the results presented in [35]. After manipulation of (156), similar to that in [35], the following expression is achieved for $\mathbf{m}_k$:

$$\mathbf{m}_k = \left(\sum_{i \in \mathcal{K}_b} \lambda_{b,i} \mathbf{h}_{b_k,i}^{\mathrm{H}} \mathbf{h}_{b_k,i} + \sum_{j \in \bar{\mathcal{K}}_b} \mu_{b,j} \mathbf{h}_{b_k,j}^{\mathrm{H}} \mathbf{h}_{b_k,j} + \mathbf{I} \right)^{-1} \\ \left(1 + \frac{1}{\gamma_k}\right) \lambda_{b,k} \mathbf{h}_{b_k,k}^{\mathrm{H}} \mathbf{h}_{b_k,k} \mathbf{m}_k \tag{157}$$

If (157) is compared to the MMSE expression of $\acute{\mathbf{w}}_k$ in (154), it can be observed that $\mathbf{m}_k$ is a scaled version of $\acute{\mathbf{w}}_k$, i.e., $\mathbf{m}_k = \sqrt{\epsilon_k} \acute{\mathbf{w}}_k$, where $\sqrt{\varepsilon_k} = \left(1 + \frac{1}{\gamma_k}\right) \lambda_{b,k} \mathbf{h}_{b_k,k} \mathbf{m}_k$. Since ε_k still depends on $\mathbf{m}_k$, an expression needs to be found where $\{\varepsilon_k\}_{k \in \mathcal{K}_b}$ are expressed only via $\{\acute{\mathbf{w}}_k\}_{k \in \mathcal{K}_b}$. In this respect, the SINR constraints are satisfied with equality at the optimal point of (14). By substituting $\mathbf{m}_k = \sqrt{\varepsilon_k} \acute{\mathbf{w}}_k$ into the SINR constraints, the following equation can be written

$$(\varepsilon_k / \gamma_k) \, |\mathbf{h}_{b_k,k} \acute{\mathbf{w}}_k|^2 - \textstyle\sum_{i \in \mathcal{K}_{b_k} \setminus k} \varepsilon_i |\mathbf{h}_{b_i,k} \acute{\mathbf{w}}_i|^2 = \\ \textstyle\sum_{b' \in \mathcal{B} \setminus \{b_k\}} \chi_{b',k} + N_0, \forall k \in \mathcal{K}_b. \tag{158}$$

Now, (158) can be solved for $\{\varepsilon_k\}_{k \in \mathcal{K}_b}$ via (28).

525. Lu, Pen-Shun (2015) Decoding and lossy forwarding based multiple access relaying

526. Suopajärvi, Terhi (2015) Functionalized nanocelluloses in wastewater treatment applications

527. Pekuri, Aki (2015) The role of business models in construction business management

528. Mantere, Matti (2015) Network security monitoring and anomaly detection in industrial control system networks

529. Piri, Esa (2015) Improving heterogeneous wireless networking with cross-layer information services

530. Leppänen, Kimmo (2015) Sample preparation method and synchronized thermography to characterize uniformity of conductive thin films

531. Pouke, Matti (2015) Augmented virtuality : transforming real human activity into virtual environments

532. Leinonen, Mikko (2015) Finite element method and equivalent circuit based design of piezoelectric actuators and energy harvester dynamics

533. Leppäjärvi, Tiina (2015) Pervaporation of alcohol/water mixtures using ultra-thin zeolite membranes : membrane performance and modeling

534. Lin, Jhih-Fong (2015) Multi-dimensional carbonaceous composites for electrode applications

535. Goncalves, Jorge (2015) Situated crowdsourcing : feasibility, performance and behaviours

536. Herrera Castro, Daniel (2015) From images to point clouds : practical considerations for three-dimensional computer vision

537. Komulainen, Jukka (2015) Software-based countermeasures to 2D facial spoofing attacks

538. Pedone, Matteo (2015) Algebraic methods for constructing blur-invariant operators and their applications

539. Karhu, Mirjam (2015) Treatment and characterisation of oily wastewaters

540. Panula-Perälä, Johanna (2015) Development and application of enzymatic substrate feeding strategies for small-scale microbial cultivations : applied for *Escherichia coli*, *Pichia pastoris*, and *Lactobacillus salivarius* cultivations

UNIVERSITY OF OULU P.O. Box 8000 FI-90014 UNIVERSITY OF OULU FINLAND

ACTA UNIVERSITATIS OULUENSIS

UNIVERSITY of OULU
OULUN YLIOPISTO

ISBN 978-952-62-0896-1 (Paperback)
ISBN 978-952-62-0897-8 (PDF)
ISSN 0355-3213 (Print)
ISSN 1796-2226 (Online)